Studies on the synthesis of bisindole *Aspidosperma* alkaloids

by

Taylor Pinto

Bachelor of Science in Chemistry
Tennessee Technological University, Cookeville, TN, 2019

Bachelor of Science in Chemical Engineering
Tennessee Technological University, Cookeville, TN, 2019

Submitted to the Department of Chemistry
in partial fulfillment of the requirements for the degree of

Doctor of Philosophy in Chemistry

at the

Massachusetts Institute of Technology

September 2024

Authored by:	Taylor Pinto Department of Chemistry August 16, 2024
Certified by:	Mohammad Movassaghi Professor of Chemistry, Thesis Supervisor
Accepted by:	Adam P. Willard Professor of Chemistry Graduate Officer, Department of Chemistry

This doctoral thesis has been examined by a committee of the Department of Chemistry as follows:

Alison Wendlandt
Associate Professor of Chemistry
Thesis Committee Chair

Mohammad Movassaghi
Professor of Chemistry
Thesis Supervisor

Timothy F. Jamison
Robert R. Taylor Professor of Chemistry
Thesis Committee Member

Studies on the synthesis of bisindole *Aspidosperma* alkaloids

by

Taylor Pinto

Submitted to the Department of Chemistry on August 16, 2024
in partial fulfillment of the requirements for the degree of

Doctor of Philosophy in Chemistry

ABSTRACT

I. Introduction and Background on Aspidosperma Alkaloids
A brief overview of monoterpene indole Aspidosperma alkaloids is discussed. The biosynthesis of the characteristic pentacyclic core from tryptamine and secologanin is summarized. Some representative examples of total syntheses of Aspidosperma alkaloids are discussed. Synthetic strategies for the synthesis of bisindole members of the family are also examined.

II. Total Synthesis of (–)-Voacinol, (–)-Voacandimine C, and related congener, (−)-methylenebisdeoxoapodine
We describe the first total synthesis of complex aspidosperma alkaloids (–)-voacinol and (–)-voacandimine C via a late-stage C7-methylenation strategy inspired by a biogenetic hypothesis. We envisioned rapid access to these natural alkaloids from a common, symmetrical precursor assembled by methylenation of a D-ring-oxidized variant of the structurally related natural product (–)-deoxoapodine. Chemoselective N9-oxidation of a pentacyclic deoxoapodine precursor enabled the synthesis of the corresponding hexacyclic C8-aminonitrile. Stereocontrolled methylenation of a C8-enamine derivative of deoxoapodine, accessed by ionization of the C8-aminonitrile, afforded a symmetrical dodecacyclic bisaminonitrile as a versatile precursor to these bisindole alkaloids. Final-stage, biosynthesis-inspired, controlled reductive opening of the oxolane substructures of this dodecacyclic intermediate provided a unified approach to (–)-voacinol and (–)-voacandimine C, while direct reduction of the same intermediate afforded the structurally related (–)-methylenebisdeoxoapodine.

III. Progress Toward the Total Synthesis of Voacandimine A
We describe our work toward the total synthesis of bisindole *Aspidosperma* alkaloid, voacandimine A. Key features of the synthetic progress include two routes for monomer synthesis, two methods for complex fragment assembly to form the bisindole structure, and strategies to address the stereochemistry of the ring fusion.

Thesis Supervisor: Mohammad Movassaghi
Professor of Chemistry

Acknowledgements

I would first like to thank my advisor, Professor Mohammad Movassaghi, for his mentorship and advice throughout my graduate school career. I appreciate all of his support for my growth as a scientist by helping to develop my scientific and chemistry problem solving skills. I always appreciated his enthusiasm and excitement about chemistry and my project. I would also like to thank Associate Professor Alison Wendlandt, my thesis committee chair, and Professor Tim Jamison for discussions and feedback at the major milestones of the graduate program. I would also like to thank Dr. Walt Massefski and Dr. Bruce Adams for their help with all of my many NMR related problems. From Tennessee Tech, I would like to thank Dr. Amanda Carroll for being one of my biggest supporters when I began to considering going to graduate school. I also want to acknowledge Dr. Daniel Swartling and Dr. William Carroll for giving me the opportunity to explore undergraduate research and sparking my interest in pursuing a future in research.

My graduate school experience would not have been as rewarding without my coworkers in the Movassaghi Lab. From the discussions about synthetic problems to the afternoon trips to get sweet treats, everything has helped to get through my Ph.D. I would like to thank Dr. Kristen Flynn for helping me get started in the Aspidosperma subgroup. Thanks to Dr. In-Soo Myeong and Robert Raclea for all of the discussions and suggestions for the Aspidosperma subgroup. I would also like to thank Dr. Katherine Walker and Dr. Tony Scott for their mentorship towards becoming a better synthetic chemist. Thanks to Dr. Walker Knauss for being a good lab bay coworker over the past few years. To Katie Downey and Rad Chrzanowski, I look forward to seeing what you accomplish as the future of the lab.

Lastly, I want to thank my family for their support and encouragement. My parents were always willing to listen to my problems even though they didn't necessarily understand the technical aspects. Their support has been invaluable for learning about the things that grad school doesn't teach about growing up and becoming independent, like taxes. I also need to thank my biggest supporter, Mya. She was always happy to see me and brighten my day even after a long day in the lab. Last but not least, thanks to Riley for your encouragement and for believing in me.

Preface

Portions of this work have been adapted from the following articles that were co-written by the author and are reproduced in part with permission from:

Flynn, K. M.; Myeong, I.-S.; Pinto, T.; Movassaghi, M. "Total Synthesis of (−)-Voacinol and (−)-Voacandimine C" *J. Am. Chem. Soc.* **2022***,* 144, 9126−9131.

Respective Contributions

This thesis contains work done in collaboration with numerous colleagues at MIT.

Chapter II was done in collaboration with Dr. Kristen M. Flynn and Dr. In-Soo Myeong. Dr. Kristen M. Flynn developed and executed the synthesis of (–)-voacinol and (–)-voacandimine C. Dr. In-Soo Myeong contributed to the synthesis of (–)-deoxoapodine and initial exploration of (–)-methylenebisdeoxoapodine.

Chapter III was done in collaboration with Dr. In-Soo Myeong. Dr. In-Soo Myeong developed parts of the synthetic route used in the study.

Table of Contents

List of Figures

Chapter I: Introduction and Background on Aspidosperma Alkaloids

Chapter II: Total Synthesis of (–)-Voacinol, (–)-Voacandimine C, and related congener, (−)-methylenebisdeoxoapodine

Chapter III. Progress Toward the Total Synthesis of Voacandimine A

List of Tables

Chapter II: Total Synthesis of (–)-Voacinol, (–)-Voacandimine C, and related congener, (−)-methylenebisdeoxoapodine

Chapter III. Progress Toward the Total Synthesis of Voacandimine A

Abbreviations

Å	angstrom
Ac	acetyl
Ar	aryl
ATR	Attenuated Total Reflectance
[α]	specific rotation
app	apparent
aq	aqueous
B_2pin_2	Bis(pinacolato)diboron
Binol	1,1′-Bi-2-naphthol
br	broad
Bu	butyl
Bn	benzyl
Boc	*tert*-butyloxycarbonyl
°C	degrees Celsius
cal	calorie
calc'd	calculated
CAM	ceric ammonium molybdate
CDI	1,1'-Carbonyldiimidazole
cm^{-1}	wavenumber
cod	1,5-cyclooctadiene
COSY	correlation spectroscopy
d	doublet
D	deuterium
δ	parts per million
DART	direct analysis in real time
DBU	1,8-diazabicyclo[5.4.0]undec-7-ene
DCE	1,2-dichloroethane
DEAD	diethyl azodicarboxylate
DEHA	diethylhydroxylamine
DIBAl	diisobutylaluminum hydride
DIPEA	diisopropylethylamine
DMAP	4-(dimethylamino)pyridine
DMF	*N,N*-dimethylformamide
DMPU	*N,N′*-dimethylpropyleneurea
DMSO	dimethylsulfoxide
DNs	dinitrobenzensulfonyl
DPAS	dihydroprecondylocarpine acetate synthase
dr	diastereomeric ratio
dtbpy	4,4'-di-*tert*-butyl bipyridine
DTBMP	2,6-di-*tert*-butyl-4-methylpyridine
EDCI	1-Ethyl-3-(3-dimethylaminopropyl)carbodiimide
ee	enantiomeric excess
ESI	electrospray ionization

Et	ethyl
ent	enantiomeric
epi	epimeric
equiv	equivalents
FT	Fourier transform
g	gram
g	gradient
GO	geissoschizine oxidase
GS	geissoschizine synthase
Glc	D-glucose
h	hour
HBpin	pinacol borane
HFIP	1,1,1,3,3,3-hexafluoroisopropanol
HMBC	heteronuclear multiple bond correlation
HPLC	high performance liquid chromatography
HRMS	high resolution mass spectrometry
HSQC	heteronuclear single quantum correlation
Hz	Hertz
IR	infrared
i	iso
IC	inhibitory concentration
ImH	imidazole
J	coupling constant
k	kilo
L	liter
LAH	lithium aluminum hydride
LC	liquid chromatography
LiHMDS	lithium bis(trimethylsilyl)amide
LDA	lithium diisopropylamide
m	medium
m	multiplet
m	milli
m	meter
m	meta
M	molar
μ	micro
mCPBA	meta-chloroperoxybenzoic acid
Me	methyl
MHz	megahertz
MIC	minimum inhibitory concentration
min	minute
MMFF	Merck Molecular Force Field
mol	mole
MS	mass spectrometry
m/z	mass to charge
n	normal

n	nano
NCS	N-chlorosuccinimide
NMR	nuclear magnetic resonance
nOe	nuclear Overhauser effect
NOESY	Nuclear Overhauser Effect Spectroscopy
Ns	nitrobenzenesulfonyl
o	ortho
p	para
PAS	precondylocarpine acetate synthase
Piv	pivalyl
PMB	*para*-methoxybenzyl
Pr	propyl
PS-BEMP	polystyrene-bound 2-*tert*-butylimino-2-diethylamino-1,3-dimethyl-perhydro-1,3,2-diazaphosphorine
ppm	parts per million
Pyr	pyridine
q	quartet
QTof	Quadrupole Time-of-Flight
Red-Al	sodium bis(2-methoxyethoxy)aluminium hydride
rel	relative
Rf	retention factor
ROESY	Rotating-Frame Overhauser Enhancement Spectroscopy
RSM	recovered starting material
rt	room temperature
s	singlet
s	strong
SAT	stemmadenine O-acetyltransferase
SGD	strictosidine β-D-glucosidase
STR	strictosidine synthase
t	tert
t	triplet
T	temperature
TS	tabersonine synthase
TBAF	tetra-*n*-butylammonium fluoride
TBDPS	*tert*-butyldiphenylsilyl
TBS	*tert*-butyldimethylsilyl
Tf	trifluoromethanesulfonyl
TFA	trifluoroacetic acid
TFAA	trifluoroacetic anhydride
TFE	2,2,2-trifluoroethanol
THF	tetrahydrofuran
TIPS	triisopropylsilyl
TLC	thin-layer chromatography
TMS	trimethylsilyl
Troc	2,2,2-trichloroethoxycarbonyl

μ	micro
UV	ultraviolet
w	weak
wt	weight

Chapter I

Introduction and Background of *Aspidosperma* Alkaloids

Introduction

The aspidosperma alkaloids are a structurally diverse family of monoterpene indole alkaloids with over 250 members[1]. They exhibit a characteristic pentacyclic 6/5/6/6/5 core, as shown by (+)-aspidospermidine (**1.1**)[2], with multiple stereocenters and varying levels and sites of oxidation (Figure 1.1). They have attracted significant interest due to their complex structure and varying biological activities. Some examples of bioactivities are (+)-haplocidine (**1.7**) is a potent caspase-8 inhibitor (IC_{50}=0.4 μM)[3] and (−)-jerantinine C (**1.6**) has cytotoxic activity against human KB cells (IC_{50}=0.81μM)[4]. Throughout the past 60 years, Aspidosperma alkaloids have prompted a number of innovative syntheses[5,6]. The Movassaghi group has had a long-standing interest in the synthesis of Aspidosperma alkaloids since our first report in 2012.[7] Our group has since reported the syntheses of (−)-mehranine (**1.2**)[8], (−)-deoxoapodine (**1.4**)[9], (+)-haplocidine (**1.7**)[10], (+)-vallesine (**1.5**)[11], and (−)-kopsifoline A (**1.10**)[12].

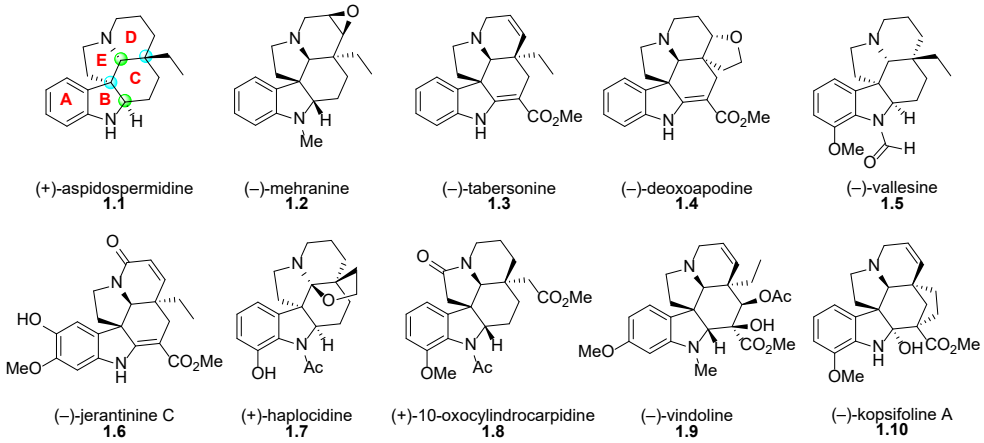

Figure 1.1 *Examples of Aspidosperma alkaloids.*

Most reported syntheses[5] of the family have been focused on members containing a single indole unit, leaving the more complex monoterpenoid bisindole Aspidosperma alkaloids[13] underexplored which provides opportunities for the development of new synthetic strategies. Our group has been interested in bisindole alkaloids due to their increased complexity, interesting bond connections, and in some cases, increased bioactivities. One of the best examples of this is

the monoterpene bisindole alkaloid (+)-vinblastine (**1.17**)[14], a potent anticancer agent[15] which has inspired studies into both its biosynthesis[16] and total synthesis[17,18]. A selection of Aspidosperma-Aspidosperma type alkaloids with a few types of connections between subunits is shown in Figure 1.2. There are a number of structural features that are typically seen in these alkaloids. Common substructures found in Aspidosperma bisindole alkaloids are (−)-mehranine (**1.2**)[19], (−)-tabersonine (**1.3**)[20], and (−)-deoxoapodine (**1.4**)[21]. For example, (+)-tabernaebovine (**1.11**)[22] consists of two mehranine units joined by a C2-C15′ bond, and (−)-melodinine K (**1.13**)[23] contains a C16 oxidized tabersonine subunit. In addition to the C2 and C15 positions, other connections between subunits are found at N1, C3, C7, C8, and C16. (−)-conophylline (**1.12**)[24] and voacandimine A (**1.15**)[25] demonstrate two different bond connections at C7 and C8.

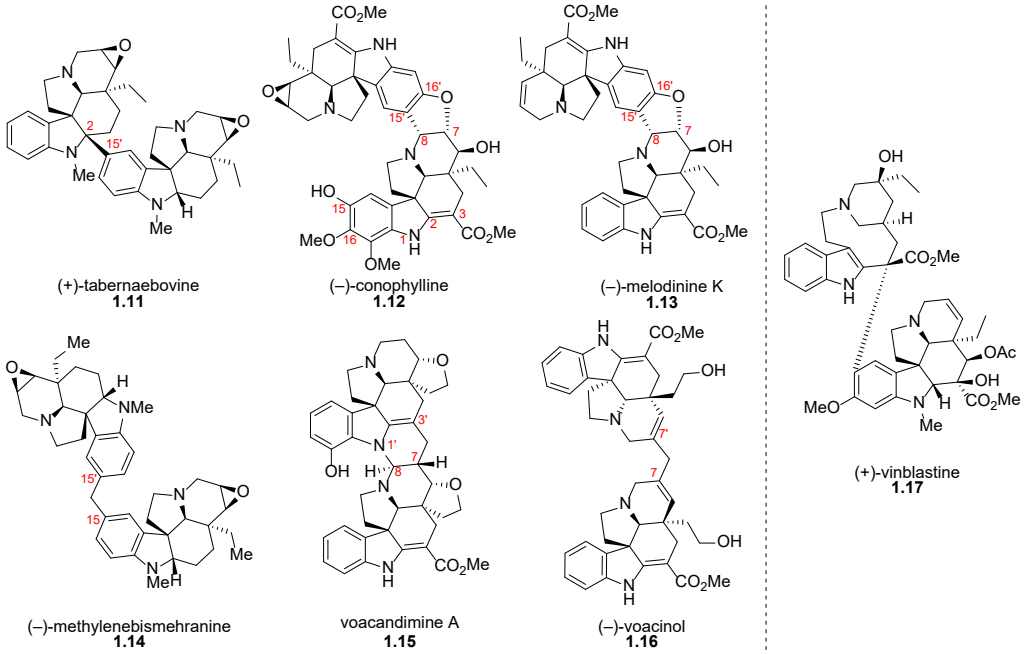

Figure 1.2 *Representative aspidosperma-aspidosperma type bisindole alkaloids.*

Another common feature is the presence of a methylene bridge, as seen in alkaloid **1.15,** (−)-methylenebismehranine (**1.14**)[22], and (−)-voacinol (**1.16**)[26].

A few of these alkaloids have been shown to have promising biological activity. (−)-melodinine K (**1.13**) has cytotoxic activity against five tumor cell lines, in some cases more

potent than the cisplatin control.[23] (−)-conophylline (**1.12**) has been found to have a variety of important biological activity.[27] It has been investigated for its anticancer activity as well as a diabetes treatment.[28] These bioactive molecules along with vinblastine demonstrate the promise of monoterpene bisindole alkaloids as leads for pharmaceutical development.

Biosynthesis

The biosynthesis of monoterpene alkaloids has been investigated for over 60 years[29]; however, the biosynthetic details of the formation of the core structure for the Aspidosperma family have been discovered recently by the O'Connor, Courdavault, and De Luca groups in their work to complete the biosynthesis of (+)-vinblastine (**1.17**) (Scheme 1.1). The biosynthesis of all terpene indole alkaloids can be traced back to tryptophan and secologanin (**1.19**), an iridoid terpene[30]. Tryptophan decarboxylase converts tryptophan to tryptamine (**1.18**)[31]. A strictosidine synthase (STR) catalyzed Pictet-Spengler condensation of tryptamine (**1.18**) and secologanin (**1.19**) yields strictosidine (**1.20**) [32]. Strictosidine (**1.20**) undergoes deglucosylation by strictosidine β-D-glucosidase (SGD)[33] followed by condensation with the secondary amine to form the iminium 4,21-dehydrogeissoschizine (**1.21**). The iminium is reduced by geissoschizine synthase (GS) to form geissoschizine (**1.22**) [34,35]. An oxidative cyclization[36] catalyzed by geissoschinzine oxidase (GO) gives a stemmadenine-type iminium intermediate **1.15** [34,35]. The iminium then undergoes two redox processes. Redox1, a cinnamyl alcohol dehydrogenase-like enzyme, reduces iminium **1.23**[34]. Redox2, an aldo-keto-type reductase, reduces the aldehyde **1.24** to give stemmadenine (**1.25**) which is the n acetylated by stemmadenine O-acetyltransferase

(SAT)[34]. **1.26** undergoes a net alkene isomerization using two enzymes; precondylocarpine acetate synthase (PAS) oxidizes **1.26** to form a conjugated iminium intermediate **1.27** followed

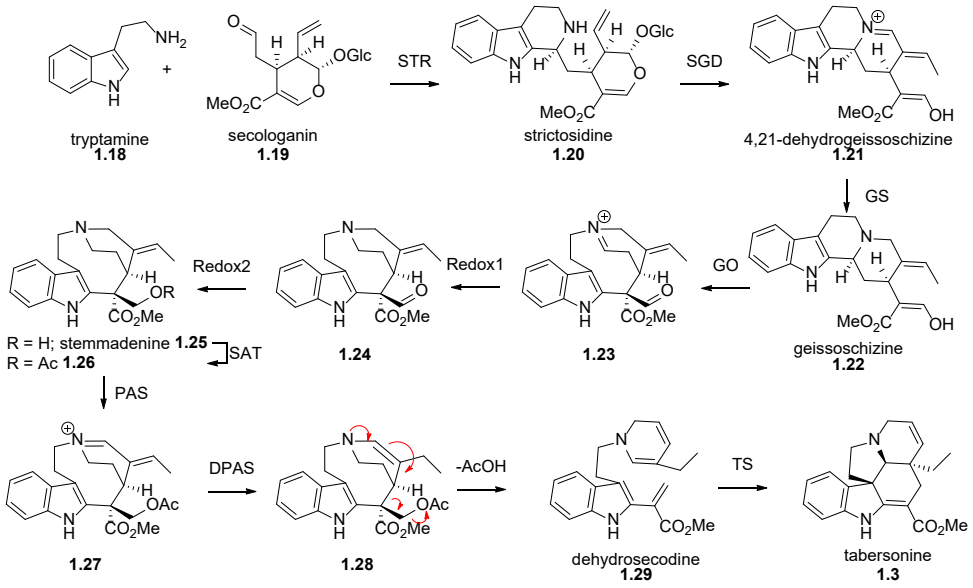

Scheme 1.1 *Aspidosperma Biosynthesis. Enzyme abbreviations: STR (strictosidine synthase), SGD (strictosidine β-D-glucosidase), GS (geissoschizine synthase), GO (geissoschizine oxidase), SAT (stemmadenine O-acetyltransferase), PAS (precondylocarpine acetate synthase), DPAS (dihydroprecondylocarpine acetate synthase), TS (tabersonine synthase).*[5c]

by dihydroprecondylocarpine acetate synthase (DPAS) catalyzing a 1,4-hydride shift to give **1.28**[37]. Grob-type fragmentation of **1.28** releases dehydrosecodine (**1.29**)[38] which serves as the branching point for Aspidosperma and Iboga alkaloids. The aspidosperma core is then formed by a [4+2] cycloaddition catalyzed by tabersonine synthase (TS), an α/β hydrolase-type cyclase[34,37,39]. From (−)-tabersonine (**1.3**), there are seven known enzymes for the conversion to vindoline (**1.9**) which then undergoes the dimerization with catharanthine catalyzed by a peroxidase to complete the biosynthesis of (+)-vinblastine (**1.17**). [29]

Synthesis

Aspidosperma alkaloids have attracted the attention of synthetic chemists for over 60 years since the first synthesis of (±)-aspidospermine (**1.36**) by Stork in 1963 (Scheme 1.2).[6a] (±)-**1.30** was prepared in 8 steps from butyraldehyde. Intramolecular aza-Michael addition of **1.30** formed the D ring. N-acetylation with chloroacetyl chloride followed by nucleophilic substitution of the primary chloride resulted in the formation of the E ring. A three step ketalization, reduction, and deprotection gave the key tricyclic aminoketone (±)-**1.34**. A Fisher indoleninization with 2-methoxyphenylhydrazine gave the pentacyclic core of aspidosperma alkaloids. Subsequent reduction and N-acetylation completed the synthesis of (±)-aspidospermine (**1.36**).

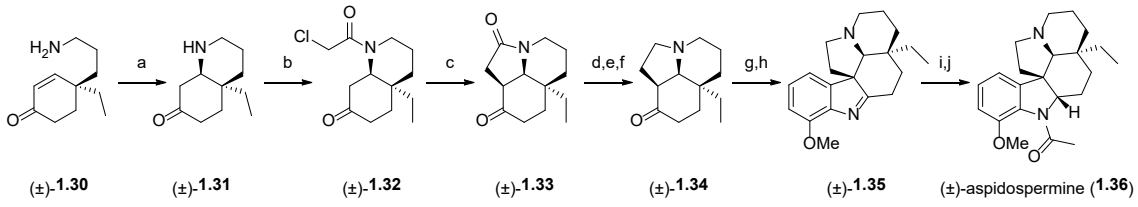

Scheme 1.2 *Stork's synthesis of (±)-aspidospermine. Reagents and conditions: a) aqueous base; b) chloroacetyl chloride; c) t-BuOK, benzene; d) $(CH_2OH)_2$, acid; e) LAH; f) aqueous acid; g) o-methoxyphenylhydrazine; h) AcOH, Δ; i) LAH; j) Ac_2O.*

The first synthesis of (±)-deoxoapodine (**1.4**) was reported by Overman in 1991 (Scheme 1.3).[40] The approach relied on a key aza-Cope rearrangement-Mannich cyclization to form the core pentacycle. Ketone **1.37** was prepared on multigram scale in 12 steps and 12% overall yield from 2-oxocyclopentaneacetate. The dianion of O-Silyl cyanohydrin **1.38**, previously used in their synthesis of 16-methoxytabersonine[41], added to ketone **1.37** and was quenched at low temperature to prevent an undesired α-ketol rearrangement. Subsequent treatment with base led to the desired tetracycle **1.39**. Wittig olefination followed by basic hydrolysis of the cyclic carbamate and pivalamide gave diamino alcohol **1.40**. Treatment with paraformaldehyde led to oxazoline **1.41**. Acid promoted aza-Cope-Mannich rearrangement of **1.41** formed the pentacyclic

imine **1.42**. Excess acid was essential to prevent a retro-Mannich fragmentation by deactivating N9 through protonation. C-acylation of imine **1.42** followed by benzyl ether deprotection using BF_3-OEt_2 in ethanethiol, to avoid alkene reduction, gave primary alcohol **1.43**. (±)-deoxoapodine (**1.4**) was accessed by an oxymercuration followed by a reductive workup.

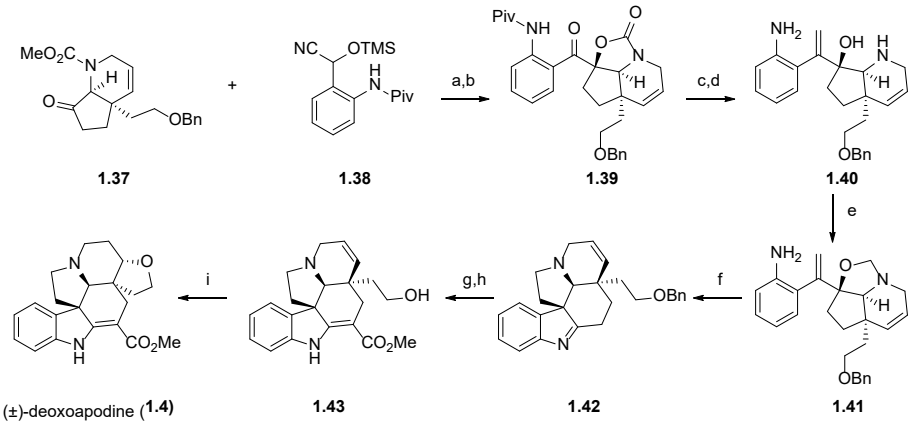

Scheme 1.3 *Overman's synthesis of (±)-deoxoapodine. Reagents and conditions: a) nBuLi, THF, −70 °C; HCl, MeOH, −70 to 0 °C; b) LiOH, H_2O, MeOH, , 0 °C to rt, 76% over 2 steps; c) methyltriphenylphosphorane, THF, −70 °C to rt, 93%; d) KOH, H_2O, EtOH, Δ, 62%; e) paraformaldehyde, Na_2SO_4, toluene, 100%; f) Na_2SO_4, camphorsulfonic acid, benzene, Δ; g) LDA, THF, −70 °C; methyl chloroformate, 36%; h) EtSH, BF_3-OEt_2, Δ, 84%; i) $Hg(OCOCF_3)_2$, THF, −70 °C to rt; NaOH, $NaBH_4$, 52%.*

The first asymmetric synthesis of the aspidosperma core was by Fuji in 1987 (Scheme 1.4).[42] Nitro olefin **1.44** was prepared in enantiomerically enriched form from 2-ethyl-δ-valerolactone via asymmetric induction through an addition-elimination sequence using a chiral nitro enamine.[43] Acid **1.45** was accessed in 6 steps from the chiral nitro olefin. Pictet-Spengler of acid **1.45** with tryptamine (**1.18**) in acetic acid followed by basic hydrolysis gave tetracyclic lactam **1.46** in 42% yield along with its epimer in equal yield separable by chromatography. Lactam **1.46** had previously been used in the synthesis of (±)-aspidospermidine (**1.1**) by Harley-Mason in 1967.[44] Fuji attempted to use boron trifluoride-etherate to affect the skeletal rearrangement from the prior report with little success; Fuji was able to use triflic acid to get the

desired formation of the pentacycle **1.47**. Reduction using LAH completed the synthesis of (−)-aspidospermidine (**1.1**).

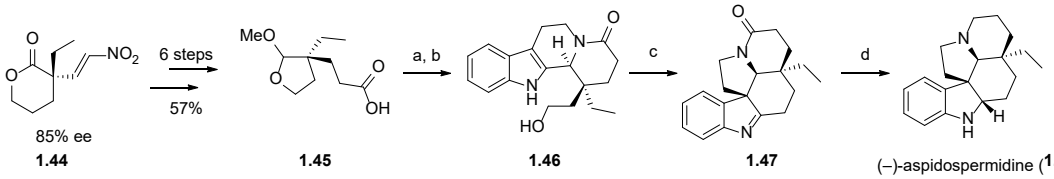

Scheme 1.4 *Fuji's synthesis of (−)-aspidospermidine. Reagents and conditions: a) tryptamine (1.18), AcOH, Δ; b) NaOH, MeOH, 42% over two steps; c) TfOH, 100 °C, 60%; d) LAH, Et_2O, 81%.*

In 2003, Fukuyama reported an enantioselective synthesis of (−)-aspidophytine (**1.55**), an aspidosperma monomer of the dimeric haplophytine, where the C, D, and E rings were formed in a single step from an 11-membered ring precursor (Scheme 1.5).[45] Corey had previously reported the first enantioselective version in 1999.[46] Iodoindole **1.48** was prepared in 7 steps from a known benzaldehyde via a tin-mediated indole formation. The key chiral alkyne **1.49** was prepared in 11 steps from cyclopentenone with an enzymatic resolution using Amano lipase PS to provide enantioenriched material that underwent a Johnson-Claisen rearrangement

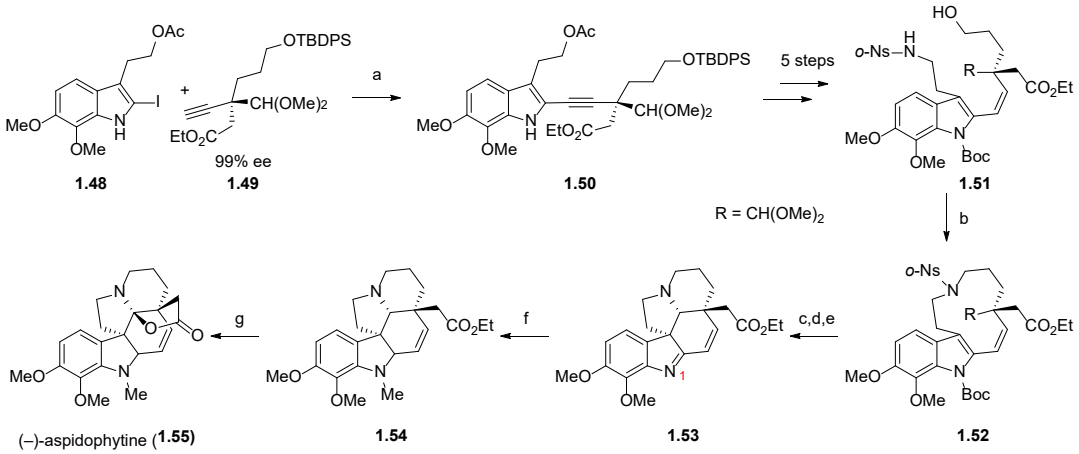

Scheme 1.5 *Fukuyama's synthesis of (−)-aspidophytine. a) $Pd(PPh_3)_4$, CuI, Et_3N, 70 °C, 2 h, 78%; b) PPh_3, DEAD, toluene, rt, 5 min, 92%; c) TMSBr, CH_2Cl_2 , -78 °C, 15 min, 92%; d) PhSH, Cs_2CO_3, MeCN, 55 °C, 20 min; e) TFA, Me_2S, CH_2Cl_2 , rt, 5 min; pH 7.8 buffer, 56% (2 steps); f) HCHO, $NaBH_3CN$, pH 7.0 buffer, -70 °C to rt, 2.5 h, 67%; g) NaOH, EtOH, 70 °C; $K_3Fe(CN)_6$, $NaHCO_3$, 5 °C to rt, 40 min, 39%.*

to set the quaternary center. The two fragments **1.48** and **1.49** were joined by a Sonogashira coupling. Indole alkyne **1.50** was then elaborated to cyclization precursor **1.51**. Intramolecular

Mitsunobu gave the 11-membered ring **1.52**. The aldehyde and amine protecting groups were removed followed by formation of the aspidosperma core as a single isomer through a Mannich-type reaction. Pentacycle **1.53** then underwent one pot 1,2 reduction and N1 reductive methylation. Saponification and oxidative lactone formation completed the synthesis of (−)-aspidophytine (**1.55**).

In 2005, Boger reported the synthesis of (−)-vindoline (**1.9**) and its enantiomer using a tandem intramolecular [4+2]/[3+2] cycloaddition cascade (Scheme 1.6).[47] Indole **1.56** was prepared from N-methyl-6-methoxytryptamine by treatment with CDI and methyl oxalylhydrazide and subsequent dehydration. EDCI coupling of indole **1.56** and isomerically pure (Z)-**1.57** provided cyclization precursor **1.58**. A cyclization cascade consisting of an intramolecular inverse electron Diels-Alder of the oxadiazole and enol ether followed by a 1,3 dipolar cycloaddition with the indole gives the pentacyclic core **1.59** as single diastereomer. This cascade forms 3 rings, 4 C-C bonds, and 6 stereocenters. The two enantiomers were

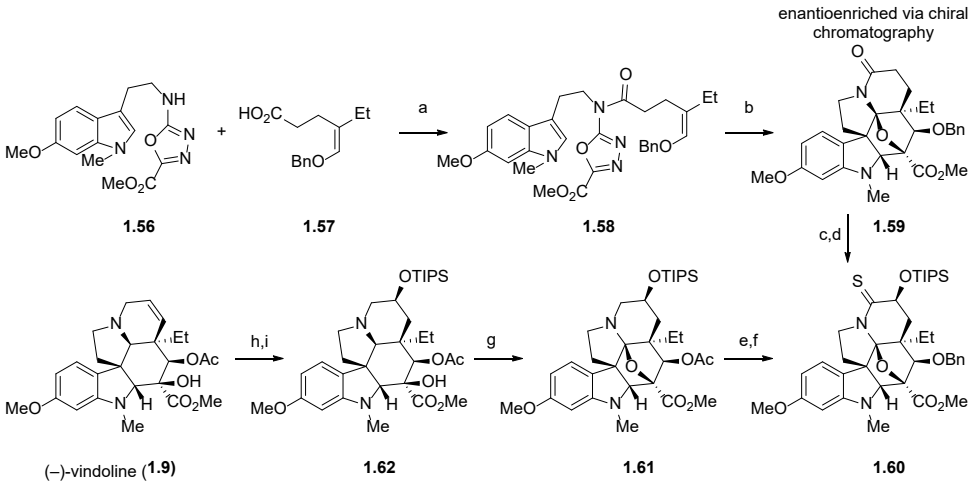

Scheme 1.6 *Boger's synthesis of (−)-vindoline. Reagents and conditions: a) EDCI, DMAP, CH_2Cl_2, 96%; b) triisopropylbenzene, 230 °C, 53%; c) LDA, $(TMSO)_2$, TIPSOTf, THF, −40 °C to RT, 64%; d) Lawesson reagent, toluene, 110 °C, 70%; e) Raney-Ni, THF, 91%; f) Ac_2O, NaOAc, 97%; g) H_2, Pt, MeOH, EtOAc, 98%; h) Bu_4NF, THF, 89%; i) Ph_3P, DEAD, THF, 75%.*

then separated using semipreparative chiral chromatography. Using enantiomerically enriched amide **1.59**, α-hydroxylation and quenching with TIPSOTf followed by conversion to the

thioamine using Lawesson's reagent gave thioamide **1.60**. Reductive desulfurization and benzyl deprotection with Raney Ni and subsequent acetylation of the free alcohol gave acetate **1.61**. Hydrogenation led to reductive ether cleavage and iminium reduction to give pentacycle **1.62**. Alcohol deprotection followed by activation using Mitsunobu conditions led to elimination furnishing (−)-vindoline (**1.9**). They later extended the [4+2]/[3+2] cycloaddition cascade to an asymmetric synthesis of alkaloid **1.9**[48] and to a synthesis of (−)-deoxoapodine (**1.4**)[49] among other members of the *Aspidosperma* family.

The Zhang group reported an enantioselective synthesis of (−)-vindorosine (**1.73**) in 2017 relying on a novel Heathcock[50]/aza-Prins sequence to form the core C and E rings (Scheme 1.7).[51] They began the synthesis with the vinylogous Mannich reaction of chiral sulfinyl imine **1.63** and ethyldioxinone **1.64** in 83% yield of the desired diastereomer and an overall d.r. of 7.6:1. Adduct **1.65** was then elaborated over four steps to the substrate for the key

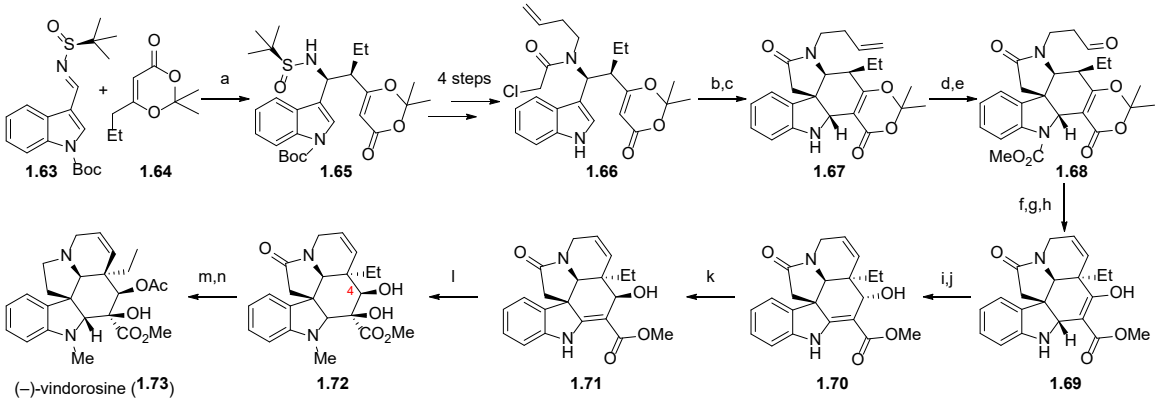

Scheme 1.7 *Zhang's synthesis of (−)-vindorosine. Reagents and conditions: a) LiHMDS, BF_3-Et_2O, THF, −78 °C, 83%; b) NaI, acetone, Δ; c) AgOTf, THF, RT, 83% over 2 steps; d) $ClCO_2Me$, $NaCO_3$, CH_2Cl_2, 96%; e) OsO_4, $NaIO_4$, THF, H_2O,* 94%; f) DBU, THF, 91%; g) $SOCl_2$, pyridine, *70 °C, 72%; h) NaOMe, MeOH, 83%; i) $CeCl_3$-$7H_2O$, O_2, iPrOH, 85%; j) $CeCl_3$-$7H_2O$,* $NaBH_4$, MeOH, 87%; k) CBr_4, Ph_3P, toluene, *80 °C; then THF, H_2O, $NaHCO_3$, 81%; l) mCPBA, CH_2Cl_2, MeOH; then HCHO, $NaBH_3CN$, 60%; m) Ac_2O, pyridine, DMAP, 99%; n) MeOTf, CH_2Cl_2, dtbpy, $NaBH_4$, MeOH, 94%.*

Heathcock/aza-Prins cyclization. Treatment of chloride **1.66** with Finkelstein conditions to form the iodide followed by silver triflate led to formation of the E ring lactam followed by aza-Prins cyclization to generate the C ring. Amine protection and oxidative alkene cleavage led to

aldehyde **1.68**. The D ring was then formed by intramolecular aldol followed by dehydration and formation of the methyl ester **1.69**. Unexpected oxidation with $CeCl_3$-$7H_2O$, and subsequent Luche reduction gave alcohol **1.70** as a single diastereomer, albeit with the wrong stereochemistry. Inversion of the stereocenter was accomplished by treatment with triphenylphosphine in carbon tetrabromide followed by aqueous sodium bicarbonate. One-pot oxidation and reductive amination with formaldehyde and sodium cyanoborohydride gave diol **1.72**. The synthesis of (−)-vindorosine (**1.73**) was achieved by acetylation of the C4 alcohol followed by selective amide reduction.

The first reported aspidosperma-aspidosperma type bisindole alkaloid synthesis was Fukuyama's synthesis of (−)-conophylline (**1.12**) in 2011[52]. The dimer features a C15′-C8 Csp^2-Csp^3 bond and a C16′-O-C7 ether linkage to form the dihydrofuran ring between the two monomeric units.[24] The synthesis of the aspidosperma core and key dimerization is shown in Scheme 1.8. Indole **1.75** was synthesized in 17 steps from commercially available phenol **1.74**. Dinitrobenzensulfonamide **1.76**, prepared in 8 steps from 2-pentenal[18h], was coupled with indole **1.75** using Mitsunobu conditions. Boc deprotection and hydration of enol ether **1.77** by TFA led to lactol **1.78**. The aspidosperma core was then formed by an intramolecular Michael addition/Mannich reaction cascade after the removal of the DNs group. Further manipulations resulted in N-oxide **1.82** for the southern portion of the dimer. Alkaloid **1.83** for the northern portion was prepared in a similar manner. For the key coupling reaction, N-oxide **1.82** was treated with TFAA to form an iminium using Polonovski-Potier-type conditions in the presence of alkaloid **1.83**. This led to the desired dimer **1.84** formed as a single isomer. Palladium catalyzed removal of the allyl group and spontaneous ring closure followed by global deprotection using LDA resulted in the completion of the synthesis of (−)-conophylline (**1.12**).

In 2020, the Andrade group reported the semi-synthesis of (−)-melodinine K (**1.13**) using the same dimerization strategy with monomers derived from (−)-tabersonine (**1.3**) isolated from *Voacanga africana* seeds.[53]

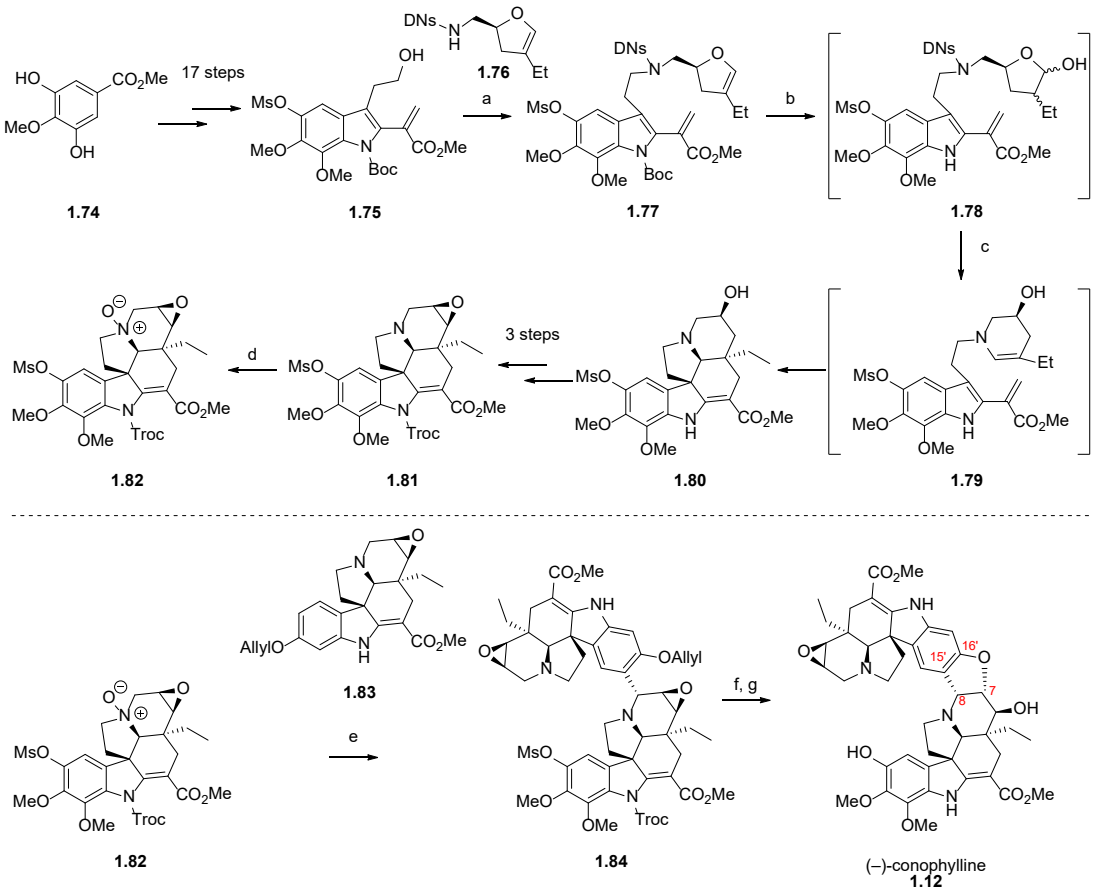

Scheme 1.8 *Key steps in Fukuyama's synthesis of (−)-conophylline. Reagents and conditions: a) PPh_3, DEAD, benzene, 0 °C→RT, 76 %; b) TFA, Me_2S, CH_2Cl_2, RT; c) pyrrolidine, MeOH/CH_3CN (5:1), 0→60 °C, 65 % (2 steps); d) mCPBA, CH_2Cl_2, 0 °C; e) TFAA, CH_2Cl_2, 0 °C→RT, 50 % (2 steps); f) [$Pd(PPh_3)_4$], pyrrolidine, CH_2Cl_2, RT, 76 %; g) LDA, THF, −78→0 °C, 72 %.*

In 2012, our group reported the synthesis of the dimeric (+)-dideepoxytabernaebovine (**1.91**)[7], a reduced form of the natural product (+)-tabernaebovine (**1.11**)[22]. Both dimers exhibit a C2-C15′ Csp^3-Csp^2 linkage between the monomer units. The key steps are shown in Scheme 1.9. N-methyl indole **1.85** was prepared in six steps from N-nosyl tryptamine using a (−)-pseudoephenamine auxiliary to introduce the C5 stereochemistry. Electrophilic amide activation

with triflic anhydride resulted in diiminium ion **1.86**. The diiminium could be reduced using sodium cyanoborohydride followed by hydrogenation to give (−)-N-methylaspidospermidine

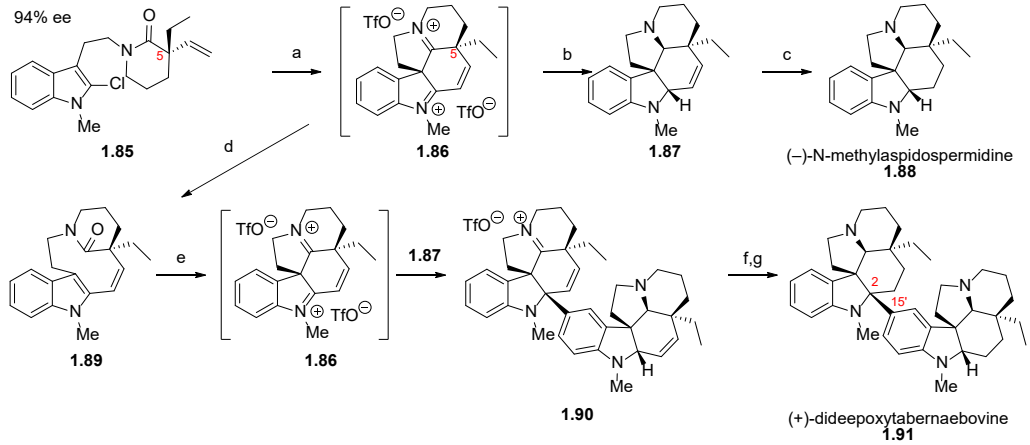

Scheme 1.9 *Key steps in Movassaghi's synthesis of (+)-dideepoxytabernaebovine and (−)-N-methylaspidospermidine. Reagents and conditions: a) Tf_2O, 3-cyanopyridine, MeCN, 85 °C; b) $NaBH_3CN$, THF, 50%; c) H_2, Pt/C, THF, 100%; d) trifluoroacetic acid, sodium trifluoroacetate, H_2O, 70 °C, 57%; e) Tf_2O, 2-ClPyr, MeCN, 23 °C; (−)-**1.87**(1.0 equiv), 85 °C, 80%; f) Red-Al, 0 °C,76%; g) H_2, Pt/C, THF, 84%.*

(**1.88**). Alternatively, heating in aqueous acid led to a Grob fragmentation to give lactam **1.89**. Electrophilic activation of lactam **1.89** followed by treatment with pentacycle **1.87** and heating led to the formation of dimeric iminium triflate **1.90**. Iminium reduction and hydrogenation gave (+)-dideepoxytabernaebovine (**1.91**). This demonstrated different connectivity than the previously reported Fukuyama report.

In 2014, our group reported a second synthesis of a bisindole aspidosperma-aspidosperma type alkaloid (Scheme 1.10).[8] (−)-methylenebismehranine (**1.14**) is a methylene bridged dimer connected at both the C15 and C15′ of two (−)-mehranine (**1.2**) monomers[22]. Amino acid **1.92** was prepared in nine steps from 2-iodoaniline using a (+)-pseudoephenamine chiral auxiliary to give the C5 stereochemistry. A lactamization followed by ring closing metathesis gave lactam **1.93**. Activation of the lactam with triflic anhydride followed by diiminium reduction using sodium trimethoxyborohydride gave the aspidosperma core with excellent diastereoselectivity (d.r. > 20:1). The pentacycle **1.94** was further elaborated to (−)-mehranine (**1.2**) by PMB

deprotection, N-formylation, epoxidation, and selective reduction of the N-formyl group. The dimerization of (−)-mehranine (**1.2**) was accomplished by using bis(4-methylpiperazin-1-yl)methane (**1.95**) as a formaldehyde equivalent. The dimerization proceeded by a Mannich reaction followed by ionization using scandium triflate and trapping with a second equivalent of (−)-mehranine (**1.2**) to give (−)-methylenebismehranine (**1.14**).

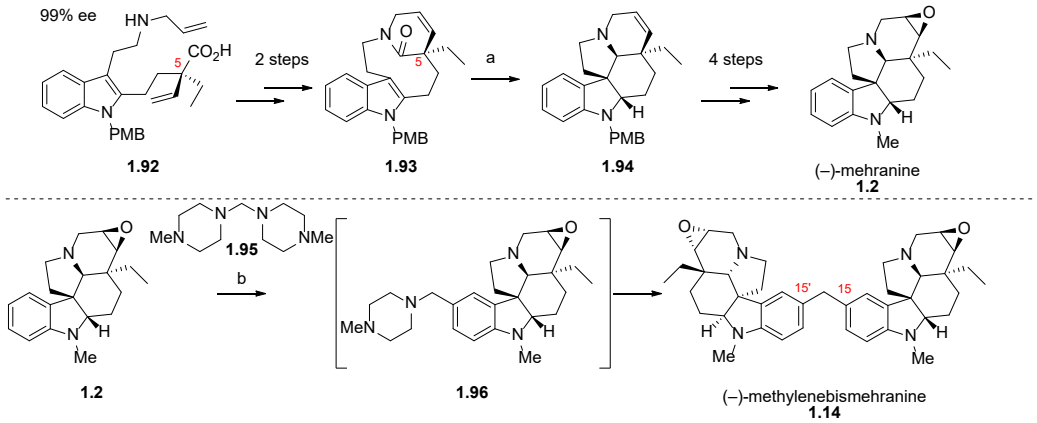

Scheme 1.10 *Key steps in Movassaghi's synthesis of (−)-mehranine and (−)-methylenebismehranine. Reagents and conditions: a) Tf_2O, n-Bu_3SnH, MeCN, −40→23°C; then $NaHB(OMe)_3$, THF, 0→23 °C, 89%; b) $Sc(OTf)_3$, MeCN, 23 °C, 49 %.*

Conclusion

The *Aspidosperma* alkaloids have a long history of scientific interest. With over 60 years of studies on their synthesis, biosynthetic origins, and bioactivity, there has been considerable progress in understanding this highly diverse family of monoterpenoid indole alkaloids. There have been a number of elegant and innovative syntheses of monomeric members of the family; however, there are limited reports of the bisindole members. The relatively underexplored area of synthesis with respect to bisindole *Aspidosperma* alkaloids coupled with promising bioactivities makes the more complex dimeric compounds attractive targets for further synthetic investigation. There are numerous opportunities for innovation and the development of new synthetic strategies.

References

1. (a) Cordell, G. A. The Aspidosperma Alkaloids. In *The Alkaloids: Chemistry and Physiology*; Manske, R. H. F., Rodrigo, R. G. A., Eds.; Academic Press: New York, 1979; Vol. 17, pp 199−384. (b) Saxton, J. E. Alkaloids of the Aspidospermine Group. In *The Alkaloids: Chemistry and Biology*; Cordell, G. A., Ed.; Academic Press: San Diego, 1998; Vol. 51, pp 1−197.

2. Biemann, K.; Friedmann-Spiteller, M.; Spiteller, G. An Investigation by Mass Spectrometry of the Alkaloids of Aspidosperm Quebracho-Blanco. *Tetrahedron Lett.* **1961**, *14*, 485–492.

3. Hart, M. J.; Glicksman, M.; Liu, M.; Sharma, M. K.; Cuny, G.; Galvan, V. Development of a high-throughput screen targeting caspase-8-mediated cleavage of the amyloid precursor protein. *Analytical Biochemistry* **2012**, *421*, 467–476.

4. Lim, K.-H. Hiraku, O.; Komiyama, K.; Kam, T.-S. Jerantinines A–G, Cytotoxic Aspidosperma Alkaloids from Tabernaemontana corymbosa. *J. Nat. Prod.* **2008**, *71*, 1591–1594.

5. For reviews on syntheses of *Aspidosperma* alkaloids: (a) Saxton, J. E. Synthesis of the Aspidosperma Alkaloids. In *The Alkaloids: Chemistry and Biology*; Cordell, G. A., Ed.; Academic Press: San Diego, 1998; Vol. 50, pp 343−376. (b) Saya, J. M.; Ruijter, E.; Orru, R. V. A. Total Synthesis of *Aspidosperma* and *Strychnos* Alkaloids through Indole Dearomatization. *Chem. Eur. J.* **2019**, 25, 8916–8935. (c) Zhao, S.; Sirasani, G.; Andrade, R. B. *Aspidosperma* and *Strychnos* alkaloids: Chemistry and biology. In *The Alkaloids: Chemistry and Biology*; Knölker, H.-J., Ed.; Academic Press: San Diego, 2021; Vol. 86, pp 1−143 and references cited therein.

6. (a) Stork, G.; Dolfini, J. E. The Total Synthesis of *dl*-Aspidospermine and of *dl*-Quebrachamine. *J. Am. Chem. Soc.* **1963**, *85*, 2872–2873. (b) Overman, L. E.; Sworin, M.; Bass, L. S.; Clardy, J. Synthesis Applications of Aza-Cope Rearrangements: A Stereoselective Synthesis of 9α-Arylhydrolilolidines [and A New Approach to the Synthesis of *Aspidosperma*] Alkaloids. *Tetrahedron* **1981**, *37*, 4041–4045. (c) Gallagher, T.; Magnus, P.; Huffman, J. Indole-2,3-quinodimethan Route to *Aspidosperma* Alkaloids: Synthesis of *dl*-Aspidospermidine. *J. Am. Chem. Soc.* **1982**, *104*, 1140–1141. (d) Kozmin, S. A.; Iwama, T.; Huang, Y.; Rawal, V. H. An Efficient Approach to *Aspidosperma* Alkaloids via [4 + 2] Cycloadditions of Aminosiloxydienes: Stereocontrolled Total Synthesis of (±)-Tabersonine. Gram-Scale Catalytic Asymmetric Syntheses of (+)-Tabersonine and (+)-16-Methoxytabersonine. Asymmetric Syntheses of (+)-Aspidospermidine and (−)-Quebrachamine. *J. Am. Chem. Soc.* **2002**, *124*, 4628–4641. (e) Wilkie, G. D.; Elliott, G. I.; Blagg, B. S. J.; Wolkenberg, S. E.; Soenen, D. R.; Miller, M. M.; Pollack, S.; Boger, D. L. Intramolecular Diels−Alder and Tandem Intramolecular Diels−Alder/1,3-Dipolar Cycloaddition Reactions of 1,3,4-Oxadiazoles. *J. Am. Chem. Soc.* **2002**, *124*, 11292–11294. (f) Jones, S. B.; Simmons, B.; Mastracchio, A.; Macmillan, D. W. C. Collective Synthesis of Natural Products by Means of Organocascade Catalysis. *Nature* **2011**, *475,* 183–188. (g) McMurray, L.; Beck, E. M.; Gaunt, M. J. Chemical

Synthesis of Aspidosperma Alkaloids Inspired by the Reverse of the Biosynthesis of the Rhazinilam Family of Natural Products. *Angew. Chem. Int. Ed.* **2012**, *51*, 9288–9291. (h) Mizoguchi, H.; Oikawa, H.; Oguri, H. Biogenetically Inspired Synthesis and Skeletal Diversification of Indole Alkaloids. *Nat. Chem.* **2014**, *6*, 57–64. (i) Tan, P. W.; Seayad, J.; Dixon, D. J. Expeditious and Divergent Total Syntheses of Aspidosperma Alkaloids Exploiting Iridium(I)-Catalyzed Generation of Reactive Enamine Intermediates. *Angew. Chem. Int. Ed.* **2016**, *55*, 13436–13440. (j) Pritchett, B.P.; Donckele, E. J.; Stoltz, B. M. Enantioselective Catalysis Coupled with Stereodivergent Cyclization Strategies Enables Rapid Syntheses of (+)-Limaspermidine and (+)-Kopsihainanine A. *Angew. Chem. Int. Ed.* **2017**, *56*, 12624–12627. (k) Wang, N.; Du, S.; Li, D.; Jiang, X. Divergent Asymmetric Total Synthesis of (+)-Vincadifformine, (−)-Quebrachamine, (+)-Aspidospermidine, (−)-Aspidospermine, (−)-Pyrifolidine, and Related Natural Products. *Org. Lett*. **2017**, *19*, 3167−3170. (l) Pandey, G.; Khamrai, J.; Mishra, A.; Maity, P.; Chikkade, P. K. Iminium ion-enamine cascade reaction enables the asymmetric total syntheses of aspidosperma alkaloids vincadifformine and ervinceine. *Tetrahedron* **2018**, *74*, 6317−6327. (m) Reuß, F.; Heretsch, P. Synthesis of Aspidodispermine via Pericyclic Framework Reconstruction. *Org. Lett*. **2020**, *22*, 3956−3959. (n) Martin, G.; Angyal, P.; Egyed, O.; Varga, S.; Soós, T. Total Syntheses of Dihydroindole *Aspidosperma* Alkaloids: Reductive Interrupted Fischer Indolization Followed by Redox Diversification. *Org. Lett*. **2020**, *22*, 4675−4679.

7. Medley, J. W.; Movassaghi, M. A Concise and Versatile Double-Cyclization Strategy for the Highly Stereoselective Synthesis and Arylative Dimerization of Aspidosperma Alkaloids. *Angew. Chem. Int. Ed*. **2012**, *51*, 4572–4576.

8. Mewald, M.; Medley, J. W.; Movassaghi, M. Concise and Enantioselective Total Synthesis of (–)-Mehranine, (–)-Methylenebismehranine, and Related *Aspidosperma* Alkaloids. *Angew. Chem. Int. Ed.* **2014**, *53*, 11634–11639.

9. White, K. L.; Movassaghi, M. Concise Total Syntheses of (+)-Haplocidine and (+)-Haplocine via Late-Stage Oxidation of (+)-Fendleridine Derivatives. *J. Am. Chem. Soc*. **2016**, *138*, 11383–11389.

10. Kang, T.; White, K. L.; Mann, T. J.; Hoveyda, A. H.; Movassaghi, M. Enantioselective Total Synthesis of (−)-Deoxoapodine. *Angew. Chem. Int. Ed*. **2017**, *56*, 13857.

11. Antropow, A. H.; Garcia, N. R.; White, K.; Movassaghi, M. Enantioselective Synthesis of (−)-Vallesine: Late-Stage C17-Oxidation via Complex Indole Boronation. *Org. Lett.* **2018**, *20*, 3647–3650.

12. Myeong, I.-S., Avci, N. H.; Movassaghi, M. Total Synthesis of (−)-Kopsifoline A and (+)-Kopsifoline. *Org. Lett*. **2021**, *23*, 9118–9122.

13. (a) Saxton, J. E. Gorman, A. A.; Hesse, M.; Schmid, H. Bisindole Alkaloids. In *The Alkaloids*, Saxton, J. E. Ed. The Royal Society of Chemistry, 1971, vol. 1, pp 200−338. (b)

Cordell, G. A.; Saxton, J. E. Bisindole Alkaloids. In *The Alkaloids*. Academic Press, 1981, vol 20, pp 1–295. (c) Kam, T.-S.; Choo,Y. -M. Bisindole Alkaloids. In *The Alkaloids: Chemistry and Biology*; Cordell, G. A., Ed.; Academic Press, 2006; Vol. 63, pp 181−337. (d) Kitajima, M.; Takayama, H. Monoterpenoid Bisindole Alkaloids. In *The Alkaloids: Chemistry and Biology*; Knölker, H.-J. Ed.; Academic Press, 2016; Vol. 76, pp 259−310.

14. (a) Noble, R. L.; Beer, C. T.; Cutts, J. H. Role of Chance Observations in Chemotherapy: *Vinca Rosea*. *Ann. N.Y. Acad. Sci.* **1958**, *76*, 882–894. (b) Svoboda, G. H.; Neuss, N.; Gorman, M. Alkaloids of *Vinca Rosea* Linn (*Catharanthus Roseus* G. Don.) V. Preparation and Characterization of Alkaloids. *J. Am. Pharm. Assoc.* **1959**, *48*, 659–666.

15. (a) Silvestri, R. New Prospects for Vinblastine Analogues as Anticancer Agents. *J. Med. Chem.* **2013**, *56*, 625–627. (b) Martino, E.; Casamassima, G.; Castiglione, S.; Cellupica, E.; Pantalone, S.; Papagni, F.; Rui, M.; Siciliano, A. M.; Collina, S. Vinca alkaloids and analogues as anti-cancer agents: Looking back, peering ahead. *Bioorganic & medicinal chemistry letters,* **2018**, *28*, 2816–2826. (c) Dhyani, P.; Quispe, C.; Sharma, E.; Bahukhandi, A.; Sati, P.; Attri, D. C.; Szopa, A.; Sharifi-Rad, J.; Docea, A. O.; Mardare, I.; Calina, D.; Cho, W. C. Anticancer potential of alkaloids: a key emphasis to colchicine, vinblastine, vincristine, vindesine, vinorelbine and vincamine. *Cancer Cell Int.* **2022**, 22, 206.

16. a) Verma, P.; Mathur, A. K.; Srivastava, A.; Mathur, A. Emerging trends in research on spatial and temporal organization of terpenoid indole alkaloid pathway in *Catharanthus roseus*: a literature update. *Protoplasma* **2012**, *249*, 255–268. (b) Salim, V. Towards Complete Elucidation of Monoterpene Indole Alkaloid Biosynthesis Pathway: *Catharanthus Roseus* as a Pioneer System. *Advances in botanical research.* **2013**, *68*, 1–37. (c) de Bernonville, T. D.; Clastre, M.; Besseau, S.; Oudin, A.; Burlat, V.; Glévarec, G.; Lanoue, A.; Papon, N.; Giglioli-Guivarc'h, N.; St-Pierre, B.; Courdavault, V. Phytochemical genomics of the Madagascar periwinkle: Unravelling the last twists of the alkaloid engine. *Phytochemistry*, **2015**, *113*, 9–23. (d) Almagro, L.; Fernández-Pérez, F.; Pedreño, M. A. Indole Alkaloids from *Catharanthus roseus*: Bioproduction and Their Effect on Human Health. *Molecules*, **2015**, *20*, 2973–3000. (e) Liu, Y.; Patra, B.; Singh, S. K.; Paul, P.; Zhou, Y.; Li, Y.; Wang, Y.; Pattanaik, S.; Yuan, L. Terpenoid indole alkaloid biosynthesis in *Catharanthus roseus*: effects and prospects of environmental factors in metabolic engineering. *Biotechnol Lett.* **2021**, *43*, 2085–2103.

17. (a) Potier, P. Synthesis of the Antitumor Dimeric Indole Alkaloids From Catharanthus Species (Vinblastine Group) *J. Nat. Prod.* **1980**, *43*, 72– 86. (b) Kuehne, M. E.; Markó, I. Syntheses of Vinblastine-Type Alkaloids. In *The Alkaloids: Chemistry and Pharmacology.* Brossi, A.; Suffness, M., Eds. Academic Press. **1990**, *37*, 77–131. (c) Sears, J. E.; Boger, D. L. Total Synthesis of Vinblastine, Related Natural Products, and Key Analogues and Development of Inspired Methodology Suitable for the Systematic Study of Their Structure–Function Properties. *Accounts of chemical research* **2015**, *48*, 653–662.

18. (a) Kutney, J. P.; Choi, L. S. L.; Nakano, J.; Tsukamoto, H.; McHugh, M.; Boulet, C. A. A Highly Efficient and Commercially Important Synthesis of the Antitumor Catharanthus Alkaloids Vinblastine and Leurosidine from Catharanthine and Vindoline. *Heterocycles* **1988**, *27*, 1845–1853. (b) Magnus, P.; Stamford, A.; Ladlow, M. Synthesis of the Antitumor Bisindole Alkaloid Vinblastine: Diastereoselectivity and Solvent Effect on the Stereochemistry of the Crucial C-15–C-18' Bond. *J. Am. Chem. Soc.* **1990**, *112*, 8210–8212. (c) Kuehne, M. E.; Matson, P. A.; Bornmann, W. G. Enantioselective Syntheses of Vinblastine, Leurosidine, Vincovaline, and 20'-*epi*-Vincovaline. *J. Org. Chem.* **1991**, *56*, 513–528. (d) Magnus, P.; Mendoza, J. S.; Stamford, A.; Ladlow, M.; Willis, P. Nonoxidative Coupling Methodology for the Synthesis of the Antitumor Bisindole Alkaloid Vinblastine and a Lower-Half Analogue: Solvent Effect on the Stereochemistry of the Crucial C-15/C-18' Bond. *J. Am. Chem. Soc.* **1992**, *114*, 10232–10245. (e) Yokoshima, S.; Ueda, T.; Kobayashi, S.; Sato, A.; Kuboyama, T.; Tokuyama, H.; Fukuyama, T. Total Synthesis of (+)-Vinblastine. *Tennen Yuki Kagobutsu Toronkai Koen Yoshishu* **2001**, *43*, 163–168. (f) Yokoshima, S.; Ueda, T.; Kobayashi, S.; Sato, A.; Kuboyama, T.; Tokuyama, H.; Fukuyama, T. Stereocontrolled Total Synthesis of (+)-Vinblastine. *Pure & Appl. Chem.* **2003**, *75*, 29–38. (g) Schneider, C. First De Novo Synthesis of the Bisindole Alkaloid Vinblastine. *Angew. Chem. Int. Ed.* **2002**, *41*, 4217–4219. (h) Yokoshima, S.; Ueda, T.; Kobayashi, S.; Sato, A.; Kuboyama, T.; Tokuyama, H.; Fukuyama, T. Stereocontrolled Total Synthesis of (+)-Vinblastine. *J. Am. Chem. Soc.* **2002**, *124*, 2137–2139. i) Kuboyama, T.; Yokoshima, S.; Tokuyama, H.; Fukuyama, T. Stereocontrolled total synthesis of (–)-vincristine. *Proc. Natl. Acad. Sci. USA* **2004**, *101*, 11966–11970. (j) Miyazaki, T.; Yokoshima, S.; Simizu, S.; Osada, H.; Tokuyama, H.; Fukuyama, T. Synthesis of (+)-Vinblastine and Its Analogues. *Org. Lett.* **2007**, *9*, 4737–4740. (k) Ishikawa, H.; Colby, D. A.; Boger, D. L. Direct Coupling of Catharanthine and Vindoline to Provide Vinblastine: Total Synthesis of (+)- and *ent*-(–)-Vinblastine. *J. Am. Chem. Soc.* **2008**, *130*, 420–421. (l) Ishikawa, H.; Colby, D. A.; Seto, S.; Va, P.; Tam, A.; Kakei, H.; Rayl, T. J.; Hwang, I.; Boger, D. L. Total Synthesis of Vinblastine, Vincristine, Related Natural Products, and Key Structural Analogues. *J. Am. Chem. Soc.* **2009**, *131*, 4904–4916.

19. Kam, T.-S.; Anuradha, S. Alkaloids from *Tabernaemontana Divaricate*. *Phytochemistry* **1995**, *40*, 313–316.

20. Janot, M.-M.; Pourrat, H., Le Men, J. Tabersonine. alkaloid extract from the seeds of *Amsonia tabernaemontana* (Apocynacees). *Bull. Soc. Chim. Fr*. **1954**, 707-708

21. a) Iglesias, R.; Diatta, L. Deoxoapodine, a new alkaloid of Tabernaemontana species. *Rev. CENIC Cienc. Fis*. **1975**, *6*, 135; b) Bui, A.-M.; Das, B. C.; Potier, P. Étude chimiotaxonomique de *Hazunta modesta. Phytochemistry* **1980**, *19*, 1473.

22. Lien, T. P.; Kamperdick, C.; Sung, T. V.; Adam, G. Ripperger, H. Bis-indole alkaloids from *Tabernaemontana bovina. Phytochemistry* **1998**, *49*, 1797−1799.

23. Feng, T.; Li, Y.; Wang, Y.-Y.; Cai, X.-H.; Liu, Y.-P.; Luo, X.-D. Cytotoxic Indole Alkaloids from *Melodinus tenuicaudatus*. J. Na. Prod. 2010, 73, 1075−1079.

24. (a) Kam, T.-S.; Loh, K.-Y.; Lim, L.-H.; Loong, W.-L., Chuah, C.-H.; Wei, C. New alkaloids from the leaves of *Tabernaemontana divaricate. Tetrahedron Lett.* **1992**, *33*, 969. (b) Kam, T.-S.; Loh, K.-Y.; Wei, C. Conophylline and Conophyllidine: New Dimeric Alkaloids from *Tabernaemontana divaricate*. *J. Nat. Prod*. **1993**, *56*, 1865−1871.

25. Kitajima, M.; Iwai, M.; Kogure, N.; Kikura-Hanajiri, R.; Goda, Y.; Takayama, H. Aspidosperma–aspidosperma-type bisindole alkaloids from *Voacanga africana. Tetrahedron* **2013**, 69, 796-801.

26. Govindachari, T. R.; Sandhya, G.; Chandrasekharan, S.; Rajagopalan, K. Voacinol: a New Bisindole Alkaloid from Voacanga Grandifoh (Miq) Rolfe. *J. Chem. Soc., Chem. Commun.* **1987**, 1137–1138.

27. Umezawa, K.; Kojima, I.; Simizu, S.; Lin, Y.; Fukatsu, H.; Koide, N.; Nakade, Y.; Yoneda, M. Therapeutic activity of plant-derived alkaloid conophylline on metabolic syndrome and neurodegenerative disease models. *Human Cell* **2018**, *31*, 95–101

28. (a) Irie, T.; Kubushiro, K.; Suzuki, K.; Tsukazaki, K.; Umezawa, K.; Nozawa, S. Inhibition of Attachment and Chemotactic Invasion of Uterine Endometrial Cancer Cells by a New Vinca Alkaloid, Conophylline. *Anticancer Res.* **1999**, *19*, 3061–3066. (b) Atsumi, S.; Nagasawa, A.; Koyano, T.; Kowithayakornd, T.; Umezawa, K. Supression of TGF- Signaling by Conophylline via Upregulation of c-Jun Expression. *Cell. Mol. Life Sci.* **2003**, *60*, 2516–2525. (c) Irie, T. Antitumor Effects of Conophylline on Uterine Endometrial Cancer. *Keio Igaku* **2005**, *82*, 313–324. (d) Ogata, T.; Li, L.; Yamada, S.; Yamamoto, Y.; Tanaka, Y.; Takei, I.; Umezawa, K.; Kojima, I. Promotion of □-Cell Differentiation by Conophylline in Fetal and Neonatal Rat Pancreas. *Diabetes* **2004**, *53*, 2596–2602. (e) Kojima, I.; Umezawa, K. Conophylline: A Novel Differentiation Inducer for Pancreatic □ Cells. *Int. J. Biochem & Cell Biology* **2006**, *38*, 923–930. (f) Roche, E.; Jones, J.; Arribas, M. I.; Leon-Quinto, T.; Soria, B. Role of Small Bioorganic Molecules in Stem Cell Differentiation to Insulin-Producing Cells. *Bioorg. Med. Chem.* **2006**, *14*, 6466–6474. (g) Kitamura, R.-I.; Ogata, T.; Tanaka, Y.; Motoyoshi, K.; Seno, M.; Takei, I.; Umezawa, K.; Kojima, I. Conophylline and Betacellulin-δ4: an Effective Combination of Differentiation Factors for Pancreatic β Cells. *Endocrine J.* **2007**, *54*, 255–264. (h) Hisanaga, E.; Park, K.-Y.; Yamada, S.; Hashimoto, H.; Takeuchi, T.; Mori, M.; Seno, M.; Umezawa, K.; Takei, I.; Kojima, I. A Simple Method to Induce Differentiation of Murine Bone Marrow Mesenchymal Cells to Insulin-Producing Cells Using Conophylline and Betacellulin-δ4. *Endocrin J.* **2008**, *55*, 535–543.

29. DeMars, M. D.; O'Connor, S. E. Evolution and diversification of carboxylesterase-like [4+2] cyclases in aspidosperma and iboga alkaloid biosynthesis. *Proc. Natl. Acad. Sci. USA* 2024, 121, e2318586121–e2318586121.

30. O'Connor, S. E.; Maresh, J. J. Chemistry and biology of monoterpene indole alkaloid biosynthesis. *Nat. Prod. Rep*. **2006**, *23*, 532–547.

31. Facchini, P. J.; Huber-Allanach, K. L.; Tari, L. W. Plant aromatic L-amino acid decarboxylases: evolution, biochemistry, regulation, and metabolic engineering applications. Phytochemistry 2000, 54, 121–138.

32. (a) Zenk, M. H.; Stöckigt, J.; Strictosidine (Isovincoside): the Key Intermediate in the Biosynthesis of Monoterpenoid Indole Alkaloids. *J. Chem. Soc., Chem. Commun*. **1977**, 646–648. (b) Kutchan, T. M. Strictosidine: From alkaloid to enzyme to gene. *Phytochemistry* **1993**, *32*, 493–506.

33. Geerlings, A.; Ibañez, M. M.-L.; Memelink, J.; van der Heijden, R.; Verpoorte, R. Molecular Cloning and Analysis of Strictosidine β-d-Glucosidase, an Enzyme in Terpenoid Indole Alkaloid Biosynthesis in *Catharanthus roseus. J. Biol. Chem.* **2000**, *275*, 3051–3056.

34. Qu, Y.; Easson, M. E. A. M.; Simionescu, R.; Hajicek, J.; Thamm, A. M. K.; Salim, V.; de Luca, V. Solution of the multistep pathway for assembly of corynanthean, strychnos, iboga, and aspidosperma monoterpenoid indole alkaloids from 19E-geissoschizine. *Proc. Natl. Acad. Sci*. **2018**, *115*, 3180–3185.

35. Tatsis, E. C.; Carqueijeiro, I.; de Bernonville, T. D.; Frank, J.; Dang, T.-T. T.; Oudin, A.; Lanoue, A.; Lafontaine, F.; Stavrinides, A. K.; Clastre, M.; Courdavault, V.; O'Connor, S. E. A three enzyme system to generate the *Strychnos* alkaloid scaffold from a central biosynthetic intermediate. *Nat. Commun*. **2017**, *8*, 316.

36. Scott, A. I.; Qureshi, A. A. Biogenesis of Strychnos, Aspidosperma, and Iboga Alkaloids. The Structure and Reactions of Preakuammicine. *J. Am. Chem. Soc*. **1969**, *91*, 5874–5876.

37. Caputi, L.; Franke, J.; Farrow, S. C.; Chung, K.; Payne, R. M. E.; Nguyen, T.-D.; Dang, T.-T. T.; Carqueijeiro, I. S. T.; Koudounas, K.; Bernonville, T. D.; Ameyaw, B.; Jones, D. M.; Vieira, I. J. C.; Courdavault, V.; O'Connor, S. E. Missing enzymes in the biosynthesis of the anticancer drug vinblastine in Madagascar periwinkle. *Science*, **2018**, *360*, 1235–1239.

38. Qureshi, A. A.; Scott, A. I. Interconversion of *Corynanthe*, *aspidosperma*, and *Iboga* alkaloids. A model for indole alkaloid biosynthesis. *Chem. Commun. (London)* **1968**, 945–946.

39. Caputi, L.; Frank, J.; Bussey, K.; Farrow, S. C.; Vieira, I. J. C.; Stevenson, C. E. M.; Lawson. D. M. O'Connor, S. E. Structural basis of cycloaddition in biosynthesis of iboga and aspidosperma alkaloids. *Nat. Chem. Bio*. **2020**, *16*, 383–386.

40. Overman, L. E.; Robertson, G. M.; Robichaud, A. J. Use of aza-Cope rearrangement-Mannich cyclization reactions to achieve a general entry to *Melodinus* and *Aspidosperma*

alkaloids. Stereocontrolled total syntheses of (±)-deoxoapodine, (±)-meloscine, and (±)-epimeloscine and a formal synthesis of (±)-1-acetylaspidoalbidine. *J. Am. Chem. Soc.* **1991,** *113*, 2598–2610.

41. Overman, L. E.; Sworin, M.; Burk, R. M. Synthesis applications of aza-Cope rearrangements. Part 10. A new approach for the total synthesis of pentacyclic Aspidosperma alkaloids. Total synthesis of dl-16-methoxytabersonine *J. Org. Chem*. **1983**, *48*, 2685.

42. Node, M.; Nagasawa, H.; Fuji, K. Expeditious enantioselective syntheses of indole alkaloids of *Aspidosperma*- and *Hunteria*-type. *J. Am. Chem. Soc.* **1987**, *109*, 7901–7903.

43. Fuji, K.; Node, M.; Nagasawa, H.; Naniwa, Y.; Terada, S. Asymmetric induction via addition-elimination process: nitroolefination of .alpha.-substituted lactones. *J. Am. Chem. Soc*. **1986**, *108*, 3855–3856.

44. Harley-Mason, J.; Kaplan, M. A simple total synthesis of (±)-aspidospermidine. *Chem. Commun*. **1967**, 915.

45. Sumi, S.; Matsumoto, K.; Tokuyama, H.; Fukuyama, T. Enantioselective Total Synthesis of Aspidophytine. *Org. Lett.* **2003**, *5*, 1891–1893.

46. He, F.; Bo, Y.; Altom, J. D.; Corey E. J. Enantioselective Total Synthesis of Aspidophytine. *J. Am. Chem. Soc.* **1999,** *121*, 6771–6772.

47. Choi, Y.; Ishikawa, H.; Velcicky, J.; Elliot, G. I.; Miller, M. M.; Boger, D. L. Total Synthesis of (−)- and *ent*-(+)-Vindoline. *Org. Lett.* **2005**, *7*, 4539–4542.

48. Sasaki, Y.; Kato, D.; Boger, D. L. Asymmetric Total Synthesis of Vindorosine, Vindoline, and Key Vinblastine Analogues. *J. Am. Chem. Soc*. **2010**, *132*, 13533–13544.

49. Lee, K.; Boger, D. L. Total Syntheses of (−)-Kopsifoline D and (−)-Deoxoapodine: Divergent Total Synthesis via Late-Stage Key Strategic Bond Formation. *J. Am. Chem. Soc*. **2014**, *136*, 3312–3317.

50. Toczko, M. A.; Heathcock, C. H. Total Synthesis of (±)-Aspidospermidine. *J. Org. Chem*. **2000**, *65*, 2642–2645.

51. Chen, W.; Yang, X.-D.; Tan, W.-Y.; Zhang, X.-Y.; Liao, X.-L.; Zhang, H. Total Synthesis of (−)-Vindorosine. *Angew. Chem. Int. Ed*. **2017**, *56*, 12327–12331.

52. Han-ya, Y.; Tokuyama, H.; Fukuyama, T. Total Synthesis of (−)-Conophylline and (−)-Conophyllidine. *Angew. Chem. Int. Ed.* **2011**, *50*, 4884–4887.

53. Walia, M.; Teijaro, C. N.; Gardner, A.; Tran, T.; Kang, J.; Zhao, S.; O'Connor, S. E.; Courdavault, V.; Andrade, R. B. Synthesis of (−)-Melodinine K: A Case Study of Efficiency in Natural Product Synthesis. *J. Nat. Prod.* **2020**, *83*, 2425-2433.

Chapter II

Total Synthesis of (–)-Voacinol, (–)-Voacandimine C, and the related congener, (−)-methylenebisdeoxoapodine

Portions of this work have been adapted from the following articles that were co-written by the author and are reproduced in part with permission from:

Flynn, K. M.; Myeong, I.-S.; Pinto, T.; Movassaghi, M. Total Synthesis of (−)-Voacinol and (−)-Voacandimine C. *J. Am. Chem. Soc.* **2022***,* 144, 9126–9131.

Chapter II was done in collaboration with Dr. Kristen M. Flynn and Dr. In-Soo Myeong.

- Dr. Kristen M. Flynn developed and executed the synthesis of (–)-voacinol and (–)-voacandimine C.
- Dr. In-Soo Myeong contributed to the initial exploration of (–)-methylenebisdeoxoapodine.

Introduction

The aspidosperma alkaloids are a structurally diverse family of monoterpene indole alkaloids with a characteristic pentacyclic skeleton (Figure 2.1; rings A–E) containing multiple stereogenic centers and varying levels of oxidation.[1] Their complex molecular structures and biological activities have attracted significant interest and has prompted the development of innovative syntheses.[2,3,4] The bisindole alkaloid (–)-voacinol (**2.1**), first isolated from *Voacanga grandifolia* in 1987 (Figure 2.1),[5] is a member of a distinct set of aspidosperma alkaloids with a methylene bridge connecting two aspidosperma units.[1] Alkaloid **2.1** was isolated again in 2013 along with the structurally related (–)-voacandimine C (**2.2**) from *Voacanga africana*.[6] Despite advancements in the total synthesis of related bisindole alkaloids,[4] there are no reported syntheses of D-ring-methylene–adjoined aspidosperma alkaloids. Alkaloids **2.1** and **2.2** have significant structural similarities with (–)-deoxoapodine (**2.4**),[7] a hexacyclic alkaloid isolated from *Tabernae armeniaca* in 1975, exhibiting a C2-vinylogous urethane along with C21-oxygenation.[1] Inspired by our observations concerning the reactivity of a transiently formed D-ring iminium ion[8] *en route* to (–)-deoxoapodine (**2.4**),[9] we hypothesized that alkaloids **2.1** and **2.2** may be biogenetically accessed from a (–)-deoxoapodine (**2.4**) derivative. Given prior isolation of natural alkaloids comprised of simpler aspidosperma alkaloids adjoined by a

methylene, such as (–)-methylenebismehranine (**2.6**),[10,11] we posited that (–)-methylenebisdeoxoapodine (**2.3**) may be of interest as a congener of alkaloids **2.1** and **2.2**. In this chapter, I describe our efforts concerning the first total synthesis of (–)-voacinol (**2.1**) and (–)-voacandimine C (**2.2**) by leveraging the reactivity of a D-ring oxidized variant of (–)-deoxoapodine (**2.4**). Our final-stage diversification of a versatile dodecacyclic intermediate, inspired by consideration of a plausible unified biosynthetic hypothesis, provides both natural alkaloids (–)-**2.1** and (–)-**2.2**, in addition to (–)-methylenebisdeoxoapodine (**2.3**).

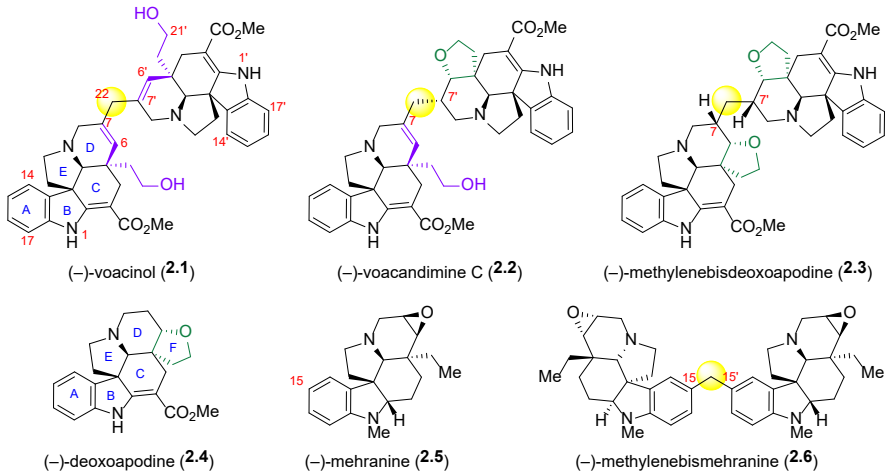

Figure 2.1 *Structures of (–)-voacinol (2.1), (–)-voacandimine C (2.2), (–)-methylenebisdeoxoapodine (2.3), and related aspidosperma alkaloids.*

Results and Discussion

Our retrosynthetic analysis for (–)-voacinol (**2.1**) and (–)-voacandimine C (**2.2**) is illustrated in Scheme 1. We envisioned accessing alkaloids (–)-**2.1** and (–)-**2.2** through a common symmetrical intermediate **2.7**. We hypothesized that opening of the two oxolane substructures of dodecacyclic bisenamine **2.7** and subsequent C8/C8' reduction of the corresponding unsaturated iminium ions would provide (–)-voacinol (**2.1**, Scheme 2.1). Furthermore, we speculated that the unsymmetrical, bisindole alkaloid (–)-voacandimine C (**2.2**) could be accessed through desymmetrization of dodecacycle **2.7** via reductive opening of a single oxolane substructure. We anticipated that electrophilic activation of one ethereal oxygen

of intermediate **2.7** may allow for generation of the corresponding unsaturated iminium ion, that upon subsequent C8- and C8'-reduction, would give (–)-voacandimine C (**2.2**). We hypothesized that bisenamine **2.7** could be accessed through an initial C7-methylenation of enamine **2.8**, yielding an unsaturated iminium ion, followed by nucleophilic addition of a second equivalent of enamine **2.8**. Enamine **2.8** could be obtained from N9-oxide alcohol **2.9** through a biogenesis-inspired dehydrative etherification.[8] We envisioned accessing the pentacyclic N-oxide **2.9** via chemoselective oxidation of vinylogous urethane (–)-**2.10**, an advanced intermediate used in our synthesis of kopsifolines A and E.[12]

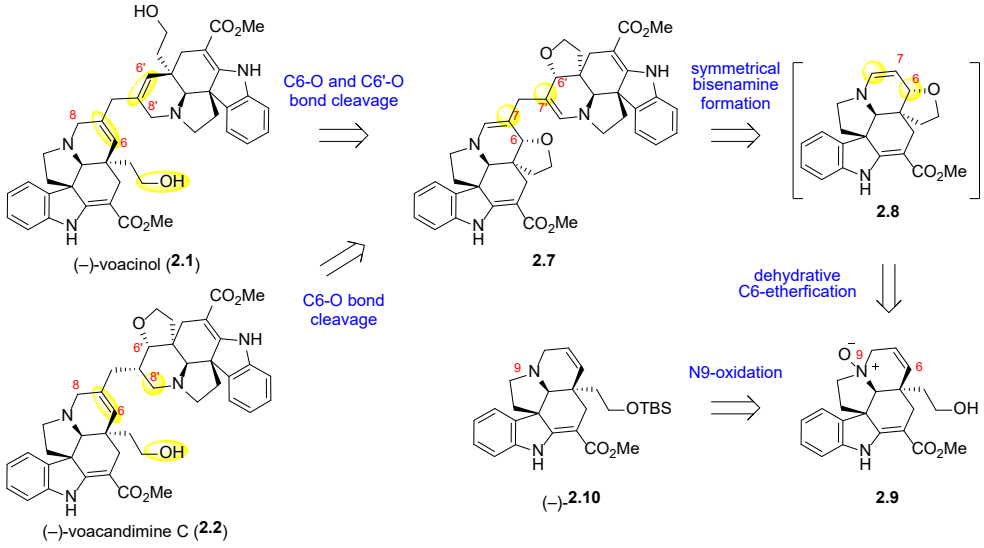

Scheme 2.1 *Retrosynthetic analysis of (–)-voacinol (2.1) and (–)-voacandimine C (2.2).*

Dr. Flynn developed our synthetic route to the key hexacyclic enamine **2.8** starting with derivatization of vinylogous urethane (–)-**2.10** (Scheme 2.2), a C21-oxygenated variant of tabersonine[13] that we have previously prepared in enantiomerically enriched form from a readily available indole derivative (Scheme 2.2).[8,11,12,14] The alkylation of **2.19** with **2.15** through the hydrolysis of the amino acid (Scheme 2.2 step h, k, and l) were performed in collaboration with Dr. Myeong and Dr. Flynn. The enzymatic resolutions were performed by Dr. Myeong and

myself (Scheme 2.2 steps p and q). We found that treatment of vinylogous urethane (–)-**2.10** (90% ee) with peracetic acid (1.3 equiv)[8,15] provided the desired N9-oxidation (70%) while minimizing a competitive C3-oxidation. Subsequent unveiling of the primary alcohol afforded the N-oxide alcohol **2.9** in 96% yield (Scheme 2.3). Exposure of N-oxide **2.9** to modified Polonovski–Potier reaction conditions[8] involving trifluoroacetic anhydride (4.0 equiv)

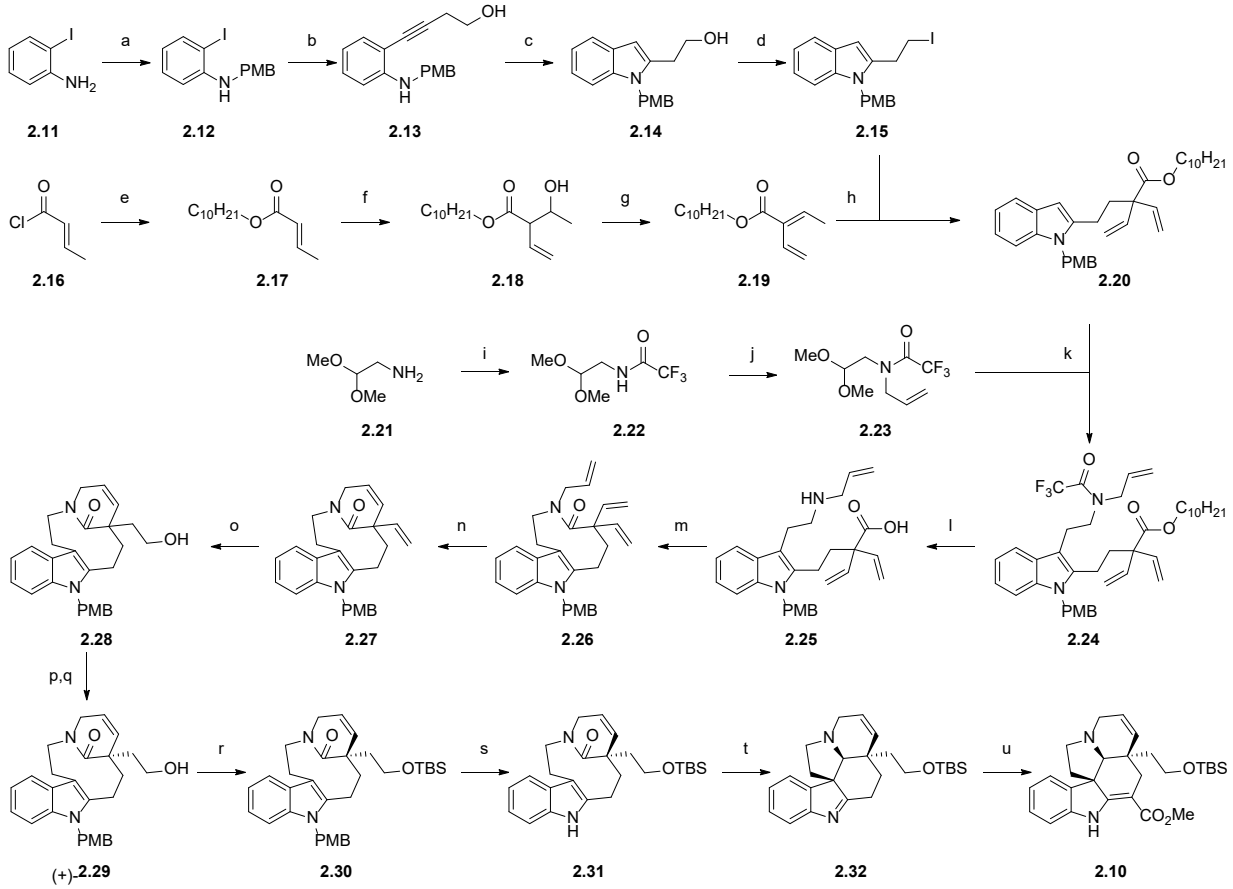

Scheme 2.2 *Synthesis of vinylogous urethane (−)-2.10. Reagents and conditions: a) 4-methoxybenzaldehyde, AcOH, MeOH, 0 °C; $NaCNBH_3$, 94%; b) 3-butyn-1-ol, $(PH_3P)_2PdCl_2$, CuI, Et_3N, 45 °C; c) CuI, DMF, 140 °C, 88% over 2 steps; d) Ph_3P, I_2, imidazole, THF; e) 1-decanol, Et_3N, DMAP, CH_2Cl_2, 91%; f) LDA, DMPU, acetaldehyde, THF, −78 °C, 79%; g) $MeSO_2Cl$, Et_3N, CH_2Cl_2, 98%; h) LDA, DMPU, THF, −78 °C, 53%; i) TFAA, Et_3N, THF; j) NaH, allyl bromide, DMF, 95% over 2 steps; k) TFA, Et_3SiH, CH_2Cl_2, 89%; l) NaOH, MeOH, H_2O, 100 °C, 92%; m) Ph_3P, I_2, DIPEA, CH_2Cl_2, 64%; n) Hoyveda-Grubbs 2nd generation, 1,2-dichloroethane, 80 °C, 80%; o) $Pd(OAc)_2$, 1,4-benzoquinone, perchloric acid, H_2O, acetonitrile, toluene; $NaBH_4$, 83%; p) Amano PS lipase, vinyl acetate, CH_2Cl_2, t-BuOMe, up to >99% ee (−)-2.29; q) lipase from Candida rugosa, Et_3N, H_2O, CH_2Cl_2, t-BuOMe, up to 95% ee (+)-2.29; r) TBSCl, imidazole, DMAP, DMF, 81%; s) Na, NH_3, THF, −78 °C, 85%; t) DIBAL, THF, 0 °C; u) n-BuLi, methyl cyanoformate, THF, −78 °C, 70% over 2 steps.*

and polystyrene-bound 2-*tert*-butylimino-2-diethylamino-1,3-dimethyl-perhydro-1,3,2-diazaphosphorine (PS-BEMP, 6.0 equiv) led to formation of the corresponding unsaturated C8-

iminium ion, which upon methanolysis of the primary trifluoroacetate gave the desired F-ring and offered the hexacyclic enamine **2.8** (Scheme 2.3). Given the sensitivity of enamine **2.8** toward isolation, we considered its conversion to the corresponding α-aminonitrile as a more stable surrogate.[16] Exposure of enamine **2.8** to *in situ* generated hydrogen cyanide in hexafluoroisopropanol afforded the C8-aminonitrile **2.34** (*ca*. 10:1 C8-epimers) in 79% yield over two steps (Scheme 2.3).

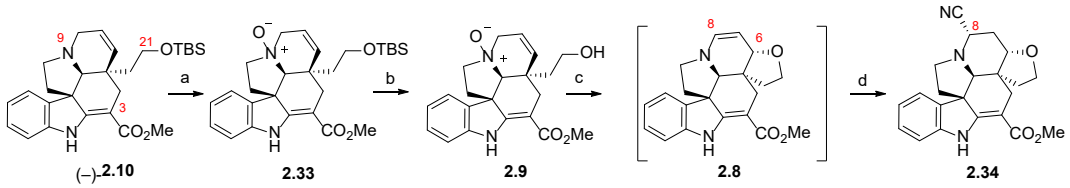

Scheme 2.3 *Dr. Kristen Flynn's synthetic route to hexacyclic aminonitrile 2.34. Reagents and conditions: (a) AcO_2H (32 wt. %) in dilute AcOH, K_2CO_3, CH_2Cl_2, 0 °C, 70%; (b) 20% TFA, CH_2Cl_2; 20% Et_3N, MeOH, 23 °C, 96%. (c) TFAA, PS-BEMP, CH_2Cl_2, 23 °C; PS-BEMP, MeOH, 23 °C; (d) TMSCN, H_2O, HFIP, 0→23 °C, 79% over two steps, 10:1 dr of C8-epimers, major diastereomer shown.*

Dr. Flynn's observations regarding the reactivity and superior stability of aminonitrile **2.34** compared to enamine **2.8** compelled us to consider a bisaminonitrile variant of bisenamine **2.7** *en route* to alkaloids **2.1** and **2.2**. We envisioned accessing the dodecacyclic bisaminonitrile **2.36** (Scheme 2.4) through activation of aminonitrile **2.15** in the presence of an electrophilic methylene reagent. Treatment of aminonitrile **2.15** with zinc (II) trifluoromethanesulfonate (1.0 equiv) in the presence of Eschenmoser's salt (0.50 equiv) led to generation of the conjugated iminium ion **2.35.** Interception of the iminium ion **2.35** by a second equivalent of enamine **2.8** led to the formation of the dodecacyclic bisaminonitrile **2.36** over 3 h in 73% yield with high stereoselectivity for the desired (C7*S*,C7'*S*)-diastereomer (C7*S*,C7'*S*-**2.36**:C7S,C7'*R*-**2.36**, *ca.* 9:1,

major epimer shown in Scheme 2.4). This strategy proved highly effective for introduction of the C7,C7'-methylene and securing four new stereogenic centers in dodecacycle **2.36**.

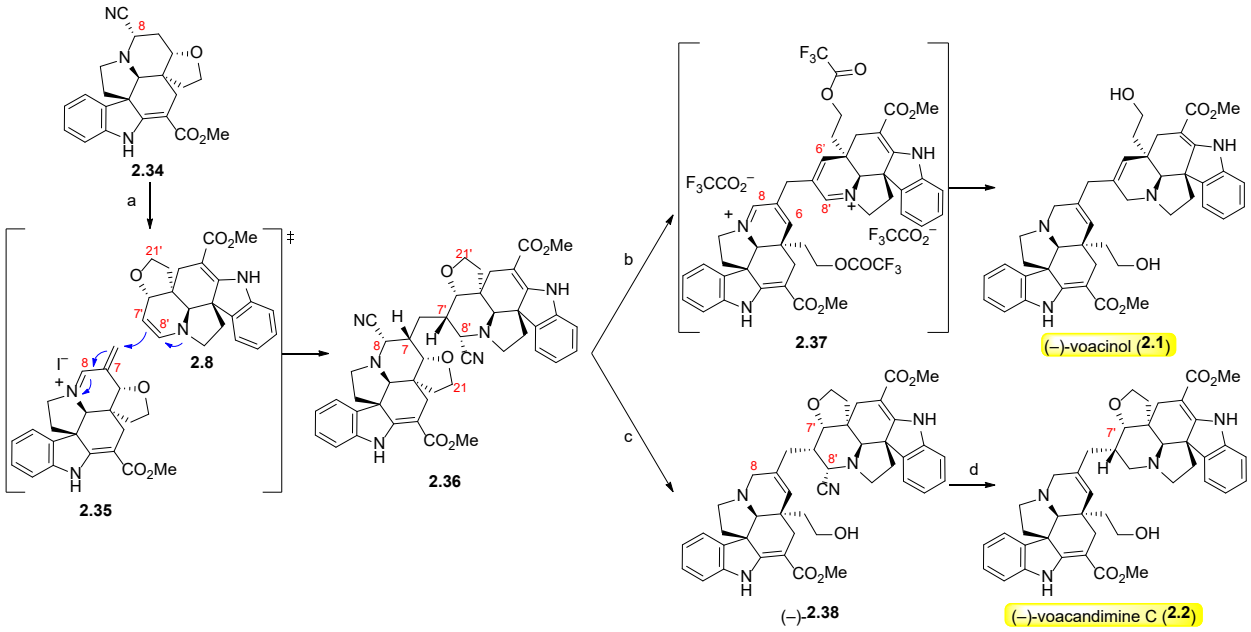

Scheme 2.4 *Dr. Kristen Flynn's synthesis of (–)-voacinol and (–)-voacandimine C. Reagents and conditions: (a) $Zn(OTf)_2$, Eschenmoser's salt, TFE, 1,2-dichloroethane, 23 °C, 73%, 9:1 dr of C7' epimers, major shown; (b) TFAA, $Zn(OTf)_2$, DTBMP, CH_2Cl_2, 23 °C; $NaBH_4$, 0→23 °C then Et_3N, MeOH, 95% over two steps; (c) TFAA, CH_2Cl_2, 23 °C; $NaBH_4$, 0→23 °C then Et_3N, MeOH, 23% over two steps; (d) $Zn(OTf)_2$, $NaBH(OAc)_3$, CH_2Cl_2, 23 °C, 63%.*

Dr. Flynn demonstrated the versatility of bisaminonitrile **2.36** by accessing (–)-voacinol (**2.1**) and (–)-voacandimine C (**2.2**) illustrated in Scheme 2.4. Addition of zinc (II) trifluoromethanesulfonate (1.0 equiv) and 2,6-di-*tert*-butyl-4-methylpyridine (DTBMP, 2.0 equiv) to bisaminonitrile **2.36** led to opening of both oxolane rings in the presence of trifluoroacetic anhydride (10 equiv), likely via C8- and C8'-enamines, to give bisiminium ion **2.37**. In-situ reduction of bisiminium ion **2.37** with sodium borohydride (20 equiv) followed by methanolysis of the trifluoroacetates provided (–)-voacinol (**2.1**) in 95% yield (2 steps, Scheme 2.4). All spectroscopic data for our synthetic (–)-voacinol (**2.1**) were consistent with literature data.[5] Treatment of bisaminonitrile **2.36** with excess trifluoroacetic anhydride (15 equiv), in the absence of other additives, favors activation of a single aminonitrile, leading to a single oxolane

ring-opening, likely due to preference for formation of a monocationic intermediate. Exposure of the resulting iminium ion to sodium borohydride (30 equiv) led to C8-reduction, which upon methanolysis afforded allylic amine (–)-**2.38** as a *single* diastereomer in 23% yield with the majority of the mass balance as recovered (C7*S*,C7'*S*)-**2.36** starting material (57%) along with (–)-voacinol (**2.1**) in 10% yield as a minor component. Under optimal conditions, treatment of (C7'*S*)-aminonitrile (–)-**2.38** with $Zn(OTf)_2$ (1.0 equiv) and sodium triacetoxyborohydride (20 equiv) provided (–)-voacandimine C (**2.2**) as a single diastereomer in 63% yield (Scheme 2.3). All spectroscopic data for our synthetic (–)-voacandimine C (**2.2**) were consistent with literature reports.[6]

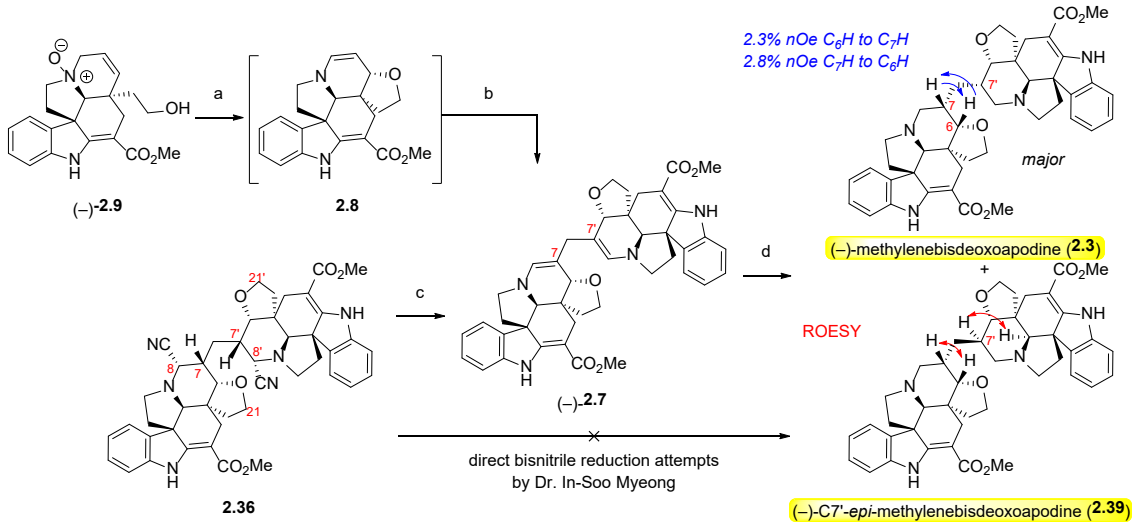

Scheme 2.5 *Synthesis of (−)-methylenebisdeoxoapodine. Reagents and conditions: (a) TFAA, PS-BEMP, CH_2Cl_2, 23 °C; PS-BEMP, MeOH, 23 °C; (b) Eschenmoser's salt, TFE, 1,2-dichloroethane, 23 °C, ~30% over two steps; (c) $AgBF_4$, DTBMP, THF, 23 °C, 73%; (d) AcOH, $NaBH(OAc)_3$, CH_2Cl_2, 23 °C, 91%, 1.75:1 dr of C7'-epimers.*

In addition to the studies described above using dodecacycle **2.36** as the key intermediate in the synthesis of (–)-voacinol (**2.1**) and (–)-voacandimine C (**2.2**), Dr. Myeong and I also pursued the synthesis of the corresponding dodecacyclic bisenamine **2.7,** our proposed key methylene bridged intermediate in our retrosynthetic analysis (Scheme 2.1). In order to study the reactivity of bisenamine **2.7**, I independently prepared N-oxide (−)-**2.9** and bisnitrile **2.36** from

the beginning of our synthetic route as shown above by following our reported procedures (Schemes 2.2−2.4) My initial attempts to access bisenamine **2.7** involved treatment of a solution of crude enamine **2.8** (filtration to remove the PS-BEMP followed by concentration) with Eschenmoser's salt (0.5 equiv) to afford C7/C7'-methylene-dodecacycle **2.7** in ~30% yield from pentacycle **2.9** (Scheme 2.5). The capricious formation of bisenamine **2.7** directly from enamine **2.8** prompted the examination of an alternative route to bisenamine **2.7**. Treatment of bisaminonitrile **2.36** with silver tetrafluoroborate (1.5 equiv) and DTBMP (3.0 equiv) provided the bisenamine (–)-**2.7** in 73% yield (Scheme 2.5). Notably, the C7,C7'-methylene substitution of bisenamine (–)-**2.7** provides greater stability toward isolation as compared to the hexacyclic enamine **2.8**. Dr. Flynn was able to use this approach to access bisenamine **2.7** in order to evaluate its potential utility in accessing the alkaloids based on our original retrosynthetic analysis.

To complete the series of 0, 1, and 2 oxolane rings in the methylene bridged dodecacycles, I pursed the synthesis of **2.3**. Initial attempts by Dr. Myeong to reduce **2.36** directly were unsuccessful, often leading to decomposition and complex mixtures of partial reduction products. However, exposure of bisenamine (–)-**2.7** to acetic acid (15 equiv) followed by addition of sodium triacetoxyborohydride (15 equiv) proceeded smoothly and afforded (–)-methylenebisdeoxoapodine (**2.3**) along with the corresponding minor C7'-epimer in 91% yield (C7*S*,C7'*S*-**2.3**: C7*S*,C7'*R*-**2.39**, *ca*. 1.75:1). The formation of the (–)-(C7'*S*)-methylenebisdeoxoapodine (**2.3**) as the major product is consistent with protonation of bisenamine (–)-**2.7** occurring from the less hindered *si*-face of the C8- and C8'-enamines, leading to the diastereomer calculated[17] to be more stable.

Conclusion

In summary, we have reported the first total synthesis of bisindole alkaloids (–)-voacinol (**2.1**) and (–)-voacandimine C (**2.2**). Late-stage diversification of a common dodecacyclic intermediate, accessed via C7-methylenation of a D-ring oxidized variant of (–)-deoxoapodine (**2.4**), formed the basis of our approach to these alkaloids inspired by a plausible unified biosynthetic lineage. Our concise and stereocontrolled synthesis of (–)-voacinol (**2.1**) and (–)-voacandimine C (**2.2**) from pentacycle **2.10**[12] was achieved in seven and eight steps, respectively. This approach provided the first synthetic samples of bisindole alkaloids (–)-**2.1** and (–)-**2.2**, along with the corresponding derivative of interest, (–)-methylenebisdeoxoapodine (**2.3**), for detailed structural analysis and characterization.[18]

References

1. (a) Cordell, G. A. The Aspidosperma Alkaloids. In *The Alkaloids: Chemistry and Physiology*; Manske, R. H. F., Rodrigo, R. G. A., Eds.; Academic Press: New York, 1979; Vol. 17, pp 199−384. (b) Saxton, J. E. Alkaloids of the Aspidospermine Group. In *The Alkaloids: Chemistry and Biology*; Cordell, G. A., Ed.; Academic Press: San Diego, 1998; Vol. 51, pp 1−197.

2. For reviews of syntheses see: (a) Saxton, J. E. Synthesis of the Aspidosperma Alkaloids. In *The Alkaloids: Chemistry and Biology*; Cordell, G. A., Ed.; Academic Press: San Diego, 1998; Vol. 50, pp 343−376. (b) Saya, J. M.; Ruijter, E.; Orru, R. V. A. Total Synthesis of *Aspidosperma* and *Strychnos* Alkaloids through Indole Dearomatization. *Chem. Eur. J.* **2019**, 25, 8916–8935. (c) Zhao, S.; Sirasani, G.; Andrade, R. B. *Aspidosperma* and *Strychnos* alkaloids: Chemistry and biology. In *The Alkaloids: Chemistry and Biology*; Knölker, H.-J., Ed.; Academic Press: San Diego, 2021; Vol. 86, pp 1−143 and references cited therein.

3. (a) Stork, G.; Dolfini, J. E. The Total Synthesis of *dl*-Aspidospermine and of *dl*-Quebrachamine. *J. Am. Chem. Soc.* **1963**, *85*, 2872–2873. (b) Overman, L. E.; Sworin, M.; Bass, L. S.; Clardy, J. Synthesis Applications of Aza-Cope Rearrangements: A Stereoselective Synthesis of 9α-Arylhydrolilolidines [and A New Approach to the Synthesis of *Aspidosperma*] Alkaloids. *Tetrahedron* **1981**, *37*, 4041–4045. (c) Gallagher, T.; Magnus, P.; Huffman, J. Indole-2,3-quinodimethan Route to *Aspidosperma* Alkaloids: Synthesis of *dl*-Aspidospermidine. *J. Am. Chem. Soc.* **1982**, *104*, 1140–1141. (d) Kozmin, S. A.; Iwama, T.; Huang, Y.; Rawal, V. H. An Efficient Approach to *Aspidosperma* Alkaloids via [4 + 2] Cycloadditions of Aminosiloxydienes: Stereocontrolled Total Synthesis of (±)-Tabersonine.

Gram-Scale Catalytic Asymmetric Syntheses of (+)-Tabersonine and (+)-16-Methoxytabersonine. Asymmetric Syntheses of (+)-Aspidospermidine and (−)-Quebrachamine. *J. Am. Chem. Soc.* **2002**, *124*, 4628–4641. (e) Wilkie, G. D.; Elliott, G. I.; Blagg, B. S. J.; Wolkenberg, S. E.; Soenen, D. R.; Miller, M. M.; Pollack, S.; Boger, D. L. Intramolecular Diels−Alder and Tandem Intramolecular Diels−Alder/1,3-Dipolar Cycloaddition Reactions of 1,3,4-Oxadiazoles. *J. Am. Chem. Soc.* **2002**, *124*, 11292–11294. (f) Jones, S. B.; Simmons, B.; Mastracchio, A.; Macmillan, D. W. C. Collective Synthesis of Natural Products by Means of Organocascade Catalysis. *Nature* **2011**, *475,* 183–188. (g) McMurray, L.; Beck, E. M.; Gaunt, M. J. Chemical Synthesis of Aspidosperma Alkaloids Inspired by the Reverse of the Biosynthesis of the Rhazinilam Family of Natural Products. *Angew. Chem. Int. Ed.* **2012**, *51*, 9288–9291. (h) Mizoguchi, H.; Oikawa, H.; Oguri, H. Biogenetically Inspired Synthesis and Skeletal Diversification of Indole Alkaloids. *Nat. Chem.* **2014**, *6*, 57–64. (i) Tan, P. W.; Seayad, J.; Dixon, D. J. Expeditious and Divergent Total Syntheses of Aspidosperma Alkaloids Exploiting Iridium(I)-Catalyzed Generation of Reactive Enamine Intermediates. *Angew. Chem. Int. Ed.* **2016**, *55*, 13436–13440. (j) Pritchett, B.P.; Donckele, E. J.; Stoltz, B. M. Enantioselective Catalysis Coupled with Stereodivergent Cyclization Strategies Enables Rapid Syntheses of (+)-Limaspermidine and (+)-Kopsihainanine A. *Angew. Chem. Int. Ed.* **2017**, *56*, 12624–12627. (k) Wang, N.; Du, S.; Li, D.; Jiang, X. Divergent Asymmetric Total Synthesis of (+)-Vincadifformine, (−)-Quebrachamine, (+)-Aspidospermidine, (−)-Aspidospermine, (−)-Pyrifolidine, and Related Natural Products. *Org. Lett*. **2017**, *19*, 3167−3170. (l) Pandey, G.; Khamrai, J.; Mishra, A.; Maity, P.; Chikkade, P. K. Iminium ion-enamine cascade reaction enables the asymmetric total syntheses of aspidosperma alkaloids vincadifformine and ervinceine. *Tetrahedron* **2018**, *74*, 6317−6327. (m) Reuß, F.; Heretsch, P. Synthesis of Aspidodispermine via Pericyclic Framework Reconstruction. *Org. Lett*. **2020**, *22*, 3956−3959. (n) Martin, G.; Angyal, P.; Egyed, O.; Varga, S.; Soós, T. Total Syntheses of Dihydroindole *Aspidosperma* Alkaloids: Reductive Interrupted Fischer Indolization Followed by Redox Diversification. *Org. Lett*. **2020**, *22*, 4675−4679. (o) Kuboyama, T.; Yokoshima, S.; Tokuyama, H.; Fukuyama, T. Stereocontrolled Total Synthesis of (+)-Vincristine. *PNAS* **2004**, *101*, 11966–11970. Sears, J. E.; Boger, D. L. Total Synthesis of Vinblastine, Related Natural Products, and Key Analogues and Development of Inspired Methodology Suitable for the Systematic Study of Their Structure-Function Properties. *Acc. Chem. Res.* **2015**, *48*, 653–662.

4. (a) Kuboyama, T.; Yokoshima, S.; Tokuyama, H.; Fukuyama, T. Stereocontrolled Total Synthesis of (+)-Vincristine. *PNAS* **2004**, *101*, 11966–11970. (b) Sears, J. E.; Boger, D. L. Total Synthesis of Vinblastine, Related Natural Products, and Key Analogues and Development of Inspired Methodology Suitable for the Systematic Study of Their Structure-Function Properties. *Acc. Chem. Res.* **2015**, *48*, 653–662. (c) Han-ya, Y.; Tokuyama, H.; Fukuyama, T. Total Synthesis of (−)-Conophylline and (−)-Conophyllidine. *Angew. Chem. Int. Ed.* **2011**, *50*, 4884–4887. (d) Satoh, H.; Ojima, K.-I.; Ueda, H.; Tokuyama, H. Bioinspired Total Synthesis of the Dimeric Indole Alkaloid (+)-Haplophytine by Direct Coupling and Late-Stage Oxidative Rearrangment. *Angew. Chem. Int. Ed.* **2016**, *55*, 15157–15161. (e) Benayad, S.; Beniddir, M. A.; Evanno, L.; Poupon, E. Biomimetic Assembly of Leucoridine A. *Eur. J. Org. Chem*. **2015**, 1894–1898. (f) Kokkonda, P.; Brown, K. R.; Seguin,

T. J.; Wheeler, S. E.; Vaddypally, S.; Zdilla, M. J.; Andrade, R. B. Biomimetic Total Syntheses of (−)-Leucoridines A and C through the Dimerization of (−)-Dihydrovalparicine. *Angew. Chem. Int. Ed*. **2015**, *54*, 12632–12635.

5. Govindachari, T. R.; Sandhya, G.; Chandrasekharan, S.; Rajagopalan, K. Voacinol: A New Bisindole Alkaloid from *Voacanga Grandifolia*(Miq) Rolfe. *J. Chem. Soc., Chem. Commun.* **1987**, 1137–1138.

6. Kitajima, M.; Iwai, M.; Kogure, N.; Kikura-Hanajiri, R.; Goda, Y.; Takayama, H. Aspidosperma–Aspidosperma-Type Bisindole Alkaloids from *Voacanga Africana*. *Tetrahedron* **2013**, *69*, 796–801.

7. (a) Iglesias, R.; Diatta, L. Deoxoapodine, A New Alkaloid of *Tabernaemontana* Species. *Rev. CENIC Cienc. Fis.* **1975**, *6*, 135–139. (b) Bui, A.-M.; Das, B. C.; Potier, P. Étude chimiotaxonomique de *Hazunta modesta*. *Phytochemistry* **1980**, *19*, 1473–1475.

8. Kang, T.; White, K. L.; Mann, T. J.; Hoveyda, A. H.; Movassaghi, M. Enantioselective Total Synthesis of (–)-Deoxoapodine. *Angew. Chem. Int. Ed.* **2017**, *56*, 13857–13860.

9. (a) Overman, L. E.; Robertson, G. M.; Robichaud, A. J. Use of Aza-Cope Rearrangement-Mannich Cyclization Reactions To Achieve a General Entry to *Melodinus* and *Aspidosperma* Alkaloids. Stereocontrolled Total Syntheses of (±)-Deoxoapodine, (±)-Meloscine, and (±)-Epimeloscine and a Formal Synthesis of (±)-1-Acetylaspidoalbidine. *J. Am. Chem. Soc.* **1991**, *113*, 2598–2610. (b) Lee, K.; Boger, D. L. Total Syntheses of (−)-Kopsifoline D and (−)-Deoxoapodine: Divergent Total Synthesis via Late-Stage Key Strategic Bond Formation. *J. Am. Chem. Soc.* **2014**, *136*, 3312–3317. (c) Zhou, Y.; Wong, H. N. C.; Peng, X. Total Syntheses of (−)-Deoxoapodine, (−)-Kopsifoline D, and (−)-Beninine. *J. Org. Chem.* **2020**, *85*, 967–976. (d) Yoshida, K.; Okada, K.; Ueda, H.; Tokuyama, H. A Concise Enantioselective Total Synthesis of (−)-Deoxoapodine. *Angew. Chem. Int. Ed.* **2020**, *59*, 23089-23093.

10. Lien, T. P.; Kamperdick, C.; Sung, T. V.; Adam, G.; Ripperger, H. Bis-indole Alkaloids from *Tabernaemontana bovina. Phytochemistry* **1998**, *49*, 1797-1799.

11. Mewald, M.; Medley, J. W.; Movassaghi, M. Concise and Enantioselective Total Synthesis of (–)-Mehranine, (–)-Methylenebismehranine, and Related *Aspidosperma* Alkaloids. *Angew. Chem. Int. Ed.* **2014**, *53*, 11634–11639.

12. Myeong, I.-S.; Avci, N. H.; Movassaghi, M. Total Synthesis of (–)-Kopsifoline A and (+)-Kopsifoline E. *Org. Lett.* **2021**, *23*, 9118–9122.

13. Janot, M.-M.; Paourrat, H.; Le Men, J. Tabersonine. Alkaloid Extract From the Seeds of *Amsonia Tabernaemontana* (Apocynacees). *Bulletin de la Societe Chemique de France* **1954**, 707–708.

14. White, K. L.; Movassaghi, M. Concise Total Syntheses of (+)-Haplocidine and (+)-Haplocine via Late-Stage Oxidation of (+)-Fendleridine Derivatives. *J. Am. Chem. Soc.* **2016**, *138*, 11383−11389.

15. Hong, A. Y.; Vanderwal, C. D. A Sequential Cycloaddition Strategy for the Synthesis of Alsmaphorazine B Traces a Path Through a Family of *Alstonia* Alkaloids. *Tetrahedron* **2017**, *73*, 416–4171.

16. (a) Myers, A. G.; Kung, D. W. A Concise, Stereocontrolled Synthesis of (–)-Saframycin A by Directed Condensation of □-Amino Aldehyde Precursors. *J. Am. Chem. Soc.* **1999**, *121*, 10828–10829. (b) Sun, P.; Sun, C.; Weinreb, S. M. A New Total Synthesis of the Marine Tunicate Alkaloid Lepadiformine. *Org. Lett.* **2001**, *3*, 3507–3510. (c) Magnus, P.; Gazzard, L.; Hobson, L.; Payne, A. H.; Rainey, T. J.; Westlund, N.; Lynch, V. Synthesis of the Kopsia Alkaloids (±)-Pauciflorine B, (±)-Lahadinine B, (±)-Kopsidasine, (±)-Kopsidasine-N-oxide, (±)-Kopsijasminilam and (±)-11-Methoxykopsilongine. *Tetrahedron* **2002**, *58*, 3423–3443. (d) Lebold, T. P.; Wood, J. L.; Deitch, J.; Lodewyk, M. W.; Tantillo, D. J.; Sarpong, R. A Divergent Approach to the Synthesis of the Yohimbinoid Alkaloids Venenatine and Alstovenine. *Nature Chemistry* **2013**, *5*, 126–131. (e) Beatty, J. W.; Stephenson, C. R. J. Synthesis of (−)-Pseudotabersonine, (−)-Pseudovincadifformine, and (+)-Coronaridine Enabled by Photoredox Catalysis in Flow. *J. Am. Chem. Soc.* **2014**, *136*, 10270–10273. (f) Pompeo, M. M.; Cheah, J. H.; Movassaghi, M. Total Synthesis and Anti-Cancer Activity of All Known Communesin Alkaloids and Related Derivatives. *J. Am. Chem. Soc.* **2019**, *141*, 14411–14420.

17 See experimental details.

18. Flynn, K. M.; Myeong, I.-S.; Pinto, T.; Movassaghi, M. Total Synthesis of (–)-Voacinol and (–)-Voacandimine C. *ChemRxiv*, March 18, 2022, ver. 1. DOI: https://doi.org/10.26434/chemrxiv-2022-l5f5h. (accessed 2022-03-21).

Experimental Details

General Procedures. All reactions were performed in oven-dried or flame-dried round bottom flasks or other style flasks as specified. The flasks were fitted with rubber septa, and reactions were conducted under a positive argon atmosphere. Cannulae or gas-tight syringes with stainless steel needles were used to transfer air- or moisture-sensitive liquids. Flash column chromatography was performed as described by Still et al.[1] using granular silica gel (60-Å pore size, 40–63 μm, 4–6% H_2O content, Zeochem) or basic alumina (70% between 0.063–0.200 mm particle size, pH value (10% suspension): 8.5–10.5). Analytical thin layer chromatography (TLC) was performed using glass plates pre-coated with 0.25 mm 230–400 mesh silica gel impregnated with a fluorescent indicator (254 nm) or 0.21–0.27 mm basic alumina impregnated with a fluorescent indicator (254 nm). Thin layer chromatography plates were visualized by exposure to short wave ultraviolet light (254 nm) and irreversibly stained by treatment with an aqueous solution of ceric ammonium molybdate (CAM) followed by heating (~ 1 min) on a hot plate (~ 250 ºC). Organic solutions were concentrated at 29–30 °C on rotary evaporators capable of achieving a minimum pressure of ~2 torr.

Materials. Commercial reagents and solvents were used as received with the following exceptions: acetonitrile, *N*,*N*-dimethylformamide, dichloromethane, methanol, tetrahydrofuran, and triethylamine were purchased from EMD Millipore (ReCycler™) or Sigma-Aldrich (Pure-Pac™) and were purified by the method of Grubbs et al. under positive argon pressure.[2] Benzene and 1,2-dichloroethane were dried by distillation over calcium hydride under an inert dinitrogen atmosphere. Deuterated solvents used for nuclear magnetic resonance (NMR) spectroscopy were purchased from Cambridge Isotope Laboratories, Inc. and were used as received with the exception of chloroform-*d*, which was stored over granular anhydrous potassium carbonate. The molarity of peracetic acid (32 weight %) was determined by titration against triphenylphosphine (average of three titrations). 2,6-di-*tert*-butyl-4-methylpyridine was purchased from Matrix Scientific and was further purified by flash column chromatography on silica gel (eluent: hexanes); Eschenmoser's salt was purchased from Alfa Aesar and stored in the glovebox; hexafluoroisopropanol was purchased from Oakwood Products, Inc. and was stored under an argon atmosphere over activated 4 Å molecular sieves; trifluoroacetic anhydride was purchased from Sigma-Aldrich and distilled over phosphorous pentoxide under argon; silver tetrafluoroborate was purchased from Matrix Scientific and stored in the glovebox. All other solvents and chemicals were purchased from Sigma-Aldrich.

Instrumentation. Proton and carbon nuclear magnetic resonance spectra were recorded on a Bruker AVANCE NEO 500 and Bruker AVANCE 600 MHz spectrometers. Proton chemical shifts are recorded in parts per million on the δ scale and are referenced from the residual protium in the NMR solvent ($CHCl_3$: δ 7.26, C_6D_6: δ 7.16). Data are reported as follows: chemical shift [multiplicity (s = singlet, d = doublet, t = triplet, q = quartet, p = pent, s = sextet, m = multiplet, br = broad), coupling constant(s) in Hertz, integration, assignment]. Carbon chemical shifts are recorded in parts per million on the δ scale and are referenced from the carbon resonances of the

1. Still, W. C.; Kahn, M.; Mitra, A. Rapid Chromatographic Technique for Preparative Separations with Moderate Resolution. *J. Org. Chem.* **1978**, *43*, 2923–2925.
2. Pangborn, A. B.; Giardello, M. A.; Grubbs, R. H.; Rosen, R. K.; Timmers, F. Safe and Convenient Procedure for Solvent Purification. *Organometallics* **1996**, 15, 1518–1520.

solvent ($CDCl_3$: δ 77.16, C_6D_6: δ 128.06). Infrared data were obtained on a Bruker ALPHA II FTIR spectrometer equipped with a diamond ATR sampling module and are reported as follows: frequency of absorption (cm^{-1}), [intensity of absorption (s = strong, m = medium, w = weak, br = broad)]. Optical rotations were measured on a Jasco P-1010 polarimeter with a sodium lamp and are reported as follows: [α]λ T °C (c = g/100 mL, solvent). High-resolution mass spectrometric data (HRMS) were recorded on an Agilent 6510 QToF with a Dual ESI spray ionization source. Circular dichroism spectra were measured on a Jasco J-1500 spectrometer with a xenon arc lamp and are reported as follows: Δε (λ) T ºC (c = mmol/L, solvent).

Positional Numbering System. At least two numbering systems exist in the literature for the aspidosperma alkaloids.[3,4,5] For direct comparison between structures, the numbering system shown below for (–)-deoxoapodine (**2.4**), (–)-voacinol (**2.1**) and (–)-voacandimine C (**2.2**) is used throughout this report.

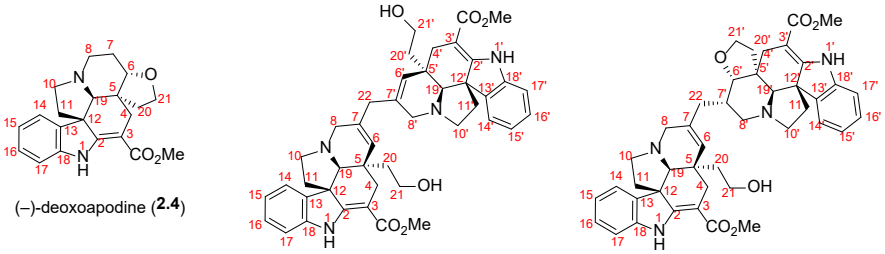

Respective Contributions The optimized procedures are reproduced from Flynn, K. M.; Myeong, I.-S.; Pinto, T.; Movassaghi, M. "Total Synthesis of (−)-Voacinol and (−)-Voacandimine C" *J. Am. Chem. Soc.* **2022***,* 144, 9126–9131.

Dr. Kristen M. Flynn characterized **2.33**, **2.9**, **2.34**, and **2.36**.
I executed the synthetic route from **2.10** to **2.3**/**2.39** using the optimized reported procedures.

---

3. (a) Yates, P.; MacLachlan, F. N.; Rae, I. D.; Rosenberger, M.; Szabo, A. G.; Willis, C. R.; Cava, M. P.; Behforouz, M.; Lakshmikantham, M. V.; Zeiger, W. Haplophytine. A Novel Type of Indole Alkaloids. *J. Am. Chem. Soc.* **1973**, *95*, 7842–7850. (b) Saxton, J. E., Alkaloids of the Aspidospermine Group. In *The Alkaloids, Chemistry and Biology*, *Vol 51* (Ed.: Cordell, G. A.), Academic Press, San Diego, **1998**, pp 1−197.
4 . Govindachari, T. R.; Sandhya, G.; Chandrasekharan, S.; Rajagopalan, K. Voacinol: A New Bisindole Alkaloid from *Voacanga Grandifolia*(Miq) Rolfe. *J. Chem. Soc., Chem. Commun.* **1987**, 1137–1138.
5. Kitajima, M.; Iwai, M.; Kogure, N.; Kikura-Hanajiri, R.; Goda, Y.; Takayama, H. Aspidosperma–Aspidosperma-Type Bisindole Alkaloids from *Voacanga Africana*. *Tetrahedron* **2013**, *69*, 796–801.

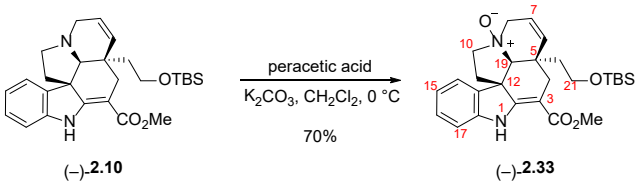

(–)-**2.10** (–)-**2.33**

***t*-Butyldimethylsilyl *N*-oxide (–)-2.33:**

Potassium carbonate (47 mg, 0.34 mmol, 1.5 equiv) was added to a solution of vinylogous urethane (–)-**2.10**[6] (110 mg, 0.22 mmol, 1 equiv) in dichloromethane (22 mL) at 0 °C. A solution of peracetic acid[7] (32 wt %, solution in dilute acetic acid, 0.67 µL, 0.29 mmol, 1.3 equiv) was added via syringe. After 20 min, a saturated aqueous sodium bicarbonate solution (10 mL) was added to the reaction mixture. The layers were separated and the aqueous layer was extracted with dichloromethane (3 × 10 mL). The combined organic layers were dried over anhydrous sodium sulfate, were filtered, and were concentrated under reduced pressure. The resulting residue was purified by flash column chromatography on silica gel (eluent: 1% → 10% methanol in dichloromethane) to give *tert*-butyldimethylsilyl *N*-oxide (–)-**2.33** (74 mg, 70%) as a yellow thin film. Structural assignments were made using additional information from gCOSY, gHSQC, and gHMBC experiments.

^{1}H NMR (600 MHz, $CDCl_3$, 25 °C): δ 9.32 (s, 1H, N1**H**), 8.78 (d, *J* = 7.8 Hz, 2H, C14**H**), 7.19 (app-t, *J* = 7.6, 1.3 Hz, 1H, C16**H**), 6.96 (app-t, *J* = 7.6, 1.1 Hz, 1H, C15**H**), 6.81 (d, *J* = 7.8, 1.0Hz, 1H, C17**H**), 5.91 (app-d, *J* = 10.7, 2.2 Hz, 1H, C6**H**), 5.71 (app-d, *J* = 10.7, 5.0, 1.9 Hz, 1 H, C7**H**), 4.35 (app-d, *J* = 17.5, 2.5 Hz, 1H, C8$\mathbf{H}_a$), 4.23 (app-d, *J* = 16.3 Hz, 1H, C8$\mathbf{H}_a$), 3.88 (s, 1H, C19**H**), 3.79 (s, 3H, $CO_2C\mathbf{H}_3$), 3.67 (app-q, *J* = 10.8, 8.5 Hz, 1H, C10$\mathbf{H}_a$), 3.59–3.52 (m, 2H, C10$\mathbf{H}_b$, C21$\mathbf{H}_a$), 3.52–3.46 (m, 1H, C21$\mathbf{H}_b$), 3.01 (app-q, *J* = 13.1, 11.1, 8.6 Hz, 1H, C11$\mathbf{H}_a$), 2.72 (app-d, *J* = 15.9, 1.2 Hz, 1H, C4$\mathbf{H}_a$), 2.25 (app-q, *J* = 11.7, 8.5 Hz, 1H, C11$\mathbf{H}_b$), 2.19 (d, *J* = 15.9 Hz, 1H, C4$\mathbf{H}_b$), 1.53 (app-p, *J* = 14.5, 7.3 Hz, 1H, C20$\mathbf{H}_a$), 1.35 (app-p, *J* = 14.3, 7.1, 5.3 Hz, 1H, C20$\mathbf{H}_b$), 0.80 (s, 9H, OSiC($C\mathbf{H}_3$)$_3$), –0.05 (s, 3H, OSiCC$\mathbf{H}_3$), –0.06 (s, 3H, OSiCC$\mathbf{H}_3$).

^{13}C NMR (150.9 MHz, $CDCl_3$, 25 °C): δ 168.5 (**C**O_2CH_3), 164.5 (**C**2), 143.2 (**C**18), 136.5 (**C**13), 132.8 (**C**6), 128.9 (**C**14), 128.6 (**C**16), 122.1 (**C**15), 117.5 (**C**7), 108.6 (**C**17), 88.2 (**C**3), 84.6 (**C**19), 68.8 (**C**10), 63.8 (**C**8), 59.0 (**C**21), 57.5 (**C**12), 51.3 ($CO_2\mathbf{C}H_3$), 42.5 (**C**11), 41.1 (**C**20), 40.9

6. For the preparation of vinylogous urethane (–)-**2.10**, see: Myeong, I.-S.; Avci, N. H.; Movassaghi, M. Total Synthesis of (–)-Kopsifoline A and (+)-Kopsifoline E. *Org. Lett.* **2021**, *23*, 9118–9122.
7. The concentration of peracetic acid (32 wt. %) was determined to be 2.49M.

	(**C**5), 32.9 (**C**4), 26.0 (3C, OSiC(**C**H_3)$_3$), 18.3 (OSi**C**(CH_3)$_3$), –5.4 (OSi(**C**H_3)$_2$), –5.4 (OSi(**C**H_3)$_2$).
FTIR (thin film) cm^{-1}:	3373 (br-w), 2952 (m), 2929 (m), 2883 (m), 2856 (m), 1682 (s), 1610 (s), 1592 (m), 1468 (s), 1437 (m), 1391 (w), 1283 (m), 1249 (s), 1208 (s).
$[\alpha]_D^{23}$:	–71 (c = 0.108, $CHCl_3$).
HRMS (ESI) (*m/z*):	calc'd for $C_{27}H_{39}N2O_4Si$ $[M+H]^+$: 483.2674, found: 483.2674.

TLC (10% methanol in dichloromethane), R*f*: 0.30 (UV, CAM).

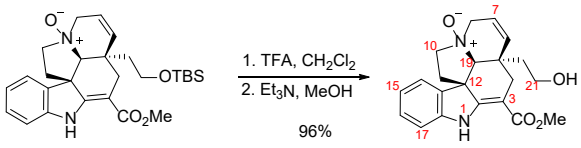

Pentacyclic *N*-oxide 2.9:

Trifluoroacetic acid (1.5 mL) was added to a solution of *tert*-butyldimethylsilyl *N*-oxide (–)-**2.33** (74 mg, 0.15 mmol, 1 equiv) in dichloromethane (7.5 mL) at 23 °C. After 2 hours, toluene (5 mL) was added and the reaction mixture was concentrated under reduced pressure. The resulting yellow residue was azeotropically dried two more times by concentration from toluene (5 mL each) and used directly in the next step.

Triethylamine (1.5 mL) was added to a solution of the yellow residue in methanol (7.5 mL) at 23 °C. After 40 min, the reaction mixture was concentrated under reduced pressure. The resulting residue was purified by flash column chromatography on basic alumina (eluent: 1% methanol, 0.1% ammonium hydroxide in chloroform → 7% methanol, 0.8% ammonium hydroxide in chloroform) to give pentacyclic *N*-oxide **2.9** (57 mg, 96%) as a white foam. Structural assignments were made using additional information from gCOSY, gHSQC, and gHMBC experiments.

^{1}H NMR (600 MHz, $CDCl_3$, 25 °C):	δ 9.30 (br-s, 1H, N1**H**), 8.71 (d, *J* = 8.1 Hz, 1H, C14**H**), 7.17 (app-t, *J* = 7.6, 1.3 Hz, 1H, C16**H**), 6.93 (app-t, *J* = 7.6, 1.1 Hz, 1H, C15**H**), 6.79 (app-d, *J* = 7.8, 1.1 Hz, 1H, C17**H**), 5.85 (app-d, *J* = 10.5, 2.9 Hz, 1H, C6**H**), 5.74 (app-d, *J* = 10.5, 5.0, 1.8 Hz, C7**H**), 4.36 (app-d, *J* = 17.4, 2.3 Hz, 1H, C8**H**$_a$), 4.16 (app-d, *J* = 17.3, 5.0 Hz, 1H, C8**H**$_b$), 4.03 (s, 1H, C19**H**), 3.78 (s, 3H, CO_2C**H**$_3$), 3.69–3.50 (m, 4H, C10**H**$_2$, C21**H**$_2$), 2.96 (app-q, *J* = 13.0, 11.0, 8.6 Hz, 1H, C20**H**$_a$), 2.70 (d, *J* = 17.0 Hz, 1H, C4**H**$_a$), 2.26–2.17 (m, 2H, C4**H**$_b$, C20**H**$_b$), 1.57 (app-p, *J* = 14.4, 7.2 Hz, 1H, C11**H**$_a$), 1.40 (m, 1H, C11**H**$_b$).
^{13}C NMR (150.9 MHz, $CDCl_3$, 25 °C):	δ 168.5 (**C**O_2CH_3), 164.2 (**C**2), 143.2 (**C**18), 136.5 (**C**13), 132.6 (**C**6), 128.8 (**C**14), 128.6 (**C**15), 122.1 (**C**16), 118.0 (**C**7), 108.7 (**C**17), 88.3 (**C**3), 84.0 (**C**19), 68.7 (**C**21), 63.5 (**C**8), 58.5 (**C**12), 57.5 (**C**10), 51.4 (CO_2**C**H_3), 42.3 (**C**20), 40.9 (**C**11), 40.8 (**C**5), 34.0 (**C**4).
FTIR (thin film) cm^{-1}:	3370 (br-w), 2926 (w), 2857 (w), 1680 (m), 1609 (s), 1592 (m), 1468 (m), 1439 (m), 1391 (m), 1284 (m), 1250 (m), 1209 (m).
HRMS (ESI) (*m/z*):	calc'd for $C_{21}H_{25}N_2O_4$ $[M+H]^+$: 369.1809, found: 369.1809.

TLC (14.4% methanol, 1.6 % ammonium hydroxide in chloroform), R*f*: 0.17 (UV, CAM).

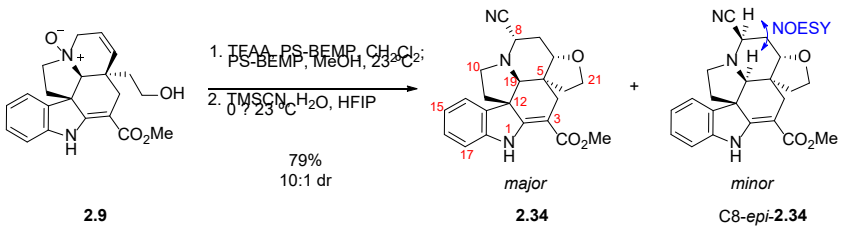

Aminonitrile 2.34 and C8-*epi*-2.34:

Pentacyclic *N*-oxide **2.9** (36.9 mg, 0.100 mmol, 1 equiv) was azeotropically dried by concentration from anhydrous benzene (3 × 300 µL) in a round bottom flask and the residue was dissolved in dichloromethane (17.0 mL). The solution was cannulated into an Erlenmeyer flask with a 24/40 joint. Polystyrene-bound 2-*tert*-butylimino-2-diethylamino-1,3-dimethyl-perhydro-1,3,2-diazaphosphorine (PS–BEMP, 273 mg, 2.20 mmol/g on 200-400 mesh polystyrene resin, 0.601 mmol, 6.00 equiv) was added followed by trifluoroacetic anhydride (3.6 M in dichloromethane, 110 µL, 0.40 mmol, 4.0 equiv). The orange suspension was shaken at 23 ºC. After 30 min, methanol (5.0 mL) and PS–BEMP (273 mg, 2.20 mmol/g on 200-400 mesh polystyrene resin, 0.601 mmol, 6.00 equiv) were then added sequentially. The reaction flask was sealed with a Teflon-lined glass stopper and shaken. After 20 h, the yellow suspension was diluted with dichloromethane (100 mL) and filtered. The resin was washed with dichloromethane (3 × 50 mL) and the light yellow filtrate was concentrated under reduced pressure. The yellow residue was used directly in the next step.

Trimethylsilyl cyanide[8] (75 µL, 0.60 mmol, 6.0 equiv) was added dropwise to a solution of the yellow residue and deionized water (16 µL, 0.90 mmol, 9.0 equiv) in hexafluoroisopropanol (HFIP, 5.0 mL) at 0 ºC. After 10 min, the ice-bath was removed and the reaction flask was sealed under an argon atmosphere with a Teflon-lined glass stopper. After 4 h, saturated aqueous sodium bicarbonate solution (10 mL) was added to the reaction mixture. The mixture was extracted with dichloromethane (3 × 10 mL). The combined organic layers were dried over anhydrous sodium sulfate, were filtered, and were concentrated under reduced pressure. The resulting residue was purified by flash column chromatography on basic alumina (eluent: 5% → 50% ethyl acetate in hexane) to give a mixture of aminonitriles **2.34** and C8-*epi*-**2.34** (**2.34**:C8-*epi*-**2.34**=10:1, 30.0 mg, 79%) as a white solid. Structural assignments were made using additional information from gCOSY, gHSQC, gHMBC and 2D NOESY experiments.

^{1}H NMR (600 MHz, $CDCl_3$, 25 °C, 10:1 mixture, * denotes minor diastereomer): δ 8.87 (br-s, 1H, N1H, N1**H***), 7.34 (d, *J* = 7.4 Hz, 1H, C14**H**), 7.22 (d, *J* = 7.4 Hz, 1H, C14**H***), 7.18 (app-t, *J* = 7.7, 1.2 Hz, 1H, C16**H**, C16**H***), 6.92 (app-t, *J* = 7.5, 1.0 Hz, 1H, C15**H**, C15**H***), 6.83 (d, *J* = 7.8 Hz, 1H, C17**H**, C17**H***), 4.11 (dd, *J* = 6.8, 2.3 Hz, 1H, C8**H**), 3.86 (q, *J* = 8.2 Hz, 2H, C21$\mathbf{H}_a$, C8**H***), 3.78 (s, 6H, $CO_2C\mathbf{H}_3$, $CO_2C\mathbf{H}_3$*), 3.77–3.69 (m, 5H, C6**H**, C6**H***, C21$\mathbf{H}_b$, C21$\mathbf{H}_2$*), 3.35–3.33 (m, 1H,

8. All operations involving trimethylsilyl cyanide were carried out in a well-ventilated fume hood. This includes but is not limited to: measuring the reagent, execution of the transformation, work-up of the reaction mixture, and concentration of the crude reaction mixture.

C10**H**$_a$*), 3.31 (s, 1H, C19**H**), 2.99–2.89 (m, 3H, C10**H**$_2$, C19**H***), 2.83–2.77 (m, 1H, C10**H**$_b$*), 2.71 (d, *J* = 14.7 Hz, 1H, C4**H**$_a$*), 2.63 (d, *J* = 14.6 Hz, 1H, C4**H**$_a$), 2.36 (app-d, *J* = 14.6, 1.9 Hz, 3H, C4**H**$_b$, C4**H**$_b$*, C7**H**$_a$*), 2.30 (app-d, *J* = 14.6, 2.7 Hz, 1H, C7**H**$_a$), 2.23–2.16 (m, 2H, C7**H**$_b$, C7**H**$_b$*), 2.09–1.99 (m, 2H, C11**H**$_a$, C11**H**$_a$*), 1.85–1.81 (m, 1H, C11**H**$_b$, C11**H**$_b$*), 1.54–1.48 (m, 1H, C20**H**$_a$, C20**H**$_a$*), 1.40–1.34 (m, 1H, C20**H**$_b$, C20**H**$_b$*).

^{13}C NMR (150.9 MHz, $CDCl_3$, 25 °C, 10:1 mixture): δ 168.7 (2C, **C**O_2C**H**$_3$, **C**O_2CH_3*), 166.5 (2C, **C**2, **C**2*), 143.2 (**C**18*), 143.1 (**C**18), 137.1 (2C, **C**13, **C**13*), 128.4 (**C**16*), 128.3 (**C**16), 121.9 (2C, **C**14, **C**14*), 121.3 (**C**15), 121.1 (**C**15*), 119.2 (C8**C**N*), 117.2 (C8**C**N), 109.8 (**C**17), 109.7 (**C**17*), 94.0 (**C**3*), 93.8 (**C**3), 79.0 (**C**6*), 78.8 (**C**6), 68.2 (**C**19*), 65.2 (2C, **C**21, **C**21*), 63.6 (**C**19), 55.2 (**C**12*), 54.4 (**C**12), 51.4 (2C, CO_2**C**H_3, CO_2**C**H_{3*}), 49.8 (**C**10*), 49.4 (**C**10), 47.3 (**C**5), 47.2 (**C**8*), 46.9 (**C**8), 46.4 (**C**5*), 44.6 (**C**11*), 44.4 (**C**11), 34.8 (**C**20*), 34.5 (**C**20), 31.4 (C7*), 30.1 (**C**7), 27.3 (**C**4*), 27.0 (**C**4).

FTIR (thin film, 10:1 mixture) cm^{-1}: 3371 (br-m), 2949 (m), 2850 (m), 2249 (w), 1677 (s), 1608 (s), 1477 (m), 1465 (m), 1437 (m), 1382 (m), 1297 (m), 1282 (m), 1252 (m).

HRMS (ESI) (*m/z*): calc'd for $C_{22}H_{24}N_3O_3$ $[M+H]^+$: 378.1812, found: 378.1811.

TLC (Basic Al_2O_3, 50 % ethyl acetate in hexane), R*f*: 0.60 (UV, CAM)

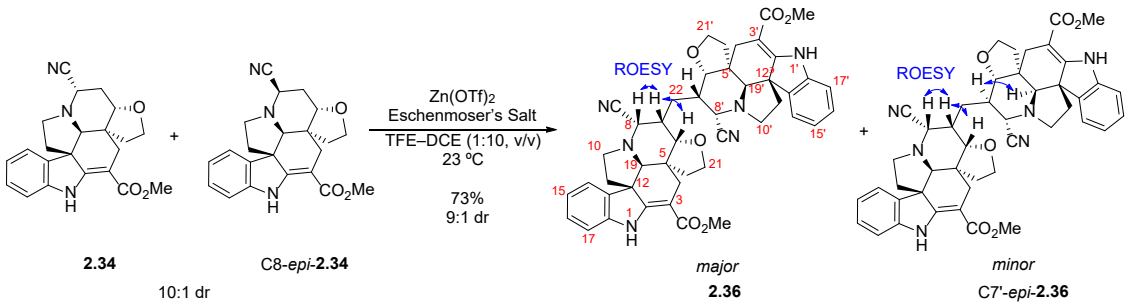

2.34 C8-*epi*-**2.34**

10:1 dr

major 2.36 **minor** C7'-*epi*-**2.36**

Bisaminonitrile 2.36 and C7'-*epi*-2.36:

Zinc trifluoromethanesulfonate[9] ($Zn(OTf)_2$, 73 mM in acetonitrile, 1.0 mL, 73 μmol, 1.0 equiv) was added to a solution of aminonitriles **2.34** and C8-*epi*-**2.34** (**2.34**:C8-*epi*-**2.34**=10:1, 27.6 mg, 73.1 μmol, 1 equiv), Eschenmoser's salt (172 mM in dimethylformamide, 215 μL, 36.6 μmol, 0.500 equiv), and trifluoroethanol (810 μL) in 1,2-dichloroethane (8.1 mL) at 23 ºC. The reaction flask was sealed under an argon atmosphere with a Teflon-lined glass stopper. After 3 h, a saturated aqueous sodium bicarbonate solution (8 mL) was added to the reaction mixture. The layers were separated and the aqueous layer was extracted with dichloromethane (3 × 10 mL). The combined organic layers were dried over anhydrous sodium sulfate, were filtered, and were concentrated under reduced pressure. The resulting residue was purified by flash column chromatography on silica gel (eluent: 5% → 50% ethyl acetate in hexanes) to give a mixture of bisaminonitriles **2.36** and C7'-*epi*-**2.36** (**2.36**:C7'-*epi*-**2.36**=9:1, 20.3 mg, 73%) as a white solid. Structural assignments were made using additional information from gCOSY, gHSQC, gHMBC, and 2D ROESY experiments.

^{1}H NMR (600 MHz, $CDCl_3$, 25 °C, 9:1 mixture, * denotes minor diastereomer): δ 8.90 (br-s, 2H, N1**H***, N1**H**'*), 8.86 (br-s, 2H, N1**H**, N1**H**'), 7.35 (d, *J* = 7.3 Hz, 4H, C14**H**, C14**H**', C14**H***, C14**H**'*), 7.18 (app-t, *J* = 7.5, 1.6 Hz, 4H, C16**H**, C16**H**', C16**H***, C16**H**'*), 6.93 (app-t, *J* = 7.3, 1.6 Hz, 4H, C15**H**, C15**H**', C15**H***, C15**H**'*), 6.84 (app-d, *J* = 7.3, 1.6 Hz, 4H, C17**H**, C17**H**', C17**H***, C17**H**'*), 4.11 (d, *J* = 5.7 Hz, 1H, C8**H***), 4.08 (d, *J* = 5.7 Hz, 2H, C8**H**, C8**H**'), 3.93 (d, *J* = 4.1 Hz, 1H, C8**H**'*), 3.89–3.76 (m, 16H, CO_2CH_3, CO_2CH_3', CO_2CH_3*, CO_2CH_3'*, C21H_a, C21H_a', C21H_a*, C21H_2'*), 3.72–3.65 (m, 5H, C6**H***, C6**H**'*, C21H_b, C21H_b', C21H_b*), 3.63 (d, *J* = 3.5 Hz, 2H, C6**H**, C6**H**'), 3.36 (s, 1H, C19**H**'*), 3.32 (s, 3H, C19**H**, C19**H**', C19**H***), 3.07–3.00 (app-s, *J* = 12.1, 8.5, 4.4 Hz, 1H, C10H_a'*), 3.00–2.92 (m, 7H, C10H_2, C10H_2', C10H_2*, C10H_b'*), 2.70 (app-d, *J* = 14.4 Hz, 3H, C4H_a, C4H_a', C4H_a*), 2.58 (s, 2H, C4H_2'*), 2.43–2.35 (m, 6H, C4H_b, C4H_b', C4H_b*, C7**H**, C7**H**',

[9]. $Zn(OTf)_2$ was flamed-dried under vacuum for 5 mins and allowed to cool to 23 ºC prior to use.

C7**H***), 2.35–2.28 (m, 1H, C7**H**'*), 2.20 (app-p, *J* = 14.6, 7.2 Hz, 1H, C22$\mathbf{H}_a$*), 2.12–2.00 (m, 6H, C11$\mathbf{H}_a$, C11$\mathbf{H}_a$', C11$\mathbf{H}_a$*, C11$\mathbf{H}_a$'*, C22$\mathbf{H}_2$), 1.95–1.89 (m, 1H, C22$\mathbf{H}_b$*), 1.88–1.81 (m, 4H, C11$\mathbf{H}_b$, C11$\mathbf{H}_b$', C11$\mathbf{H}_b$*, C11$\mathbf{H}_b$'*), 1.60–1.51 (m, 4H, C20$\mathbf{H}_a$, C20$\mathbf{H}_a$', C20$\mathbf{H}_a$*, C20$\mathbf{H}_a$'*), 1.43–1.37 (m, 4H, C20$\mathbf{H}_b$, C20$\mathbf{H}_b$', C20$\mathbf{H}_b$*, C20$\mathbf{H}_b$'*).

^{13}C NMR (150.9 MHz, $CDCl_3$, 25 °C, 9:1 mixture, * denotes minor diastereomer): δ 168.6 (4C, **C**O_2CH_3, **C**O_2CH_3', **C**O_2CH_3*, **C**O_2CH_3'*), 166.6 (3C, **C**2, **C**2', **C**2*), 165.4 (**C**2'*), 143.1 (**C**18'*), 143.0 (3C, **C**18, **C**18', **C**18*), 137.01 (3C, **C**13, **C**13', **C**13*), 136.97 (**C**13'*), 128.5 (**C**16'*), 128.4 (3C, **C**16, **C**16', **C**16*), 121.9 (3C, **C**14, **C**14', **C**14*), 121.8 (**C**14'*), 121.4 (3C, **C**15, **C**15', **C**15*), 121.3 (**C**15'*), 117.3 (**C**8CN'*), 115.9 (2C, C8**C**N, C8**C**N'), 115.8 (C8**C**N*), 109.7 (4C, **C**17, **C**17', **C**17*, **C**17'*), 93.8 (**C**3*), 93.7 (**C**3'*), 93.6 (2C, **C**3, **C**3'), 84.3 (**C**6'*), 80.8 (**C**6*), 79.9 (2C, **C**6, **C**6'), 66.1 (**C**19'*), 66.0 (**C**21'*), 64.9 (2C, **C**21, **C**21'), 64.8 (**C**21*), 63.1 (2C, **C**19, **C**19'), 63.0 (**C**19*), 54.41 (**C**12*), 54.40 (2C, **C**12, **C**12'), 54.3 (**C**12'*), 53.0 (2C, **C**8, **C**8'), 52.9 (**C**8'*), 52.3 (**C**8*), 51.4 (2C, CO_2**C**H_3, CO_2**C**H_3'), 51.39 (2C, CO_2**C**H_3*, CO_2**C**H_3'*), 49.6 (**C**10*), 49.5 (2C, **C**10, **C**10'), 49.3 (**C**10'*) 48.8 (**C**5'*), 47.0 (3C, **C**5, **C**5', **C**5*), 44.7 (3C, **C**11, **C**11', **C**11*), 43.5 (**C**11'*), 38.9 (**C**7'*), 37.3 (**C**7*), 35.5 (2C, **C**7**,** **C**7'), 34.7 (2C, **C**20, **C**20'), 34.6 (**C**20*), 34.5 (**C**20'*), 31.5 (**C**22*), 28.2 (**C**4'*), 27.2 (**C**22), 27.0 (2C, **C**4, **C**4'), 26.9 (**C**4*).

FTIR (thin film, 9:1 mixture) cm^{-1}: 3370 (br-m), 2948 (m), 2850 (m), 2252 (w), 1677 (s), 1608 (s), 1467 (m), 1465 (m), 1437 (m), 1383 (w), 1297 (m), 1279 (m), 1252 (m).

HRMS (ESI) (*m/z*): calc'd for $C_{45}H_{47}N_6O_6$ $[M+H]^+$: 767.3552, found: 767.3549.

TLC (60% ethyl acetate in hexane), R*f*: 0.64 (UV, CAM).

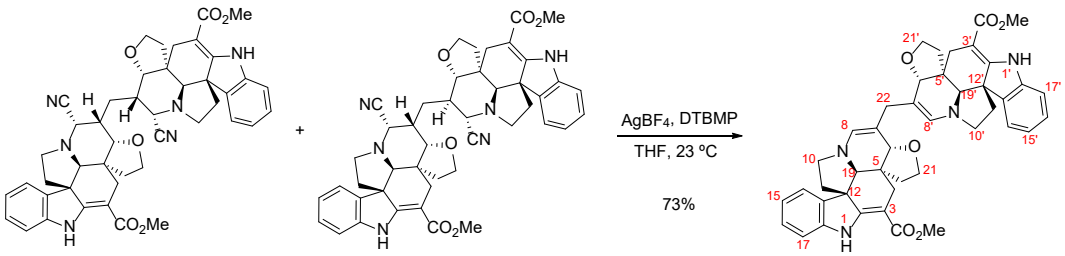

Bisenamine (–)-2.7:

Silver tetrafluoroborate (2.4 mM in toluene, 83 µL, 0.020 mmol, 1.5 equiv) was added to a solution of bis-aminonitriles **2.36** and C7'-*epi*-**2.36** (**2.36**:C7'-*epi*-**2.36**=9:1, 9.7 mg, 13 µmol, 1 equiv) and 2,6-di-*tert*-butyl-4-methylpyridine (DTBMP, 8.1 mg, 39 µmol, 3.0 equiv) in tetrahydrofuran (2.6 mL) at 23 ºC. After 3 h, a solution of ammonium hydroxide (28.0–30%, 5 mL) and ethyl acetate (5 mL) were added sequentially. The layers were separated and the aqueous layer was extracted with dichloromethane (3 × 5 mL). The combined organic layers were dried over anhydrous sodium sulfate, were filtered, and were concentrated under reduced pressure. The resulting residue was purified by flash column chromatography on silica gel (eluent: 30% → 50% ethyl acetate in hexanes with 1% triethylamine) to give bisenamine (–)-**2.7** (6.6 mg, 73%) as a thin film. Structural assignments were made using additional information from gCOSY, gHSQC, and gHMBC experiments.

^{1}H NMR (600 MHz, C_6D_6, 25 °C): δ 9.27 (s, 2H, N1**H**, N1**H'**), 6.90 (app-t, *J* = 7.7 Hz, 2H, C16**H**, C16**H'**), 6.80 (d, *J* = 7.3 Hz, 2H, C14**H**, C14**H'**), 6.68 (app-t, *J* = 7.4 Hz, 2H, C15**H**, C15**H'**), 6.34 (s, 2H, C8**H**, C8**H'**), 6.24 (d, *J* = 7.7 Hz, 2H, C17**H**, C17**H'**), 3.94 (s, 2H, C6**H**, C6**H'**), 3.64 (s, 6H, CO_2CH_3, CO_2CH_3'), 3.63–3.58 (m, 2H, C21H_a, C21H_a'), 3.57 (s, 2H, C19**H**, C19**H'**), 3.54 (s, 2H, C22H_2), 3.52–3.46 (m, 2H, C21H_b, C21H_b'), 3.07 (app-td, *J* = 9.0, 5.7 Hz, 2H, C10H_a, C10H_a'), 2.76–2.70 (m, 2H, C10H_b, C10H_b'), 2.61 (d, *J* = 15.0 Hz, 2H, C4H_a, C4H_a'), 2.24 (d, *J* = 14.9 Hz, 2H, C4H_b, C4H_b'), 1.84–1.76 (m, 2H, C11H_a, C11H_a'), 1.62–1.55 (m, 2H, C11H_b, C11H_b'), 1.52–1.44 (m, 2H, C20H_a, C20H_a'), 1.23–1.15 (m, 2H, C20H_b, C20H_b').

^{13}C NMR (150.9 MHz, C_6D_6, 25 °C): δ 168.7 (2C, **C**O_2CH_3, **C**O_2CH_3'), 167.4 (2C, **C**2, **C**2'), 143.8 (2C, **C**18, **C**18'), 136.8 (2C, **C**13, **C**13'), 131.3 (2C, **C**8, **C**8'), 128.4 (2C, **C**16, **C**16'), 121.9 (2C, **C**14, **C**14'), 121.4 (2C, **C**15, **C**15'), 109.6 (2C, **C**17, **C**17'), 105.7 (2C, **C**7, **C**7'), 94.6 (2C, **C**3, **C**3'), 78.6 (2C, **C**6, **C**6'), 63.7 (2C, **C**21, **C**21'), 63.6 (2C, **C**19, **C**19'), 56.8 (2C, **C**12, **C**12'), 51.0 (2C, CO_2**C**H_3, CO_2**C**H_3'), 50.0 (2C, **C**10, **C**10'), 44.8 (2C,

	C11, **C**11'), 43.8 (2C, **C**5, **C**5'), 37.2 (2C, **C**20, **C**20'), 36.0 (**C**22), 28.7 (2C, **C**4, **C**4').
FTIR (thin film) cm^{-1}:	3375 (br-w), 2847 (br-m), 2850 (br-m), 1678 (m), 1609 (s), 1289 (m), 1248 (m), 1199 (m).
$[\alpha]_D^{23}$:	–218 (c = 0.243, MeOH).
HRMS (ESI) (*m/z*):	calc'd for $C_{43}H_{45}N_4O_6$ $[M+H]^+$: 713.3334, found: 713.3354.
TLC (50% ethyl acetate in hexane), R*f*:	0.23 (UV, CAM).

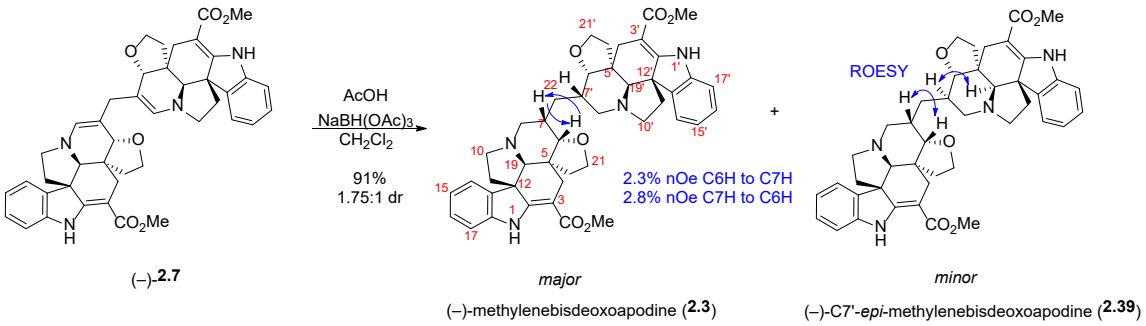

(–)-**2.7**

(–)-methylenebisdeoxoapodine (**2.3**)

(–)-C7'-*epi*-methylenebisdeoxoapodine (**2.39**)

(–)-Methylenebisdeoxoapodine (2.3) and (–)-C7'-*epi*-methylenebisdeoxoapodine (2.16):

Sodium triacetoxyborohydride (78 mg, 370 µmol, 15 equiv) was added to a solution of bisenamine (–)-**2.7** (17.5 mg, 24.5 µmol, 1 equiv) and acetic acid (21 µL, 370 µmol, 15 equiv) in dichloromethane (5.0 mL) at 23 ºC. After 5.5 h, a saturated aqueous sodium bicarbonate solution (5 mL) was added. The layers were separated and the aqueous layer was extracted with dichloromethane (3 × 5 mL). The combined organic layers were dried over anhydrous sodium sulfate, were filtered, and were concentrated under reduced pressure. The resulting residue was purified by flash column chromatography on basic alumina (eluent: 15% → 20% acetone in hexanes) to give a mixture of (–)-methylenebisdeoxoapodine (**2.3**) and (–)-C7'-*epi*-methylenebisdeoxoapodine (**2.39**) (**2.3**:**2.39** = 1.75:1, 16.0 mg, 91%) as a thin film. Additional column chromatography afforded a sample of the major diastereomer used for characterization. Structural assignments for (–)-methylenebisdeoxoapodine (**2.3**) were made using additional information from gCOSY, gHSQC, gHMBC, and 1D NOESY experiments. Structural assignments for (–)-C7'-*epi*-methylenebisdeoxoapodine (**2.39**) were made using additional information from gCOSY, gHSQC, gHMBC, and 2D ROESY experiments.

(–)-methylenebisdeoxoapodine (**2.3**):

^{1}H NMR (600 MHz, $CDCl_3$, 25 °C): δ 8.93 (br-s, 2H, N1**H**, N1**H'**), 7.24 (d, *J* = 7.4 Hz, 2H, C14**H**, C14**H'**), 7.16 (app-t, *J* = 7.6 Hz, 2H, C16**H**, C16**H'**), 6.89 (app-t, *J* = 7.6 Hz, 2H, C15**H**, C15**H'**), 6.82 (d, *J* = 7.7 Hz, 2H, C17**H**, C17**H'**), 3.79 (s, 6H, CO_2CH_3, CO_2CH_3'), 3.78–3.73 (m, 2H, C21H_a, C21H_a'), 3.69 (app-q, *J* = 8.9, 5.8 Hz, 2H, C21H_b, C21H_b'), 3.54 (d, *J* = 4.3 Hz, 2H, C6**H**, C6**H'**), 2.96–2.88 (m, 6H, C8H_a, C8H_a', C10H_a, C10H_a', C19**H**, C19**H'**), 2.84 (dd, *J* = 10.8, 4.0 Hz, 2H, C8H_b, C8H_b'), 2.77–2.67 (m, 4H, C4H_a, C4H_a', C10H_b, C10H_b'), 2.48 (d, *J* = 14.5 Hz, 2H, C4H_b, C4H_b'), 2.09 (app-td, *J* = 11.3, 6.0 Hz, 2H, C11H_a, C11H_a'), 2.03–1.96 (m, 2H, C7**H'**, C7**H**), 1.84–1.76 (m, 4H, C11H_b, C11H_b', C22H_2), 1.53–1.46 (m, 2H, C20H_a, C20H_a'), 1.31–1.23 (m, 2H, C20H_b, C20H_b').

^{13}C NMR (150.9 MHz, $CDCl_3$, 25 °C): δ 169.0 (**C**O_2CH_3, **C**O_2CH_3'), 166.8 (**C**2, **C**2'), 143.3 (**C**18, **C**18'), 137.9 (**C**13, **C**13'), 128.0 (**C**16, **C**16'),

	121.8 (**C**14, **C**14'), 120.9 (**C**15, **C**15'), 109.5 (**C**17, **C**17'), 94.2 (**C**3, **C**3'), 86.3 (**C**6, **C**6'), 70.4 (**C**19, **C**19'), 65.6 (**C**21, **C**21'), 55.3 (**C**12, **C**12'), 51.9 (**C**10, **C**10'), 51.3 ($CO_2\mathbf{C}H_3$, $CO_2\mathbf{C}H_3$'), 51.0 (**C**8, **C**8'), 48.4 (**C**5, **C**5'), 44.8 (**C**11, **C**11'), 36.3 (**C**7, **C**7'), 35.1 (**C**20, **C**20'), 34.9 (**C**22), 28.8 (**C**4, **C**4').
FTIR (thin film) cm^{-1}:	3373 (br-w), 2922 (m), 2851 (m), 2803 (w), 1677 (s), 1609 (s), 1465 (m), 1437 (m), 1293 (m), 1250 (m), 1205 (m).
$[\alpha]_D^{23}$:	–392 (c = 0.080, $CHCl_3$).
HRMS (ESI) (*m/z*):	calc'd for $C_{43}H_{49}N_4O_6$ $[M+H]^+$: 717.3647, found: 717.3654.
TLC (Al_2O_3, 30% acetone in hexane), R*f*:	0.40 (UV, CAM).

(–)-C7'-*epi*-methylenebisdeoxoapodine (**2.39**):

^{1}H NMR (600 MHz, $CDCl_3$, 25 °C):	δ 8.91 (app-d, *J* = 13.2 Hz, 2H, N1**H**, N1**H**'), 7.25 (d, *J* = 7.2 Hz, 2H, C14**H**, C14**H**'), 7.15 (app-td, *J* = 7.6, 7.6, 3.5 Hz, 2H, C16**H**, C16**H**'), 6.89 (app-td, *J* = 7.5, 7.5, 2.7 Hz, 2H, C15**H**, C15**H**'), 6.81 (d, *J* = 7.7 Hz, 2H, C17**H**, C17**H**'), 3.79 (app-d, *J* = 5.1 Hz, 6H, CO2C$\mathbf{H}_3$, $CO_2C\mathbf{H}_3$'), 3.77–3.72 (m, 2H, C21$\mathbf{H}_a$, C21$\mathbf{H}_a$'), 3.72–3.64 (m, 2H, C21$\mathbf{H}_b$, C21$\mathbf{H}_b$'), 3.61 (d, *J* = 3.3 Hz, 1H, C6**H**), 3.57 (d, *J* = 3.6 Hz, 1H, C6**H**'), 2.99–2.88 (m, 5H, C8$\mathbf{H}_a$, C8$\mathbf{H}_a$', C10$\mathbf{H}_a$, C10$\mathbf{H}_a$', C19**H**'), 2.87 (s, 1H, C19**H**) 2.81 (dd, *J* = 10.9, 3.4 Hz, 1H, C8$\mathbf{H}_b$'), 2.78 (d, *J* = 14.5 Hz, 1H, C4$\mathbf{H}_a$), 2.75 (d, *J* = 14.4 Hz, 1H, C4$\mathbf{H}_a$'), 2.75–2.68 (m, 2H, C10$\mathbf{H}_b$, C10$\mathbf{H}_b$'), 2.54 (t, *J* = 11.0, 11.0 Hz, 1H, C8$\mathbf{H}_b$), 2.45 (d, *J* = 14.5 Hz, 1H, C4$\mathbf{H}_b$'), 2.33 (d, *J* = 14.5 Hz, 1H, C4$\mathbf{H}_b$'), 2.16–2.09 (m, 1H, C7**H**), 2.09–2.01 (m, 3H, C7**H**', C11$\mathbf{H}_a$, C11$\mathbf{H}_a$'), 1.87–1.80 (m, 1H, C22$\mathbf{H}_a$), 1.80–1.75 (m, 2H, C11$\mathbf{H}_b$, C11$\mathbf{H}_b$), 1.66–1.59 (m, 1H, C22$\mathbf{H}_b$), 1.52–1.42 (m, 2H, C20$\mathbf{H}_b$, C20$\mathbf{H}_b$'), 1.34–1.25 (m, C20$\mathbf{H}_b$, C20$\mathbf{H}_b$).
^{13}C NMR (150.9 MHz, $CDCl_3$, 25 °C):	δ 168.9 ($\mathbf{C}O_2CH_3$, $\mathbf{C}O_2CH_3$'), 167.6 (**C**2), 166.9 (**C**2'), 143.3 (**C**18, **C**18'), 138.0 (**C**13 or **C**13'), 137.9 (**C**13 or **C**13'), 127.9 (**C**16, **C**16'), 121.8 (**C**14 or **C**14'), 121.5 (**C**14 or **C**14'), 120.9 (**C**15 or **C**15'), 120.8 (**C**15 or **C**15'), 109.5 (**C**17, **C**17'), 94.3 (**C**3'),

	93.9 (**C**3), 85.4 (**C**6'), 82.1 (**C**6), 70.2 (**C**19'), 68.2 (**C**19), 65.4 (**C**21 or **C**21'), 64.9 (**C**21 or **C**21'), 55.3 (**C**12 or **C**12'), 55.2 (**C**12 or **C**12'), 51.9 (**C**8 or **C**8', **C**10, **C**10'), 51.5 (**C**8 or **C**8'), 51.3 (CO_2**C**H_3 or CO_2**C**H_3'), 51.2 (CO_2**C**H_3 or CO_2**C**H_3'), 48.2 (**C**5'), 46.9 (**C**5), 45.6 (**C**11), 44.9 (**C**11'), 35.1 (**C**7, **C**7', **C**20, **C**20'), 32.5 (**C**22), 28.6 (**C**4'), 27.8 (**C**4).
FTIR (thin film) cm^{-1}:	3379 (br-w), 2932 (m), 2867 (m), 22796 (w), 1677 (s), 1609 (s), 1465 (m), 1294 (m), 1279 (s), 1247 (m), 1153 (m).
$[\alpha]_D^{23}$:	–289 (c = 0.094, $CHCl_3$).
HRMS (ESI) (*m/z*):	calc'd for $C_{43}H_{49}N_4O_6$ $[M+H]^+$: 717.3647, found: 717.3643.
TLC (Al_2O_3, 30% acetone in hexane), R*f*:	0.40 (UV, CAM).

Table 2.1 Comparison of our ^{1}H NMR data for (–)-methylenebisdeoxoapodine (2.3) with related compounds ($CDCl_3$).

Assignment	**Our Previous Synthesis**[10] (–)-deoxoapodine (**2.4**) ^{1}H NMR, 400 MHz, $CDCl_3$	**Isolation Report**[2] deoxoapodine–substructure of voacandimine C (**2.2**) ^{1}H NMR, 600 MHz, $CDCl_3$	**This Work** (–)-methylene-bisdeoxoapodine (**2.3**) ^{1}H NMR, 600 MHz, $CDCl_3$
N1	8.90 (br. s, 1H)	8.88 (br. s, 1H)	8.93 (br. s, 2H)
C4	2.76 (d, *J* = 14.7 Hz, 1H) 2.31 (dd, *J* = 14.6, 1.8 Hz, 1H)	2.74 (d, *J* = 14.6, 1H) 2.33 (d, *J* = 14.6, 1H)	2.77–2.67 (m 2H) 2.48 (d, *J* = 14.5 Hz. 2H)
C6	3.70–3.65 (m, 1H)	3.56 (d, *J* =2.5, 1H)	3.54 (d, *J* = 4.3 Hz, 2H)
C7	2.00–1.92 (m, 2H)	2.19–2.13 (m, 1H)	2.03–1.96 (m, 2H)
C8	2.99–2.91 (m, 1H) 2.77–2.70 (m, 1H)	2.98–2.94 (m, 1H) 2.51–2.46 (m, 1H)	2.96–2.88 (m, 2H) 2.84 (app-d, *J* = 10.8, 4.0 Hz, 2H)
C10	2.99–2.91 (m, 1H) 2.67 (ddd, *J* = 11.1, 8.5, 4.6 Hz, 1H)	2.98–2.94 (m, 1H) 2.77–2.69 (m, 1H)	2.96–2.88 (m, 2H) 2.77–2.67 (m , 2H)
C11	2.04 (ddd, *J* = 11.2, 11.2, 6.2 Hz, 1H) 1.77 (dd, *J* = 11.5, 4.4 Hz, 1H)	2.10–2.02 (m, 1H) 1.79 (dd, *J* =11.3, 4.1, 1H)	2.09 (app-s, *J* = 11.3, 6.0 Hz, 2H) 1.84–1.76 (m, 2H)
C14	7.24 (d, *J* = 7.4 Hz, 1H)	7.24 (d, *J* = 7.4, 1H)	7.24 (d, *J* = 7.4 Hz, 2H)
C15	6.88 (td, *J* = 7.5, 1.0 Hz, 1H)	6.90 (dd, *J* = 7.4, 7.4, 1H)	6.89 (app-t, *J* = 7.6 Hz, 2H)
C16	7.14 (td, *J* = 7.7, 1.2 Hz, 1H)	7.15 (dd, *J* = 7.4, 7.4, 1H)	7.16 (app-t, *J* = 7.6 Hz, 2H)
C17	6.81 (d, *J* = 7.7 Hz, 1H)	6.81 (d, *J* = 7.4, 1H)	6.82 (d, *J* = 7.7 Hz, 2H)
C19	2.83 (s, 1H)	2.86 (s, 1H)	2.96–2.88 (m, 2H)
C20	1.45 (ddd, *J* = 12.8, 9.9, 7.4 Hz, 1H) 1.29 (ddd, *J* = 13.0, 8.4, 4.7 Hz, 1H)	1.46 (m, 1H) 1.34–1.28 (m, 1H)	1.53–1.46 (m, 2H) 1.31–1.23 (m, 2H)
C21	3.81–3.73 (m, 1H) 3.72–3.65 (m, 1H)	3.74 (ddd, *J* = 8.9, 8.9, 8.9, 1H)	3.78–3.73 (m, 2H) 3.69 (app-q, *J* = 8.6, 5.8 Hz, 2H)

[10] Kang, T.; White, K. L.; Mann, T. J.; Hoveyda, A. H.; Movassaghi, M. Enantioselective Total Synthesis of (−)-Deoxoapodine. *Angew. Chem. Int. Ed*. **2017**, *56*, 13857.

		3.66 (ddd, J = 8.9, 8.9, 3.9, 1H)	
C22	–	2.28 (m, 1H) 2.19–2.13 (m, 1H)	1.84–1.76 (m, 2H)
CO_2CH_3	3.78 (s, 3H)	3.80 (s, 3H)	3.79 (s, 6H)

Table 2.2 Comparison of our ^{13}C NMR data of (–)-methylenebisdeoxoapodine (2.3) with related compounds ($CDCl_3$).

Assignment	**Our Previous Synthesis**[10] (–)-deoxoapodine (**2.4**) ^{13}C NMR, 400 MHz, $CDCl_3$	**Isolation Report**[2] deoxoapodine– substructure of voacandimine C (**2.2**) ^{13}C NMR, 600 MHz, $CDCl_3$	**This Work** (–)-methylene-bisdeoxoapodine (**2.3**) ^{13}C NMR, 600 MHz, $CDCl_3$
C2	167.5	167.3	166.8
C3	94.1	93.7	94.2
C4	27.8	27.7	28.8
C5	46.8	46.9	48.4
C6	80.1	82.2	86.3
C7	27.0	35.4	36.3
C8	46.1	51.4	51.0
C10	51.6	51.4	51.9
C11	45.4	45.5	44.8
C12	55.3	55.0	55.3
C13	138.0	137.84	137.9
C14	121.5	121.3	121.8
C15	120.9	120.7	120.9
C16	127.9	127.77	128.0
C17	109.5	109.4	109.5
C18	143.3	143.1	143.3
C19	68.9	68.4	70.4
C20	35.1	34.9	35.1
C21	65.1	64.8	65.6
C22	–	36.1	34.9
$\mathbf{C}O_2CH_3$	168.9	168.7	169.0
$CO_2\mathbf{C}H_3$	51.2	51.08	51.3

Figure 2.2 Comparison of the relative energies for (–)-methylenebisdeoxoapodine (2.3) and its isomers.

The geometries (gas phase) in the ground state of the three diastereomers were optimized with Merck Molecular Force Field (MMFF)[11] followed by density functional theory at B3LYP level with 6-31g(d,p) as basis set (Gaussian09, by Gaussian, Inc.).[12]

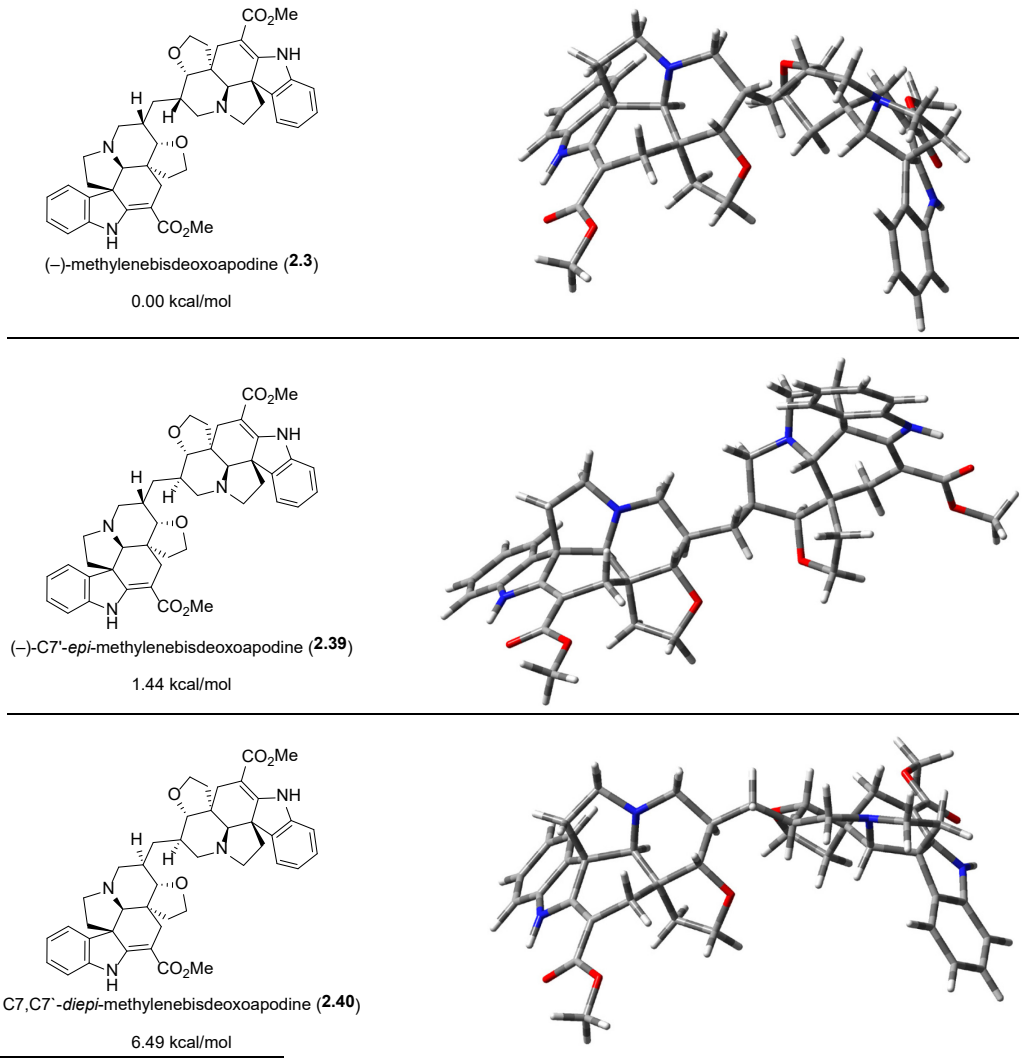

11. Halgren, T. A. Merck molecular force field. I. Basis, form, scope, parameterization, and performance of MMFF94. J. Comput. Chem. 1996, 17, 490–519.
12. Frisch, M. J. T., G. W.; Schlegel, H. B.; Scuseria, G. E.; Robb, M. A.; Cheeseman, J. R.; Scalmani, G.; Barone, V.; Mennucci, B.; Petersson, G. A.; Nakatsuji, H.; Caricato, M.; Li, X.; Hratchian, H. P.; Izmaylov, A. F.; Bloino, J.; Zheng, G.; Sonnenberg, J. L.; Hada, M.; Ehara, M.; Toyota, K.; Fukuda, R.; Hasegawa, J.; Ishida, M.; Nakajima, T.; Honda, Y.; Kitao, O.; Nakai, H.; Vreven, T.; Montgomery, J. A., Jr.; Peralta, J. E.; Ogliaro, F.; Bearpark, M.; Heyd, J. J.; Brothers, E.; Kudin, K. N.; Staroverov, V. N.; Kobayashi, R.; Normand, J.; Raghavachari, K.; Rendell, A.; Burant, J. C.; Iyengar, S. S.; Tomasi, J.; Cossi, M.; Rega, N.; Millam, M. J.; Klene, M.; Knox, J. E.; Cross, J. B.; Bakken, V.; Adamo, C.; Jaramillo, J.; Gomperts, R.; Stratmann, R. E.; Yazyev, O.; Austin, A. J.; Cammi, R.; Pomelli, C.; Ochterski, J. W.; Martin, R. L.; Morokuma, K.; Zakrzewski, V. G.; Voth, G. A.; Salvador, P.; Dannenberg, J. J.; Dapprich, S.; Daniels, A. D.; Farkas, Ö.; Foresman, J. B.; Ortiz, J. V.; Cioslowski, J.; Fox, D. J.; Gaussian, Inc.: Wallingford CT, 2009; Vol. Revision D.01.

Table 2.3 Optimized cartesian coordinates (atom, x, y, z) for (–)-methylenebisdeoxoapodine (2.3).

O	-6.84562100	1.69647700	2.12205600	C	-6.12485400	2.09884300	1.20649500
O	-5.98009500	3.42622400	0.95077400	C	6.12439000	-2.09945300	1.20610700
C	-6.71511100	4.30035000	1.81636100	H	-6.40205200	4.17375700	2.85611300
O	6.84533000	-1.69740400	2.12167500	H	-7.78779600	4.10144200	1.74974800
O	5.97914900	-3.42677100	0.95031800	H	-6.49255400	5.31054500	1.47186300
C	6.71392800	-4.30120000	1.81579800	H	7.78671700	-4.10298400	1.74873700
C	-3.95830500	-4.43267000	1.51021900	H	6.49061900	-5.31131700	1.47155800
C	-4.88196200	-4.22449700	2.53536900	H	6.40134800	-4.17421500	2.85564100
C	-5.62115500	-3.03743500	2.61602900	H	-3.39079800	-5.35713500	1.47269500
C	-5.39888600	-2.07237700	1.64027600	H	-5.02923600	-4.99118400	3.29038800
C	-4.47608900	-2.26816800	0.59516000	H	-6.33342700	-2.87365700	3.41870300
C	-3.75698400	-3.45216200	0.52567000	H	-3.03445900	-3.61913800	-0.26822000
N	-5.98191100	-0.80479900	1.51069600	H	-6.49215200	-0.29127400	2.22227600
C	-5.36415100	-0.09818800	0.51146000	H	-4.24052000	2.85472300	-0.57818400
C	-4.56472200	-1.06762500	-0.33852700	H	-4.75609900	1.64930000	-1.74238900
C	-5.35092200	1.25164300	0.31174600	H	-2.39869300	-1.04443500	-0.46408500
C	-4.37798700	1.78088300	-0.72048700	H	-2.62148800	2.14195400	-2.47577200
C	-3.00861200	1.04229200	-0.63156800	H	-0.69485500	1.12168800	-3.28834900
C	-3.23074800	-0.46358400	-0.89473600	H	-1.51684800	-1.50452900	-3.04323200
C	-2.03207400	1.61437600	-1.71411000	H	-2.28110000	-0.32713900	-4.11684300
C	-1.15380300	0.57203300	-2.45734100	H	-3.77663300	-2.70866900	-2.52856800
C	-2.05929400	-0.54004200	-3.06332600	H	-4.57735400	-1.63952300	-3.69918700
N	-3.32385500	-0.62021000	-2.34988200	H	-5.97243800	-0.63329900	-1.97545200
C	-4.23038800	-1.70616700	-2.66107700	H	-5.98843800	-2.33841100	-1.47957400
C	-5.34920700	-1.46944500	-1.64668400	H	-1.53964800	0.60725200	0.92315900
C	-2.27050700	1.38609200	0.67920300	H	-2.94399300	1.49285000	1.53343800
O	-1.19087000	2.57177800	-1.05502200	H	-2.21860100	3.55763900	0.46750300
C	-1.55649900	2.69044100	0.32229000	H	-0.64397100	2.86320000	0.90277800
C	-0.00006300	0.00036600	-1.60301800	H	-0.37017400	-0.80148800	-0.95904100
C	3.95933900	4.43246100	1.51096800	H	0.37000500	0.80213200	-0.95888800
C	4.88292100	4.22386800	2.53610100	H	3.39203000	5.35705400	1.47362000
C	5.62185100	3.03662700	2.61652300	H	5.03033400	4.99035700	3.29129500
C	5.39938900	2.07182900	1.64055800	H	6.33409300	2.87251700	3.41915700
C	4.47662100	2.26801000	0.59549700	H	3.03537100	3.61952400	-0.26766500
C	3.75781200	3.45219400	0.52622700	H	6.49227700	0.29037500	2.22219500
N	5.98220400	0.80417500	1.51068500	H	4.24001900	-2.85462100	-0.57879700
C	5.36424300	0.09787500	0.51136500	H	4.75580000	-1.64905100	-1.74277400
C	4.56498200	1.06762400	-0.33843100	H	2.39890600	1.04483900	-0.46379300
C	5.35074300	-1.25192100	0.31142300	H	2.62125200	-2.14112200	-2.47622800
C	4.37769300	-1.78078000	-0.72088900	H	0.69472500	-1.12058000	-3.28860200
C	3.00845400	-1.04195500	-0.63180100	H	2.28081400	0.32880600	-4.11674500
C	3.23082300	0.46393100	-0.89465000	H	1.51680200	1.50568200	-3.04239800
C	2.03184700	-1.61368700	-1.71446300	H	3.77704800	2.70927300	-2.52800700
C	1.15365200	-0.57113400	-2.45744000	H	4.57742100	1.64023800	-3.69896200
C	2.05916300	0.54116900	-3.06308700	H	5.97241900	0.63329000	-1.97557100
N	3.32383100	0.62086800	-2.34977900	H	5.98889700	2.33828900	-1.47933900
C	4.23057300	1.70670800	-2.66080200	H	1.53960100	-0.60696500	0.92305600
C	5.34942700	1.46951900	-1.64655800	H	2.94377900	-1.49297000	1.53311100
C	2.27030000	-1.38588700	0.67889900	H	2.21804600	-3.55739100	0.46692500
O	1.19062200	-2.57120700	-1.05559700	H	0.64347900	-2.86274300	0.90212200
C	1.55609400	-2.69007500	0.32173800				

Table 2.4 Optimized cartesian coordinates (atom, x, y, z) for (–)-C7'-epi-methylenebisdeoxoapodine (2.39).

O	-7.75900700	2.34401300	1.27063500	C	-6.53802400	2.50657900	1.22313200
O	-5.93132500	3.51853100	1.89742800	C	7.39747700	-0.96189100	1.48458100
C	-6.80698600	4.36084300	2.65758200	H	-7.32590700	3.78772100	3.43058000
O	8.35368900	-0.18563900	1.43295000	H	-7.55391000	4.82875400	2.01137100
O	7.33674900	-1.95016800	2.41546000	H	-6.16630600	5.11761400	3.11085700
C	8.44849400	-2.01207500	3.31762000	H	8.53296300	-1.08868200	3.89675800
C	-6.90995600	-3.82450600	-1.47211700	H	9.38306600	-2.16734400	2.77258500
C	-8.19110000	-3.43301200	-1.08126800	H	8.24575700	-2.85703300	3.97608600
C	-8.45135500	-2.12462700	-0.65436900	H	-6.73038500	-4.84610600	-1.79178200
C	-7.38658400	-1.23087600	-0.62909600	H	-9.00305300	-4.15398500	-1.10105600
C	-6.08896300	-1.60674100	-1.02551800	H	-9.44705700	-1.82365700	-0.34391600
C	-5.84998000	-2.90419900	-1.45294000	H	-4.85442500	-3.21516800	-1.75671200
N	-7.37624500	0.11055800	-0.22557100	H	-8.08417300	0.58935800	0.32220300
C	-6.09108300	0.58747000	-0.19340600	H	-3.83765000	2.51633700	1.34600800
C	-5.20649500	-0.36622800	-0.97556800	H	-3.68899900	2.23903100	-0.37914900
C	-5.60701600	1.67191500	0.47821900	H	-3.62914600	-1.55304000	-0.06572200
C	-4.10147400	1.81981500	0.54762300	H	-1.56828000	1.58821200	0.40497400
C	-3.41331900	0.44507200	0.78178900	H	-1.40398100	-1.44247400	0.63398000
C	-3.76146200	-0.50550700	-0.38823700	H	-0.85815400	0.10215100	-1.93476600
C	-1.85639500	0.62575900	0.85294200	H	-1.31930400	-1.59420900	-1.72717100
C	-1.08133800	-0.50938800	0.15091400	H	-3.57590100	-1.42769100	-3.06529400
C	-1.49091000	-0.57063000	-1.33950500	H	-3.05820400	0.19629700	-3.56286900
N	-2.87159100	-0.14804900	-1.49479800	H	-4.94277800	1.25224200	-2.44593600
C	-3.54740200	-0.36316200	-2.75640600	H	-5.71961300	-0.18931200	-3.13210600
C	-4.94946700	0.15895900	-2.44120500	H	-3.57821500	-1.20998600	2.19315300
C	-3.72545700	-0.12365400	2.18287400	H	-4.74831000	0.07927000	2.51040800
O	-1.50344100	0.64939000	2.24333700	H	-3.00374800	1.55519600	3.37358200
C	-2.67254100	0.55394700	3.05708700	H	-2.41535200	-0.01560400	3.95595500
C	0.43689800	-0.39471200	0.38666700	H	0.56597900	-0.26044300	1.46183900
C	4.72188700	3.80222300	-2.71513300	H	0.80970600	0.51392900	-0.10582800
C	5.98238200	4.23424200	-2.30054500	H	4.07520600	4.47422800	-3.27039800
C	6.83461400	3.39359900	-1.57331800	H	6.31048600	5.24189600	-2.53820900
C	6.37836400	2.11453600	-1.27507900	H	7.81193300	3.73373900	-1.24537700
C	5.11213600	1.65973200	-1.69014700	H	3.30100900	2.17189000	-2.74037500
C	4.28371400	2.50245800	-2.41605600	H	7.81979500	1.20278000	0.06470800
N	7.01885400	1.10115500	-0.55069300	H	5.08321400	-2.34154200	1.72700600
C	6.16105900	0.05204400	-0.34067300	H	4.96898000	-2.58796400	-0.00587700
C	4.98695800	0.19481600	-1.29098100	H	2.95030600	0.57097900	-0.63126500
C	6.24153800	-0.93162400	0.60083400	H	2.79369800	-2.96231900	0.65072600
C	5.02438300	-1.81576900	0.77197100	H	0.59055400	-2.50066800	0.07517500
C	3.71005100	-0.98324400	0.69433400	H	1.54804800	-2.58030800	-2.01306000
C	3.62770200	-0.29767700	-0.68691700	H	1.12783700	-0.86800400	-2.09971500
C	2.47804200	-1.93285700	0.86675700	H	3.23318700	-0.25769500	-3.48627000
C	1.25403400	-1.63577800	-0.04880700	H	3.65858800	-1.98090400	-3.55589100
C	1.72415900	-1.60780900	-1.53536800	H	5.71510200	-1.62283700	-2.29997900
N	3.14565400	-1.31763700	-1.62467900	H	5.70417200	-0.19760200	-3.35915800
C	3.72457600	-1.08223600	-2.93101400	H	2.88679000	0.78418300	1.67681500
C	5.16310500	-0.71736800	-2.56619900	H	4.51478700	0.38102000	2.23891100
C	3.56318000	-0.04518500	1.91052300	H	3.70406500	-1.52376900	3.51110900
O	2.08765000	-1.86359600	2.24156900	H	2.31824500	-0.42828200	3.69239700
C	2.93391700	-0.96202400	2.96106900				

Table 2.5 Optimized cartesian coordinates (atom, x, y, z) for C7,C7'-diepi-methylenebisdeoxoapodine (2.40).

O	7.27499100	-2.47433600	1.52234000	C	6.32908100	-2.63943000	0.74912000
O	5.84744700	-3.88083600	0.47504200	C	-6.32891200	2.63957800	0.74900500
C	6.51130400	-4.95781400	1.14794300	H	6.42466300	-4.85278600	2.23267900
O	-7.27484700	2.47457800	1.52221200	H	7.57189900	-4.98572500	0.88522400
O	-5.84719900	3.88093900	0.47487200	H	6.01135400	-5.86673700	0.81232400
C	-6.51098300	4.95798800	1.14773500	H	-7.57144900	4.98633600	0.88452900
C	5.79796600	4.16451700	1.69319400	H	-6.01057500	5.86681900	0.81254700
C	6.81798300	3.68147700	2.51404100	H	-6.42488200	4.85266500	2.23248100
C	7.26738700	2.35881500	2.41066700	H	5.46078400	5.19103800	1.79676300
C	6.65740100	1.54310300	1.46429700	H	7.27054500	4.33751000	3.25182700
C	5.63116400	2.01522500	0.62396600	H	8.05621600	1.98225700	3.05436100
C	5.20331600	3.32981900	0.73370700	H	4.40881900	3.71099700	0.09845800
N	6.90236300	0.19303800	1.18059600	H	7.40260000	-0.47260200	1.76122100
C	5.97051500	-0.28310500	0.29480300	H	4.02238000	-2.83004900	-0.64785200
C	5.27609500	0.90094300	-0.35197000	H	4.58163200	-1.68974900	-1.85715900
C	5.61558700	-1.57867400	0.05410600	H	3.16787700	1.36033000	-0.07944500
C	4.37546600	-1.80598200	-0.78553000	H	2.24668400	-1.64844200	-2.17539700
C	3.25474200	-0.79239400	-0.41557600	H	1.01203600	0.81328000	-0.86460100
C	3.76477200	0.64533300	-0.67220700	H	1.97673400	2.15591900	-2.52275200
C	1.97907900	-1.04925600	-1.29226300	H	2.23684600	0.81047900	-3.64473300
C	1.28849800	0.24640300	-1.75791100	H	4.51077000	2.83046100	-2.31042400
C	2.28485200	1.09395000	-2.58324400	H	4.83902600	1.69808900	-3.63854700
N	3.64208500	0.88015000	-2.11269400	H	6.24912900	0.29959200	-2.23459700
C	4.69901700	1.76515800	-2.55300600	H	6.73015900	1.92046600	-1.69152400
C	5.89400700	1.22282700	-1.76870700	H	2.22676000	-0.12790200	1.38847000
C	2.70975200	-1.03549900	1.00801700	H	3.48444100	-1.32946400	1.72065200
O	1.07346700	-1.82504500	-0.48562600	H	2.12952200	-3.12313900	0.75986800
C	1.66534700	-2.12494900	0.77884400	H	0.87131700	-2.13819600	1.53281400
C	0.00000100	-0.00021800	-2.57137100	H	0.17323600	-0.85915600	-3.23591600
C	-5.79829600	-4.16438000	1.69334400	H	-0.17324200	0.85860400	-3.23606500
C	-6.81827900	-3.68123300	2.51416900	H	-5.46119300	-5.19092300	1.79694900
C	-7.26758000	-2.35853900	2.41074800	H	-7.27089600	-4.33720500	3.25197500
C	-6.65752700	-1.54290600	1.46435300	H	-8.05638400	-1.98189800	3.05442500
C	-5.63131700	-2.01513600	0.62404600	H	-4.40910200	-3.71102200	0.09860300
C	-5.20357300	-3.32975800	0.73383300	H	-7.40261900	0.47285400	1.76117000
N	-6.90237500	-0.19283500	1.18061000	H	-4.02220000	2.82997400	-0.64800800
C	-5.97049300	0.28320900	0.29479800	H	-4.58153100	1.68961400	-1.85723300
C	-5.27615500	-0.90091200	-0.35192100	H	-3.16796700	-1.36043500	-0.07937200
C	-5.61547500	1.57874000	0.05404900	H	-2.24659500	1.64815300	-2.17550300
C	-4.37534900	1.80592000	-0.78561500	H	-1.01205600	-0.81353200	-0.86453000
C	-3.25468800	0.79228800	-0.41560700	H	-1.97687000	-2.15623400	-2.52258400
C	-3.76480900	-0.64542300	-0.67216600	H	-2.23686700	-0.81084900	-3.64466100
C	-1.97901500	1.04902800	-1.29232100	H	-4.51095200	-2.83057600	-2.31022300
C	-1.28849300	-0.24670100	-1.75787700	H	-4.83910200	-1.69828800	-3.63845000
C	-2.28490500	-1.09424600	-2.58315500	H	-6.24909700	-0.29954600	-2.23459800
N	-3.64213200	-0.88030900	-2.11264100	H	-6.73029800	-1.92035300	-1.69145700
C	-4.69912200	-1.76528400	-2.55290300	H	-2.22677300	0.12781700	1.38848400
C	-5.89407800	-1.22279800	-1.76866000	H	-3.48434600	1.32951600	1.72057600
C	-2.70967500	1.03543100	1.00796900	H	-2.12925900	3.12302100	0.75981300
O	-1.07338500	1.82486800	-0.48575700	H	-0.87111800	2.13794100	1.53269200
C	-1.66517900	2.12478700	0.77875100				

Chapter III

Progress Toward the Total Synthesis of Voacandimine A

Chapter III was done in collaboration with Dr. In-Soo Myeong. Dr. In-Soo Myeong developed parts of the synthetic route used in the study.

Introduction

The aspidosperma alkaloids are a structurally diverse family of monoterpene indole alkaloids containing over 200 members.[1] Aspidosperma alkaloids have a characteristic pentacyclic skeleton (Figure 3.1; rings A–E) containing multiple stereogenic centers and varying levels and sites of oxidation. Their complex molecular structures and biological activities have attracted significant interest and has prompted the development of innovative syntheses.[2]

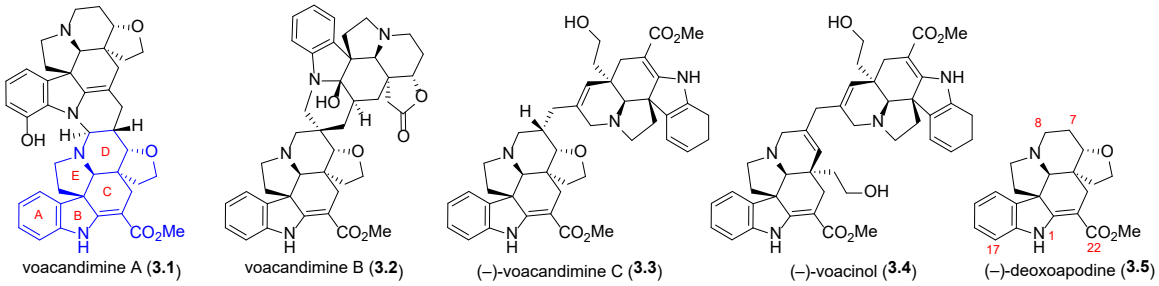

Figure 3.1 *Aspidosperma-Aspidosperma bisindole alkaloids isolated from Voacanga africana.*

Continuing the Movassaghi group's interest in the bisindole members of the Aspidosperma family[3,4], we recently reported the total synthesis of (−)-voacinol (**3.4**) and (−)-voacandimine C (**3.3**).[5] (See Chapter II). We then began to investigate the synthesis of voacandimine A (**3.1**), another bisindole alkaloid isolated along with alkaloids **3.3** and **3.4** from *Voacanga africana* in 2013.[6] The southern portion of the molecule contains a (−)-deoxoapodine (**3.5**)[7] subunit while the northern portion has C17′ oxygenation and a C22 methylene as opposed to the carbomethoxy group of (−)-deoxoapodine (**3.5**). Alkaloid **3.1** has a tridecacyclic skeleton with ten stereocenters, with 6 and 4 contiguous stereocenters. Alkaloid **3.1** also features a unique fused piperidine ring linkage found for the first time in aspidosperma alkaloids.[8]

Results and Discussion

Our initial retrosynthetic analysis for voacandimine A (**3.1**) is shown in Scheme 3.1. We envisioned nucleophilic attack on α,β-unsaturated imine **3.6** by enamine **3.8** and trapping of the resulting iminium by N1 of **3.6** would lead to voacandimine A (**3.1**). Imine **3.6** could come from the C22 reduction and subsequent dehydration of benzyl ether **3.7**. The C17 oxygenation could be introduced to (−)-deoxoapodine (**3.5**) via the iridium catalyzed borylation and oxidation strategy we have previously used in our group's syntheses of (+)-vallesine[9] and (−)-kopsifoline A[10]. Enamine **3.8** could be accessed through a dehydrative etherification of N-oxide **3.9**[11] or through in-situ generation via an aminonitrile surrogate similar to our approach used for (−)-voacinol (**3.4**)[5]. For a summary of the synthetic route to N-oxide **3.9**, see Scheme 2.2 and Scheme 2.3 in Chapter II. Both enantiomers were accessed over the course of this study from the enzymatic resolution steps.

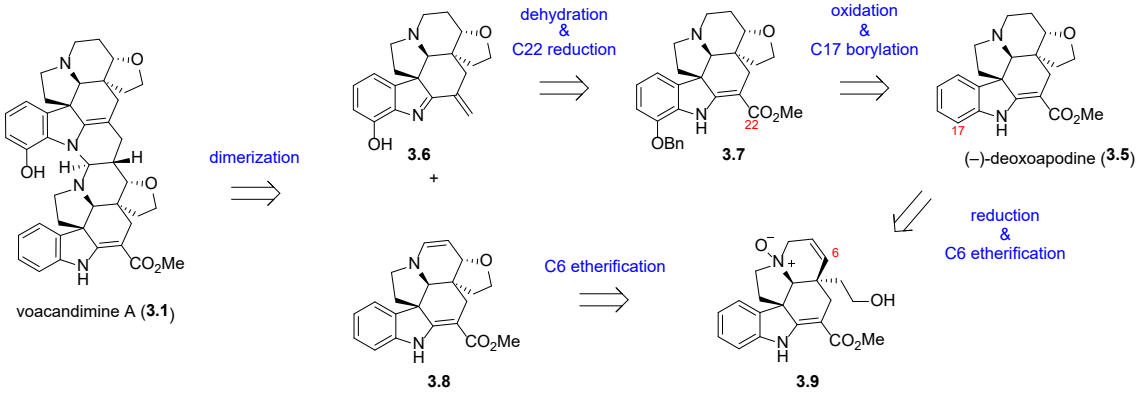

Scheme 3.1 *Initial voacandimine A retrosynthesis.*

Iridium catalyzed borylation of (–)-deoxoapodine (**3.5**) followed by oxidation with diethylhydroxylamine (DEHA) and protection of the resulting phenol with benzyl bromide gave C17 oxidized indoline **3.10** (Scheme 3.2). The vinylogous urethane of benzyl ether **3.10** proved to be highly resistant to neutral reduction conditions, such as DIBAL or LAH. In an attempt to make the ester more susceptible to reduction, the ester was removed from conjugation by

chlorination of C3 with NCS to form the α-chloro imine. There was some selectivity for the ester over the imine at decreased temperature; however, this approach was complicated due to overreduction and the need to remove the C3 chlorine. Ultimately, the vinylogous urethane was fully reduced using lithium borohydride to give alcohol **3.11**. The alcohol was then protected in order to oxidize the aniline to imine **3.12** using N-t-butylbenzenesulfinimidoyl chloride[12]. Subjecting the imine to trifluoroacetic acid led to net elimination of the silanol and the formation of α,β-unsaturated imine **3.13**. The free phenol **3.6** could be accessed via hydrogenation prior to TBS protection and a TBAF deprotection following formation of the unsaturated imine.

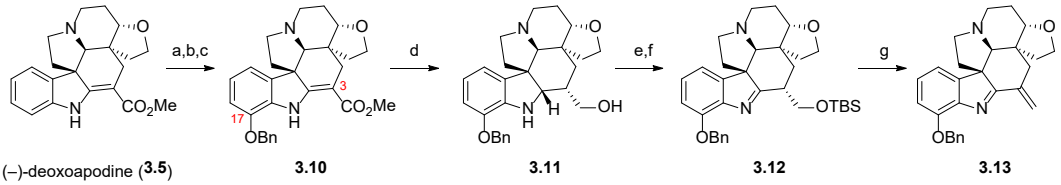

Scheme 3.2 *First generation α,β-unsaturated imine synthesis. Reagents and conditions: a) [Ir(cod)OMe]$_2$, dtbpy, HBpin, B$_2$pin$_2$, THF. 60 °C; b) DEHA, Et$_3$N, MeCN, 60 °C, 79% over two steps; c) Cs$_2$CO$_3$, benzyl bromide, acetone, 23°C, 73%; d) LiBH$_4$, THF, 23 °C, 97%; e) TBSCl, ImH, DMAP, DMF, 23 °C, 72%; f) N-t-butylbenzenesulfinimidoyl chloride, DBU, CH$_2$Cl$_2$, −78 °C, 85%; g) TFA, CH$_2$Cl$_2$, 23 °C, 67%.*

This approach to α,β-unsaturated imine **3.13** was able to provide material for initial dimerization studies, but it had a number of drawbacks. Material throughput was challenging due to starting with an already advanced intermediate. There were also the redox state adjustments and the extra protection/deprotection steps. Another issue was that the benzyl protecting group could not be removed from the dimer. Contemporaneously, Dr. In-Soo Myeong developed a new synthetic route for the C17 methoxy **3.14** (R=Me) during his studies of related aspidosperma alkaloids (Scheme 3.3).

Starting with primary alcohol (+)-**3.17**[13], a palladium catalyzed oxidative cyclization to form the F ring gave enamide **3.18** along with the uncyclized C8 imide (8%) as a side product (Scheme 3.4). Platinum (IV) oxide catalyzed hydrogenation and PMB deprotection using Birch

conditions gave indole (+)-**3.20**. Application of the iridium catalyzed borylation gave boronic ester (+)-**3.21**. Attempts at oxidation to the C17 phenol using DEHA or similar conditions

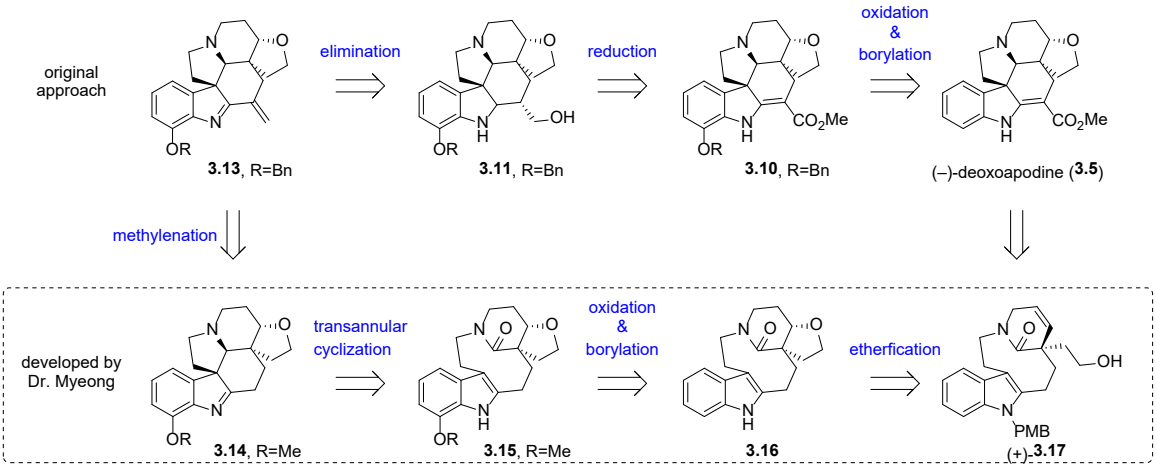

Scheme 3.3 *Retrosynthesis of α,β-unsaturated imine*

led to decomposition. A Chan-Lam coupling of the boronic ester with 4-methoxybenzyl alcohol to give the C17 ether proved to be an effective way to introduce the oxygenation. The PMB group was chosen to provide more options for removal over the benzyl group. Reductive transannular cyclization by partial amide reduction using DIBAL gave hexacyclic imine (−)-**3.23**. An unexpected complication was the undesired side product given by full amide reduction before the cyclization could occur which had not been observed under these conditions on related substrates. This was minimized by running the reaction in toluene at −78 °C. Initial attempts at performing a methylenation of imine **3.23** using Eschenmoser's salt led to the formation of an undesired adduct that was unable to be isolated to determine the structure. Triethylamine was found to be necessary to get formation of the desired C3 adduct **3.24**. Elimination of N,N-dimethylamine using acetic acid and heat gave α,β-unsaturated imine **3.25**.

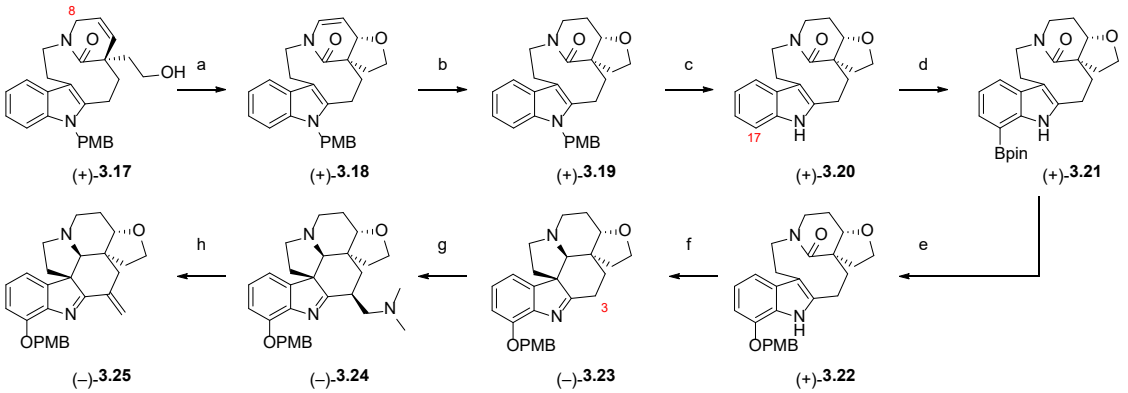

Scheme 3.4 *Second generation α,β-unsaturated imine synthesis. Reagents and conditions: a) $Pd(OAc)_2$, O_2, DMSO, 23 °C, 48%; b) PtO_2, H_2, MeOH, CH_2Cl_2, 23 °C, 83%; c) Na, NH_3, THF, −78 °C, 90%; d) $[Ir(cod)OMe]_2$, tmphen, HBpin, THF, 60 °C, 91%; e) $Cu(OAc)_2$, DMAP, PMBOH, CH_2Cl_2, 23 °C, 71%; f) DIBAL, toluene, −78 °C, 74%; g) Eschenmoser's salt, Et_3N, CH_2Cl_2, 23 °C, 96%; h) AcOH, 1,2-dichloroethane, 60 °C, 79%.*

After securing access to the requisite α,β-unsaturated imine, we turned our attention to gaining a better understanding of the key enamine **3.8** before commencing dimerization studies. There had been questions to its stability and isolation during our previous work. The aminonitrile surrogate had proven to be beneficial in order to access (−)-voacandimine C (**3.3**) with the correct stereochemistry in our prior report.[5] Initial attempts at using an aminonitrile for dimerization had limited success. The initial major product of the Polonovski-Potier/dehydrative cyclization reaction sequence (Scheme 3.5) is indeed enamine **3.8**, which has been characterized by 2D NMR on the crude reaction mixture after aqueous bicarbonate workup but before chromatography. However, upon column chromatography on either silica or basic alumina, **3.8** undergoes self-dimerization to give a mixture of C8′ epimers of enamine **3.26**. The reversibility of the dimerization was examined to see if the dimer would be a competent enamine surrogate. A mixture of C8′ epimers of enamine **3.26** (~1.7:1 C8′*R*:C8′*S* by NMR) was dissolved in 20% trifluoroethanol in dichloroethane for 22 hours. Upon concentration and redissolving in chloroform, the ratio had changed to ~8:1 C8′*R*:C8′*S.* This experiment along with calculations (C8′*S* is 1.37 kcal/mol higher in energy) suggests that the *R* isomer is the thermodynamically preferred product. Additionally, when a mixture of epimers of enamine **3.26** was dissolved in

trifluoroethanol-d_3 for 26 hours, double deuterium incorporation at C7′ as well as N1 and N1′ prime was observed by LC-MS and NMR. Exact amount of incorporation was unable to be determined due to the mixture of epimers present; however for C8′*R*-**3.26**, the C8′H signal went from a doublet of doublet to a singlet and one of the C7′H_2 signals appeared to go away. The other C7′H_2 is overlapped with other signals so no conclusive determination could be made. Mechanistically, both of the observations can be explained by the dimer breaking apart in solution and reforming. Additionally, small amounts of monomeric enamine **3.8** can be observed in the NMR.

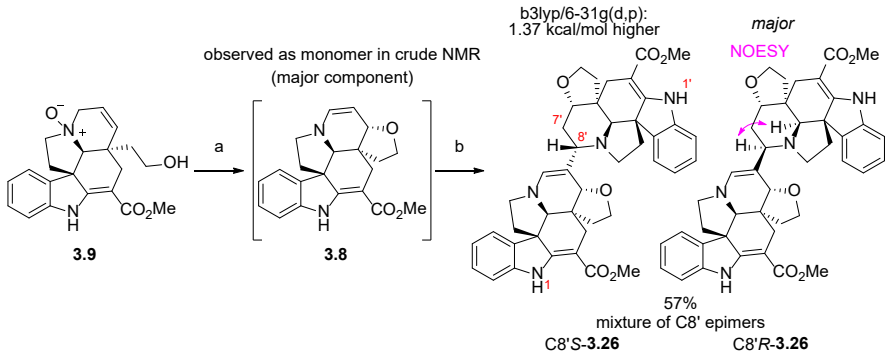

Scheme 3.5 *Enamine dimer synthesis. Reagents and conditions: TFAA, CH_2Cl_2, 23 °C; DBU, MeOH; b) silica or alumina column chromatography.*

In the process of investigating the above reaction, a number of other side products were observed that had previously not been observed (Scheme 3.6). Work done using the enantiomer of N-oxide **3.9**, prepared as described from alcohol (−)-**17**, resulted in a number of undesired products. On one occasion, the side products accounted for ~57% of the material. The formation of enamine **3.28** and C19 hemiaminal **3.29** along with the desired enamine **3.26** suggested that the Polonovski-Potier reaction was not completely regioselective under the reaction conditions. The expected product should be the C8 iminium formation based off of prior work and the presence of the C6-C7 alkene.[14] However, enamine **3.28** was evidence for the C10 iminium formation; ether **3.29** showed C19 iminium formation. Another issue was the formation of the

methylene bridged bisenamine **3.27**. Methanol was hypothesized to be the source of the methylene. Modification of the reaction conditions by changing solvents and incorporation of DTMBP led to only products from the desired iminium regioisomer being observed and elimination of the methylene bridged product. Enamine **3.30** is formed as a side product; however, the C8′ connection of enamine **3.30** is evidence of the desired iminium formation. Based on the observations of **3.26**, **3.30** was found to readily be converted to desired enamine **3.26** by dissolving in a 1:1 mixture of trifluoroethanol and dichloromethane overnight.

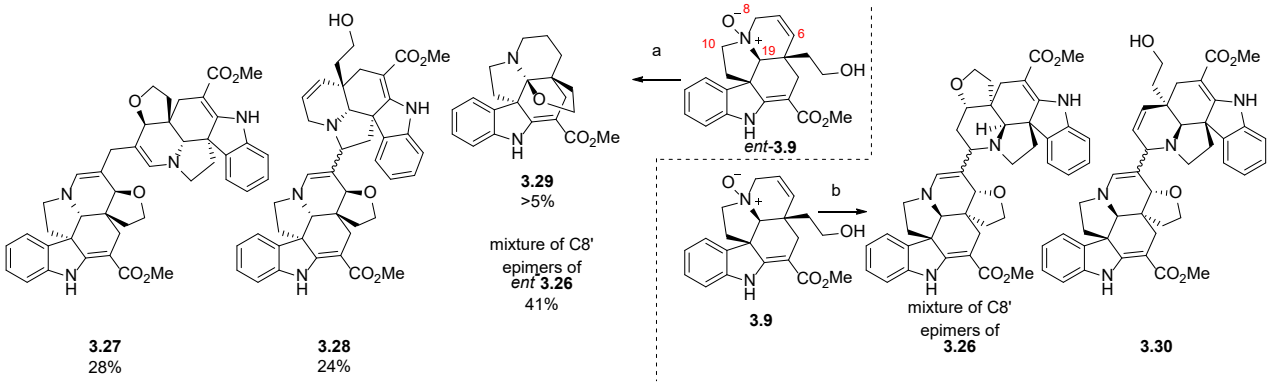

Scheme 3.6 *Dehydrative cyclization of 3.9. Reagents and conditions: a) TFAA, CH_2Cl_2, 0 to 23 °C; MeOH; DBU; b) TFAA, DTBMP, 1,2-dichloroethane, 23 °C; EtOH; DBU, 45% of 3.26, 32% of 3.30.*

The dimerization of unsaturated imine **3.25** and enamine **3.26** promoted by trifluoroethanol proceeds to give a single cis-fused product **3.31** (Scheme 3.7). Benzyl and TBS protecting groups were briefly examined. The benzyl group was unable to be removed, and the TBS group led to a much slower reaction. We also explored the reaction using the free phenol **3.6**, but there was no observed product formation. The rate of the reaction can be accelerated by adding a Lewis acid such as scandium (III) triflate; however, this also leads to undesired self-dimerization of the α,β-unsaturated imine. The stereochemistry of the product was initially challenging to determine. There was a clear NOESY correlation between the C8H and C19H to confirm the C8 stereocenter. The complication was that there were correlations of approximately the same magnitude between the C7H and C8H and the C7H and C6H with C6H and C8H being

on opposite faces of the D ring. The conclusive correlation was the NOESY correlation between a C4H and a C22H. The protons are 6 bonds apart and can only be in close proximity if the molecule is in a folded conformation. This is only possible with a C7-C8 *cis* ring fusion.

Hydrogenation and DDQ oxidation were not effective in removing the PMB group. Deprotection of the phenol using trifluoromethanesulfonic acid led to the formation of C7-*epi*-voacandimine A (**3.32**). A number of acidic and basic conditions were explored to see if the C8 aminal could be opened and subsequently closed to affect isomerization of the C7 stereocenter through a transiently formed enamine. With the conditions explored, there was no observed evidence of reaction. Deuterium sources were also examined to see if deuterium incorporation could be observed with no success.

The only successful attempt at observing ring opening was when subjecting tridecacycle *ent*-**3.32** to TMSCN in hexafluoroisopropanol. Aminonitrile **3.33** was isolated as a single diastereomer. Subjecting aminonitrile **3.33** to zinc triflate and deuterated methanol for 4.5 hours led to ~100% C7 deuterium incorporation. This was reversible by using methanol as the solvent. This supported that upon aminonitrile activation with zinc that the enamine was being accessed. However, there was no evidence of isomerization. Tridecacycle *ent*-**3.32** could be reformed by subjecting the aminonitrile **3.33** to zinc triflate in dichloromethane and acetonitrile.

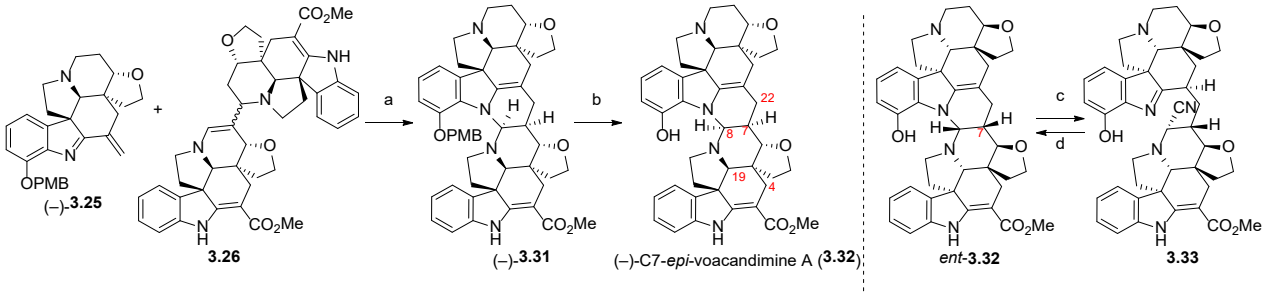

Scheme 3.7 *1st generation synthesis of C7-epi-voacandimine A. Reagents and conditions: a) 1,2 dichloroethane, TFE, 23 °C, 44%; b) TfOH, CH_2Cl_2, 23 °C, 55%; c) TMSCN, H_2O, HFIP, 23 °C, 93%; d) $Zn(OTf)_2$, CH_2Cl_2, MeCN, 23 °C, 58%.*

The cyclization of aminonitrile **3.33** to give the cis-fused tridecacycle **3.32** along with work by Dr. Myeong inspired a new strategy to arrive at voacandimine A (**3.1**) (Scheme 3.8). A stereo-controlled cyclization of a dimeric compound with no C7 or C8 stereochemical information could give voacandimine A. We had seen that it was possible to get cyclization of the aminonitrile, but there was a question whether the initial stereochemistry was biasing the outcome. Dr. Myeong had developed a method to arrive at a methylene bridged dimer of the type like dodecacycle **3.34**. The approached used a reversed nucleophile-electrophile pair. Nucleophilic attack by the enamine tautomer of imine **3.36** on conjugated iminium **3.35**, a proposed intermediate from our (−)-voacinol synthesis[5], could give an enamine **3.34** with no C7 or C8 stereochemistry.

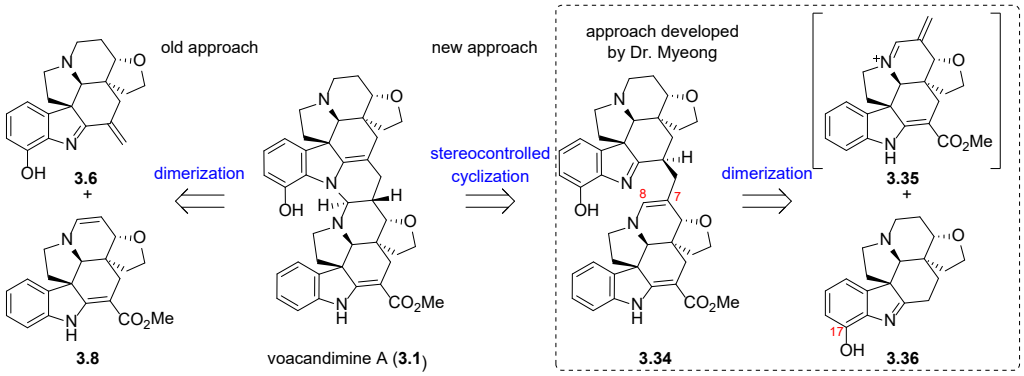

Scheme 3.8 *New voacandimine A retrosynthesis.*

Similarly to the dimer, C17 ether (−)-**3.23** was deprotected using triflic acid to give phenol (−)-**3.36** (Scheme 3.9). Initial dimerization reactions were performed using the crude Eschenmoser's salt monomeric adduct of enamine **3.26**. There were some problems with reproducibility, but it was not possible to isolate the adduct using chromatography. In order to improve the reliability of the reaction, a morpholine adduct was examined in place of the dimethyl amine. Depending on the column eluent, it was possible to isolate either the morpholine adduct or, with methanol in dichloromethane, the methoxy adduct **3.37**. Both adducts were

evaluated for use as conjugated iminium precursors. The dimerization was more reliable with both of the adducts. However, the morpholine adduct also led to the formation of side products resulting from the expulsion of the methylenemorpholinium ion. Similar side products were not observed with methoxy methylene adduct **3.37**. Unlike the earlier dimerization, the new approach was compatible with either the C17 ether or C17 phenol. Unfortunately, treatment of enamine **3.34** with trifluoroacetic acid led to the *cis*-fused tridecacycle **3.32**.

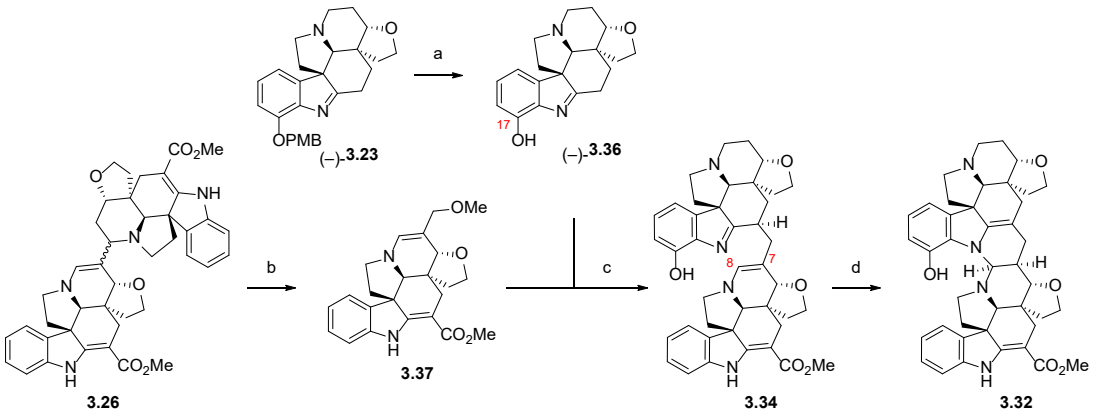

Scheme 3.9 *2nd generation synthesis of C7-epi-voacandimine A. Reagents and conditions: a) TfOH, CH_2Cl_2, 23 °C, 95%; b) Eschenmoser's salt, CH_2Cl_2, 23 °C; morpholine; silica column with 2 to 4% MeOH in CH_2Cl_2, 89%; c) AcOH, 1,2-dichloroethane, TFE, 23 °C,48%; d) TFA, CH_2Cl_2, 23 °C, 27%.*

Numerous attempts at affecting a stereocontrolled cyclization of enamine **3.34** were attempted. A variety of BINOL derived chiral phosphoric acids were examined to try and affect the stereochemistry via chiral acid catalysis.[15] There was little to no evidence of stereochemical control for the C7 protonation either *R* or *S* acids. The chiral acids were also examined for the dimerization reaction with no real success. It could be a problem of finding a specific catalyst with an active site to match the complex substrate. One interesting side product, *trans*-fused tridecacycle **3.38**, was observed over a number of attempted cyclizations ranging from <5% to ~50% (Figure3.2). Column fractions from multiple reactions containing the product were combined to be able to isolate and determine the structure of the side product. Since being

identified, tridecacycle **3.38** has also been observed as a minor side product (0-10%) in the dimerization reaction above.

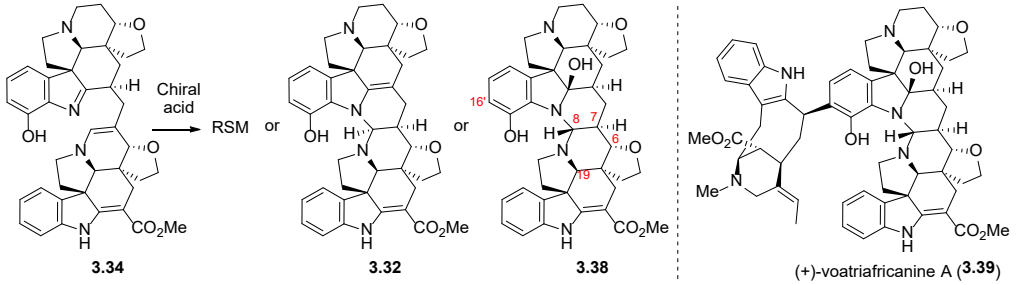

Figure 3.2 *Products observed from stereocontrolled cyclization attempts.*

The key C7 and C8 stereocenters of tridecacycle **3.38** were determined by ROESY correlations. There was a correlation between the C7H and C19H, and there was a correlation between C6H and C8H. Both the C7 and C8 stereocenters are opposite those found in voacandimine A (**3.1**) in addition to the hydration of the C2′-C3′ alkene. This was particularly interesting because tridecacycle **3.38** maps onto the monoterpene trisindole alkaloid, (+)-voatriafricanine A (**3.39**).[16] Alkaloid (+)-**3.39** was isolated in 2021 from the stem bark of *Voacanga africana.* It is a vobasine-Aspidosperma-Aspidosperma type alkaloid that has shown antimycobacterial activity against *M. smegmatis*, *M. abscessus*, and *M. bovis BCG* (MIC: 25 μg/mL). C16′ functionalization of tridecacycle **3.38** with a vobasine unit could lead to the synthesis of (+)-voatriafricanine A.

With little success in controlling both stereocenters in the same reaction, we thought about ways to set each stereocenter in separate reactions. Inspired by the oxolane ring opening used in our synthesis of (−)-voacinol (**3.4**), TFAA was used to open the southern oxolane ring, forming the conjugated iminium that was then trapped by the N1′ imine to give trifluoroacetate **3.40** with the desired C8 stereochemistry as determined by a ROESY correlation between C8H and C19H (Scheme 3.10). The C2′ hydration happens upon workup of the reaction; longer

reaction times leads to C2′-C3′ unsaturation. Trifluoroacetate **3.40** provides an opportunity to set the last stereocenter when reforming the oxolane ring of the southern portion. The C6-O bond should only be able to form on the bottom face of the ring based off the C5 stereocenter. The desired face for the C7H is the top face of the D ring. One initial observation from work done on trifluoroacetate *ent*-**3.40** is that the C2′ alcohol versus the C2′-C3′ unsaturated compound appears to be important for reactivity of the C6-C7 alkene. Our observations suggest that the more electron rich C2′-C3′ alkene reacts faster the C6-C7 alkene towards electrophiles, and the hydration of the C2′-enamine to the C2′-alcohol presents a single alkene for selective chemistry.

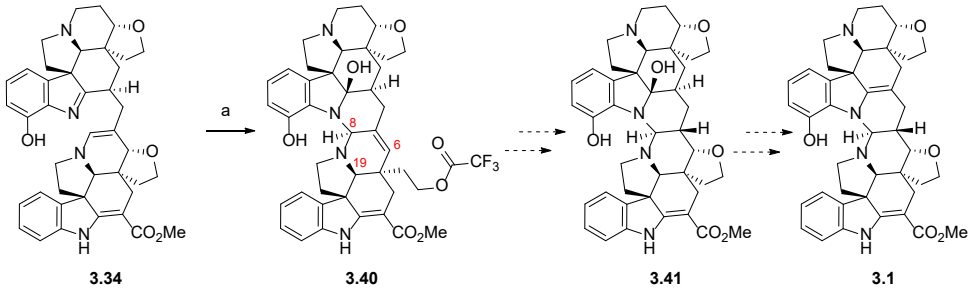

Scheme 3.10 *New late-stage approach. Reagents and conditions: a) TFAA, CH_2Cl_2, 23 °C, 15%.*

Conclusion

In conclusion, we have demonstrated two different approaches for complex fragment assembly of Aspidosperma monomers of *en route* to voacandimine A (**3.1**). We have accessed an epimer of the natural product, (−)-C7-epi-voacandimine A **(3.32)**, from both a formal [4+2] approach and through acid promoted cyclization of a dodecacyclic methylene bridged dimeric intermediate. Attempts thus far at affecting a C7 epimerization have proven futile; however, our new strategy of setting one stereocenter at a time provides new opportunities for stereochemical control. We hope to apply these learnings to the first total synthesis of voacandimine A (**3.1**). Additionally during the course of our investigations, we have identified a recurring key minor side product (<10%), (−)-C7,C8-diepi-C2′,C3′-hydrovoacandimine A (**3.38**), which is a subunit of the trisindole alkaloid, voatriafricanine A (**3.39**).

References

1. (a) Cordell, G. A. The Aspidosperma Alkaloids. In *The Alkaloids: Chemistry and Physiology*; Manske, R. H. F., Rodrigo, R. G. A., Eds.; Academic Press: New York, 1979; Vol. 17, pp 199−384. (b) Saxton, J. E. Alkaloids of the Aspidospermine Group. In *The Alkaloids: Chemistry and Biology*; Cordell, G. A., Ed.; Academic Press: San Diego, 1998; Vol. 51, pp 1−197.

2. For reviews on syntheses of *Aspidosperma* alkaloids: (a) Saxton, J. E. Synthesis of the Aspidosperma Alkaloids. In *The Alkaloids: Chemistry and Biology*; Cordell, G. A., Ed.; Academic Press: San Diego, 1998; Vol. 50, pp 343−376. (b) Saya, J. M.; Ruijter, E.; Orru, R. V. A. Total Synthesis of *Aspidosperma* and *Strychnos* Alkaloids through Indole Dearomatization. *Chem. Eur. J.* **2019**, 25, 8916–8935. (c) Zhao, S.; Sirasani, G.; Andrade, R. B. *Aspidosperma* and *Strychnos* alkaloids: Chemistry and biology. In *The Alkaloids: Chemistry and Biology*; Knölker, H.-J., Ed.; Academic Press: San Diego, 2021; Vol. 86, pp 1−143 and references cited therein.

3. Medley, J. W.; Movassaghi, M. A Concise and Versatile Double-Cyclization Strategy for the Highly Stereoselective Synthesis and Arylative Dimerization of Aspidosperma Alkaloids. *Angew. Chem. Int. Ed*. **2012**, *51*, 4572–4576.

4. Mewald, M.; Medley, J. W.; Movassaghi, M. Concise and Enantioselective Total Synthesis of (–)-Mehranine, (–)-Methylenebismehranine, and Related *Aspidosperma* Alkaloids. *Angew. Chem. Int. Ed.* **2014**, *53*, 11634–11639.

5. Flynn, K. M.; Myeong, I.-S.; Pinto, T.; Movassaghi, M. "Total Synthesis of (−)-Voacinol and (−)-Voacandimine C" *J. Am. Chem. Soc.* **2022***,* 144, 9126–9131.

6. Kitajima, M.; Iwai, M.; Kogure, N.; Kikura-Hanajiri, R.; Goda, Y.; Takayama, H. Aspidosperma–Aspidosperma-Type Bisindole Alkaloids from *Voacanga Africana*. *Tetrahedron* **2013**, *69*, 796–801.

7. (a) Iglesias, R.; Diatta, L. Deoxoapodine, A New Alkaloid of *Tabernaemontana* Species. *Rev. CENIC Cienc. Fis.* **1975**, *6*, 135–139. (b) Bui, A.-M.; Das, B. C.; Potier, P. Étude chimiotaxonomique de *Hazunta modesta*. *Phytochemistry* **1980**, *19*, 1473–1475.

8. (a) Kam, T.-S.; Choo,Y. -M. Bisindole Alkaloids. In *The Alkaloids: Chemistry and Biology*; Cordell, G. A., Ed.; Academic Press, 2006; Vol. 63, pp 181−337. (b) Kitajima, M.; Takayama, H. Monoterpenoid Bisindole Alkaloids. In *The Alkaloids: Chemistry and Biology*; Knölker, H.-J. Ed.; Academic Press, 2016; Vol. 76, pp 259−310.

9. Antropow, A. H.; Garcia, N. R.; White, K.; Movassaghi, M. Enantioselective Synthesis of (−)-Vallesine: Late-Stage C17-Oxidation via Complex Indole Boronation. *Org. Lett.* **2018**, *20*, 3647–3650.

10. Myeong, I.-S., Avci, N. H.; Movassaghi, M. Total Synthesis of (−)-Kopsifoline A and (+)-Kopsifoline. *Org. Lett*. **2021**, *23*, 9118–9122.

11. Kang, T.; White, K. L.; Mann, T. J.; Hoveyda, A. H.; Movassaghi, M. Enantioselective Total Synthesis of (−)-Deoxoapodine. *Angew. Chem. Int. Ed*. **2017**, *56*, 13857.

12. (a) Mukaiyama, T.; Matsuo, J.-i.; Yanagisawa, M. A New and Efficient Method for Oxidation of Various Alcohols by Using N-tert-Butyl Phenylsulfinimidoyl Chloride. *Chem. Lett*. **2000**, *29*, 1072-1073. (b) Mukaiyama, T.; Kawana, A.; Fukuda, Y.; Matsuo, J.-I. Oxidation of Various Secondary Amines to Imines with N-tert-Butylphenylsulfinimidoyl Chloride. *Chem. Lett*. **2001**, *30*, 390-391

13. White, K. L.; Movassaghi, M. Concise Total Syntheses of (+)-Haplocidine and (+)-Haplocine via Late-Stage Oxidation of (+)-Fendleridine Derivatives. *J. Am. Chem. Soc*. **2016**, *138*, 11383–11389.

14. Grierson, D.; The Polonovski Reaction. *Organic Reactions*. 1990, 85–295.

15. (a) Mahlau, M.; List, B. Asymmetric Counteranion-Directed Catalysis: Concept, Definition, and Applications. *Angew. Chem. Int. Ed*. **2012**, *52,* 518–533. (b) Parmar, D.; Sugiono, E.; Raja, S.; Rueping, M.; Complete Field Guide to Asymmetric BINOL-Phosphate Derived Brønsted Acid and Metal Catalysis: History and Classification by Mode of Activation; Brønsted Acidity, Hydrogen Bonding, Ion Pairing, and Metal Phosphates. *Chem. Rev*. **2014**, *114*, 9047–9153.

16. Fouotsa, H.; Le Pogam, P.; Mkounga, P.; Lannang, A. M.; Bernadat, G. Vanheuverzwijn, J.; Zhou, Z.; Leblanc, K; Rharrabti, S.; Nkengfack, A. E.; Gallard, J.-F.; Fontaine, V.; Meyer, F.; Poupo, E. Beniddir, M. H. Voatriafricanines A and B, Trimeric Vobasine-Aspidosperma-Aspidosperma Alkaloids from *Voacanga africana*. *J. Nat. Prod*. **2021**, *84*, 2755–2761.

Experimental Details

General Procedures. All reactions were performed in oven-dried or flame-dried round-bottom flasks fitted with rubber septa and were conducted under positive argon pressure using standard Schlenk techniques, unless noted otherwise. Cannulae or gas-tight syringes with stainless steel needles were used to transfer air- or moisture-sensitive liquids. Where necessary (so noted), solutions were degassed by sparging with argon for a minimum of 10 min. Flash column chromatography was performed as described by Still et al.[1] using granular silica gel (60-Å pore size, 40–63 μm, 4–6% H_2O content, Zeochem) or basic alumina (70% between 0.063–0.200 mm particle size, pH value (10% suspension): 8.5–10.5). Analytical thin layer chromatography (TLC) was performed using glass plates pre-coated with 0.25 mm 230–400 mesh silica gel impregnated with a fluorescent indicator (254 nm) or 0.21–0.27 mm basic alumina impregnated with a fluorescent indicator (254 nm). TLC plates were visualized by exposure to short wave ultraviolet light (254 nm) and irreversibly stained by treatment with an aqueous solution of ceric ammonium molybdate (CAM) or an aqueous solution of potassium permanganate ($KMnO_4$) followed by heating (~ 1 min) on a hot plate (~250 ºC). Organic solutions were concentrated at 30–35 °C on rotary evaporators capable of achieving a minimum pressure of ~10 Torr.

Materials. Commercial reagents and solvents were used as received with the following exceptions: acetonitrile, dichloromethane, *N*,*N*-dimethylformamide, methanol, tetrahydrofuran, toluene, and triethylamine were purchased from Sigma-Aldrich and were purified by the method of Grubbs et al. under positive argon pressure.[2] Deuterated solvents used for nuclear magnetic resonance (NMR) spectroscopy were purchased from Cambridge Isotope Laboratories, Inc. and were used as received with the exception of chloroform-*d*, which was stored over granular anhydrous potassium carbonate. 4-(Dimethylamino)pyridine was purchased from Chem-Impex International. All other solvents and chemicals were purchased from Sigma-Aldrich.

Instrumentation. Proton nuclear magnetic resonance (^{1}H NMR) spectra were recorded with a Bruker AVANCE NEO 600 or a Bruker AVANCE NEO 500 spectrometer. Spectra were processed with MestReNova 14.1.2 using the automatic phasing and third-order polynomial baseline correction capabilities. Chemical shifts are recorded in parts per million on the δ scale and are referenced from the residual protium in the NMR solvent ($CHCl_3$: δ 7.26, CD_2HCN: δ 1.94, C_6D_6: δ 7.16).[3] Data are reported as follows: chemical shift [multiplicity (s = singlet, d = doublet, t = triplet, q = quartet, m = multiplet, br = broad), coupling constant(s) in Hertz, integration, assignment]. Carbon-13 nuclear magnetic resonance (^{13}C NMR) spectra were recorded with a Bruker AVANCE NEO 600 or a Bruker AVANCE NEO 500 spectrometer and are recorded in parts per million on the δ scale and are referenced from the carbon resonances of the solvent ($CDCl_3$: δ 77.16, CD_3CN: δ 118.26, C_6D_6: δ 128.06).[4] Data are reported as follows: chemical shift (assignment). Infrared data were obtained with a Perkin−Elmer 2000 FTIR and are reported as follows: frequency of absorption (cm^{-1}) [intensity of absorption (s = strong, m = medium, w =

[1] Still, W. C.; Kahn, M.; Mitra, A. *J. Org. Chem.* **1978**, *43*, 2923.
[2] Pangborn, A. B.; Giardello, M. A.; Grubbs, R. H.; Rosen, R. K.; Timmers, F. *Organometallics* **1996**, *15*, 1518.
[3] (a) Gottlieb, H. E.; Kotlyar, V.; Nudelman, A. *J. Org. Chem.* **1997**, *62*, 7512; (b) Fulmer, G. R.; Miller, A. J. M.; Sherden, N. H.; Gottlieb, H. E.; Nudelman, A.; Stoltz, B. M.; Bercaw, J. E.; Goldberg, K. I. *Organometallics* **2010**, *29*, 2176.

weak, br = broad)]. Optical rotations were measured on a Jasco P2000 polarimeter with a sodium lamp and are reported as follows: [α]λ T °C (c = g/100 mL, solvent). High-resolution mass spectra (HRMS) were recorded on a Bruker Daltonics APEXIV 4.7 Tesla FT-ICR-MS using electrospray ionization (ESI) source, a Q-TOF LC/MS using ESI or direct analysis in real time (DART) ionization source. LC-MS analysis and mass-directed semi-preparative HPLC were performed on an Agilent Technologies 1260 Infinity II series instrument equipped with an Agilent 6125B single quadrupole MSD, a diode array detector, and a multicolumn compartment thermostatted to 35 °C.

Positional Numbering System. At least two numbering systems exist in the literature for the aspidosperma alkaloids.[4,5] For direct comparison between structures, the numbering system shown below for (–)-deoxoapodine (**3.5**) and (–)-voacandimine A (**3.1**)[6] is used throughout this report.

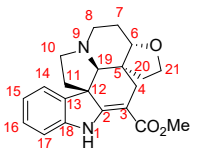

(–)-deoxoapodine (**3.5**)

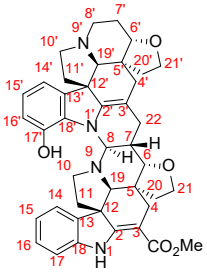

voacandimine A (**3.1**)

Respective Contributions

Dr. In-Soo Myeong developed the initial procedures and performed the characterization of **3.18**, **3.19**, and **3.20**. All of the experimental procedures were executed by myself.

---

[4] Saxton, J. E. Alkaloids of the Aspidospermine Group. In *The Alkaloids, Chemistry and Biology*, *Vol 51* (Ed.: Cordell, G. A.), Academic Press, San Diego, **1998**, pp 1−197.

[5] Zhou, Y.-G.; Wong, H. N. C.; Peng, X.-S. *J. Org. Chem.* **2020**, *85*, 967.

[6] Kitajima, M.; Iwai, M.; Kogure, N.; Kikura-Hanajiri, R.; Goda, Y.; Takayama, H. Aspidosperma–Aspidosperma-Type Bisindole Alkaloids from *Voacanga Africana*. *Tetrahedron* **2013**, *69*, 796–801.

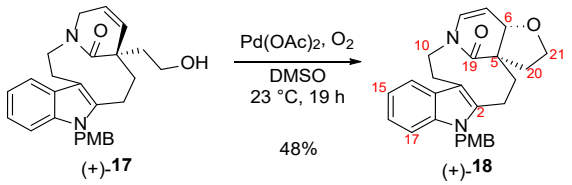

enamide (+)-3.18:

Palladium (II) acetate (177 mg, 788 μmol, 0.10 equiv) was added to a solution of (+)-**3.17**[7] (3.39 g, 7.87 mmol, 1 equiv) in dimethyl sulfoxide (150 mL) at 23 °C under argon. The reaction flask was evacuated and backfilled with an atmosphere of oxygen gas (balloon). After 19 h, the reaction mixture was opened to air, and then water (150 mL) was added to the reaction mixture. The layers were separated, and the aqueous layer was further extracted with ethyl acetate (3 × 50 mL). The combined organic extracts were dried over anhydrous sodium sulfate, were filtered, and were concentrated under reduced pressure. The residue was purified by flash column chromatography on silica gel (eluent: 75% ethyl acetate in hexanes to 100% ethyl acetate) to afford enamide (+)-**3.18** (1.6365 g, 3.80 mmol, 48%) as a residue. Structural assignments were made using additional information from gCOSY, gHSQC, and gHMBC experiments. Additional ^{13}C signals were identified from gHSQC, and gHMBC.

^{1}H NMR (500 MHz, $CDCl_3$, 25 °C): δ 7.56–7.48 (m, 1H, C_{14}**H**), 7.12–7.01 (m, 3H, C_{15}**H**, C_{16}**H**, C_{17}**H**), 6.86–6.81 (m, 2H, Ar_{PMB}**H**), 6.80–6.76 (m, 2H, Ar_{PMB}**H**), 6.30 (br s, 1H, C_8**H**), 5.43 (br s, 1H, C_7**H**), 5.29 (d, J = 17.3 Hz, 1H, N_1CH_a), 5.12 (d, J = 17.0 Hz, 1H, N_1CH_b), 4.45 (ddd, J = 13.1, 11.2, 2.2 Hz, 1H, $C_{10}H_a$), 3.87 (d, J = 4.7 Hz, 1H, C_6H_a), 3.74 (s, 3H, OCH_3), 3.72–3.67 (m, 2H, $C_{21}H_2$), 3.22–3.07 (m, 2H, $C_{10}H_b$, $C_{11}H_a$), 2.87 (dd, J = 15.8, 10.9 Hz, 1H, C_3H_a), 2.82–2.71 (m, 3H, C_3H_b, $C_{11}H_b$, $C_{20}H_a$), 2.31 (t, J = 12.3 Hz, 1H, C_4H_a), 1.97 (dd, J = 13.8, 8.2 Hz, 1H, C_4H_b), 1.66 (dt, J = 12.8, 8.4 Hz, 1H, $C_{20}H_b$).

^{13}C NMR (125.8 MHz, $CDCl_3$, 25 °C): δ 172.8 (**C**$_{19}$), 158.9 (**C**OCH_3), 137.0 (**C**$_2$), 136.6 (**C**$_{13}$), 133.7 (**C**$_8$), 129.9 (N_1CH_2**C**), 127.5 (**C**$_{18}$), 127.2 (Ar_{PMB}), 121.6 (**C**$_{15}$), 119.4 (**C**$_{16}$), 117.9 (**C**$_{14}$), 114.2 (Ar_{PMB}), 109.8 (**C**$_{17}$), 109.5 (**C**$_{12}$), 102.8 (**C**$_7$), 80.2 (**C**$_6$), 65.2 (**C**$_{21}$), 55.4 (O**C**H_3), 50.3 (**C**$_5$), 47.7 (**C**$_{10}$), 46.2 (N_1**C**H_2), 39.7 (**C**$_4$), 37.7 (**C**$_{20}$), 24.8 (**C**$_{11}$), 20.4 (**C**$_3$).

FTIR (thin film) cm^{-1}: 2932 (br), 1670 (s), 1512 (s), 1468 (m), 1248 (s), 1176 (m), 1036 (m), 747 (s).

---

[7] (a) Mewald, M.; Medley, J. W.; Movassaghi, M. *Angew. Chem. Int. Ed.* **2014**, *53*, 11634.; (b) White, K. L.; Movassaghi, M. *J. Am. Chem. Soc.* **2016**, *138*, 11383.

HRMS (DART) (*m/z*):	calc'd for $C_{27}H_{29}N_2O_3$ $[M+H]^+$: 429.2173, found: 429.2162.
$[\alpha]_D^{20}$:	+65.0 (*c* = 0.50, $CHCl_3$).
TLC (30% acetone in hexanes), R*f*:	0.40 (UV, CAM).

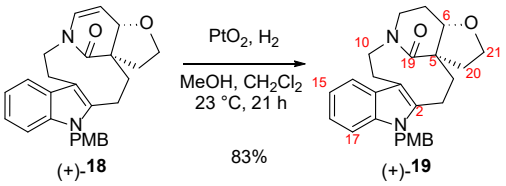

pentacyclic lactam (+)-3.19:

Platinum dioxide (87 mg, 0.38 μmol, 0.10 equiv) was added as a solid to a solution of enamide (+)-**3.18** (1.6365 g, 3.80 mmol, 1 equiv) in methanol (75 mL) and dichloromethane (75 mL) at 23 ºC. The reaction mixture was purged with hydrogen gas for 5 min and then stirred under an atmosphere of hydrogen gas (balloon) at 23 ºC. After 21 h, the reaction mixture was opened to air and filtered over Celite. The solids were rinsed with acetone (100 mL), and the combined filtrates were concentrated under reduced pressure. The resulting residue was purified by flash column chromatography on silica gel (eluent: 20% acetone in hexanes to 30% acetone in hexanes) to afford lactam (+)-**3.19** (1.3634 g, 3.17 mmol, 83%) as a residue. Structural assignments were made using additional information from gCOSY, gHSQC, and gHMBC experiments.

^{1}H NMR (500 MHz, CD_3CN, 25 °C):	δ 7.54–7.49 (m, 1H, C_{14}**H**), 7.12–7.06 (m, 1H, C_{17}**H**), 7.05–6.99 (m, 2H, C_{15}**H**, C_{16}**H**) 6.90–6.84 (m, 2H, Ar_{PMB}**H**), 6.82–6.76 (m, 2H, Ar_{PMB}**H**), 5.35 (d, *J* = 17.0 Hz, 1H, N_1C**H**$_a$), 5.15 (d, *J* = 17.0 Hz, 1H, N_1C**H**$_b$), 4.25–4.15 (m, 1H, C_{10}**H**$_a$), 3.94 (br s, 1H, C_6**H**$_a$), 3.76–3.64 (m, 2H, C_{21}**H**$_2$) 3.71 (s, 3H, O**C**H$_3$), 3.28–3.16 (m, 1H, C_8**H**$_a$) 3.00 (br d, *J* = 14.7 Hz, 1H, C_{11}**H**$_a$), 2.93–2.81 (m, 3H, C_3**H**$_a$, C_{10}**H**$_b$, C_{11}**H**$_b$), 2.66 (dd, *J* = 15.6, 10.0 Hz, 1H, C_3**H**$_b$), 2.30 (dd, *J* = 13.5, 8.5 Hz, 1H, C_4**H**$_a$), 2.19 (dt, *J* = 12.9, 7.6 Hz, 1H, C_{20}**H**$_a$), 2.13–1.99 (m, 2H, C_4**H**$_b$, C_7**H**$_a$), 1.68–1.56 (m, 2H, C_7**H**$_b$, C_{20}**H**$_b$).
^{13}C NMR (125.8 MHz, CD_3CN, 25 °C):	δ 175.5 (**C**$_{19}$), 159.8 (**C**OCH$_3$), 138.3 (**C**$_2$), 137.5 (**C**$_{13}$), 131.4 (N_1CH_2**C**), 128.9 (**C**$_{18}$), 128.3 (Ar_{PMB}), 121.8 (**C**$_{15}$), 119.8 (**C**$_{16}$), 118.7 (**C**$_{14}$), 114.8 (Ar_{PMB}), 111.4 (**C**$_{12}$), 110.5 (**C**$_{17}$), 81.7 (**C**$_6$), 66.4 (**C**$_{21}$), 55.8 (O**C**H$_3$), 55.2 (**C**$_5$), 48.8 (**C**$_{10}$), 46.7 (N_1**C**H$_2$), 45.3 (**C**$_8$), 43.8 (**C**$_4$), 38.2 (**C**$_{20}$), 29.1 (**C**$_7$), 23.3 (**C**$_{11}$), 21.4 (**C**$_3$).
FTIR (thin film) cm^{-1}:	2929 (br), 1642 (s), 1512 (s) 1468 (m), 1248 (s), 1176 (m), 747 (s).
HRMS (DART) (*m/z*):	calc'd for $C_{27}H_{31}N_2O_3$ $[M+H]^+$: 431.2329, found: 431.2314.
$[\alpha]_D^{20}$:	+32.1 (*c* = 0.50, $CHCl_3$).
TLC (40% ethyl acetate in hexanes), R*f*:	0.30 (UV, CAM).

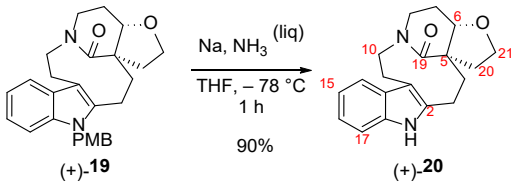

pentacyclic indole (+)-3.20:

A solution of the lactam (+)-**3.19** (1.3634 g, 3.17 mmol, 1 equiv) in THF (150 mL) was cannulated to liquid ammonia (300 mL) at –78 °C under argon. After 5 min, sodium (728 mg, 31.7 mmol, 10 equiv) was added to the mixture as solid, and the reaction mixture was stirred at –78 °C. After 1 h, solid ammonium chloride (3 g) was added to the reaction mixture. After 5 min, the ammonia was evaporated by slowly warming the colorless suspension to 23 °C. After evaporation of the ammonia, water (100 mL) and dichloromethane (100 mL) were added to the flask and the layers were separated. The aqueous layer was extracted with dichloromethane (2 × 100 mL). The combined organic layers were dried over anhydrous sodium sulfate, were filtered, and were concentrated under reduced pressure. The resulting residue was purified by flash column chromatography on silica gel (eluent: 40% acetone in hexanes) to afford indole (+)-**3.20** (883.8 mg, 2.85 mmol, 90%) as a residue. Structural assignments were made using additional information from gCOSY, gHSQC, and gHMBC experiments.

^{1}H NMR (500 MHz, $CDCl_3$, 25 °C):	δ 7.83 (br s, 1H, N_1**H**), 7.48 (d, *J* = 7.6 Hz, 1H, C_{14}**H**), 7.23 (d, *J* = 7.6 Hz, 1H, C_{17}**H**), 7.14–7.03 (m, 2H, C_{15}**H**, C_{16}**H**), 4.38–4.29 (m, 1H, C_{10}**H**$_a$), 3.93–3.80 (m, 3H, C_6**H**, C_{21}**H**$_2$), 3.25–3.02 (m, 3H, C_{11}**H**$_a$, C_8**H**$_2$), 3.00–2.90 (m, 1H, C_3**H**$_a$), 2.85–2.75 (m, 2H, C_{10}**H**$_b$, C_{11}**H**$_b$), 2.59 (ddd, *J* = 15.3, 7.2, 3.7 Hz, 1H, C_3**H**$_b$), 2.42 (dt, *J* = 12.9, 7.6 Hz, 1H, C_{20}**H**$_a$), 2.35–2.24 (m, 2H, C_4**H**$_2$), 1.99–1.82 (m, 2H, C_7**H**$_a$, C_{20}**H**$_b$), 1.69–1.54 (m, 1H, C_7**H**$_b$).
^{13}C NMR (125.8 MHz, $CDCl_3$, 25 °C):	δ 174.6 (**C**$_{19}$), 135.7 (**C**$_2$), 135.3 (**C**$_{13}$), 128.3 (**C**$_{18}$), 121.7 (**C**$_{15}$), 119.4 (**C**$_{16}$), 117.8 (**C**$_{14}$), 110.7 (**C**$_{17}$), 110.0 (**C**$_{12}$), 81.6 (**C**$_6$), 66.4 (**C**$_{21}$), 54.4 (**C**$_5$), 48.4 (**C**$_{10}$), 45.7 (**C**$_8$), 43.1 (**C**$_4$), 37.7 (**C**$_{20}$), 28.0 (**C**$_7$), 22.9 (**C**$_3$), 22.0 (**C**$_{11}$).
FTIR (thin film) cm^{-1}:	3281 (br), 2928 (br), 1631 (s), 1440 (w), 1333 (w), 746 (m).
HRMS (ESI) (*m/z*):	calc'd for $C_{19}H_{23}N_2O_2$ $[M+H]^+$: 311.1754, found: 311.1756.
$[\alpha]_D^{23}$:	+41.8 (*c* = 0.40, $CHCl_3$).
TLC (40% acetone in hexanes), R*f*:	0.40 (UV, CAM).

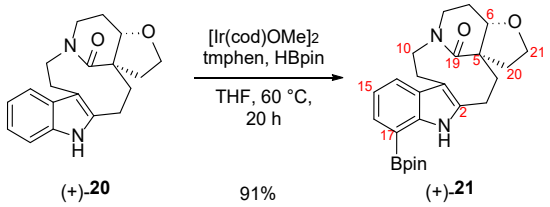

(+)-**20** 91% (+)-**21**

C17 boronic ester (+)-3.21:

Pinacolborane (4.1 mL, 28 mmol, 9.8 equiv) was added to a solution of 3,4,7,8-tetramethyl-1,10-phenanthroline (66 mg, 0.28 mmol, 9.8 mol%) and (1,5-cyclooctadiene)(methoxy)iridium(I) dimer (93 mg, 0.14 mmol, 4.9 mol%) in THF (20 mL) at 23 °C. A solution of indole (+)-**3.20** (883 mg, 2.85 mmol, 1 equiv) in THF (30 mL) was added to the reaction mixture at 23 °C. The reaction mixture was heated to 60 °C. After 20 h, the reaction mixture was concentrated under reduced pressure. The resulting residue was purified by flash column chromatography on silica gel (eluent: 20% acetone in hexanes to 30% acetone in hexanes) to afford C17-boronic ester (+)-**3.21** (1.1322 g, 2.59 mmol, 91%) as a white foam. Structural assignments were made using additional information from gCOSY, gHSQC, and gHMBC experiments. Additional ^{13}C signals were identified from gHSQC, and gHMBC.

^{1}H NMR (600 MHz, $CDCl_3$, 25 °C): δ 8.64 (br s, 1H, N_1**H**), 7.59 (d, *J* = 7.9, 1H, C_{14}**H**), 7.56 (d, *J* = 7.0, 1H, C_{16}**H**), 7.09 – 7.06 (m, 1H, C_{15}**H**), 4.39 – 4.31 (m, 1H, C_{10}**H**), 3.98 – 3.88 (m, 1H, C_6**H**), 3.90 – 3.83 (m, 2H, C_{21}**H₂**), 3.15 – 3.06 (m, 3H, C_8**H₂**, C_{11}**H$_a$**), 3.04 (ddd, *J* = 15.3, 8.5, 2.9 Hz, 1H, C_3**H$_a$**), 2.85 – 2.77 (m, 2H, C_{10}**H$_a$**,C_{11}**H$_b$**), 2.65 (ddd, *J* = 15.4, 8.5, 2.5 Hz, 1H, C_3**H$_b$**), 2.46 – 2.30 (m, 3H, C_4**H₂**, C_{20}**H$_a$**), 2.01 1.93 (m, 1H, C_7**H$_a$**), 1.90 (dt, *J* = 12.6, 6.0 Hz, 1H, C_{20}**H$_b$**), 1.69 – 1.59 (m, 1H, C_7**H$_b$**), 1.39 (s, 12H, C**H₃**).

^{13}C NMR (150.8 MHz, $CDCl_3$, 25 °C): δ 174.8 (**C**$_{19}$), 141.1 (**C**$_{18}$), 135.1 (**C**$_2$), 129.0 (**C**$_{16}$), 127.2 (**C**$_{13}$), 121.2 (**C**$_{14}$), 118.8 (**C**$_{15}$), 109.5 (**C**$_{17}$), 109.1 (**C**$_{12}$), 83.8 (2C, pinacol C), 81.6 (**C**$_6$), 66.4 (**C**$_{21}$), 54.2 (**C**$_5$), 48.6 (**C**$_{10}$), 45.9 (**C**$_8$), 43.1 (**C**$_4$), 37.7 (**C**$_{20}$), 28.3 (**C**$_7$), 25.3 (2C, **C**H$_3$) 25.2 (2C, **C**H$_3$), 23.0(**C**$_3$), 21.7 (**C**$_{11}$).

FTIR (thin film) cm^{-1}: 3445 (m), 2977 (m), 2927 (m), 2856 (m), 1641 (s), 1452 (m), 1375 (s), 1321 (s), 1280 (s), 1129 (s), 751 (s), 678 (m).

HRMS (ESI) (*m/z*): calc'd for $C_{25}H_{34}BN_2O_4$ $[M+H]^+$: 437.2606, found: 437.2596.

$[\alpha]_D^{20}$: +26.8 (*c* = 0.205, $CHCl_3$).

TLC (30% acetone in hexanes), R*f*: 0.35 (UV, CAM).

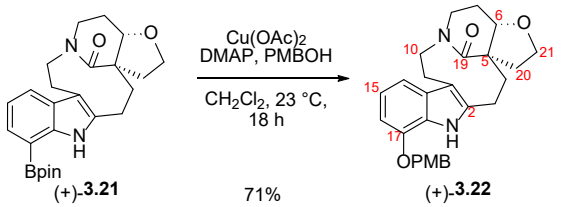

PMB ether : (+)-3.22

Copper (II) acetate (230 mg, 1.27 mmol, 2.0 equiv), molecular sieves (4 Å, 280 mg), and 4-dimethylaminopyridine (155 mg, 1.27 mmol, 2.0 equiv) were added to a solution of C17-boronic ester (+)-**3.21** (277 mg, 0.645 mmol, 1 equiv) in dichloromethane (6 mL) and 4-methoxybenzyl alcohol (1.5 mL) at 23 °C. After 4 days, the reaction mixture was filtered over Celite. The solids were rinsed with acetone (50 mL), and the combined filtrates were concentrated under reduced pressure. The resulting residue was purified by flash column chromatography on silica gel (eluent: 20% acetone in hexanes to 40% acetone in hexanes) to afford *p*-methoxybenzyl ether (+)-**3.22** (203 mg, 0.455 mmol, 71%) as a white foam. Structural assignments were made using additional information from gCOSY, gHSQC, and gHMBC experiments. Additional ^{13}C signals were identified from gHSQC, and gHMBC.

^{1}H NMR (600 MHz, $CDCl_3$, 25 °C): δ 7.97 (br s, 1H, N_1**H**), 7.43 (app-d, *J* = 8.6 Hz, 2H, Ar_{PMB}), 7.11 (d, *J* = 7.9 Hz, 1H, C_{14}**H**), 6.99 (t, *J* = 7.8 Hz, 1H, C_{15}**H**), 6.95 (app-d, *J* = 8.6 Hz, 2H, Ar_{PMB}), 6.68 (d, *J* = 7.2 Hz, 1H, C_{16}**H**), 5.12–5.04 (m, 2H, $C_{17}OC$**H₂**), 4.38–4.30 (m, 1H, C_{10}**H**$_a$), 3.84 (s, 3H, OC**H**$_3$), 3.86–3.80 (m, 3H, C_6**H**, C_{21}**H₂**), 3.17–3.03 (m, 3H, C_8**H₂**, C_{11}**H**$_a$), 2.98–2.92 (m, 1H, C_3**H**$_a$), 2.82–2.75 (m, 2H, C_{10}**H**$_b$, C_{11}**H**$_b$), 2.61–2.55 (m, 1H, C_3**H**$_b$), 2.40 (app-dt, *J* = 12.7, 7.6 Hz, 1H, C_{20}**H**$_a$), 2.31–2.23 (m, 2H, C_4**H₂**), 1.93–1.81 (m, 2H, C_7**H**$_a$, C_{20}**H**$_b$), 1.64–1.53 (m, 1H, C_7**H**$_b$).

^{13}C NMR (150.8 MHz, $CDCl_3$, 25 °C): δ 174.7 (**C**$_{19}$), 159.8 (Ar_{PMB}), 145.2 (**C**$_{17}$), 135.0 (**C**$_2$), 130.1 (2C, Ar_{PMB}), 129.7 (Ar_{PMB}), 129.3 (**C**$_{13}$), 126.1 (**C**$_{18}$), 119.7 (**C**$_{15}$), 114.1 (2C, Ar_{PMB}), 110.9 (**C**$_{14}$), 110.4 (**C**$_{12}$), 103.0 (**C**$_{16}$), 81.6 (**C**$_6$), 70.0 ($C_{17}OCH_2$), 66.4 (**C**$_{21}$), 55.5 (OCH_3), 54.3 (**C**$_5$), 48.5 (**C**$_{10}$), 45.3 (**C**$_8$), 43.1 (**C**$_4$), 37.7 (**C**$_{20}$), 28.0 (**C**$_7$), 22.9 (**C**$_3$), 22.3 (**C**$_{11}$).

FTIR (thin film) cm^{-1}: 3322 (br), 2928 (br), 2870 (br), 1634 (s), 1514 (m), 1457 (m), 1247 (s), 1173 (m), 1077 (m), 1033 (m), 750 (m)

HRMS (ESI) (*m/z*): calc'd for $C_{27}H_{31}N_2O_4$ $[M+H]^+$: 447.2278, found: 447.2267.

$[\alpha]_D^{20}$:	+49.1 (*c* = 0.385, $CHCl_3$).
TLC (40% acetone in hexanes), R*f*:	0.21 (UV, CAM).

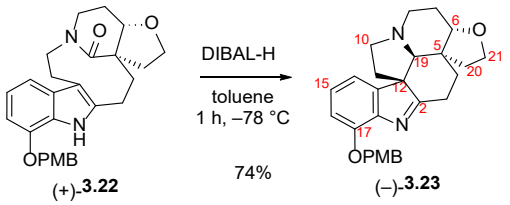

hexacyclic imine (–)-3.23:

Diisobutylaluminum hydride (1.0 M in hexane, 7.8 mL, 7.8 mmol, 6.0 equiv) was added slowly via syringe to a solution of *p*-methoxybenzyl ether (+)-**3.22** (581 mg, 1.30 mmol, 1 equiv) in toluene (50 mL) at –78 °C under argon. After 1 hr, –78 °C methanol (8 mL) was added followed by a saturated aqueous solution of Rochelle's salt (50 mL). The solution was stirred vigorously and allowed to warm to 23 °C. Ethyl acetate (50 mL) was added and the layers were separated. The aqueous layer was extracted further with ethyl acetate (2 × 50 mL) and the combined organic layers were dried over anhydrous sodium sulfate, were filtered, and were concentrated under reduced pressure. The resulting residue was purified by flash column chromatography on silica gel (eluent: 10% acetone in hexanes to 20% acetone in hexanes to 40% acetone in hexanes) to afford hexacyclic imine (–)-**3.23** (411.5 mg, 0.956 mmol, 74%) as a foam. Structural assignments were made using additional information from gCOSY, gHSQC and gHMBC experiments.

^{1}H NMR (600 MHz, $CDCl_3$, 25 °C): δ 7.40 (app-d, J = 8.6 Hz, 2H, Ar_{PMB}) 7.06 (t, J = 7.8 Hz, 1H, C_{15}**H**), 6.95 (d, J = 7.4 Hz, 1H, C_{14}**H**), 6.89–6.84 (m, 3H, C_{16}**H**, Ar_{PMB}), 5.27–5.20 (m, 2H, $C_{17}OC$**H**$_2$), 3.78 (s, 3H, OC**H**$_3$), 3.61–3.53 (m, 2H, C_{21}**H**$_2$), 3.46 (dd, J = 3.7, 2.2 Hz, 1H, C_6**H**), 3.21 (app-dd, J = 8.6, 6.5 Hz, 1H, C_{10}**H**$_a$) 3.07–3.01 (m, 1H, C_3**H**$_a$), 3.00–2.92(m, 2H, C_3**H**$_b$, C_8**H**$_a$), 2.70–2.62 (m, 3H, C_4**H**$_a$, C_{10}**H**$_b$, C_{19}**H**), 2.50 (td, J = 11.4, 3.9 Hz, 1H, C_8**H**$_b$), 2.22 (td, J = 11.9, 6.6 Hz, 1H, C_{11}**H**$_a$), 2.01–1.89 (m, 2H, C_7**H**$_2$), 1.71 (app-dd, J = 12.3, 5.1 Hz, 1H, C_{11}**H**$_b$), 1.65–1.57 (m, 1H, C_4**H**$_b$), 1.45–1.36 (m, 1H, C_{20}**H**$_a$), 1.01 (ddd, J = 12.6, 7.8, 4.6 Hz, 1H, C_{20}**H**$_b$).

^{13}C NMR (150.8 MHz, $CDCl_3$, 25 °C): δ 189.1 (**C**$_2$), 159.4 (Ar_{PMB}), 150.4 (**C**$_{17}$), 150.1 (**C**$_{13}$), 142.7 (**C**$_{18}$), 129.5 (Ar_{PMB}), 129.3 (Ar_{PMB}), 126.7 (**C**$_{15}$), 114.1 (**C**$_{14}$), 114.0 (Ar_{PMB}), 113.1 (**C**$_{16}$), 80.4 (**C**$_6$), 73.5 (**C**$_{19}$), 70.8 ($C_{17}O$**C**H_2), 65.5 (**C**$_{21}$), 61.2 (**C**$_{12}$), 55.4 (OCH_3), 54.4 (**C**$_{10}$), 47.6 (**C**$_8$), 44.1 (**C**$_5$), 35.3 (**C**$_{11}$), 35.0 (**C**$_{20}$), 29.6 (**C**$_4$), 26.1 (**C**$_7$), 24.1 (**C**$_3$).

FTIR (thin film) cm^{-1}: 2933 (br), 2874 (m), 2808 (br), 1611 (m), 1589 (m), 1514 (m), 1482 (br), 1247 (s), 1173 (m), 1074 (m), 1033 (br), 821 (m), 747 (m).

HRMS (ESI) (*m/z*):	calc'd for $C_{27}H_{31}N_2O_3$ $[M+H]^+$: 431.2329, found: 431.2305.
$[\alpha]_D^{20}$:	–94.3 (*c* = 0.215, $CHCl_3$).
TLC (40% acetone in hexanes), R*f*:	0.34 (UV, CAM).

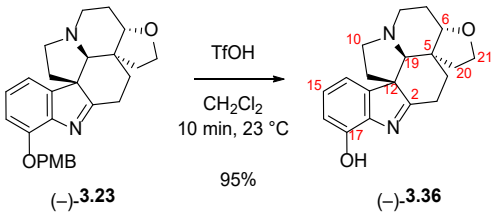

(–)-**3.23** (–)-**3.36**

hexacyclic phenol (−)-3.36

Trifluoromethanesulfonic acid (310 µL, 3.84 mmol, 5.0 equiv) was added to a solution of (–)-**3.23** (330 mg, 0.768 mmol, 1 equiv) in dichloromethane (15 mL) at 23 °C under argon. After 10 minutes, the reaction mixture was opened to air, and then saturated aqueous sodium bicarbonate solution (30 mL) was added to the reaction mixture. The layers were separated, and the aqueous layer was further extracted with dichloromethane (3 × 20 mL). The combined organic extracts were dried over anhydrous sodium sulfate, were filtered, and were concentrated under reduced pressure. The resulting residue was purified by flash column chromatography on silica gel (eluent: 30% acetone in hexanes) to afford phenol (–)-**3.36** (227 mg, 0.731 mmol, 95%) as a white foam. Structural assignments were made using additional information from gCOSY, gHSQC, and gHMBC experiments.

^{1}H NMR (600 MHz, $CDCl_3$, 25 °C):	δ 9.63 (br s, 1H, N_1**H**), 7.10 (dd, *J* = 8.2, 7.2 Hz, 1H, C_{15}**H**), 6.91– 6.88 (m, 2H, C_{14}**H**, C_{16}**H**), 3.65 – 3.55 (m, 2H, C_{21}**H$_2$**), 3.49 – 3.44 (m, 1H, C_6**H**), 3.23 – 3.18 (m, 1H, C_{10}**H$_a$**), 3.10 – 2.96 (m, 3H, C_3**H$_2$**, C_8**H$_a$**), 2.72 – 2.62 (m, 3H, C_{10}**H$_b$**, C_4**H$_a$**, C_{19}**H**), 2.50 (td, *J* = 11.2, 4.3 Hz, 1H, C_8**H$_b$**), 2.23 (td, *J* = 11.9, 6.5 Hz, 1H, C_{11}**H$_a$**), 2.04 – 1.90 (m, 2H, C_7**H$_2$**), 1.78 – 1.66 (m, 2H, C_{11}**H$_b$**, C_4**H$_b$**), 1.44 (dt, *J* = 12.8, 8.8 Hz, 1H, C_{20}**H$_a$**), 1.02 (dt, *J* = 12.8, 6.0 Hz, 1H, C_{20}**H$_b$**).
^{13}C NMR (150.9 MHz, $CDCl_3$, 25 °C):	δ 190.0 (**C**$_2$), 149.1 (**C**$_{13}$), 148.6 (**C**$_{17}$), 140.1 (**C**$_{18}$), 127.5 (**C**$_{15}$), 116.3 (**C**$_{14}$), 113.1 (**C**$_{16}$), 80.4 (**C**$_6$), 74.5 (**C**$_{19}$), 65.5 (**C**$_{21}$), 61.5 (**C**$_{12}$), 54.4 (**C**$_{10}$), 47.7 (**C**$_8$), 44.0 (**C**$_5$), 35.4 (**C**$_{11}$), 34.9 (**C**$_{20}$), 29.9 (**C**$_4$), 26.1 (**C**$_7$), 23.5 (**C**$_3$).
FTIR (thin film) cm^{-1}:	2932 (br), 2802 (br), 1612 (m) 1446 (m), 1278 (m), 1217 (m), 1155 (m), 747 (s).
HRMS (ESI) (*m/z*):	calc'd for $C_{19}H_{23}N_2O_2$ $[M+H]^+$: 311.1754, found: 311.1744.
$[\alpha]_D^{20}$:	–81.0 (*c* = 0.59, $CHCl_3$).
TLC (30% acetone in hexanes), R*f*:	0.21 (UV, CAM).

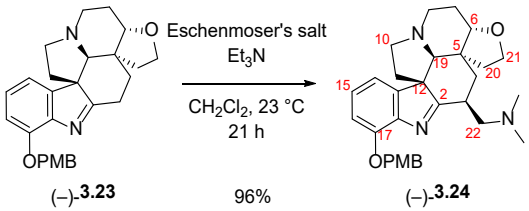

(–)-**3.23** 96% (–)-**3.24**

N,N-dimethylaminomethylene adduct (−)-3.24:

Eschenmoser's salt (91 mg, 0.49 mmol, 4.0 equiv) was added to a solution of (–)-**3.23** (52.7 mg, 0.122 mmol, 1 equiv) and triethylamine (170 µL, 1.22 mmol, 10.0 eq) in dichloromethane (10 mL) at 23 °C under argon. After 21 hours, the reaction mixture was opened to air, and then saturated aqueous sodium bicarbonate solution (10 mL) was added to the reaction mixture. The layers were separated, and the aqueous layer was further extracted with dichloromethane (3 × 10 mL). The combined organic extracts were dried over anhydrous sodium sulfate, were filtered, and were concentrated under reduced pressure. The resulting residue was purified by flash column chromatography on silica gel (eluent: 1.8% methanol in chloroform with 0.2% ammonium hydroxide to 3.6% methanol in chloroform with 0.4% ammonium hydroxide) to afford phenol (–)-**3.24** (56.9 mg, 0.117 mmol, 96%) as a white foam. Structural assignments were made using additional information from gCOSY, gHSQC, gHMBC, and NOESY experiments.

^{1}H NMR (600 MHz, $CDCl_3$, 25 °C): δ 7.40 (app-d, J = 8.6 Hz, 2H, Ar_{PMB}), 7.04 (dd, J = 8.2, 7.4 Hz, 1H, C_{15}**H**), 6.91 (dd, J = 7.4, 0.9 Hz, 1H, C_{14}**H**), 6.90 – 6.86 (m, 2H, Ar_{PMB}), 6.81 (dd, J = 8.3, 0.9 Hz, 1H, C_{16}**H**), 5.31 – 5.23 (m, 2H, $C_{17}OC$**H**$_2$), 3.79 (s, 3H, OC**H**$_3$), 3.63 – 3.58 (m, 2H, C_{21}**H**$_2$), 3.51 – 3.42 (m, 2H, C_6**H**, C_3**H**), 3.20 – 3.15 (m, 1H, C_{10}**H**$_a$), 2.96 (ddd, J = 11.1, 5.8, 1.7 Hz, 1H, C_8**H**$_a$), 2.83 (dd, J = 11.6, 6.8 Hz, 1H, C_{22}**H**$_a$), 2.76 (ddd, J = 11.1, 8.5, 5.2 Hz, 1H, C_{10}**H**$_b$), 2.72 – 2.64 (m, 2H, C_{19}**H**, C_{22}**H**$_b$), 2.62 – 2.51 (m, 2H, C_4**H**$_a$, C_8**H**$_b$), 2.46 – 2.38 (m, 1H, C_{11}**H**$_a$), 2.33 (s, 6H, $N(C$**H**$_3)_2$), 1.98 (tdd, J = 12.3, 5.8, 2.9 Hz, 1H, C_7**H**$_a$), 1.88 (ddt, J = 14.5, 3.6, 1.9 Hz, 1H, C_7**H**$_b$), 1.74 – 1.66 (m, 2H, C_4**H**$_b$, C_{11}**H**$_b$), 1.52 – 1.44 (m, 1H, C_{20}**H**$_a$), 1.07 – 1.00 (m, 1H, C_{20}**H**$_b$).

^{13}C NMR (150.9 MHz, $CDCl_3$, 25 °C): δ 188.1 (**C**$_2$), 159.4 (Ar_{PMB}), 150.9 (**C**$_{17}$), 150.4 (**C**$_{13}$), 142.1 (**C**$_{18}$), 129.7 (Ar_{PMB}), 129.1 (2C, Ar_{PMB}), 127.0 (**C**$_{15}$), 114.0 (**C**$_{14}$), 114.0 (2C, Ar_{PMB}), 113.2 (**C**$_{16}$), 80.9 (**C**$_6$), 72.0 (**C**$_{19}$), 70.9 (C_{17}**OCH2**), 65.3 (**C**$_{21}$), 64.6 (**C**$_{22}$), 61.9 (**C**$_{12}$), 55.4 (OCH_3), 53.7 (**C**$_{10}$), 46.9 (**C**$_8$), 45.7 (2C, $N(CH_3)_2$), 44.7 (**C**$_5$), 38.3 (**C**$_3$), 35.5 (**C**$_{11}$), 34.0 (2C, **C**$_4$, **C**$_{20}$), 26.2 (**C**$_7$).

FTIR (thin film) cm^{-1}:	2940 (br), 2815 (m), 2774 (m), 1611 (m), 1514 (s), 1463 (m), 1248 (s), 1173 (m), 1076 (m), 1034 (m), 821 (w), 748 (m).
HRMS (ESI) (*m/z*):	calc'd for $C_{30}H_{38}N_3O_3$ $[M+H]^+$: 488.2908, found: 488.2850.
$[\alpha]_D^{20}$:	–137.2 (*c* = 0.635, $CHCl_3$).

TLC (3.6% methanol in chloroform with 0.4% ammonium hydroxide), R*f*: 0.17 (UV, CAM).

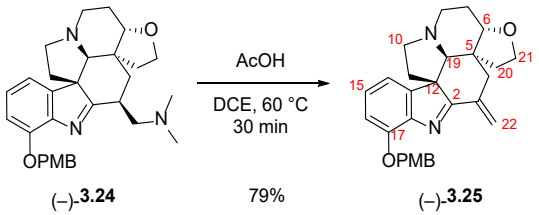

(–)-**3.24** 79% (–)-**3.25**

α,β-unsaturated imine (−)-3.25

Acetic acid (1.2 mL) was added to a solution of (–)-**3.24** (56.9 mg, 0.117 mmol, 1 equiv) in 1,2-dichloroethane (4.8 mL) at 23 °C under argon. The reaction mixture was heated to 60 °C. After 30 minutes, the reaction mixture was opened to air, and then saturated aqueous sodium bicarbonate solution (20 mL) was added to the reaction mixture. The layers were separated, and the aqueous layer was further extracted with dichloromethane (3 × 5 mL). The combined organic extracts were dried over anhydrous sodium sulfate, were filtered, and were concentrated under reduced pressure. The resulting residue was purified by flash column chromatography on silica gel (eluent: 20% acetone in hexanes) to afford phenol (–)-**3.25** (41.2 mg, 0.093 mmol, 79%) as a foam. Structural assignments were made using additional information from gCOSY, gHSQC, and gHMBC experiments.

^{1}H NMR (600 MHz, $CDCl_3$, 25 °C): δ 7.42 (app-d, J = 7.8 Hz, 2H, Ar_{PMB}), 7.08 (t, J = 7.8 Hz, 1H, C_{15}**H**), 6.96 (d, J = 7.2 Hz, 1H, C_{14}**H**), 6.91 – 6.85 (m, 3H, C_{16}**H**, Ar_{PMB}), 6.16 (br s, 1H, C_{22}**H$_a$**), 5.34 – 5.24 (m, 3H, $C_{17}OC$**H$_2$**, C_{22}**H$_b$**), 3.80 (s, 3H, OC**H$_3$**), 3.72 – 3.61 (m, 2H, C_{22}**H$_2$**), 3.56 (dd, J = 3.8, 2.3 Hz, 1H, C_6**H**), 3.52 (dt, J = 15.9, 3.0 Hz, 1H, C_4**H$_a$**), 3.15 – 3.10 (m, 1H, C_{10}**H$_a$**), 2.97 (ddd, J = 11.2, 5.7, 2.0 Hz, 1H, C_8**H$_a$**), 2.84 (ddd, J = 10.9, 8.4, 4.7 Hz, 1H, C_{10}**H$_b$**), 2.81 (d, J = 1.7 Hz, 1H, C_{19}**H**), 2.72 (td, J = 11.4, 3.8 Hz, 1H, C_8**H$_b$**), 2.22 – 2.13 (m, 2H, C_{11}**H$_a$**, C_4**H$_b$**), 2.01 – 1.88 (m, 2H, C_7**H$_2$**), 1.61 (dd, J = 11.9, 4.6 Hz, 1H, C_{11}**H$_b$**), 1.51 (ddd, J = 13.0, 10.0, 7.5 Hz, 1H, C_{20}**H$_a$**), 1.05 (ddd, J = 12.8, 8.2, 4.5 Hz, 1H, C_{20}**H$_b$**).

^{13}C NMR (150.9 MHz, $CDCl_3$, 25 °C): δ 183.5 (**C**$_2$), 159.4 (Ar_{PMB}), 151.1 (**C**$_{17}$), 150.2 (**C**$_{13}$), 142.6 (**C**$_{18}$), 138.9 (**C**$_3$), 129.6 (Ar_{PMB}), 129.2 (2C, Ar_{PMB}), 127.1 (**C**$_{15}$), 116.8 (**C**$_{22}$), 114.1 (**C**$_{14}$), 114.0 (2C, Ar_{PMB}), 113.5 (**C**$_{16}$), 80.5 (**C**$_6$), 71.1 (C_{17}**O**CH2), 70.4 (**C**$_{19}$), 65.4 (**C**$_{21}$), 61.2 (**C**$_{12}$), 55.4 (O**C**H$_3$), 52.7 (**C**$_{10}$), 46.1 (**C**$_8$), 45.3 (**C**$_5$), 36.7 (**C**$_{11}$), 36.2 (**C**$_4$), 34.2 (**C**$_{20}$), 26.4 (**C**$_7$).

FTIR (thin film) cm^{-1}: 2929 (br), 2808 (br), 1610 (m), 1587 (m), 1514 (m), 1248 (s), 1174 (m), 1076 (m), 1033 (m), 822 (m), 749 (m).

HRMS (ESI) (*m/z*):	calc'd for $C_{28}H_{31}N_2O_3$ $[M+H]^+$: 443.2329, found: 443.2305.
$[\alpha]_D^{20}$:	–18.9 (*c* = 0.135, $CHCl_3$).
TLC (20% acetone in hexanes), R*f*:	0.17 (UV, CAM).

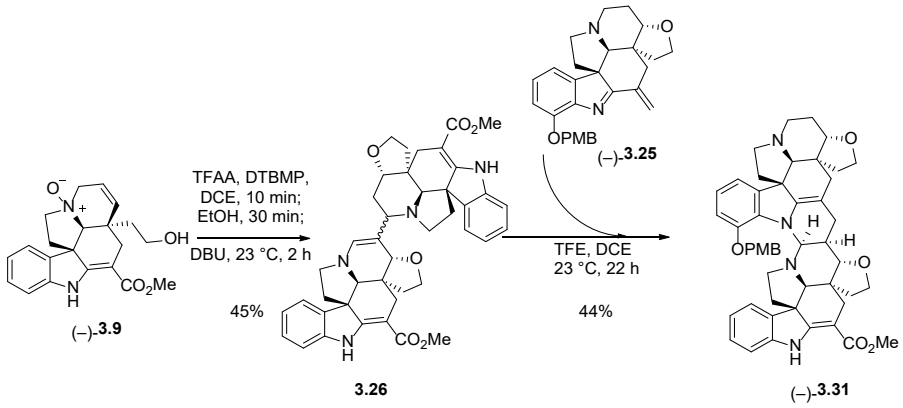

cis-fused tridecacycle (−)-3.31:

Trifluoroacetic anhydride (440 μL, 3.17 mmol, 4.0 equiv) was added dropwise via syringe to a solution of pentacyclic *N*-oxide **3.9**[8] (292 mg, 0.792 mmol, 1 equiv) and 2,6-di-*tert*-butyl-4-methylpyridine (650 mg, 3.17 mmol, 4.0 equiv) in 1,2-dichloroethane (40 mL) at 23 °C under argon. After 10 minutes, ethanol (40 mL) was added to the reaction. After 30 minutes, 1,8-diazabicyclo[5.4.0]undec-7-ene (DBU, 710 μL, 4.75 mmol, 6.0 equiv) was added. After 2 h, saturated aqueous sodium bicarbonate solution (60 mL) and ethyl acetate (40 mL) were added to the reaction mixture. The layers were separated, and the aqueous layer was extracted with ethyl acetate (2 × 40 mL). The combined organic layers were dried over anhydrous sodium sulfate, were filtered, and were concentrated under reduced pressure. The resulting residue was purified by flash column chromatography on silica gel (eluent: 30% ethyl acetate in hexanes to 50% ethyl acetate in hexanes) to afford a mixture of C8′ epimers of dimeric enamine **3.26** (125.5 mg, 0.179 mmol, 45%) and also open dimer **3.30** (89 mg, 0.127 mmol, 32%). **3.30** is readily converted to **3.26** by dissolving in equal parts dichloromethane and 2,2,2-trifluoroethanol.

2,2,2-trifluoroethanol (300 μL) was added to a solution of above enamine **3.26** (26.5 mg, 37.8 μmol, 0.7 equiv) and unsaturated imine **3.25** (23.6 mg, 53.3 μmol, 1 equiv) in 1,2-dichloroethane (300 μL) at 23 ºC under argon. After 22 h, the reaction mixture was concentrated under reduced pressure. The resulting residue was purified by flash column chromatography on silica gel (eluent: 30% ethyl acetate in dichloromethane to 50% ethyl acetate in dichloromethane) to afford tridecacycle (–)-**3.31** (18.6 mg, 23.5 μmol, 44%) as a residue. Structural assignments were made using additional information from gCOSY, gHSQC, gHMBC, and ROESY experiments.

^{1}H NMR (600 MHz, $CDCl_3$, 25 °C): δ 8.83 (s, 1H, N_1**H**), 7.57 (app-d, J = 8.6, 2H, Ar_{PMB}), 7.04 (td, J = 7.6, 1.2 Hz, 1H, C_{16}**H**), 6.97 – 6.82 (m, 4H, Ar_{PMB}, $C_{14'}$**H**, $C_{16'}$**H**), 6.77 – 6.72 (m, 1H, $C_{15'}$**H**), 6.71 (d, J = 7.6 Hz, 1H, C_{17}**H**), 6.54 (td, J = 7.5, 1.0 Hz, 1H, C_{15}**H**), 6.11 (d, J = 7.3 Hz, 1H, C_{14}**H**), 5.94 (d, J = 3.4 Hz, 1H, C_8**H**), 5.10 (s, 2H, $C_{17'}$C**H₂**), 3.88 – 3.79 (m, 2H, C_{21}**H$_a$**, $C_{21'}$**H$_a$**), 3.77 (s, 3H, CO_2C**H₃**), 3.75 – 3.68 (m, 2H, C_{21}**H$_b$**, $C_{21'}$**H$_b$**), 3.67 (d, J = 1.3

[8] Flynn, K. M.; Myeong, I.-S.; Pinto, T.; Movassaghi M.; *J. Am. Chem. Soc.* **2022**, *144*, 9126.

	Hz, 1H, C_6**H**), 3.64 (s, 3H, OC**H₃**), 3.61 (t, J = 3.1 Hz, 1H, $C_{6'}$**H**), 3.05 – 2.99 (m, 2H, C_{19}**H**, $C_{4'}$**H$_a$**), 2.97 (dd, J = 8.8, 5.9 Hz, 1H, C_{10}**H$_a$**), 2.95 – 2.91 (m, 1H, $C_{8'}$**H$_a$**), 2.89 (dd, J = 8.5, 6.4 Hz, 1H, $C_{10'}$**H$_a$**), 2.84 (dd, J = 14.2, 1.9 Hz, 1H, $C_{4'}$**H$_a$**), 2.78 (ddd, J = 12.4, 8.6, 4.1 Hz, 1H, C_{10}**H$_b$**), 2.75 – 2.69 (m, 2H, C_{22}**H$_a$**, $C_{19'}$**H**), 2.65 – 2.56 (m, 1H, $C_{8'}$**H$_b$**), 2.48 (ddd, J = 11.5, 8.5, 5.0 Hz, 1H, $C_{10'}$**H$_b$**), 2.37 (dd, J = 14.2, 1.8 Hz, 1H, C_4**H$_b$**), 2.12 (dt, J = 12.5, 4.2 Hz, 1H, C_7**H**), 2.03 – 1.88 (m, 4H, $C_{7'}$**H₂**, C_{11}**H$_a$**, $C_{11'}$**H$_a$**), 1.75 (dd, J = 15.3, 5.6 Hz, 1H, C_{22}**H$_b$**), 1.67 – 1.59 (m, 2H, $C_{11'}$**H$_b$**, $C_{20'}$**H$_a$**), 1.57 – 1.53 (m, 1H, C_{11}**H$_b$**), 1.53 – 1.46 (m, 1H, $C_{20'}$**H$_b$**), 1.47 – 1.40 (m, 2H, $C_{4'}$**H$_b$**, C_{20}**H$_a$**), 1.34 – 1.23 (m, 1H, C_{20}**H$_b$**).
^{13}C NMR (150.9 MHz, $CDCl_3$, 25 °C):	δ 168.8 (**C**O_2CH_3), 167.2 (**C**$_2$), 159.8 (Ar_{PMB}), 143.5 (**C**$_{2'}$), 143.4 (**C**$_{18'}$), 142.9 (**C**$_{18}$), 140.0 (**C**$_{13'}$), 137.7 (**C**$_{13}$), 134.2 (**C**$_{17'}$), 130.1 (2C, Ar_{PMB}), 129.2 (Ar_{PMB}), 127.4 (**C**$_{16}$), 121.5 (**C**$_{14}$), 121.1 (**C**$_{15}$), 119.2 (**C**$_{15'}$), 114.8 (**C**$_{14'}$), 114.3 (2C, Ar_{PMB}), 112.9 (**C**$_{16'}$), 109.1 (**C**$_{17}$), 101.9 (**C**$_{3'}$), 94.2 (**C**$_3$), 86.1 (**C**$_6$), 80.2 (**C**$_{6'}$), 77.4 (**C**$_{2'}$), 71.2 (**C**$_{17'}$O**C**H_2), 69.4 (**C**$_{19}$), 68.8 (**C**$_{19'}$), 68.2 (**C**$_8$), 65.3 (**C**$_{21}$), 65.1 (**C**$_{21'}$), 55.8 (**C**$_{12}$), 55.3 (O**C**H_3), 52.3 (**C**$_{10'}$), 51.2 (CO_2**C**H_3), 50.9 ($C_{12'}$), 47.4 (**C**$_{2'}$), 47.4 (2C, **C**$_{5'}$, **C**$_{8'}$), 47.2 (**C**$_5$), 46.8 (**C**$_{10}$), 44.9 (**C**$_{11'}$), 44.3 (**C**$_{11}$), 35.5 (2C, **C**$_{20}$, **C**$_{20'}$), 35.2 (2C, **C**$_7$, **C**$_{4'}$), 29.3 (**C**$_{22}$), 28.7 (**C**$_4$), 27.5 (**C**$_{7'}$).
FTIR (thin film) cm^{-1}:	2945 (br), 2821 (br), 1677 (m), 1608 (s), 1515 (m), 1464 (m), 1439 (m), 1293 (m), 1250 (s), 1201 (m), 1070 (m), 751 (m)
HRMS (ESI) (*m/z*):	calc'd for $C_{49}H_{53}N_4O_6$ $[M+H]^+$: 793.3959, found: 793.3954.
$[\alpha]_D^{20}$:	–370 (*c* = 0.175, $CHCl_3$).

TLC (50% ethyl acetate in dichloromethane), R*f*: 0.32 (UV, CAM).

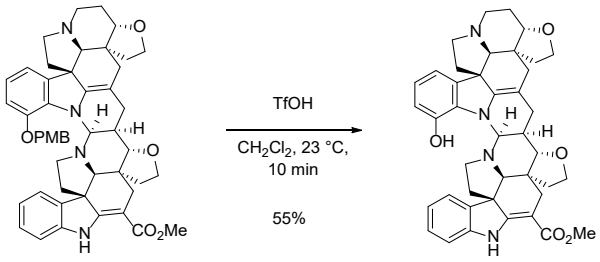

(–)-**3.31** (–)-**3.32**

(−)-C7-*epi*-voacandimine A (3.32):

Trifluoromethanesulfonic acid (16 µl, 0.20 mmol, 10.0 equiv) was added to a solution of (–)-**3.31** (15.8 mg, 0.020 mmol, 1 equiv) in dichloromethane (1.0 mL) at 23 °C under argon. After 10 minutes, the reaction mixture was opened to air, and then saturated aqueous sodium bicarbonate solution (3 mL) was added to the reaction mixture. The layers were separated, and the aqueous layer was further extracted with dichloromethane (3 × 3 mL). The combined organic extracts were dried over anhydrous sodium sulfate, were filtered, and were concentrated under reduced pressure. The resulting residue was purified by flash column chromatography on silica gel (eluent: 10% acetone in hexanes to 20% acetone in hexanes) to afford phenol (–)-**3.32** (7.4 mg, 0.011 mmol, 55%) as a residue. Structural assignments were made using additional information from gCOSY, gHSQC, and gHMBC experiments. The ^{13}C resonances for this compound are provided from HSQC of *ent*-**3.32** prepared in the method described.

^1H NMR (600 MHz, $CDCl_3$, 25 °C): δ 8.95 (s, 1H, N_1**H**), 7.35 (d, *J* = 7.4 Hz, 1H, C_{14}**H**), 7.16 (t, *J* = 7.8 Hz, 1H, C_{16}**H**), 6.92 (t, *J* = 7.6 Hz, 1H, C_{15}**H**) , 6.85 – 6.80 (m, 2H, C_{17}**H**, $C_{14'}$**H**), 6.72 – 6.63 (m, 2H, $C_{16'}$**H**, $C_{15'}$**H**), 5.52 (br s, 1H, C_8**H**), 3.83 – 3.75 (m, 6H, CO_2C**H**$_3$, C_6**H**, C_{21}**H**$_a$, $C_{21'}$**H**$_a$), 3.71 – 3.64 (m, 2H, C_{21}**H**$_b$, $C_{21'}$**H**$_b$), 3.62 (t, *J* = 3.1 Hz, 1H, $C_{6'}$**H**), 3.38 (s, 1H, C_{19}**H**), 3.31 – 3.25 (m, 1H, C_{10}**H**$_a$), 3.18 – 3.13 (m, 1H, C_{10}**H**$_b$), 2.98 – 2.83 (m, 4H, C_4**H**$_a$, $C_{10'}$**H**$_a$, $C_{8'}$**H**$_a$, $C_{4'}$**H**$_a$), 2.72 (s, 1H, $C_{19'}$**H**,), 2.69 – 2.60 (m, 2H, C_{22}**H**$_a$, $C_{8'}$**H**$_b$), 2.54 – 2.45 (m, 2H, C_4**H**$_b$, $C_{10'}$**H**$_b$), 2.16 – 2.08 (m, 1H, C_{11}**H**$_a$), 2.07 – 1.99 (m, 1H, C_7**H**), 1.99 – 1.94 (m, 2H, $C_{7'}$**H**$_2$), 1.94 – 1.82 (m, 3H, C_{22}**H**$_b$, C_{11}**H**$_b$, $C_{11'}$**H**$_a$), 1.68 – 1.63 (m, 1H, $C_{11'}$**H**$_b$), 1.63 – 1.50 (m, 2H, C_{20}**H**$_a$, $C_{20'}$**H**$_a$), 1.48 – 1.38 (m, 3H, C_{20}**H**$_b$, $C_{4'}$**H**$_b$, $C_{20'}$**H**$_b$).

^{13}C NMR (from *ent*-**3.32** HSQC): δ 127.9 (**C**$_{16}$), 121.8 (**C**$_{14}$), 121.1 (**C**$_{15}$), 119.9 (**C**$_{15'}$), 116.0 (**C**$_{16'}$), 114.0 (**C**$_{14'}$), 109.3 (**C**$_{17}$), 85.7 (**C**$_6$), 80.1 (**C**$_{6'}$), 69.3 (**C**$_{19}$), 69.1 (**C**$_{19'}$), 68.0 (**C**$_8$), 65.0 (**C**$_{21'}$), 64.6 (**C**$_{21}$), 52.0 (**C**$_{10'}$), 51.0 (CO_2**C**H_3), 47.7 (**C**$_{10}$), 47.0 (**C**$_{8'}$), 45.5 (**C**$_{11'}$), 44.2 (**C**$_{11}$), 37.1 (**C**$_{20}$), 35.4 (**C**$_4$, **C**$_{20}$, **C**$_{20'}$), 30.3 (**C**$_{22}$), 30.1 (**C**$_{4'}$), 27.3 (**C**$_{7'}$).

FTIR (thin film) cm^{-1}:	2924 (br), 2834 (br), 1677 (m), 1609 (s), 1477 (m), 1465 (m), 1439 (m), 1293 (m), 1247 (m),1196 (m), 1201 (m), 1069 (m), 753 (m)
HRMS (ESI) (*m/z*):	calc'd for $C_{41}H_{45}N_4O_5$ $[M+H]^+$: 673.3395, found: 673.3388.
$[\alpha]_D^{20}$:	–57 (*c* = 0.14, $CHCl_3$).
TLC (20% acetone in hexanes), R*f*:	0.24 (UV, CAM).

Table 3.1 Comparison of our ^{13}H NMR data of C7-epi-voacandimine A (**3.32**) with literature data ($CDCl_3$).

Assignment	Isolation Report[6] voacandimine A (**3.1**, ^{1}H NMR, 600 MHz, $CDCl_3$)	Our synthetic (–)-C7-*epi*-voacandimine A (**3.32**, ^{1}H NMR, 600 MHz, $CDCl_3$)
N1-H	9.11 (br. s)	8.95 (s)
C4	2.58 (d, J = 15.4) 2.51 (d, J = 15.4 Hz)	2.98 – 2.83 (m, 4H) 2.54 – 2.45 (m, 2H)
C6	3.92 (br d, J = 1.6 Hz)	3.83 – 3.75 (m, 3H)
C7	2.58 (m)	2.07 – 1.99 (m, 1H)
C8	4.77 (d, J = 10.4 Hz)	5.52 (br s)
C10	3.51 (br ddd, J = 10.0, 6.8, 3.6) 3.23 (ddd, J = 9.5, 9.5, 9.5)	3.31 – 3.25 (m, 1H) 3.18 – 3.13 (m, 1H)
C11	2.44 – 2.39 (2H, overlapped)	2.16 – 2.08 (m, 1H) 1.94 – 1.82 (m, 3H)
C14	7.79 (d, J = 7.6 Hz)	7.35 (d, J = 7.4 Hz)
C15	7.09 (dd, J = 7.6, 7.6 Hz)	6.92 (t, J = 7.6 Hz)
C16	7.21 (dd, J = 7.6, 7.6 Hz)	7.16 (t, J = 7.8 Hz)
C17	6.85 (d, J = 7.6 Hz)	6.85 – 6.80 (m, 2H)
C19	3.63 (s)	3.38 (s)
C20	1.53 (2H, overlapped)	1.63 – 1.50 (m, 2H) 1.48 – 1.38 (m, 3H)
C21	3.82 (overlapped) 3.77 (m)	3.83 – 3.75 (m, 3H) 3.71 – 3.64 (m, 2H)
C22	2.44 – 2.39 (overlapped) 2.09 (dd, J = 16.9, 4.8 Hz)	2.69 – 2.60 (m, 2H) 1.94 – 1.82 (m, 3H)
CO_2CH_3	3.80 (3H, s)	3.79 (s, 3H)
C4′	2.73 (d, J = 15.1) 1.51 (d, J = 15.1)	2.98 – 2.83 (m, 4H) 1.48 – 1.38 (m, 3H)
C6′	3.58 (br s)	3.62 (t, J = 3.1 Hz)
C7′	2.03 – 1.98 (2H, overlapped)	1.99 – 1.94 (m, 2H) 1.99 – 1.94 (m, 2H
C8′	2.52 (ddd, J = 10.7, 10.7, 5.2 Hz) 2.94 (overlapped)	2.98 – 2.83 (m, 4H) 2.69 – 2.60 (m, 2H)
C10′	2.94 (overlapped) 2.44 – 2.39 (overlapped)	2.98 – 2.83 (m, 4H) 2.54 – 2.45 (m, 2H)
C11′	2.04 (ddd, J = 12.1, 12.1, 6.9 Hz) 1.77 (dd, J = 12.5, 5.2 Hz)	1.94 – 1.82 (m, 3H) 1.68 – 1.63 (m, 1H)
C14′	6.71 (dd, J = 7.2, 1.9 Hz)	6.85 – 6.80 (m, 2H)
C15′	6.78 – 6.82 (overlapped)	6.72 – 6.63 (m, 2H)
C16′	6.78 – 6.82 (overlapped)	6.72 – 6.63 (m, 2H)
C17′-O**H**	12.76 (s)	6.25 (br s)
C19′	2.64 (s)	2.72 (s)
C20′	1.63 (ddd, J = 12.6, 8.3, 4.0 Hz) 1.43 (m)	1.63 – 1.50 (m, 2H) 1.48 – 1.38 (m, 3H)

C21′	3.82 (overlapped) 3.71 (br ddd, J = 9.2, 9.2, 4.0 Hz)	3.83 – 3.75 (m, 3H) 3.71 – 3.64 (m, 2H)

Table 3.2 Comparison of our ^{13}C NMR data of ent-C7-epi-voacandimine A (**3.32**) with literature data ($CDCl_3$).

Assignment	Isolation Report[6] voacandimine A (**3.1**, ^{13}C NMR, 125 MHz, $CDCl_3$)	Our synthetic *ent*-C7-*epi*-voacandimine A (**3.32**, ^{1}H-^{13}C HSQC, 600 MHz (H), 150.9 MHz (C), $CDCl_3$)[9]	Chemical Shift Difference [10]
C2	165.4	-	-
C3	91.4	-	-
C4	32.9	35.4	2.5
C5	44.5	-	-
C6	83.9	85.7	1.8
C7	29.2	35.4	6.2
C8	65.6	68.0	2.4
C10	46.0	47.7	1.7
C11	43.3	44.2	0.9
C12	56.3	-	-
C13	137.4	-	-
C14	122.9	121.8	-1.1
C15	122.4	121.1	-1.3
C16	128.2	127.9	-0.3
C17	109.1	109.3	-0.2
C18	142.6	-	-
C19	66.9	69.3	2.4
C20	40.0	37.1	-2.9
C21	65.3	64.6	-0.7
C22	29.7	30.3	0.6
$\mathbf{C}O_2CH_3$	168.5	-	-
$CO_2\mathbf{C}H_3$	51.2	51.0	-0.2
C2′	145.7	-	-
C3′	104.6	-	-
C4′	32.6	30.1	-2.5
C5′	46.1	-	-
C6′	79.8	80.1	0.3
C7′	27.2	27.3	0.1
C8′	48.0	47.0	-1.0
C10′	52.7	52.0	-0.7

[9] Due to the stability of synthetic *ent*-C7-*epi*-voacandimine A (**3.32**) sample, the carbon shifts were exclusively obtained from HSQC.

[10] Chemical Shift Difference, $\Delta\,\delta = \delta$ (this work, solvent ref. δ 77.16) – δ (previously reported voacandimine A (**3.1**))

C11′	43.0	45.5	2.5
C12′	50.1	-	-
C13′	140.7	-	-
C14′	111.5	114.0	2.5
C15′	122.1	119.9	-2.2
C16′	116.2	116.0	-0.2
C17′	143.9	-	-
C18′	132.9	-	-
C19′	68.5	69.1	0.6
C20′	34.9	35.4	0.5
C21′	65.2	65.0	-0.2

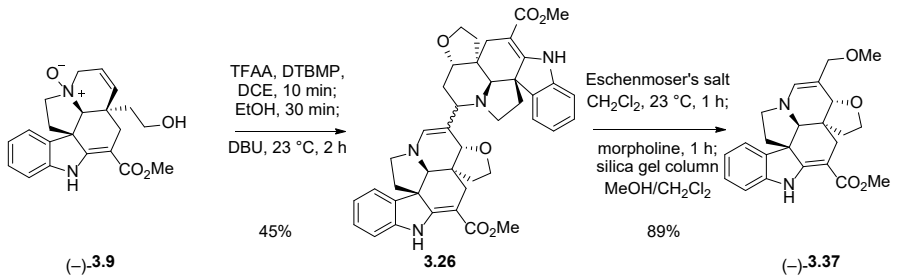

Methoxy methylene adduct (−)-3.37:

Trifluoroacetic anhydride (440 μL, 3.17 mmol, 4.0 equiv) was added dropwise via syringe to a solution of pentacyclic *N*-oxide **3.9**[8] (292 mg, 0.792 mmol, 1 equiv) and 2,6-di-*tert*-butyl-4-methylpyridine (650 mg, 3.17 mmol, 4.0 equiv) in 1,2-dichloroethane (40 mL) at 23 °C under argon. After 10 minutes, ethanol (40 mL) was added to the reaction. After 30 minutes, 1,8-diazabicyclo[5.4.0]undec-7-ene (DBU, 710 μL, 4.75 mmol, 6.0 equiv) was added. After 2 h, saturated aqueous sodium bicarbonate solution (60 mL) and ethyl acetate (40 mL) were added to the reaction mixture. The layers were separated, and the aqueous layer was extracted with ethyl acetate (2 × 40 mL). The combined organic layers were dried over anhydrous sodium sulfate, were filtered, and were concentrated under reduced pressure. The resulting residue was purified by flash column chromatography on silica gel (eluent: 30% ethyl acetate in hexanes to 50% ethyl acetate in hexanes) to afford a mixture of C8′ epimers of dimeric enamine **3.26** (125.5 mg, 0.179 mmol, 45%) and also open dimer **3.30** (89 mg, 0.127 mmol, 32%). **3.30** is readily converted to **3.26** by dissolving in equal parts dichloromethane and 2,2,2-trifluoroethanol.

Eschenmoser's salt (131 mg, 0.71 mmol, 5.1 equiv), was added to a solution of above **3.26** (99 mg, 0.14 mmol, 1 equiv) in dichloromethane (5.5 mL) at 23 ºC. After 1 h, morpholine (10 equiv) was added to the reaction. After 1 h, saturated aqueous sodium bicarbonate solution (10 mL) was added to the reaction mixture. The layers were separated and the aqueous layer was extracted with dichloromethane (3 × 10 mL). The combined organic layers were dried over anhydrous sodium sulfate, were filtered, and were concentrated under reduced pressure. The resulting residue was purified by flash column chromatography on silica gel (eluent: 2% methanol in dichloromethane to 4% methanol in dichloromethane.) to afford (–)-**3.37** (97 mg, 0.25 mmol, 89%) as a foam. Structural assignments were made using additional information from gCOSY, gHSQC, and gHMBC experiments.

^{1}H NMR (600 MHz, $CDCl_3$, 25 °C): δ 8.93 (s, 1H, N_1**H**), 7.23 (d, J = 7.4 Hz, 1H, C_{14}**H**), 7.19 (td, J = 7.7, 1.2 Hz, 1H, C_{16}**H**), 6.92 (td, J = 7.5, 1.0 Hz, 1H, C_{15}**H**), 6.86 (d, J = 7.8 Hz, 1H, C_{17}**H**), 6.57 (s, 1H, C_8**H**), 4.09 (d, J = 11.0 Hz, 1H, C_7C**H$_a$**), 3.90 (d, J = 10.9 Hz, 1H, C_7C**H$_b$**), 3.90 (s, 1H, C_6**H**) 3.77 (s, 3H, CO_2C**H$_3$**), 3.79 – 3.73 (m, C_{21}**H$_a$**), 3.66 (m, 2H, C_{10}**H$_a$**, C_{21}**H$_b$**), 3.52 (d, J = 2.0 Hz, 1H, C_{19}**H**), 3.38 (ddd, J = 10.0, 7.2, 2.8 Hz, 1H, C_{10}**H$_b$**), 3.32 (s, 3H, OC**H$_3$**), 2.32 (dd, J = 15.1, 2.1 Hz, 1H, C_4**H$_a$**), 2.04 (td, J = 10.7, 10.2, 7.1 Hz, 1H, C_{11}**H$_a$**), 1.94 – 1.87 (m, 2H, C_4**H$_b$**, C_{11}**H$_b$**), 1.63 (ddd, J =

	13.0, 9.5, 5.9 Hz, 1H, $C_{20}\mathbf{H_a}$), 1.33 (ddd, J = 12.9, 8.6, 6.1 Hz, 1H, $C_{20}\mathbf{H_b}$).
^{13}C NMR (150.9 MHz, $CDCl_3$, 25 °C):	δ 168.7 (2C, $\mathbf{C}O_2CH_3$, $\mathbf{C}_2$), 143.5 ($\mathbf{C}_{18}$), 136.2 ($\mathbf{C}_{13}$), 135.0 ($\mathbf{C}_8$), 128.4 ($\mathbf{C}_{16}$), 121.8 ($\mathbf{C}_{14}$), 121.3 ($\mathbf{C}_{15}$), 109.7 ($\mathbf{C}_{17}$), 100.4 ($\mathbf{C}_7$), 93.7 ($\mathbf{C}_3$), 78.1 ($\mathbf{C}_6$), 74.2 ($C_7\mathbf{C}H_2$), 63.7 ($\mathbf{C}_{21}$), 63.0 ($\mathbf{C}_{19}$), 57.2 ($O\mathbf{C}H_3$), 51.3 ($CO_2\mathbf{C}H_3$), 50.3 ($\mathbf{C}_{10}$), 44.4 ($\mathbf{C}_{11}$), 43.0 ($\mathbf{C}_5$), 36.8 ($\mathbf{C}_{20}$), 27.4 ($\mathbf{C}_4$).
FTIR (thin film) cm^{-1}:	2938 (br), 2848 (br), 1674 (s), 1655 (s), 1607 (s), 1464 (m), 1378 (m), 1289 (m), 1247 (m), 1198 (m), 747 (m).
HRMS (ESI) (*m/z*):	calc'd for $C_{22}H_{23}N_2O_3$ $[M-OCH_3]^+$: 363.1705, found: 363.1698.
$[\alpha]_D^{20}$:	–96 (*c* = 0.485, $CHCl_3$).

TLC (3% methanol in dichloromethane), R*f*: 0.27 (UV, CAM).

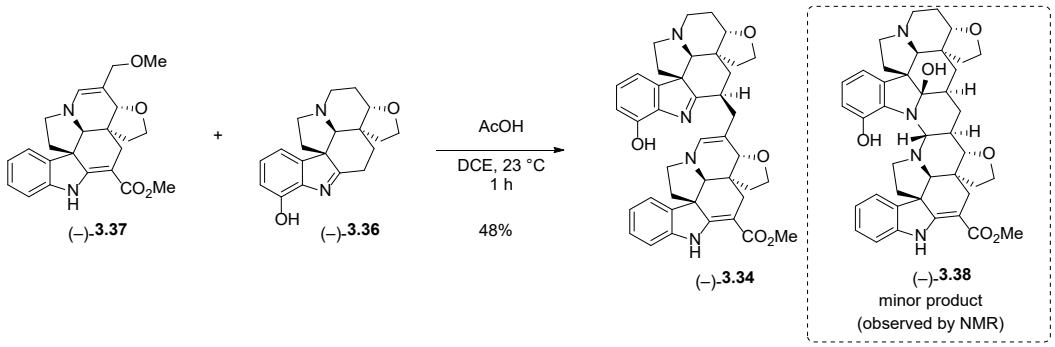

methylene bridged dodecacycle (−)-3.34

Acetic acid (14 μL, 0.240 mmol, 9.8 equiv) was added to a solution of hexacyclic imine (–)-**3.36** (15.8 mg, 50 μmol, 2.0 equiv) and **3.37** (9.8 mg, 25 μmol, 1 equiv) in 1,2-dichloroethane (0.20 mL) and 2,2,2-trifluoroethanol (0.20 mL) at 23 °C. After 1 h, saturated aqueous sodium bicarbonate solution (5 mL) and dichloromethane (5 mL) were added to the reaction mixture. The layers were separated, and the aqueous layer was extracted with dichloromethane (2 × 5 mL). The combined organic layers were dried over anhydrous sodium sulfate, were filtered, and were concentrated under reduced pressure. The resulting residue was purified by flash column chromatography on silica gel (eluent: 60% ethyl acetate in hexanes to 100% ethyl acetate in hexanes) to afford heterodimeric intermediate (–)-**3.34** (8.4 mg, 12 μmol, 48%) as a residue. Structural assignments were made using additional information from gCOSY, gHSQC, gHMBC, and ROESY experiments.

(−)-**3.38** (<5%) can be observed by NMR as part of a mixture with recovered imine (−)-**3.36**. Due to the low amount of material, samples containing (−)-**3.38** from various attempts were combined and purified by flash column chromatography on silica gel (eluent: 20% acetone in hexanes to 30% acetone in hexanes) for characterization. Structural assignments were made using additional information from gCOSY, gHSQC, gHMBC, and ROESY experiments.

^{1}H NMR (600 MHz, $CDCl_3$, 25 °C): δ 8.92 (s, 1H, N_1**H**), 7.25 (d, J = 7.5 Hz, 1H, C_{14}**H**), 7.18 (td, J = 7.7, 1.2 Hz, 1H, C_{16}**H**), 7.08 (t, J = 7.8 Hz, 1H, $C_{15'}$**H**), 6.92 (td, J = 7.5, 0.9 Hz, 1H, C_{15}**H**), 6.88 (app-d, J = 7.8 Hz, 2H, $C_{14'}$**H**, $C_{16'}$**H**), 6.85 (d, J = 7.8 Hz, 1H, C_{17}**H**), 6.44 (s, 1H, C_8**H**), 3.80 (s, 3H, CO_2C**H**$_3$), 3.70 (td, J = 8.8, 5.7 Hz, 1H, C_{21}**H**$_a$), 3.67 – 3.63 (m, 2H, $C_{21'}$**H**$_2$), 3.60 (td, J = 9.4, 5.5 Hz, 1H, C_{10}**H**$_a$), 3.55 (s, 1H, C_6**H**), 3.54 – 3.50 (m, 2H, $C_{6'}$**H**, C_{21}**H**$_b$), 3.49 (d, J = 1.9 Hz, 1H, C_{19}**H**), 3.32 (ddd, J = 10.1, 6.9, 3.6 Hz, 1H, C_{10}**H**$_b$), 3.27 (dd, J = 9.1, 6.6 Hz, 1H, $C_{3'}$**H**), 3.20 (dd, J = 8.4, 6.3 Hz, 1H, $C_{10'}$**H**$_a$), 2.98 (ddd, J = 11.1, 5.8, 1.8 Hz, 1H, $C_{8'}$**H**$_a$), 2.86 – 2.79 (m, 2H, C_{22}**H**$_a$, $C_{10'}$**H**$_b$), 2.71 (s, 1H, $C_{19'}$**H**), 2.64 (td, J = 11.7, 3.5 Hz, 1H, $C_{8'}$**H**$_b$), 2.57 (dd, J = 13.4, 9.8 Hz, 1H, $C_{4'}$**H**$_a$), 2.54 – 2.58 (m, 2H, C_{22}**H**$_b$, $C_{11'}$**H**$_a$), 2.21 (dd, J = 15.1, 2.0 Hz, 1H, C_4**H**$_a$), 2.08 (ddd, J = 12.0, 9.2, 6.9 Hz, 1H, C_{11}**H**$_a$), 2.00 – 1.95 (m, 2H, C_4**H**$_b$, $C_{7'}$**H**$_a$), 1.95 – 1.89 (m, 2H, C_{11}**H**$_b$,

	$C_{7'}\mathbf{H_b}$), 1.76 – 1.62 (m, 2H, $C_{4'}\mathbf{H_b}$, $C_{11'}\mathbf{H_b}$), 1.60 – 1.52 (m, 2H, $C_{20}\mathbf{H_a}$, $C_{20'}\mathbf{H_a}$), 1.29 (ddd, J = 12.8, 8.7, 6.3 Hz, 1H, $C_{20}\mathbf{H_b}$), 1.05 (ddd, J = 12.6, 7.8, 4.6 Hz, 1H, $C_{20}\mathbf{H_b}$).
^{13}C NMR (150.9 MHz, $CDCl_3$, 25 °C):	δ 189.3 ($\mathbf{C}_{2'}$), 168.7 ($\mathbf{C}O_2CH_3$), 166.8 ($\mathbf{C}_2$), 150.1 ($\mathbf{C}_{13'}$), 148.0 ($\mathbf{C}_{17'}$), 143.5 ($\mathbf{C}_{18}$), 140.0 ($\mathbf{C}_{18'}$), 136.2 ($\mathbf{C}_{13}$), 132.5 ($\mathbf{C}_8$), 128.3 ($\mathbf{C}_{16}$), 127.4 ($\mathbf{C}_{15'}$), 121.8 ($\mathbf{C}_{14}$), 121.3 ($\mathbf{C}_{15}$), 115.2 ($\mathbf{C}_{14'}$), 113.3 ($\mathbf{C}_{16'}$), 109.7 ($\mathbf{C}_{17}$), 101.8 ($\mathbf{C}_7$), 93.7 ($\mathbf{C}_3$), 81.0 ($\mathbf{C}_{6'}$), 79.0 ($\mathbf{C}_6$), 72.1 ($\mathbf{C}_{19'}$), 65.3 ($\mathbf{C}_{21'}$), 63.5 ($\mathbf{C}_{21}$), 62.9 ($\mathbf{C}_{19}$), 62.7 ($\mathbf{C}_{12'}$), 56.7 ($\mathbf{C}_{12}$), 53.5 ($\mathbf{C}_{10'}$), 51.3 ($CO_2\mathbf{C}H_3$), 50.3 ($\mathbf{C}_{10}$), 46.7 ($\mathbf{C}_{8'}$), 45.2 ($\mathbf{C}_{5'}$), 44.7 ($\mathbf{C}_{11}$), 43.1 ($\mathbf{C}_5$), 40.4 ($\mathbf{C}_{3'}$), 38.6 ($\mathbf{C}_{22}$), 36.7 ($\mathbf{C}_{20}$), 35.9 ($\mathbf{C}_{11'}$), 34.9 ($\mathbf{C}_{4'}$), 33.7 ($\mathbf{C}_{20'}$), 27.8 ($\mathbf{C}_4$), 26.5 ($\mathbf{C}_{7'}$).
FTIR (thin film) cm^{-1}:	3378 (br w), 2924 (br), 2850 (br), 1675 (m), 1608 (s), 1477 (m), 1438 (m), 1290 (m), 1250 (s), 1200 (m), 1045 (m), 749 (s).
HRMS (ESI) (*m/z*):	calc'd for $C_{41}H_{45}N_4O_5$ $[M+H]^+$: 673.3386, found: 673.3380.
$[\alpha]_D^{20}$:	–141 (*c* = 0.215, $CHCl_3$)
TLC (60% ethyl acetate in hexanes), R*f*:	0.61 (UV, CAM).

(−)-C7,C8-*diepi*-C2′,C3′-hydrovoacandimine A (3.38):

^{1}H NMR (600 MHz, $CDCl_3$, 25 °C):	δ 13.15 (s, 1H, $C_{17'}O\mathbf{H}$), 9.01 (s, 1H, $N_1\mathbf{H}$), 7.61 (d, J = 7.4 Hz, 1H, $C_{14}\mathbf{H}$), 7.19 (td, J = 7.7, 1.2 Hz, 1H, $C_{16}\mathbf{H}$), 7.03 (td, J = 7.5, 1.0 Hz, 1H, $C_{15}\mathbf{H}$), 6.83 (d, J = 7.8 Hz, 1H, $C_{17}\mathbf{H}$), 6.80 – 6.72 (m, 2H, $C_{15'}\mathbf{H_b}$, $C_{16'}\mathbf{H_b}$), 6.61 (dd, J = 6.9, 1.6 Hz, 1H, $C_{14'}\mathbf{H}$), 4.24 (d, J = 12.0 Hz, 1H, $C_8\mathbf{H}$), 4.08 – 3.98 (m, 2H, $C_{19}\mathbf{H}$, $C_{21}\mathbf{H_a}$), 3.88 (ddd, J = 11.1, 8.5, 3.0 Hz, 1H, $C_{21}\mathbf{H_b}$), 3.79 (s, 3H, $CO_2C\mathbf{H_3}$), 3.70 – 3.65 (m, 2H, $C_{10}\mathbf{H_a}$, $C_{21'}\mathbf{H_a}$), 3.62 (dt, J = 9.1, 6.7 Hz, 1H, $C_{21'}\mathbf{H_b}$), 3.53 (d, J = 8.2 Hz, 1H, $C_6\mathbf{H}$), 3.45 – 3.42 (m, 1H, $C_{6'}\mathbf{H}$), 3.06 (td, J = 9.3, 3.6 Hz, 1H, $C_{10'}\mathbf{H_a}$), 2.96 (td, J = 10.7, 6.0 Hz, 1H, $C_{10}\mathbf{H_b}$), 2.89 (ddd, J = 13.4, 9.4, 6.8 Hz, 1H, $C_{11'}\mathbf{H_a}$), 2.86 – 2.81 (m, 1H, $C_{8'}\mathbf{H_a}$), 2.67 (dd, J = 15.8, 2.1 Hz, 1H, $C_4\mathbf{H_a}$), 2.59 (s, 1H, $C_{19'}\mathbf{H}$), 2.36 (ddd, J = 13.1, 6.0, 2.0 Hz, 1H, $C_{11}\mathbf{H_a}$), 2.33 – 2.19 (m, 5H, $C_4\mathbf{H_b}$, $C_{11}\mathbf{H_b}$, $C_{8'}\mathbf{H_b}$, $C_{10'}\mathbf{H_b}$, $C_{20'}\mathbf{H_a}$), 2.07 –

	2.00 (m, 1H, $C_{3'}$**H**), 1.99 – 1.83 (m, 4H, C_7**H**, C_{22}**H$_a$**, $C_{7'}$**H$_2$**), 1.76 (t, J = 13.1 Hz, 1H, $C_{4'}$**H$_a$**), 1.60 – 1.55 (m,1H, C_{22}**H$_b$**), 1.52 – 1.43 (m, 2H, C_{20}**H$_a$**, $C_{20'}$**H$_b$**), 1.34 (ddd, J = 14.2, 11.2, 3.7 Hz, 1H, $C_{11'}$**H$_b$**), 1.29 – 1.24 (m, 1H, C_{20}**H$_b$**), 0.93 – 0.88 (m, 1H, $C_{4'}$**H$_b$**).
^{13}C NMR (150.9 MHz, $CDCl_3$, 25 °C):	δ 168.6 (**C**O_2CH_3), 166.5 (**C**$_2$), 144.0 (**C**$_{17'}$), 143.1 (**C**$_{18}$), 137.0 (**C**$_{13'}$), 135.1 (**C**$_{13}$), 134.0 (**C**$_{18'}$), 128.5 (**C**$_{16}$), 122.5 (**C**$_{14}$), 122.2 (**C**$_{15}$), 121.4 (**C**$_{15'}$), 116.6 (**C**$_{16'}$), 112.7 (**C**$_{14'}$), 109.5 (**C**$_{17}$), 95.8 (**C**$_{2'}$), 94.2 (**C**$_3$), 88.2 (**C**$_6$), 80.6 (**C**$_{6'}$), 71.2 (**C**$_8$), 66.8 (**C**$_{19}$), 66.0 (**C**$_{21'}$), 65.6 (**C**$_{21}$), 63.7 (**C**$_{19'}$), 57.3 (**C**$_{12}$), 55.6 (**C**$_{12'}$), 52.9 (**C**$_{10}$), 52.2 (**C**$_{10'}$), 51.4 (CO_2**C**H_3), 48.7 (2C, **C**$_5$, **C**$_{8'}$), 44.3 (**C**$_{5'}$), 44.0 (**C**$_{11}$), 39.8 (**C**$_7$), 39.4 (**C**$_{20}$), 36.9 (**C**$_{20'}$), 34.5 (**C**$_4$), 34.0 (**C**$_{3'}$), 33.8 (**C**$_{22}$), 32.5 (**C**$_{4'}$), 29.8 (**C**$_{11'}$), 25.9 (**C**$_{7'}$).
FTIR (thin film) cm^{-1}:	2940 (br), 2860 (br), 1681 (m), 1611 (s), 1475 (m), 1330 (m), 1238 (m), 1158 (m), 1075 (m), 1037 (m), 753 (m).
HRMS (ESI) (*m/z*):	calc'd for $C_{41}H_{47}N_4O_6$ $[M+H]^+$: 691.3493, found: 691.3490.
$[\alpha]_D^{20}$:	–307 (*c* = 0.11, $CHCl_3$)
TLC (40% acetone in hexanes), R*f*:	0.31 (UV, CAM).

Table 3.3 Comparison of our ^{13}H NMR data of (−)-C7,C8-*diepi*-C2′,C3′-hydrovoacandimine A (**3.38)** with literature data ($CDCl_3$).

Assignment	Isolation Report voatriafricanine A[11] Aspidosperma subunit (**3.39**, ^{1}H NMR, 600 MHz, $CDCl_3$)	Our synthetic (−)-**3.38** (^{1}H NMR, 600 MHz, $CDCl_3$)
N1-H	9.07 (s)	9.01 (s)
C4	2.74 (d, J = 15.7 Hz) 2.32 (d, J = 15.7 Hz)	2.67 (dd, J = 15.8, 2.1 Hz) 2.33 – 2.19 (m, 5H)
C6	3.62 (d, J = 9.1 Hz)	3.53 (d, J = 8.2 Hz)
C7	1.94 (overlapped)	1.99 – 1.83 (m, 4H)
C8	4.35 (d, J = 12.0 Hz)	4.24 (d, J = 12.0 Hz)
C10	3.76 (overlapped) 3.03 (td, J = 10.9, 5.7)	3.70 – 3.65 (m, 2H) 2.96 (td, J = 10.7, 6.0 Hz)
C11	2.46 (overlapped) 2.29 (overlapped)	2.36 (ddd, J = 13.1, 6.0, 2.0 Hz) 2.33 – 2.19 (m, 5H)
C14	8.08 (d, J = 7.3 Hz)	7.61 (d, J = 7.4 Hz)
C15	7.14 (br t, J = 7.3 Hz)	7.03 (td, J = 7.5, 1.0 Hz)
C16	7.18 (br t, J = 7.3 Hz)	7.19 (td, J = 7.7, 1.2 Hz)
C17	6.85 (d, J = 7.3 Hz)	6.83 (d, J = 7.8 Hz)
C19	4.16 (s)	4.08 – 3.98 (m, 2H)
C20	1.55 (overlapped) 1.35 (overlapped)	1.52 – 1.43 (m, 2H) 1.29 – 1.24 (m, 1H)
C21	3.75 (overlapped)	4.08 – 3.98 (m, 2H) 3.88 (ddd, J = 11.1, 8.5, 3.0 Hz)
C22	1.97 (overlapped) 1.68 (overlapped)	1.99 – 1.83 (m, 4H) 1.60 – 1.55 (m, 1H)
CO_2CH_3	3.82 (s)	3.79 (s, 3H)
C3′	2.09 (overlapped)	2.07 – 2.00 (m, 1H)
C4′	1.93 (overlapped) 0.98 (br d, J = 13.0)	1.76 (t, J = 13.1 Hz) 0.93 – 0.88 (m, 1H)
C6′	3.47 (br s)	3.45 – 3.42 (m, 1H)
C7′	2.00 (overlapped) 2.28 (overlapped)	1.99 – 1.83 (m, 4H) 1.99 – 1.83 (m, 4H)
C8′	3.44 (overlapped) 2.46 (overlapped)	2.86 – 2.81 (m, 1H) 2.33 – 2.19 (m, 5H)
C10′	3.75 (m) 1.54 (m)	3.06 (td, J = 9.3, 3.6 Hz) 2.33 – 2.19 (m, 5H)

[11] Fouotsa, H.; Le Pogam, P.; Mkounga, P.; Lannang, A. M.; Bernadat, G. Vanheuverzwijn, J.; Zhou, Z.; Leblanc, K; Rharrabti, S.; Nkengfack, A. E.; Gallard, J.-F.; Fontaine, V.; Meyer, F.; Poupo, E. Beniddir, M. H. Voatriafricanines A and B, Trimeric Vobasine-Aspidosperma-Aspidosperma Alkaloids from *Voacanga africana*. *J. Nat. Prod*. **2021**, *84*, 2755-2761.

C11′	2.95 (m) 1.34 (overlapped)	2.89 (ddd, J = 13.4, 9.4, 6.8 Hz) 1.34 (ddd, J = 14.2, 11.2, 3.7 Hz)
C14′	6.42 (d, J = 7.3 Hz)	6.61 (dd, J = 6.9, 1.6 Hz)
C15′	6.29 (d, J = 7.3 Hz)	6.80 – 6.72 (m, 2H)
C16′	-	6.80 – 6.72 (m, 2H)
C17′-O**H**	14.39 (s)	13.15 (s)
C19′	2.74 (s)	2.59 (s)
C20′	2.26 (overlapped) 1.51 (overlapped)	2.33 – 2.19 (m, 5H) 1.52 – 1.43 (m, 2H)
C21′	3.94 (overlapped) 3.84 (overlapped)	3.70 – 3.65 (m, 2H) 3.62 (dt, J = 9.1, 6.7 Hz)

Table 3.4 Comparison of our ^{13}C NMR data of (−)-C7,C8-*diepi*-C2′,C3′-hydrovoacandimine A (**3.38**) with literature data ($CDCl_3$).

Assignment	Isolation Report[11] voatriafricanine A Aspidosperma subunit (**3.39**, ^{13}C NMR, 150 MHz, $CDCl_3$)	Our synthetic **3.38** (^{13}C NMR, 150.9 MHz, $CDCl_3$)	Chemical Shift Difference[12]
C2	166.3	166.5	0.2
C3	94.1	94.2	0.1
C4	34.4	34.5	0.1
C5	48.8	48.7	-0.1
C6	87.6	88.2	0.6
C7	40.0	39.8	-0.2
C8	71.0	71.2	0.2
C10	53.2	52.9	-0.3
C11	44.8	44.0	-0.8
C12	56.8	57.3	0.5
C13	135.3	135.1	-0.2
C14	122.5	122.5	0.0
C15	122.6	122.2	-0.4
C16	128.7	128.5	-0.2
C17	109.7	109.5	-0.2
C18	143.0	143.1	0.1
C19	67.2	66.8	-0.4
C20	39.8	39.4	-0.4
C21	66.0	65.6	-0.4
C22	33.1	33.8	0.7
$\mathbf{C}O_2CH_3$	168.6	168.6	0.0
$CO_2\mathbf{C}H_3$	51.5	51.4	-0.1
C2′	95.8	95.8	0.0
C3′	34.8	34.0	-0.8
C4′	31.8	32.5	0.7
C5′	44.8	44.3	-0.5
C6′	79.6	80.6	1.0
C7′	25.1	25.9	0.8
C8′	49.2	48.7	-0.5
C10′	51.8	52.2	0.4
C11′	29.8	29.8	0.0
C12′	55.5	55.6	0.1
C13′	134.5	137.0	2.5
C14′	112.2	112.7	0.5

[12] Chemical Shift Difference, $\Delta\,\delta = \delta$ (this work, solvent ref. δ 77.16) – δ (previously reported voatriafricanine A (**3.39**))

C15′	119.6	121.4	1.8
C16′	132.4	116.6	-15.8
C17′	141.3	144.0	2.7
C18′	134.2	134.0	-0.2
C19′	64.7	63.7	-1.0
C20′	37.1	36.9	-0.2
C21′	65.3	66.0	0.7

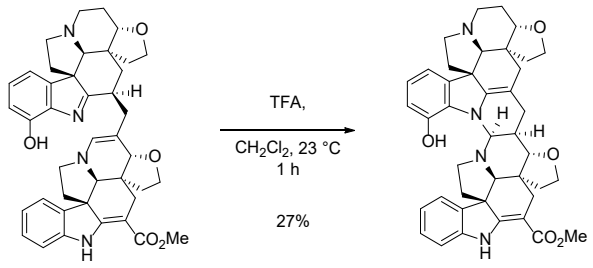

(–)-**3.34** (–)-**3.32**

(−)-C7-*epi*-voacandimine A (3.32):

Trifluoroacetic acid (9.0 µL, 0.117 mmol, 20 equiv) was added to a solution of (–)-**3.34** (4.0 mg, 5.9 µmol, 1 equiv) in dichloromethane (0.5 mL) under argon at 23 °C. After 1 h, saturated aqueous sodium bicarbonate solution (3mL) and dichloromethane (3 mL) were added to the reaction mixture. The layers were separated, and the aqueous layer was extracted with dichloromethane (2 × 3 mL). The combined organic layers were dried over anhydrous sodium sulfate, were filtered, and were concentrated under reduced pressure. The resulting residue was purified by flash column chromatography on silica gel (eluent: 10% acetone in hexanes to 20% acetone in hexanes) to afford (–)-**3.32** (1.1 mg, 1.6 µmol, 27%) as a residue.

Appendix A. Spectra for Chapter II

Respective Contributions

Dr. Kristen M. Flynn collected the spectral data for **2.33**, **2.9**, **2.34**, and **2.36**.

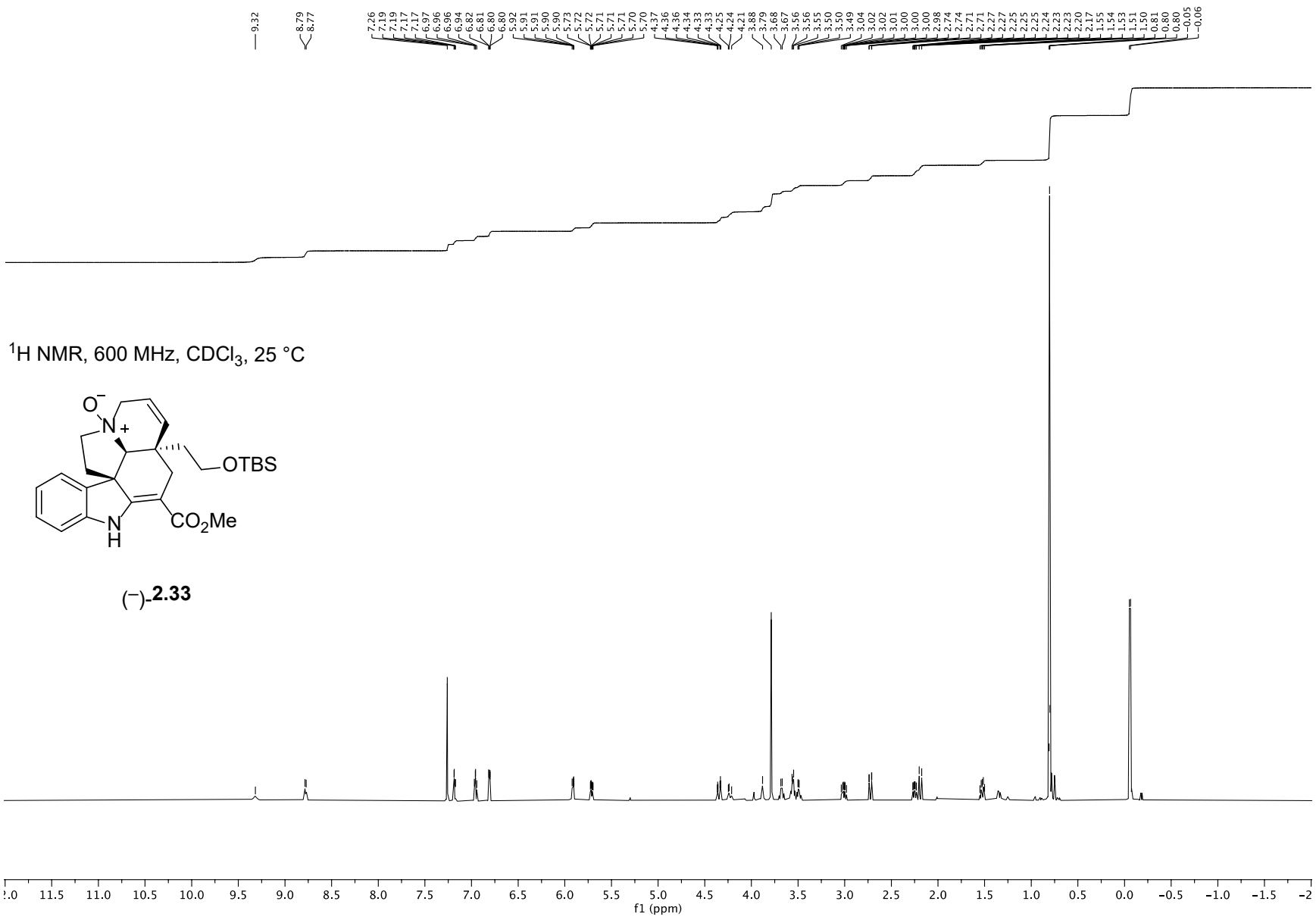
9.32
8.79
8.77
7.26
7.19
7.19
7.17
7.17
6.97
6.96
6.96
6.94
6.82
6.81
6.80
6.80
5.92
5.91
5.91
5.90
5.90
5.73
5.72
5.72
5.71
5.71
5.71
5.70
5.70
4.37
4.36
4.36
4.34
4.33
4.33
4.25
4.24
4.21
3.88
3.79
3.68
3.67
3.56
3.56
3.55
3.50
3.50
3.49
3.04
3.02
3.02
3.01
3.00
3.00
3.00
2.98
2.74
2.74
2.71
2.71
2.27
2.27
2.25
2.25
2.25
2.24
2.23
2.20
2.17
1.55
1.54
1.53
1.51
1.50
0.81
0.80
0.80
-0.05
-0.06
1H NMR, 600 MHz, CDCl3, 25 °C
O
N
OTBS
CO2Me
N
H
(−)-2.33
11.5
11.0
10.5
10.0
9.5
9.0
8.5
8.0
7.5
7.0
6.5
6.0
5.5
5.0
4.5
4.0
3.5
3.0
2.5
2.0
1.5
1.0
0.5
0.0
-0.5
-1.0
-1.5
f1 (ppm)

^{13}C NMR, 150.9 MHz, $CDCl_3$, 25 °C

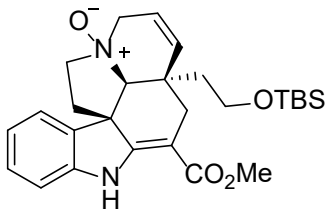

(–)-**2.33**

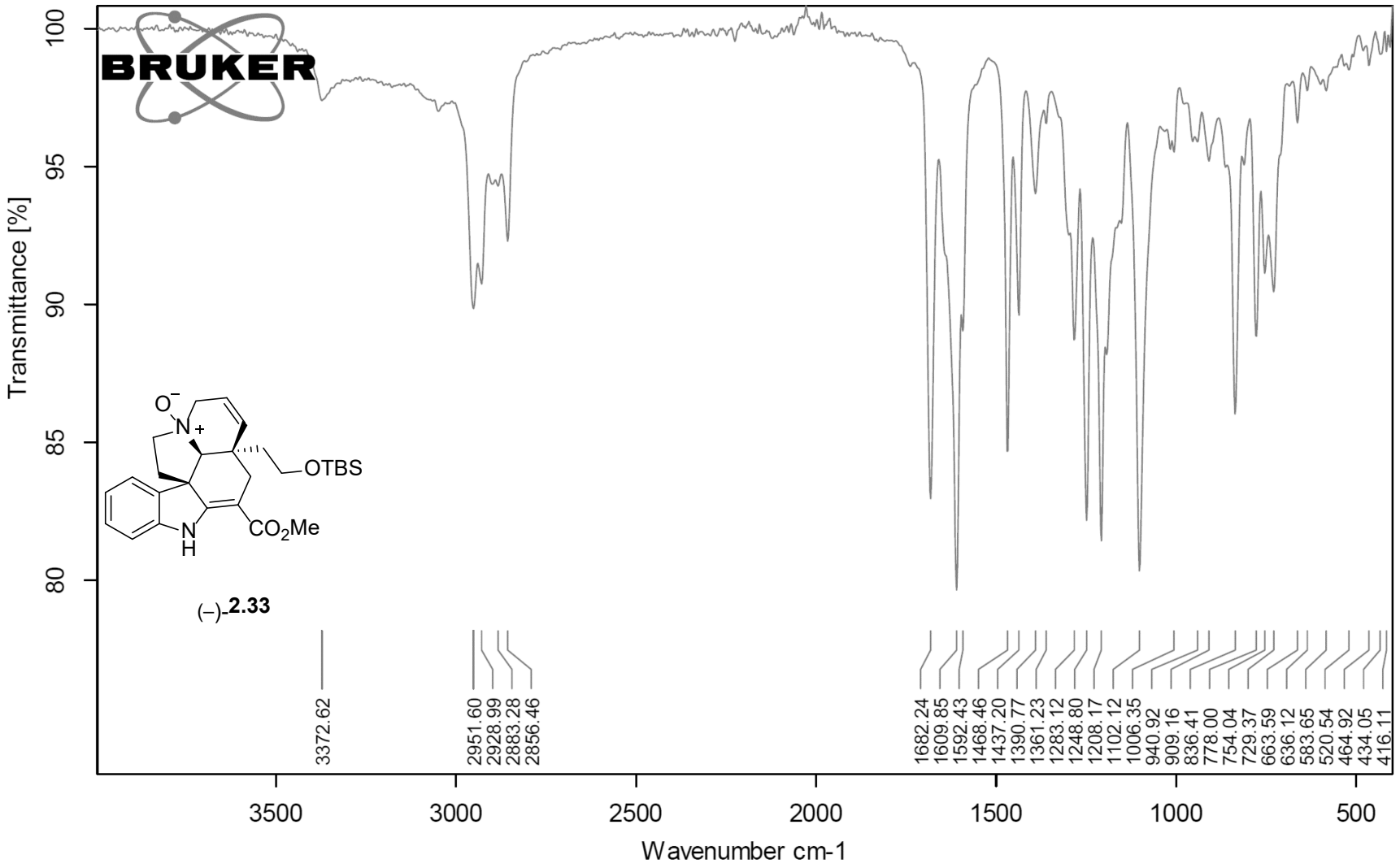
BRUKER
Transmittance [%]
100
95
90
85
80
OTBS
CO2Me
N
H
(–)-2.33
3372.62
2951.60
2928.99
2883.28
2856.46
1682.24
1609.85
1592.43
1468.46
1437.20
1390.77
1361.23
1283.12
1248.80
1208.17
1102.12
1006.35
940.92
909.16
836.41
778.00
754.04
729.37
663.59
636.12
583.65
520.54
464.92
434.05
416.11
3500
3000
2500
2000
1500
1000
500
Wavenumber cm-1

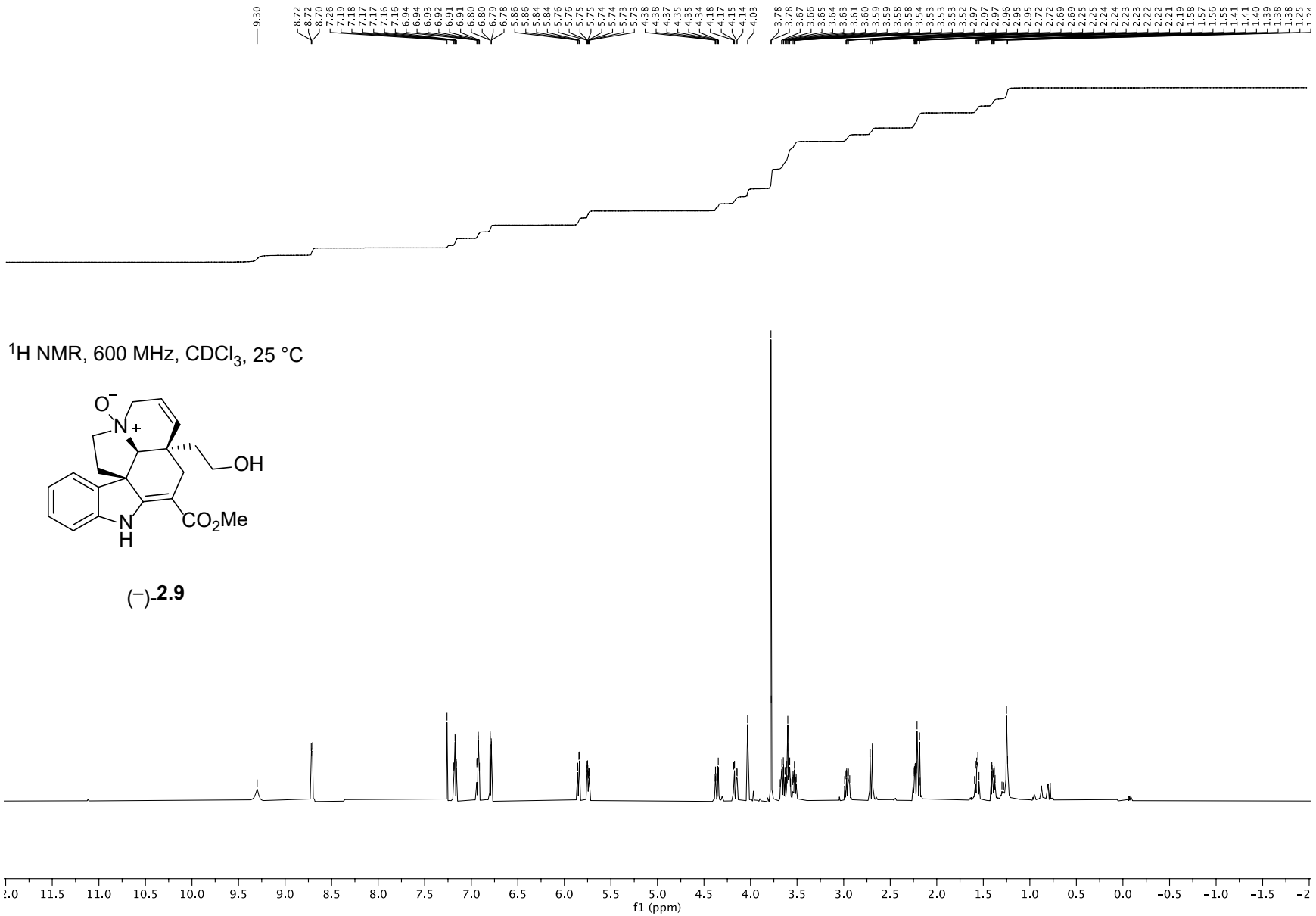
9.30
8.72
8.72
8.70
7.26
7.19
7.18
7.17
7.17
7.16
7.16
6.94
6.94
6.93
6.92
6.91
6.91
6.80
6.80
6.79
6.78
5.86
5.86
5.84
5.84
5.76
5.76
5.75
5.75
5.75
5.74
5.74
5.73
5.73
4.38
4.38
4.37
4.35
4.34
4.18
4.17
4.15
4.14
4.03
3.78
3.78
3.67
3.67
3.66
3.65
3.64
3.63
3.61
3.60
3.59
3.59
3.58
3.58
3.54
3.53
3.53
3.53
3.52
2.97
2.97
2.97
2.96
2.95
2.95
2.72
2.72
2.69
2.69
2.25
2.25
2.24
2.24
2.23
2.22
2.22
2.21
2.19
1.58
1.57
1.56
1.55
1.41
1.41
1.40
1.39
1.38
1.38
1.25
1.24
^{1}H NMR, 600 MHz, $CDCl_3$, 25 °C
O
N
OH
CO_2Me
N
H
(−)-2.9
f1 (ppm)

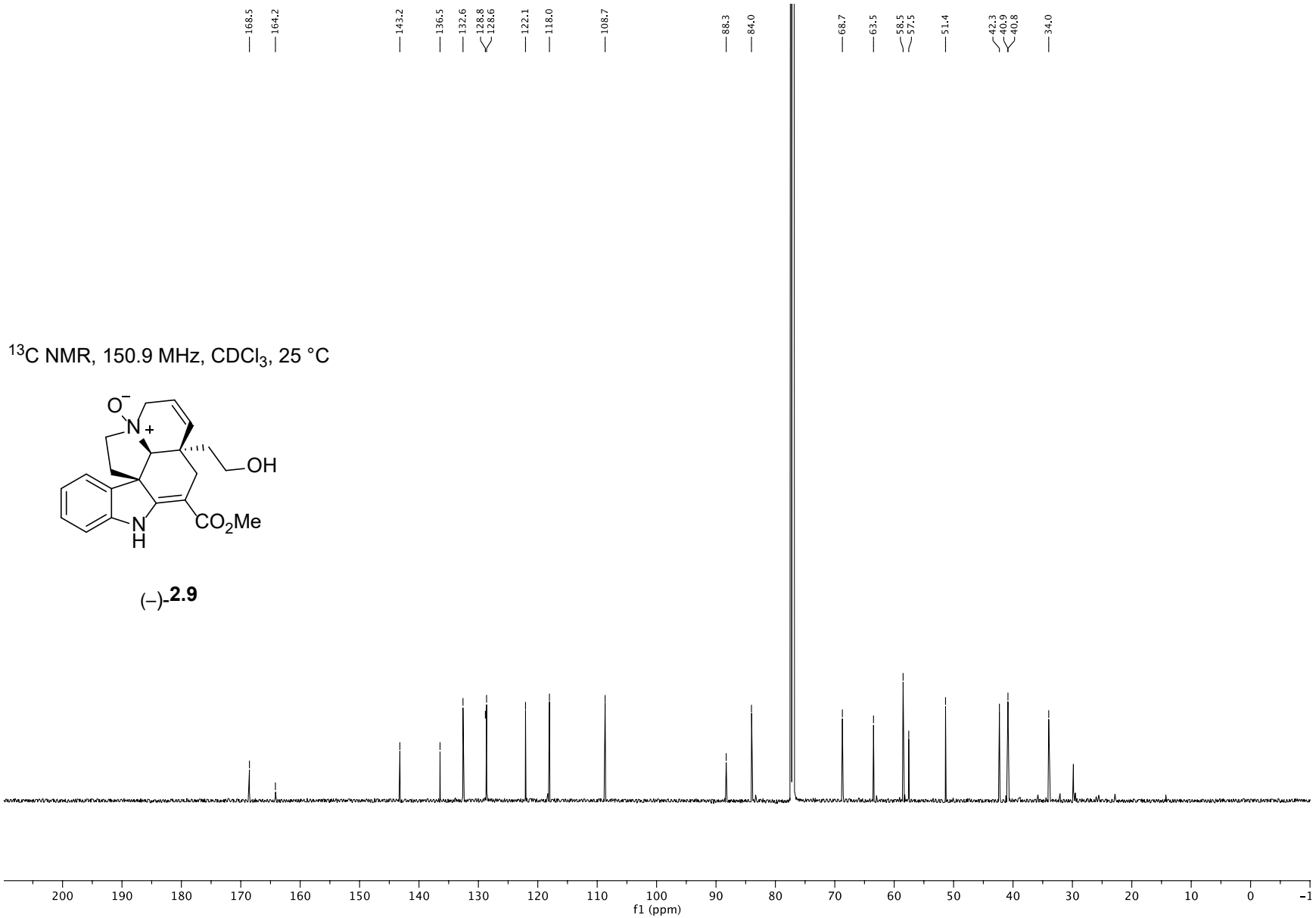

^{13}C NMR, 150.9 MHz, $CDCl_3$, 25 °C

(–)-**2.9**

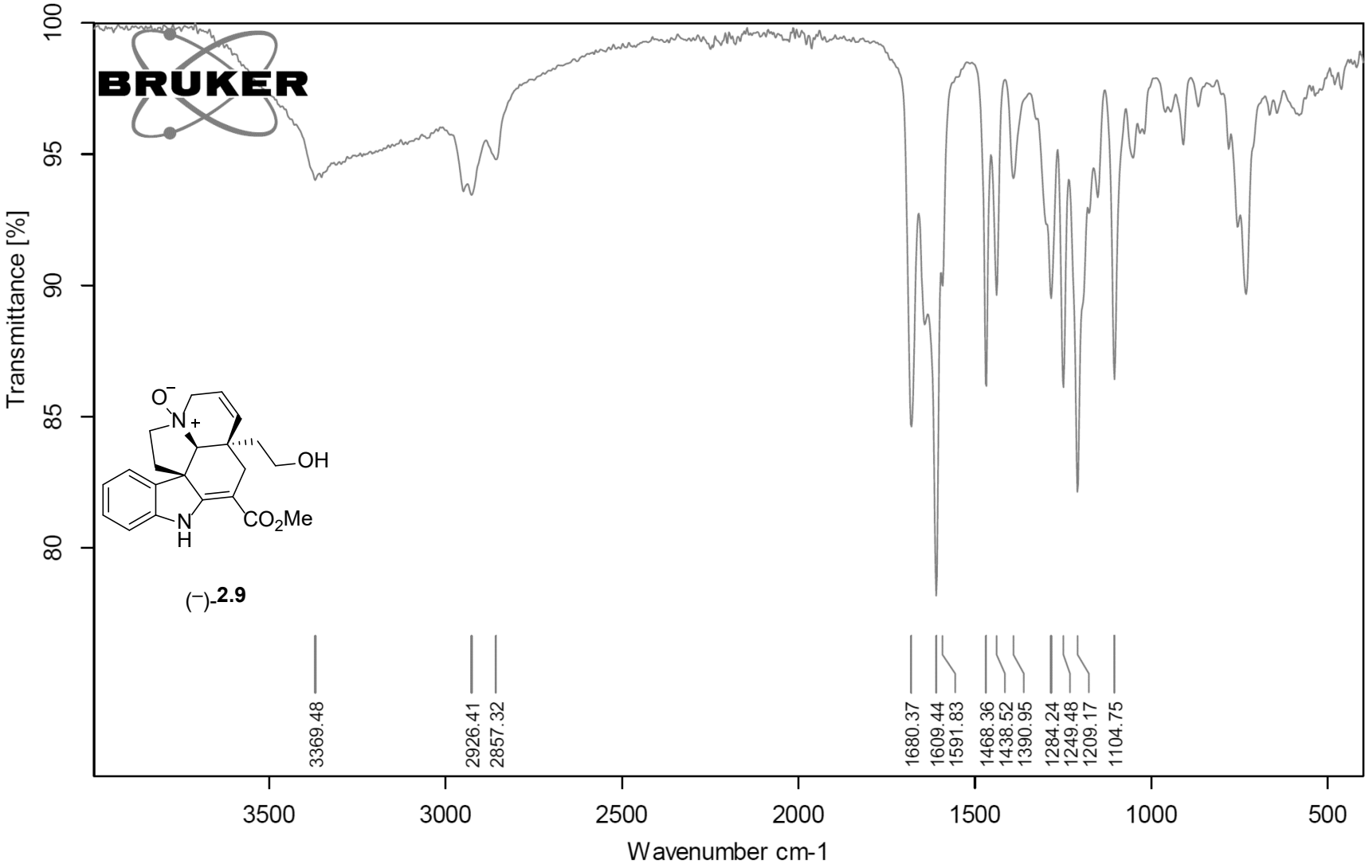
BRUKER
Transmittance [%]
100
95
90
85
80
3500
3000
2500
2000
1500
1000
500
Wavenumber cm-1
3369.48
2926.41
2857.32
1680.37
1609.44
1591.83
1468.36
1438.52
1390.95
1284.24
1249.48
1209.17
1104.75
OH
CO2Me
N
H

(−)-**2.9**

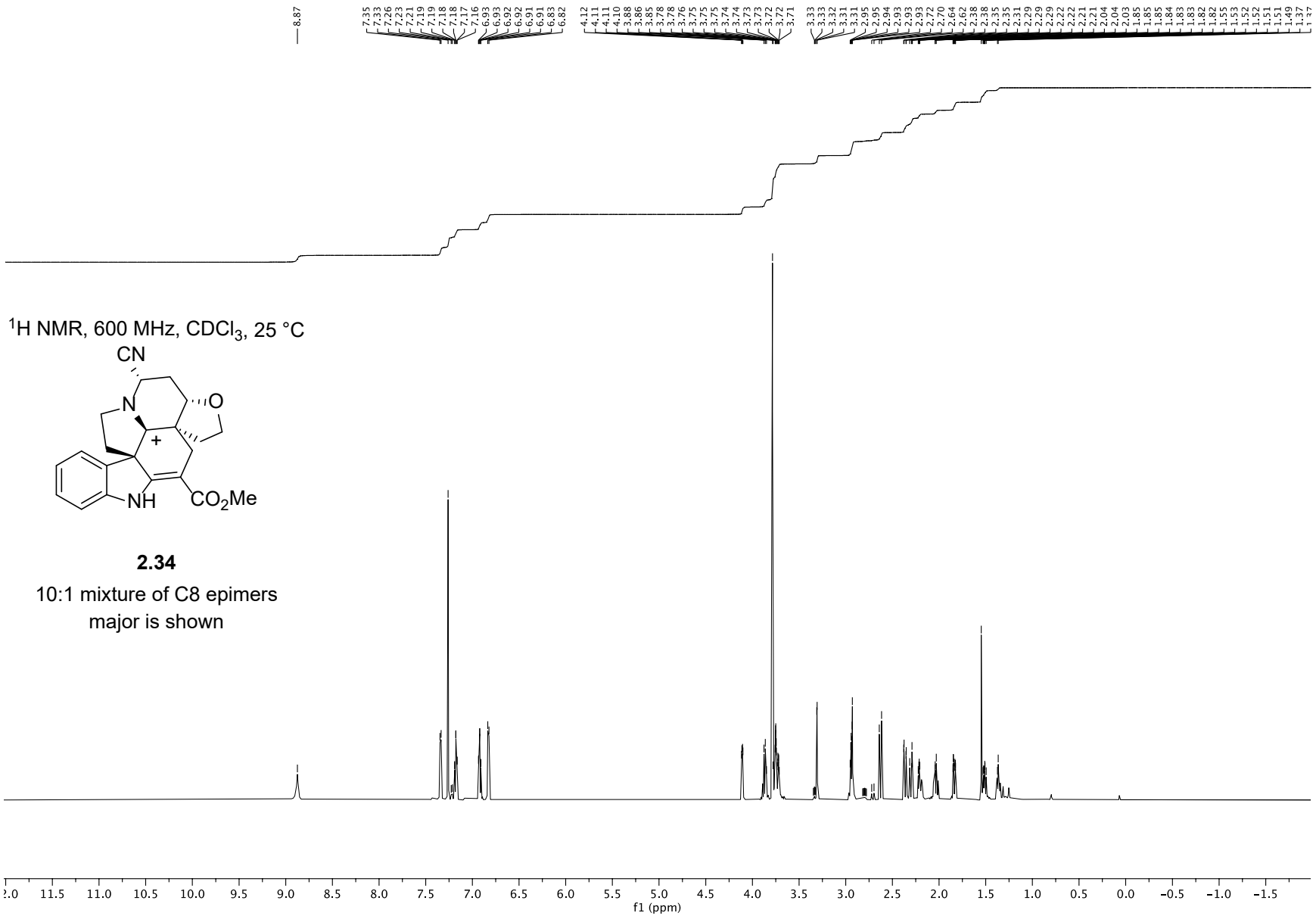
^{1}H NMR, 600 MHz, $CDCl_3$, 25 °C
CN
N
O
+
NH
CO_2Me
2.34
10:1 mixture of C8 epimers
major is shown
f1 (ppm)

^{13}C NMR, 150.9 MHz, $CDCl_3$, 25 °C

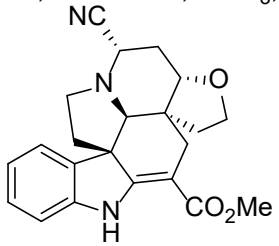

2.34

10:1 mixture of C8 epimers
major is shown

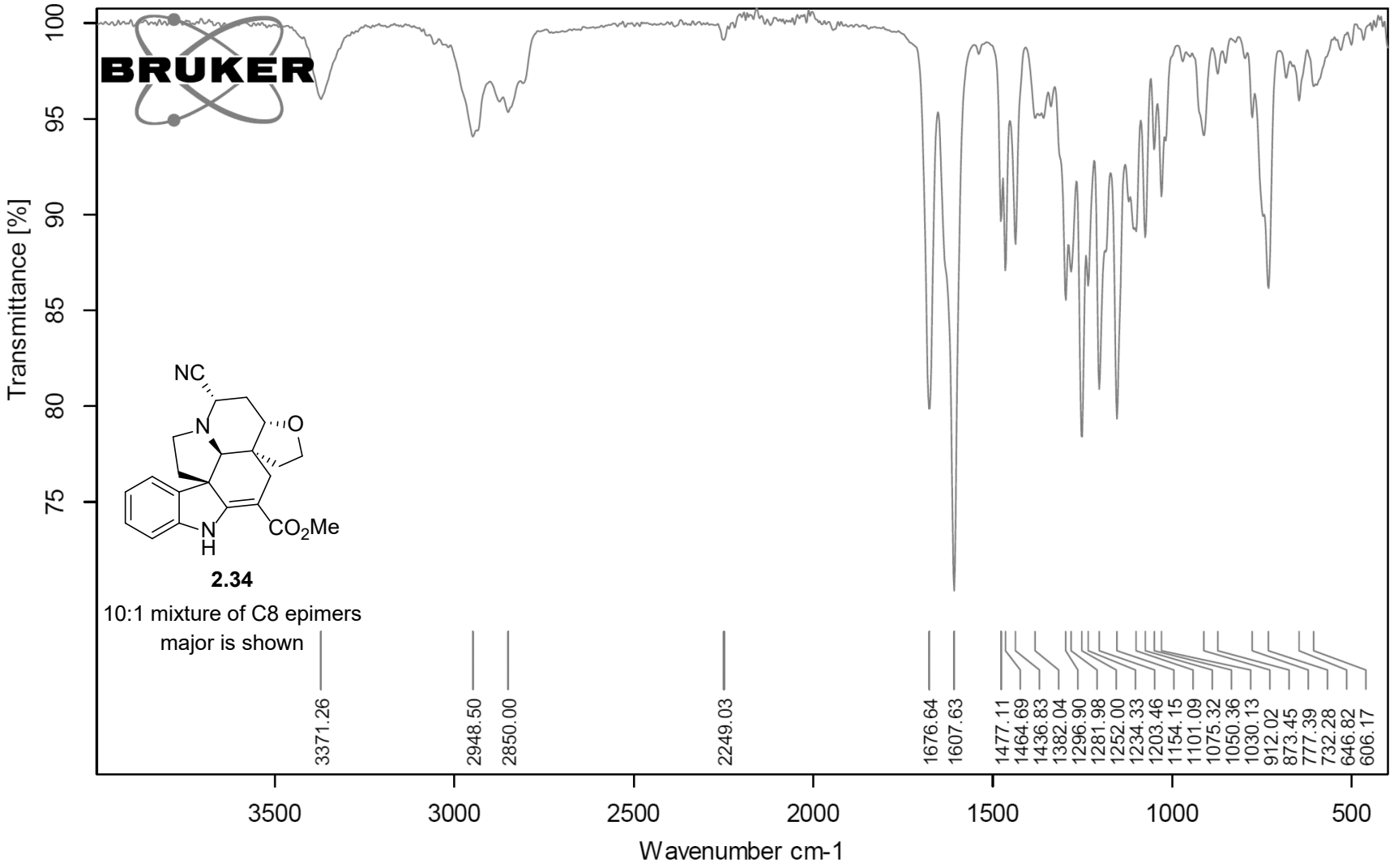
BRUKER
Transmittance [%]
100
95
90
85
80
75
NC
N
O
N
H
CO2Me
2.34
10:1 mixture of C8 epimers
major is shown
3371.26
2948.50
2850.00
2249.03
1676.64
1607.63
1477.11
1464.69
1436.83
1382.04
1296.90
1281.98
1252.00
1234.33
1203.46
1154.15
1101.09
1075.32
1050.36
1030.13
912.02
873.45
777.39
732.28
646.82
606.17
3500
3000
2500
2000
1500
1000
500
Wavenumber cm-1

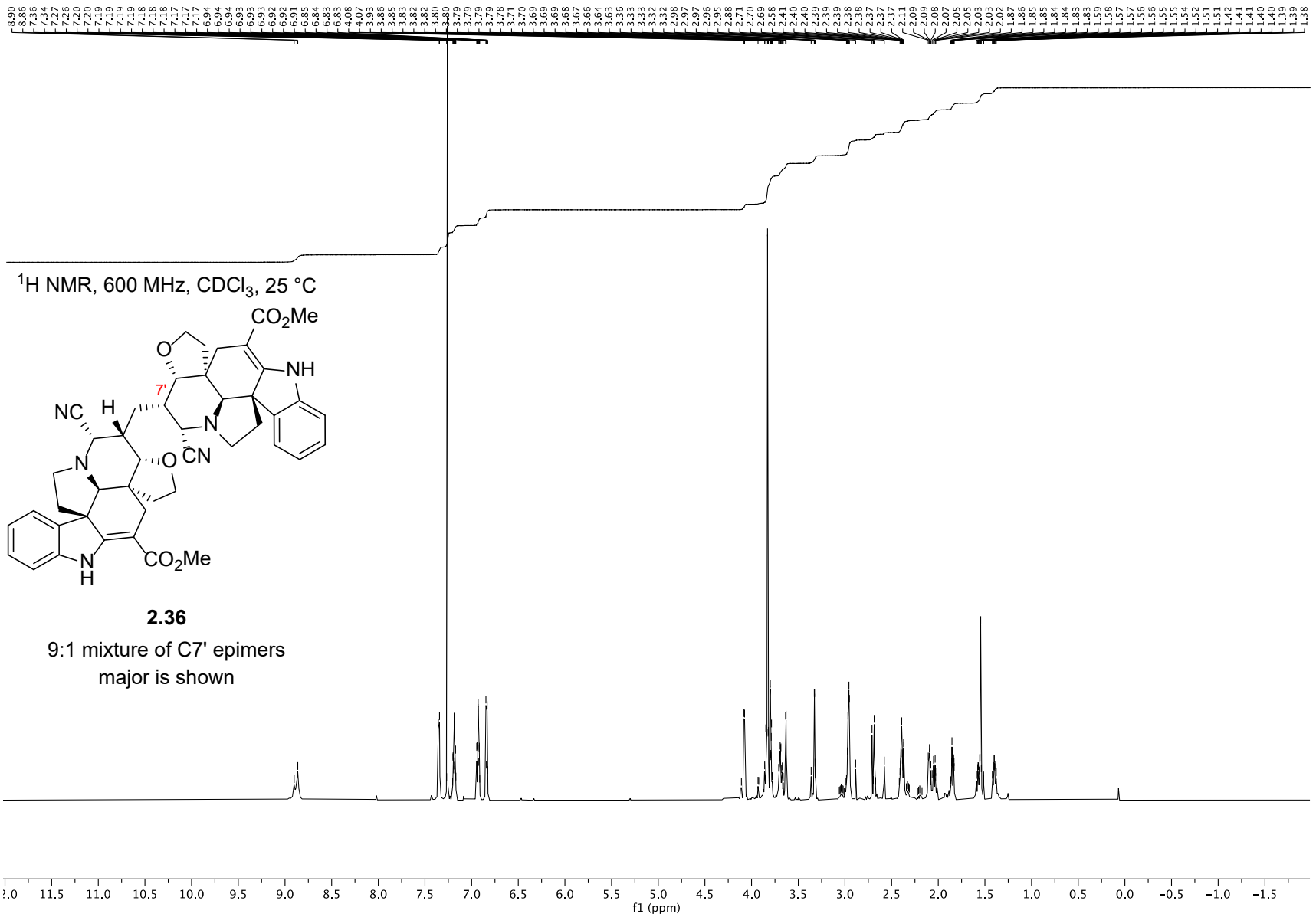

2.36

9:1 mixture of C7' epimers
major is shown

^{13}C NMR, 150.8 MHz, $CDCl_3$, 25 °C

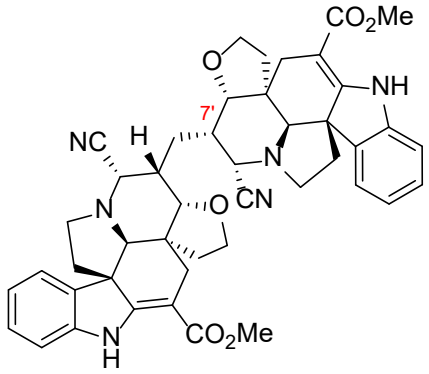

2.36

9:1 mixture of C7' epimers
major is shown

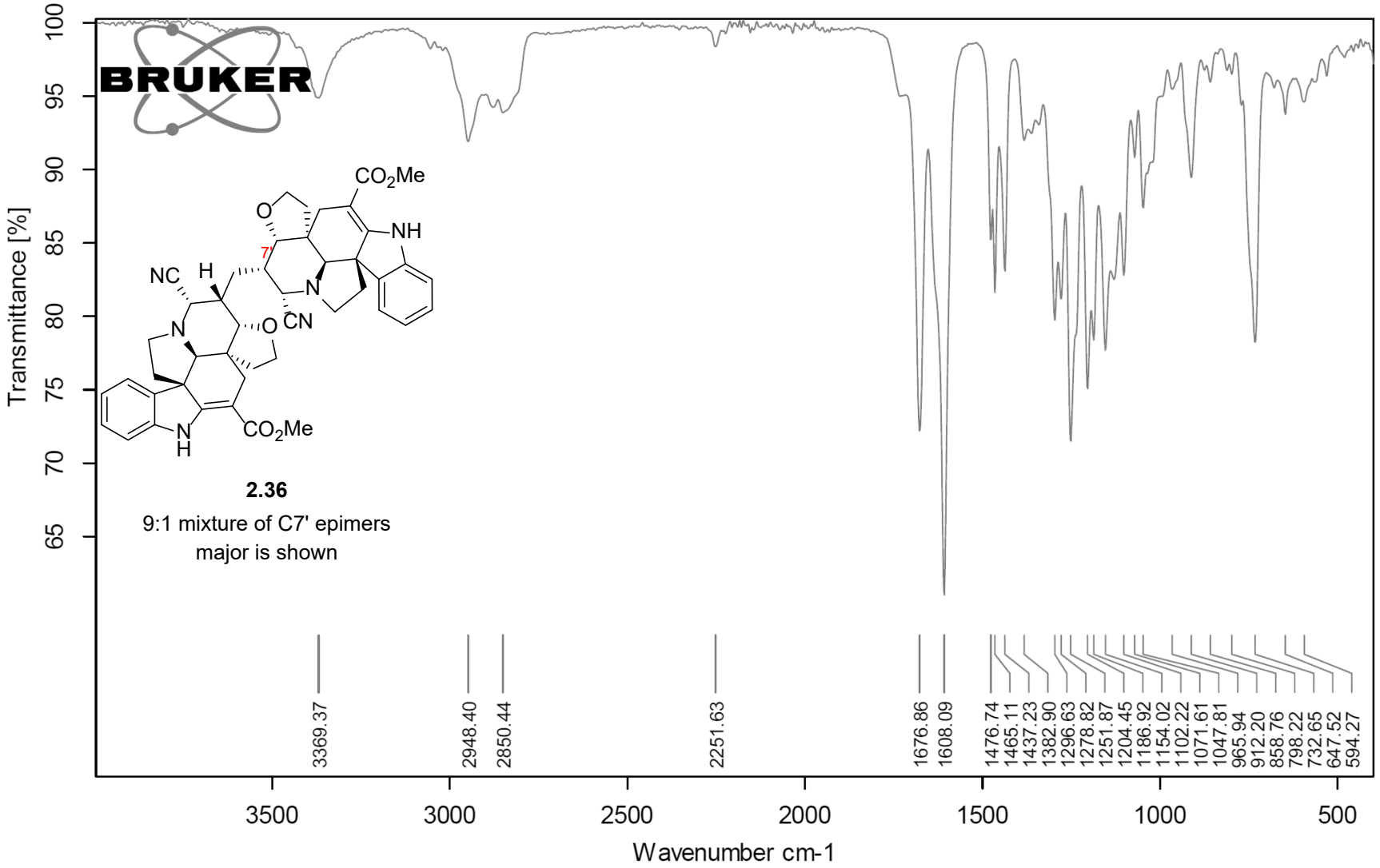
BRUKER
CO2Me
NH
O
7'
NC
H
N
O
CN
N
H
CO2Me
2.36
9:1 mixture of C7' epimers
major is shown
Transmittance [%]
100
95
90
85
80
75
70
65
3369.37
2948.40
2850.44
2251.63
1676.86
1608.09
1476.74
1465.11
1437.23
1382.90
1296.63
1278.82
1251.87
1204.45
1186.92
1154.02
1102.22
1071.61
1047.81
965.94
912.20
858.76
798.22
732.65
647.52
594.27
3500
3000
2500
2000
1500
1000
500
Wavenumber cm-1

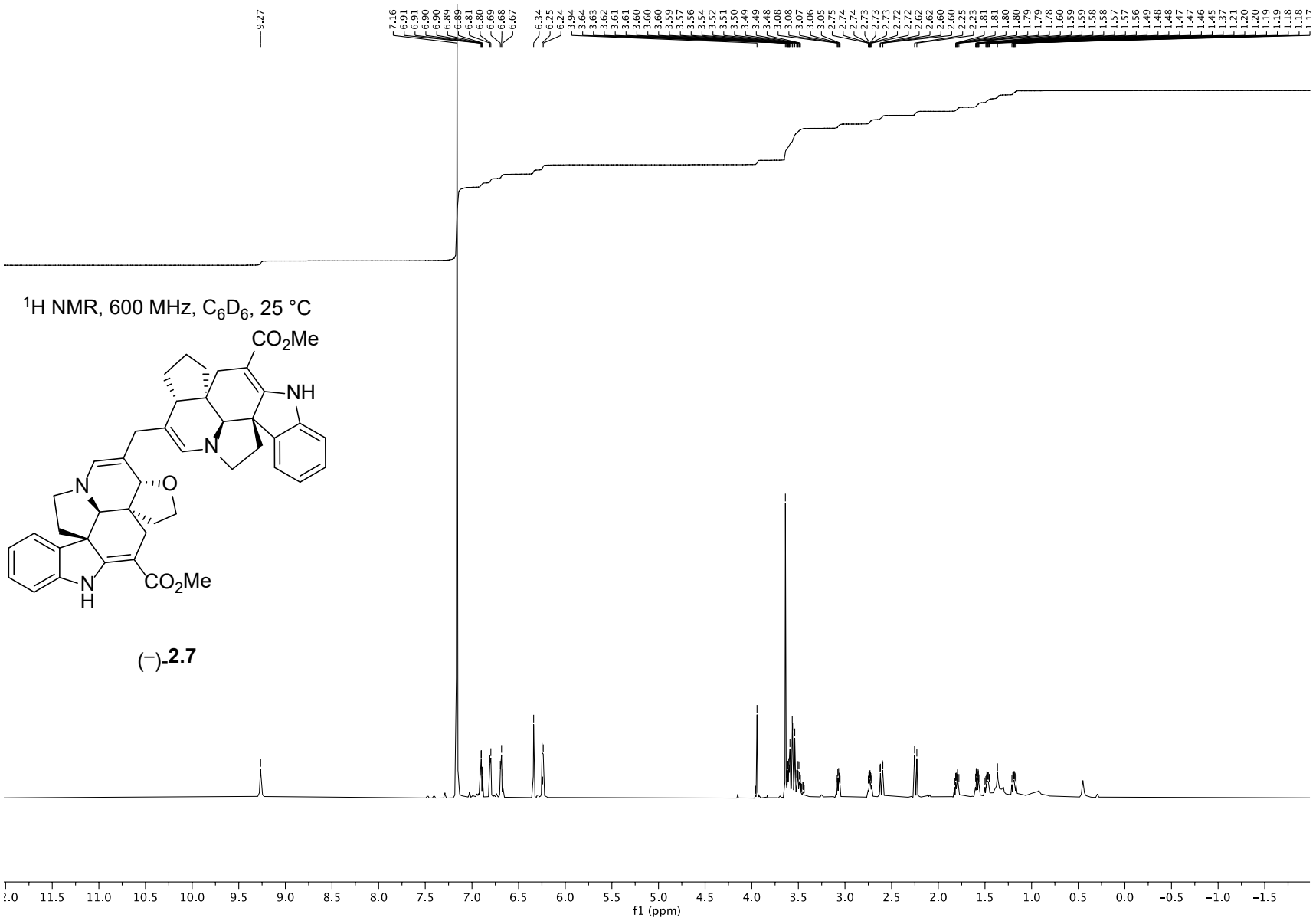
9.27
7.16
6.91
6.91
6.90
6.90
6.89
6.89
6.81
6.80
6.69
6.68
6.67
6.34
6.25
6.24
3.94
3.64
3.63
3.62
3.61
3.61
3.60
3.60
3.60
3.59
3.57
3.56
3.54
3.52
3.51
3.50
3.49
3.49
3.48
3.08
3.08
3.07
3.06
3.05
2.75
2.74
2.74
2.73
2.73
2.72
2.72
2.62
2.62
2.60
2.60
2.25
2.23
1.81
1.81
1.80
1.80
1.79
1.79
1.78
1.60
1.59
1.59
1.58
1.58
1.57
1.57
1.56
1.49
1.48
1.48
1.47
1.47
1.46
1.45
1.37
1.21
1.20
1.19
1.19
1.18
1.18
1H NMR, 600 MHz, C6D6, 25 °C
CO2Me
NH
N
N
O
N
H
CO2Me
(−)-2.7
f1 (ppm)

^{13}C NMR, 150.8 MHz, C_6D_6, 25 °C

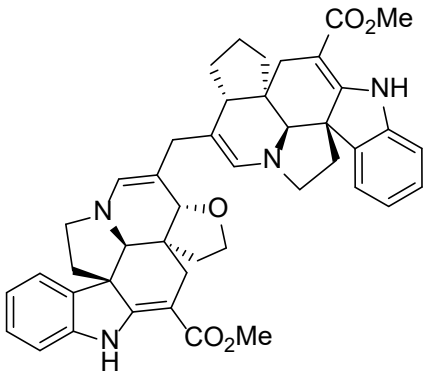

(–)-**2.7**

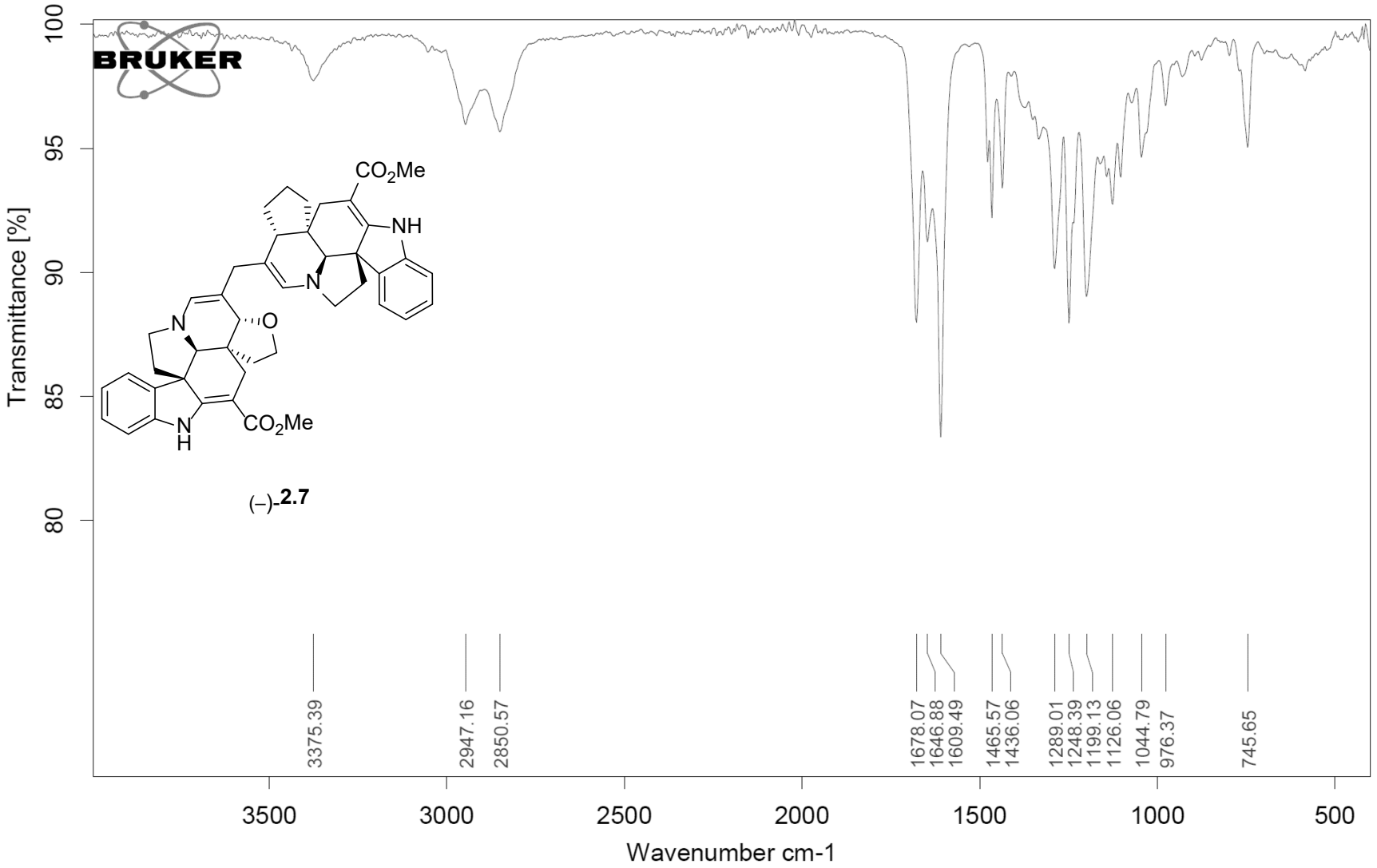
BRUKER
Transmittance [%]
100
95
90
85
80
CO2Me
NH
N
O
N
H
CO2Me
3375.39
2947.16
2850.57
1678.07
1646.88
1609.49
1465.57
1436.06
1289.01
1248.39
1199.13
1126.06
1044.79
976.37
745.65
3500
3000
2500
2000
1500
1000
500
Wavenumber cm-1

(–)-**2.7**

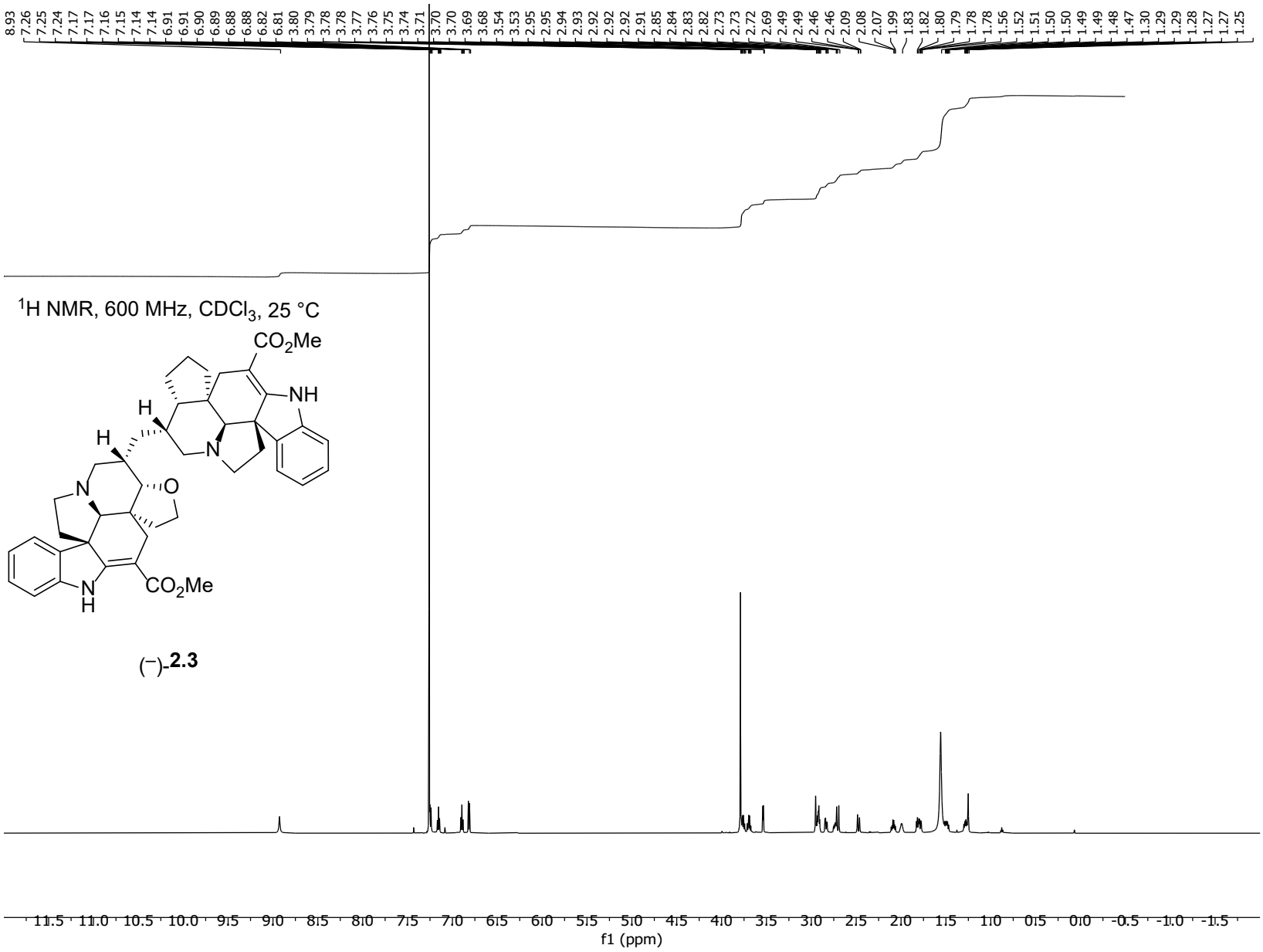
8.93 7.26 7.25 7.24 7.17 7.17 7.16 7.15 7.14 7.14 6.91 6.91 6.90 6.89 6.88 6.88 6.82 6.81 3.80 3.79 3.78 3.78 3.77 3.76 3.75 3.74 3.71 3.70 3.70 3.69 3.68 3.54 3.53 2.95 2.95 2.94 2.93 2.92 2.92 2.92 2.91 2.85 2.84 2.83 2.82 2.73 2.73 2.72 2.69 2.49 2.49 2.46 2.46 2.09 2.08 2.07 1.99 1.83 1.82 1.80 1.79 1.78 1.78 1.56 1.52 1.51 1.50 1.50 1.49 1.49 1.48 1.47 1.30 1.29 1.29 1.28 1.27 1.27 1.25
^{1}H NMR, 600 MHz, $CDCl_3$, 25 °C
CO_2Me
NH
H
H
N
O
N
H
CO_2Me
(−)-**2.3**
11.5 11.0 10.5 10.0 9.5 9.0 8.5 8.0 7.5 7.0 6.5 6.0 5.5 5.0 4.5 4.0 3.5 3.0 2.5 2.0 1.5 1.0 0.5 0.0 -0.5 -1.0 -1.5
f1 (ppm)

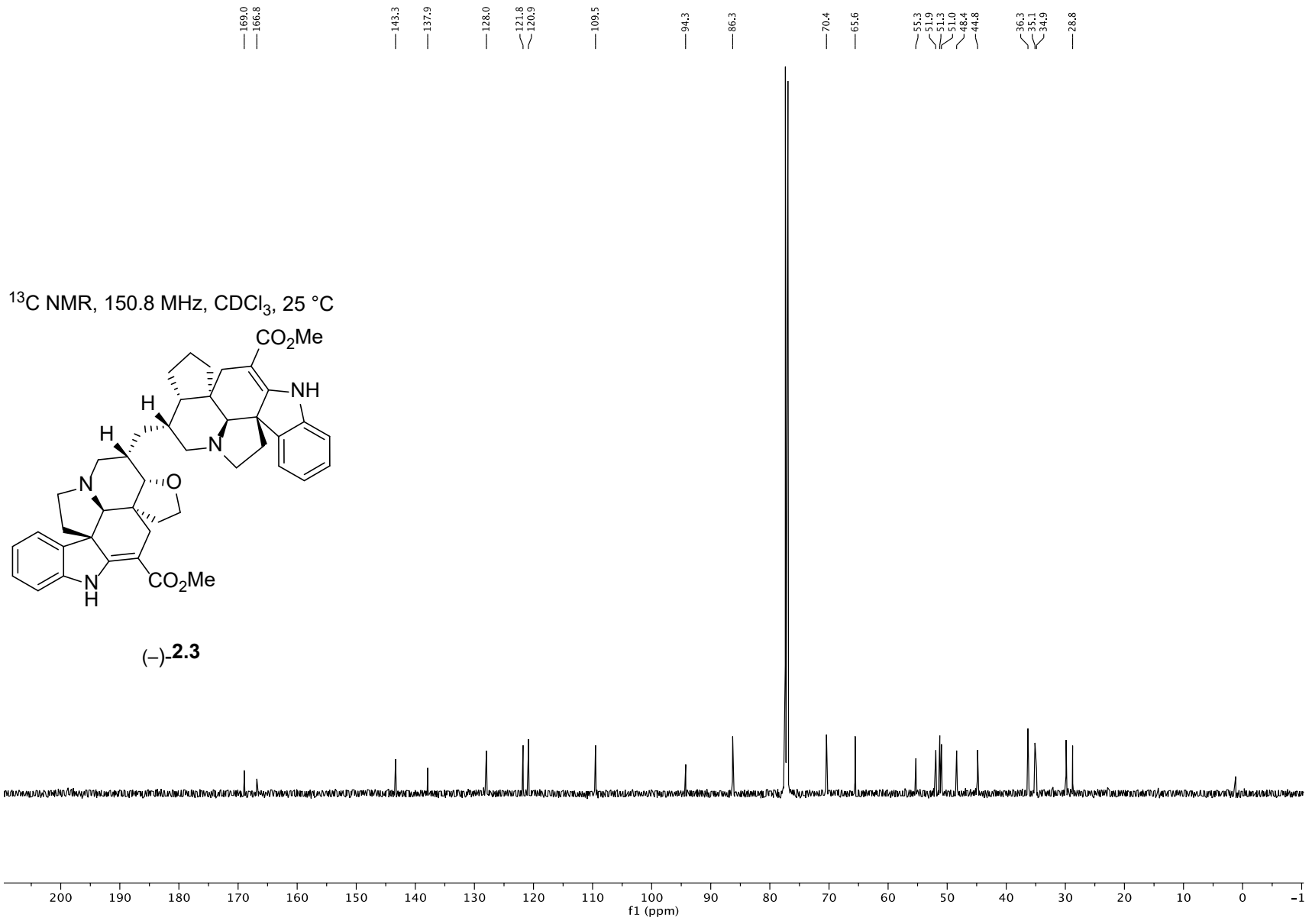
169.0
166.8
143.3
137.9
128.0
121.8
120.9
109.5
94.3
86.3
70.4
65.6
55.3
51.9
51.3
51.0
48.4
44.8
36.3
35.1
34.9
28.8
^{13}C NMR, 150.8 MHz, $CDCl_3$, 25 °C
CO_2Me
NH
H
H
N
N
O
N
H
CO_2Me
(–)-**2.3**
200
190
180
170
160
150
140
130
120
110
100
90
80
70
60
50
40
30
20
10
0
-1
f1 (ppm)

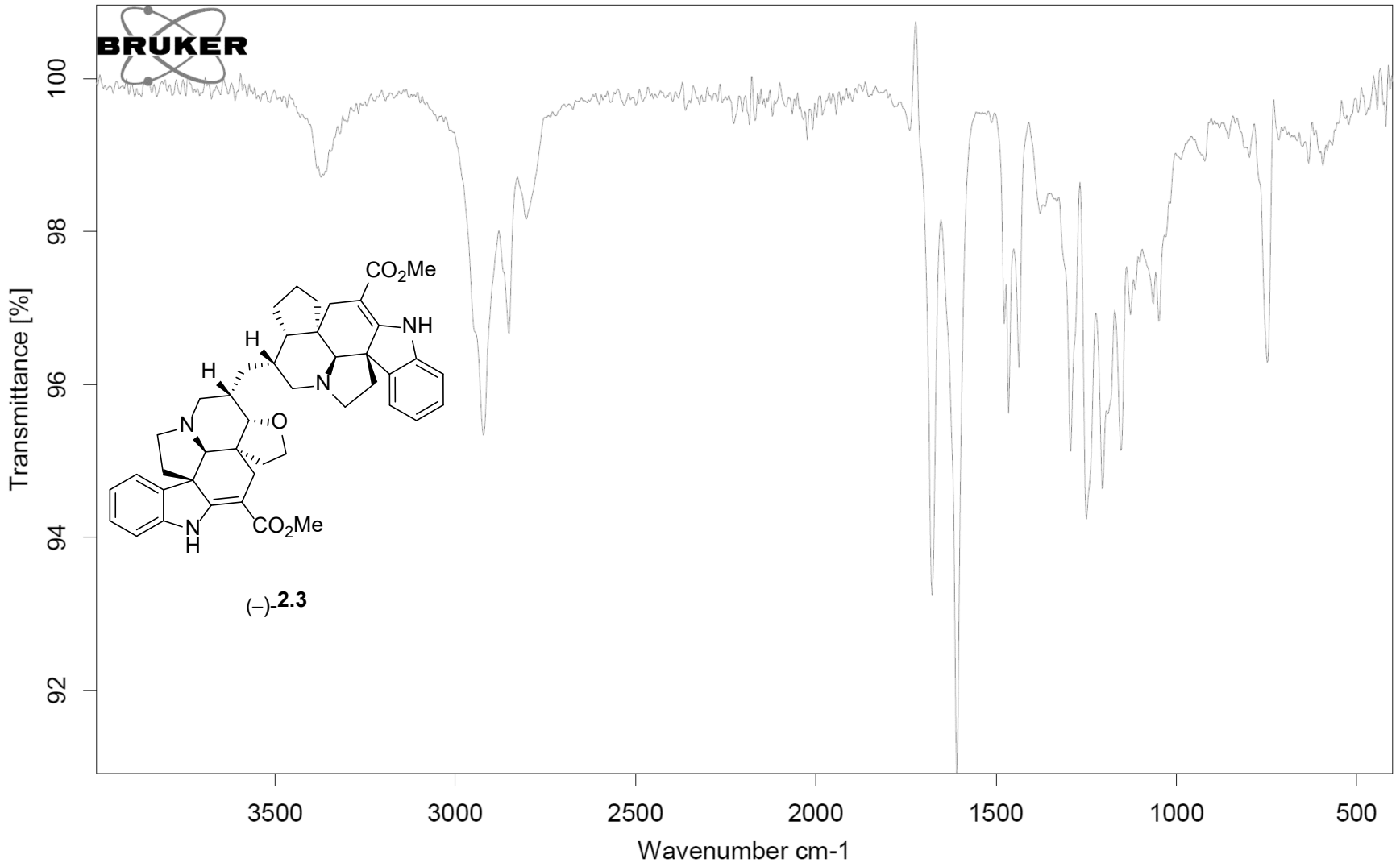
BRUKER
Transmittance [%]
100
98
96
94
92
3500
3000
2500
2000
1500
1000
500
Wavenumber cm-1
CO2Me
NH
H
H
N
N
O
N
H
CO2Me

(–)-**2.3**

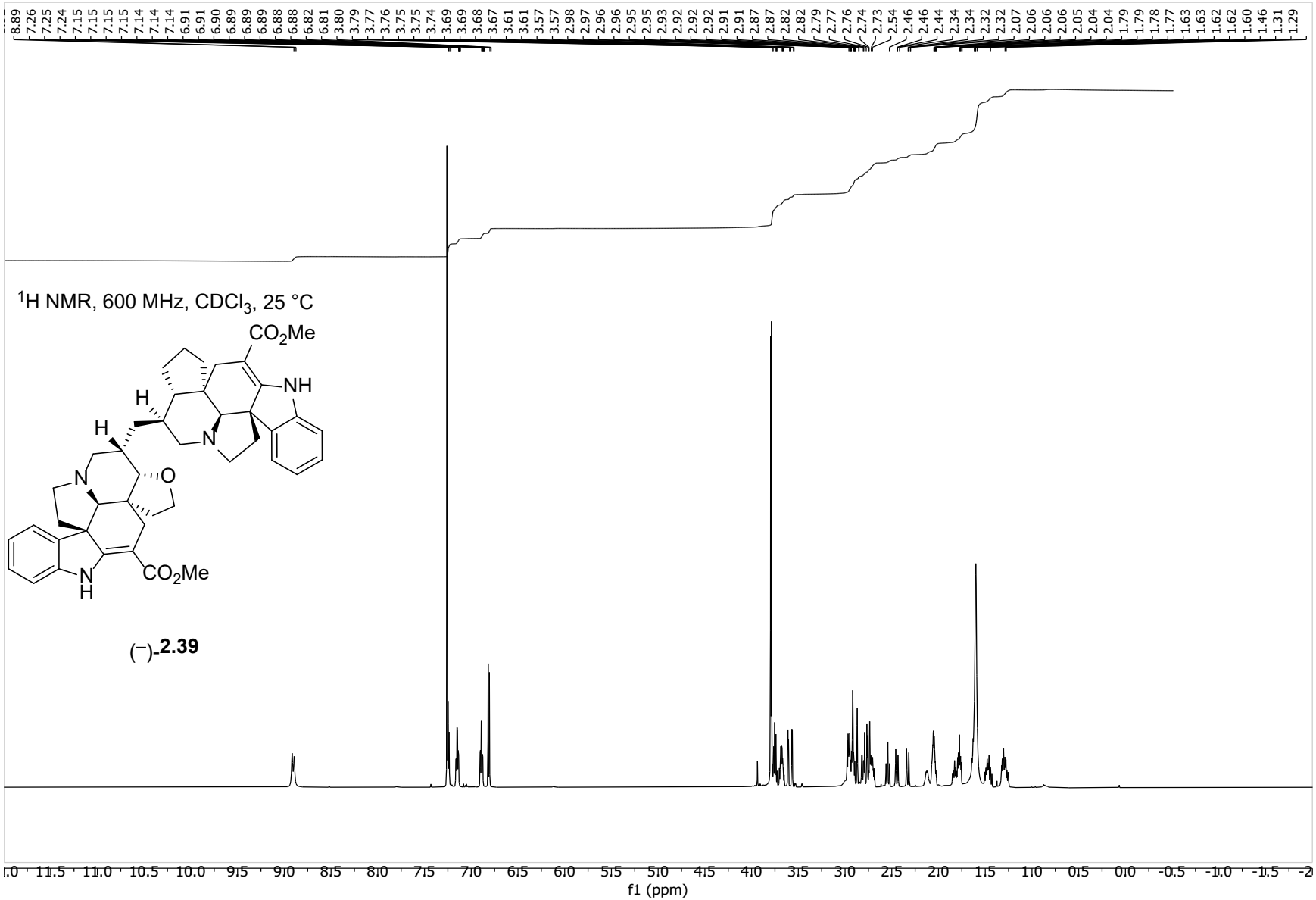
^{1}H NMR, 600 MHz, $CDCl_3$, 25 °C
CO_2Me
NH
H
H
N
O
N
H
CO_2Me
(−)-**2.39**
f1 (ppm)

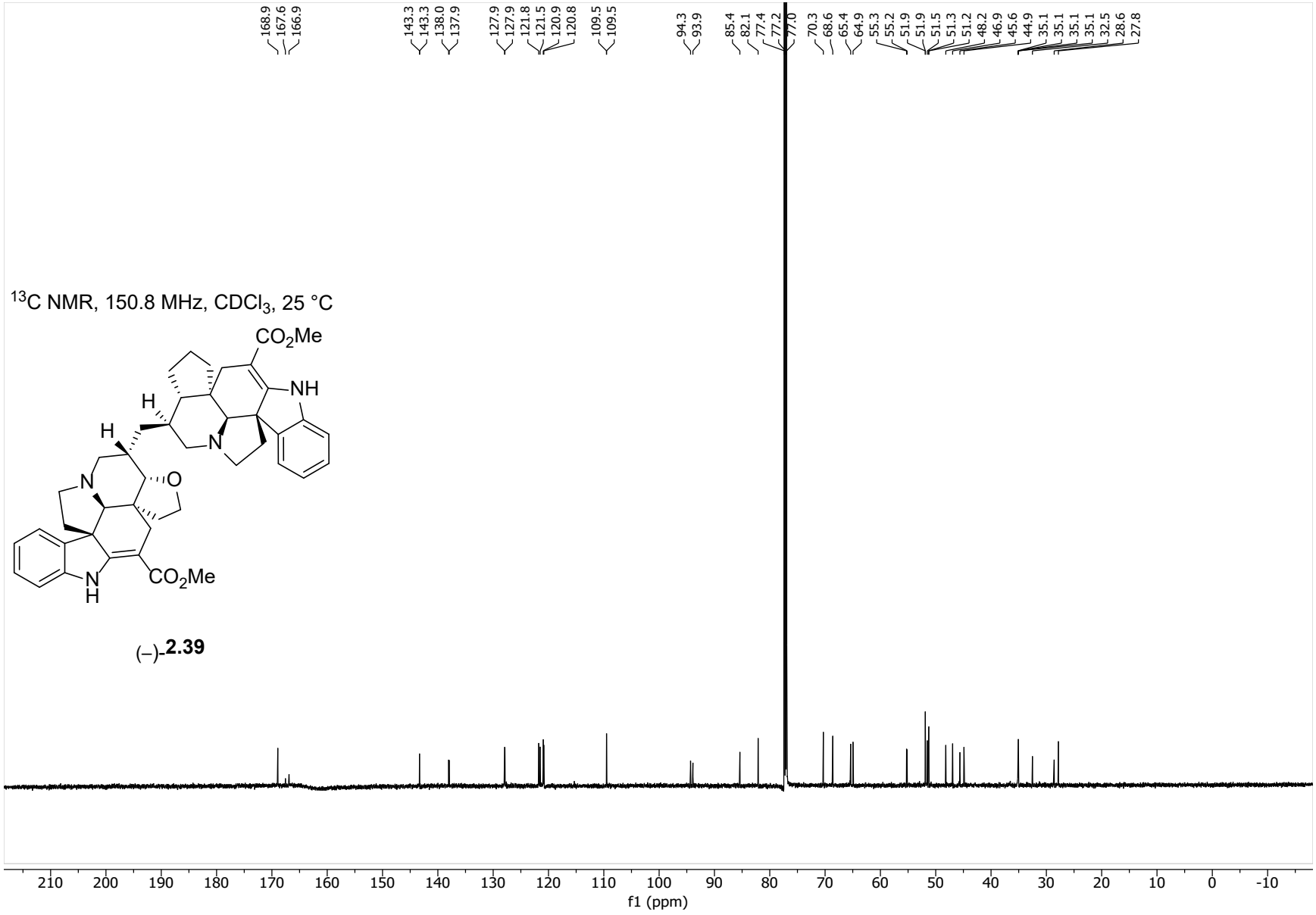
168.9
167.6
166.9
143.3
143.3
138.0
137.9
127.9
127.9
121.8
121.5
120.9
120.8
109.5
109.5
94.3
93.9
85.4
82.1
77.4
77.2
77.0
70.3
68.6
65.4
64.9
55.3
55.2
51.9
51.9
51.5
51.3
51.2
48.2
46.9
45.6
44.9
35.1
35.1
35.1
32.5
28.6
27.8
^{13}C NMR, 150.8 MHz, $CDCl_3$, 25 °C
CO_2Me
NH
H
H
N
N
O
N
H
CO_2Me
(–)-**2.39**
210
200
190
180
170
160
150
140
130
120
110
100
90
80
70
60
50
40
30
20
10
0
-10
f1 (ppm)

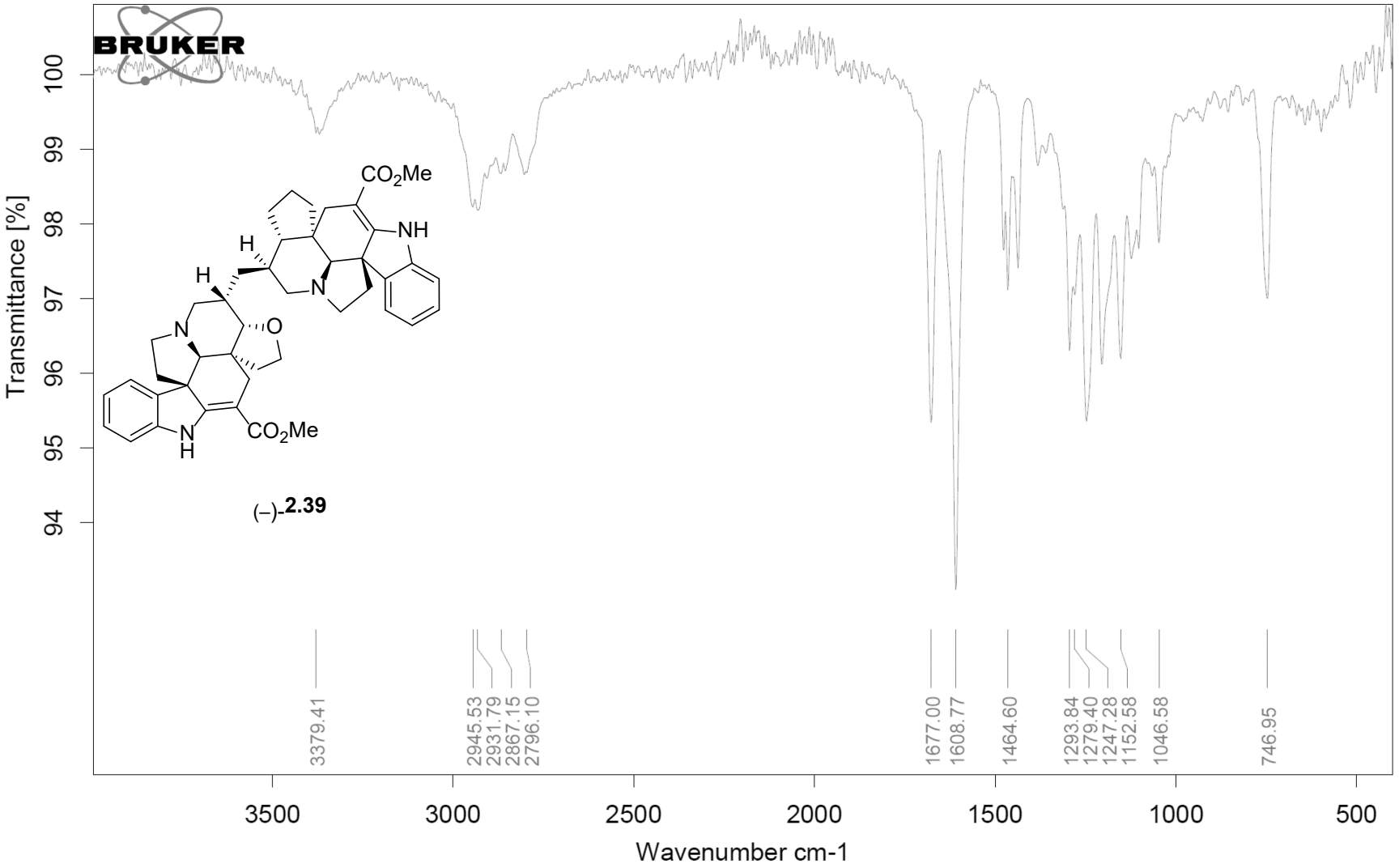
BRUKER
Transmittance [%]
100
99
98
97
96
95
94
CO2Me
NH
H
H
N
N
O
N
H
CO2Me
(–)-2.39
3379.41
2945.53
2931.79
2867.15
2796.10
1677.00
1608.77
1464.60
1293.84
1279.40
1247.28
1152.58
1046.58
746.95
3500
3000
2500
2000
1500
1000
500
Wavenumber cm-1

Appendix B Spectra for Chapter III

Respective Contributions

Dr. In-Soo Myeong collected the spectral data for **3.18**, **3.19**, and **3.20**.

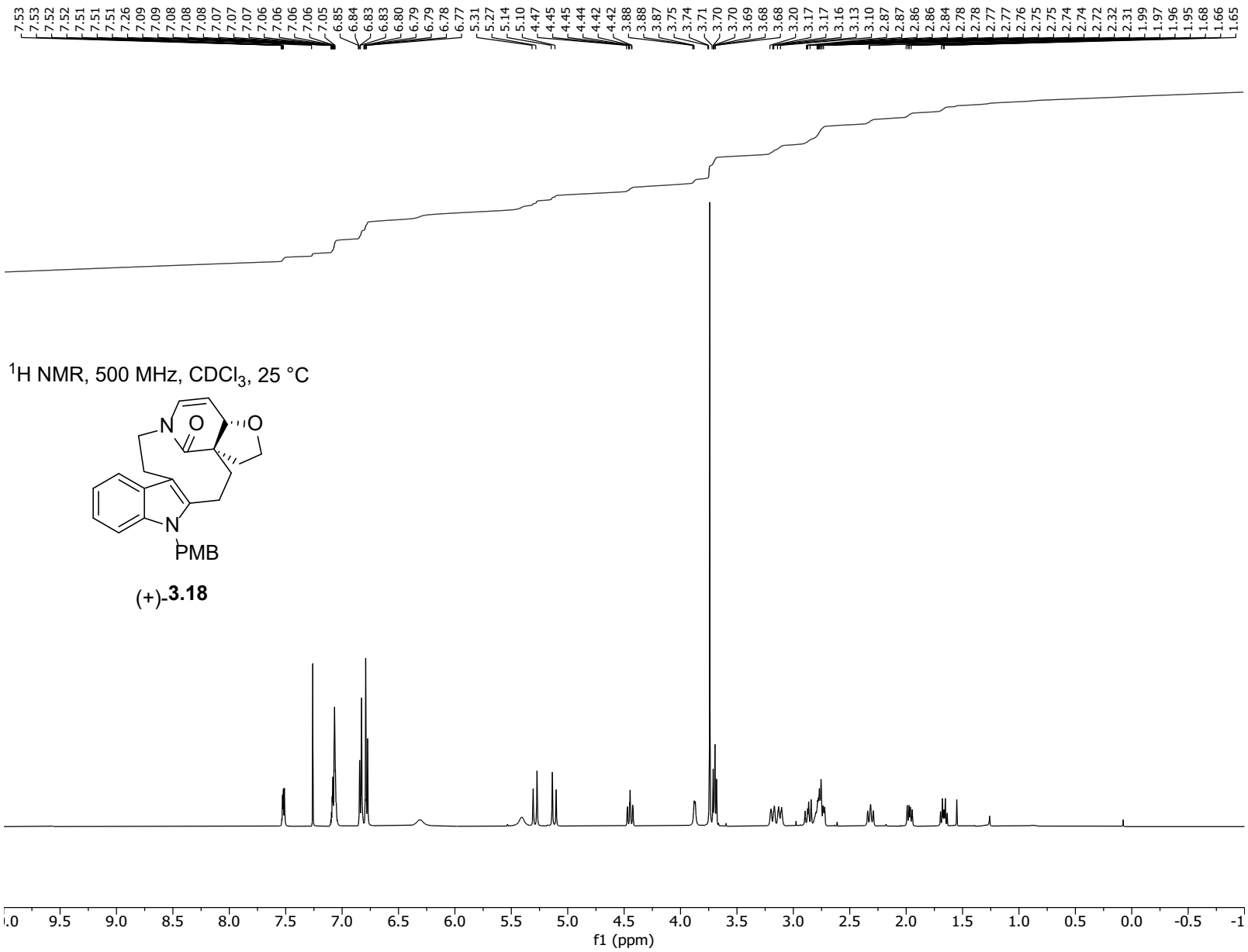
7.53 7.53 7.52 7.52 7.51 7.51 7.51 7.26 7.09 7.09 7.08 7.08 7.08 7.07 7.07 7.07 7.06 7.06 7.06 7.06 7.05 6.85 6.84 6.83 6.83 6.80 6.79 6.79 6.78 6.77
5.31 5.27 5.14 5.10 4.47 4.45 4.45 4.44 4.42 4.42 3.88 3.88 3.87 3.75 3.74 3.71 3.70 3.70 3.69 3.68 3.68 3.20 3.17 3.17 3.16 3.13 3.10 2.87 2.87 2.86 2.86 2.84 2.78 2.78 2.77 2.77 2.76 2.75 2.75 2.74 2.74 2.72 2.32 2.31 1.99 1.97 1.96 1.95 1.68 1.66 1.65
1H NMR, 500 MHz, CDCl3, 25 °C
N
O
O
N
PMB
(+)-3.18
9.5 9.0 8.5 8.0 7.5 7.0 6.5 6.0 5.5 5.0 4.5 4.0 3.5 3.0 2.5 2.0 1.5 1.0 0.5 0.0 -0.5
f1 (ppm)

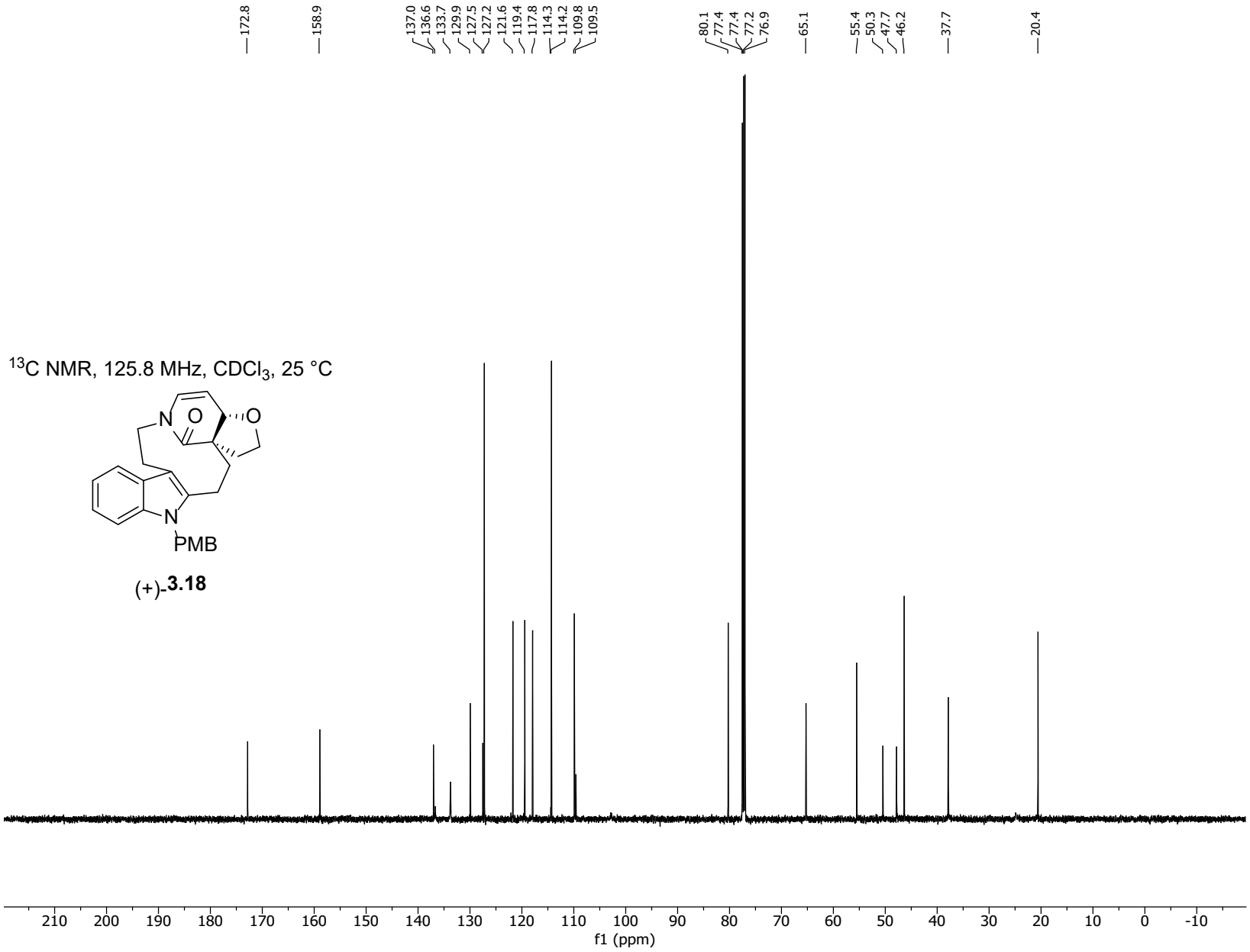
172.8
158.9
137.0
136.6
133.7
129.9
127.5
127.2
121.6
119.4
117.8
114.3
114.2
109.8
109.5
80.1
77.4
77.4
77.2
76.9
65.1
55.4
50.3
47.7
46.2
37.7
20.4
13C NMR, 125.8 MHz, CDCl3, 25 °C
N
O
O
N
PMB
(+)-3.18
210
200
190
180
170
160
150
140
130
120
110
100
90
80
70
60
50
40
30
20
10
0
-10
f1 (ppm)

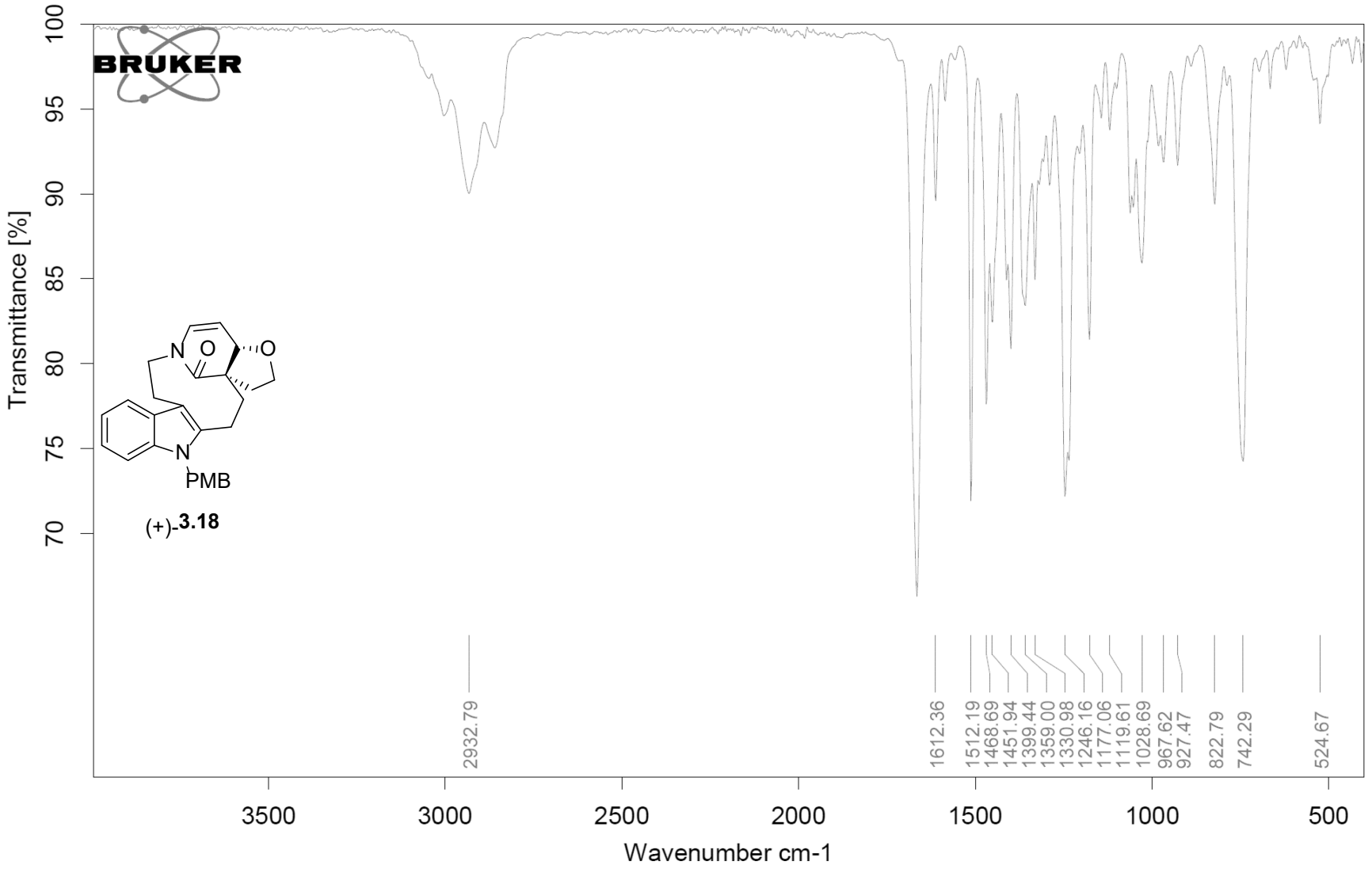
BRUKER
Transmittance [%]
100
95
90
85
80
75
70
N
O
O
N
PMB
(+)-3.18
2932.79
1612.36
1512.19
1468.69
1451.94
1399.44
1359.00
1330.98
1246.16
1177.06
1119.61
1028.69
967.62
927.47
822.79
742.29
524.67
3500
3000
2500
2000
1500
1000
500
Wavenumber cm-1

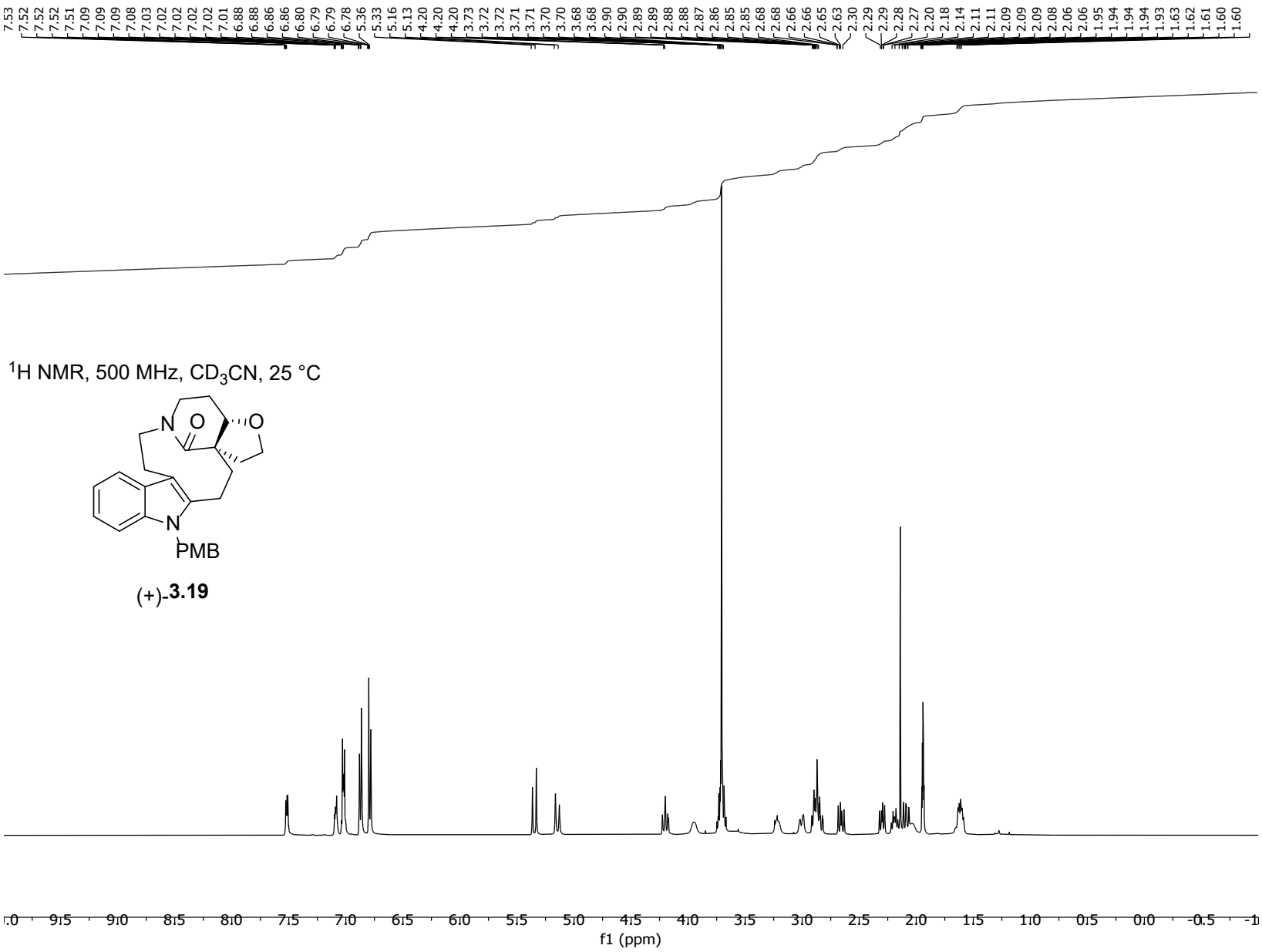
7.53 7.52 7.52 7.52 7.51 7.09 7.09 7.09 7.08 7.03 7.02 7.02 7.02 7.02 7.01 6.88 6.88 6.86 6.86 6.80 6.79 6.78 6.36 5.33 5.16 5.13 4.20 4.20 3.73 3.72 3.72 3.71 3.71 3.70 3.70 3.68 3.68 2.90 2.90 2.89 2.89 2.88 2.88 2.87 2.86 2.85 2.85 2.68 2.68 2.66 2.66 2.65 2.63 2.30 2.29 2.29 2.28 2.27 2.20 2.18 2.14 2.11 2.11 2.09 2.09 2.09 2.08 2.06 2.06 1.95 1.94 1.94 1.94 1.93 1.63 1.62 1.61 1.60 1.60
1H NMR, 500 MHz, CD3CN, 25 °C
N
O
O
N
PMB
(+)-3.19
f1 (ppm)

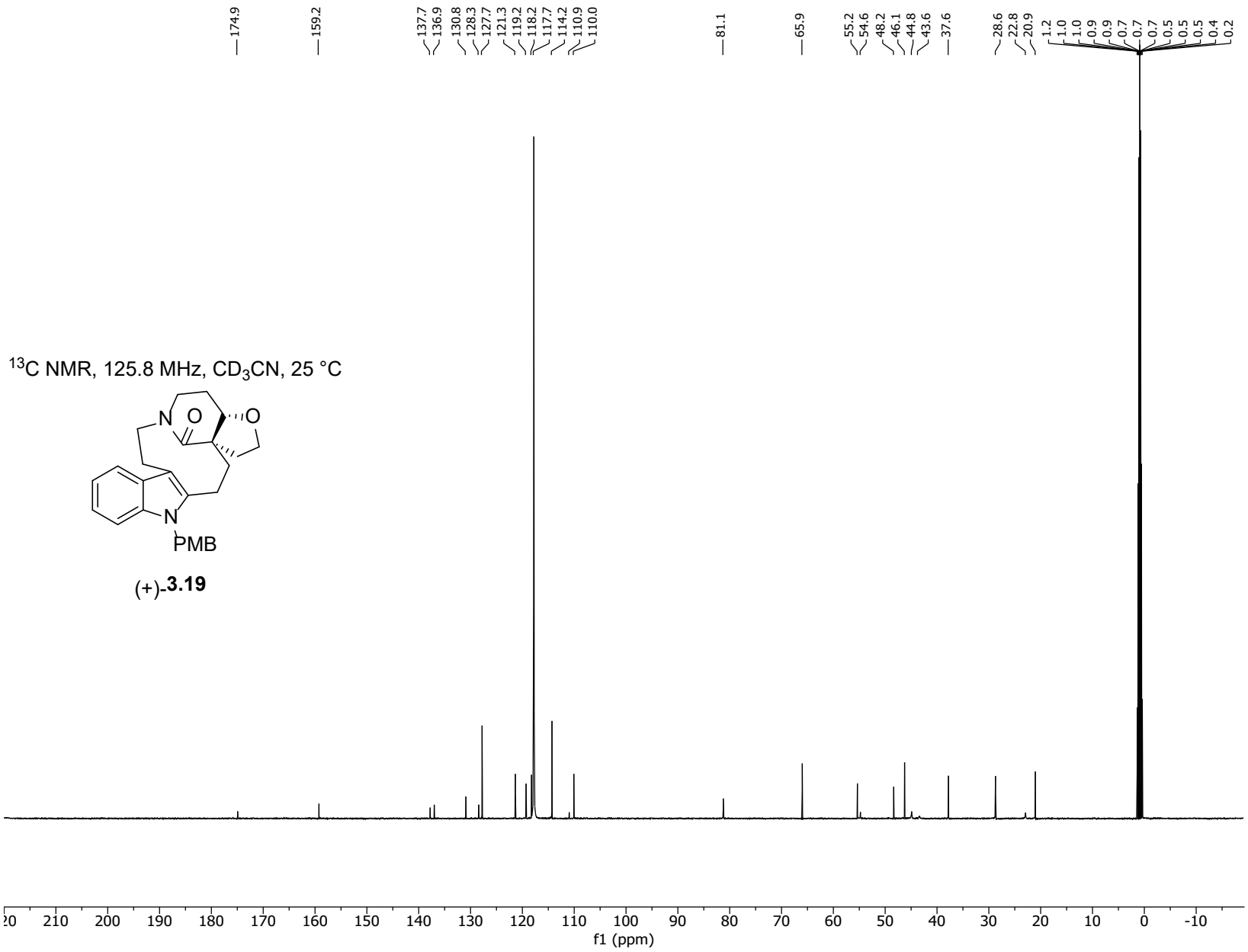
174.9
159.2
137.7
136.9
130.8
128.3
127.7
121.3
119.2
118.2
117.7
114.2
110.9
110.0
81.1
65.9
55.2
54.6
48.2
46.1
44.8
43.6
37.6
28.6
22.8
20.9
1.2
1.0
1.0
0.9
0.9
0.7
0.7
0.7
0.5
0.5
0.5
0.4
0.2
13C NMR, 125.8 MHz, CD3CN, 25 °C
N
O
O
N
PMB
(+)-3.19
f1 (ppm)

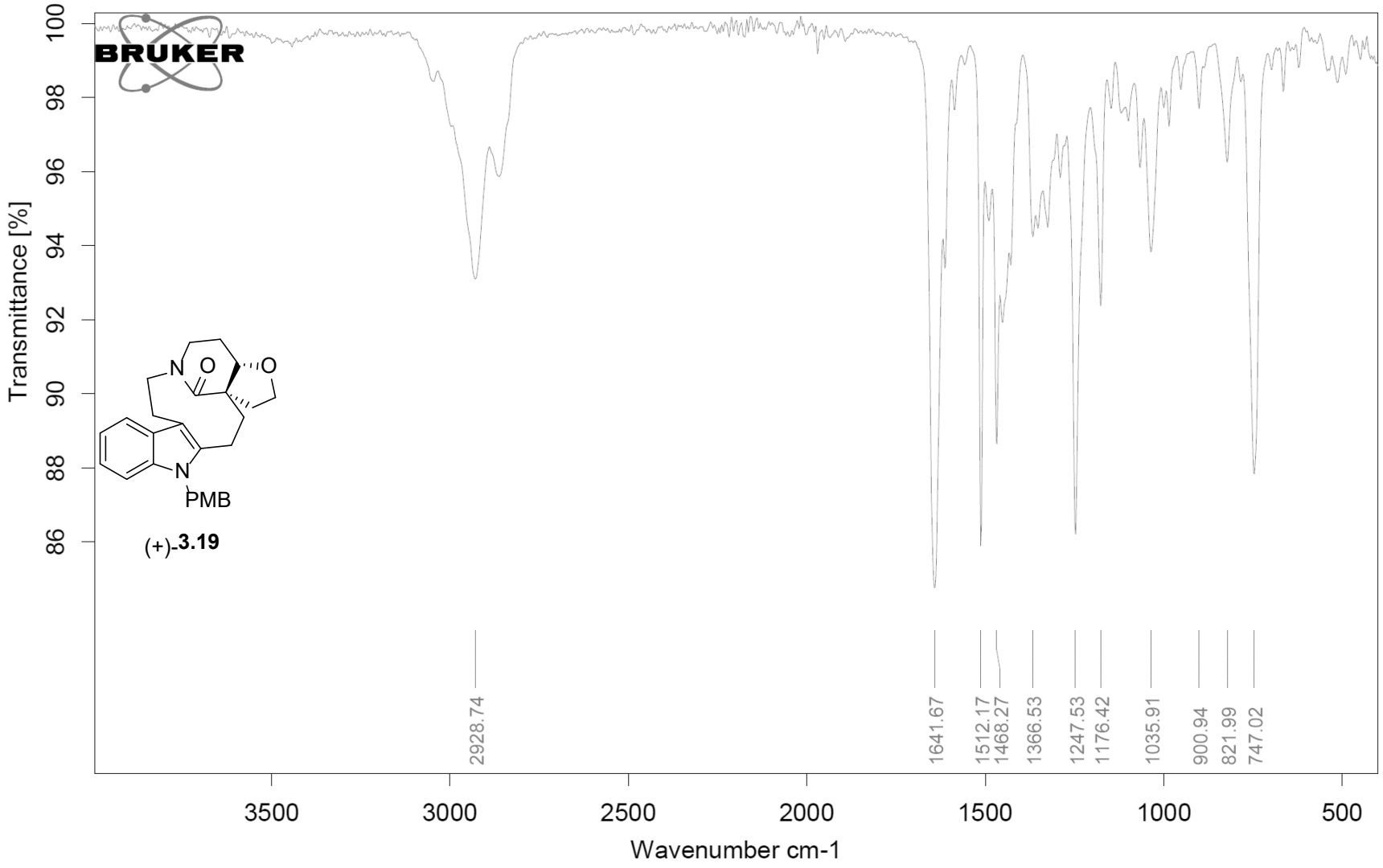
BRUKER
Transmittance [%]
100
98
96
94
92
90
88
86
N
O
O
N
PMB
(+)-3.19
2928.74
1641.67
1512.17
1468.27
1366.53
1247.53
1176.42
1035.91
900.94
821.99
747.02
3500
3000
2500
2000
1500
1000
500
Wavenumber cm-1

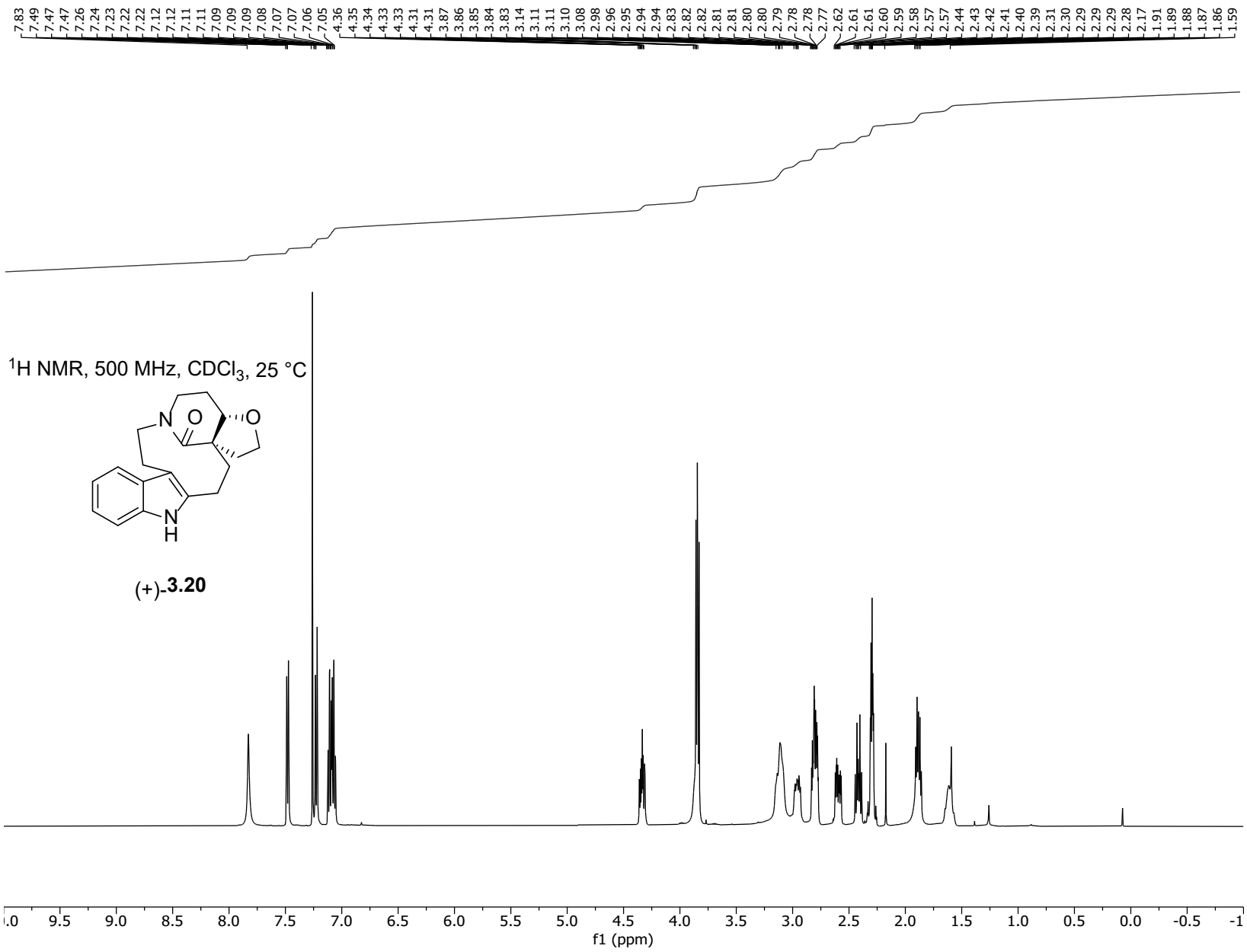
7.83 7.49 7.47 7.47 7.26 7.24 7.23 7.22 7.22 7.12 7.12 7.11 7.11 7.09 7.09 7.09 7.08 7.07 7.07 7.06 7.05 4.36 4.35 4.34 4.33 4.33 4.31 4.31 3.87 3.86 3.85 3.84 3.83 3.14 3.11 3.11 3.10 3.08 2.98 2.96 2.95 2.94 2.94 2.83 2.82 2.82 2.81 2.81 2.80 2.80 2.79 2.78 2.78 2.77 2.62 2.61 2.61 2.60 2.59 2.58 2.57 2.57 2.44 2.43 2.42 2.41 2.40 2.39 2.31 2.30 2.29 2.29 2.29 2.28 2.17 1.91 1.89 1.88 1.87 1.86 1.59
1H NMR, 500 MHz, CDCl3, 25 °C
N
O
O
N
H
(+)-3.20
9.5 9.0 8.5 8.0 7.5 7.0 6.5 6.0 5.5 5.0 4.5 4.0 3.5 3.0 2.5 2.0 1.5 1.0 0.5 0.0 -0.5
f1 (ppm)

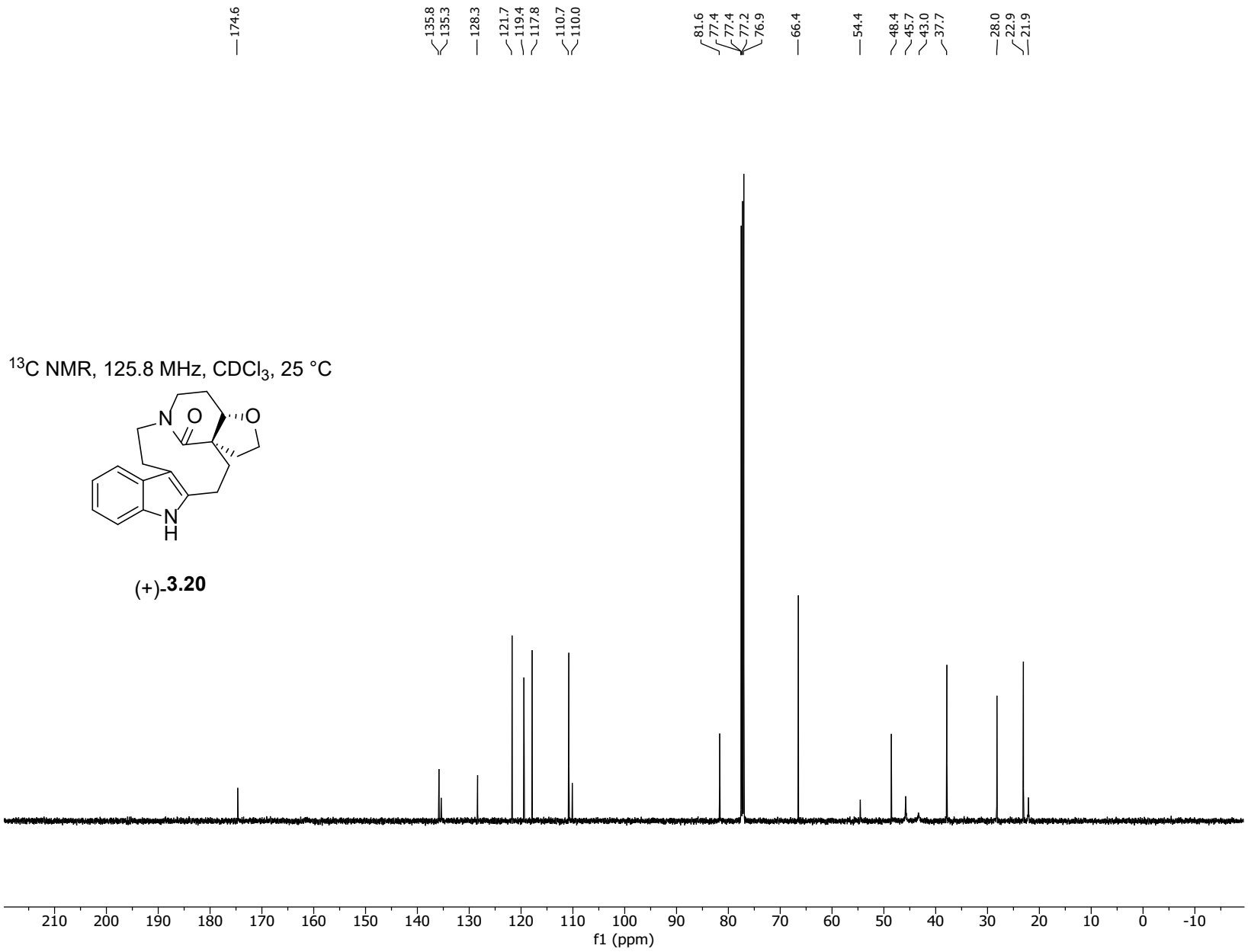
174.6
135.8
135.3
128.3
121.7
119.4
117.8
110.7
110.0
81.6
77.4
77.4
77.2
76.9
66.4
54.4
48.4
45.7
43.0
37.7
28.0
22.9
21.9
13C NMR, 125.8 MHz, CDCl3, 25 °C
N
O
O
N
H
(+)-3.20
210
200
190
180
170
160
150
140
130
120
110
100
90
80
70
60
50
40
30
20
10
0
-10
f1 (ppm)

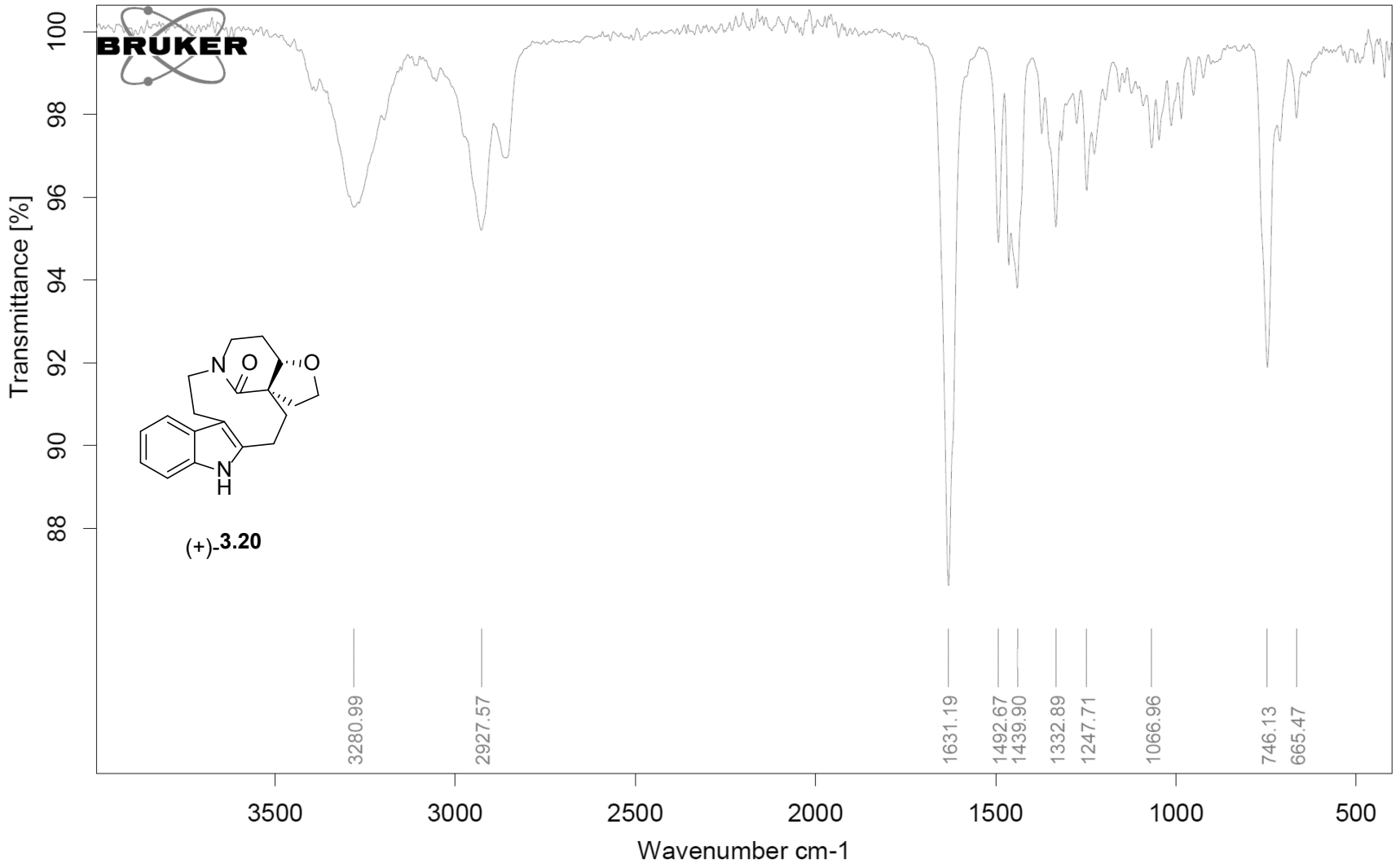
BRUKER
Transmittance [%]
100
98
96
94
92
90
88
3280.99
2927.57
1631.19
1492.67
1439.90
1332.89
1247.71
1066.96
746.13
665.47
3500
3000
2500
2000
1500
1000
500
Wavenumber cm-1
N
O
O
N
H

(+)-**3.20**

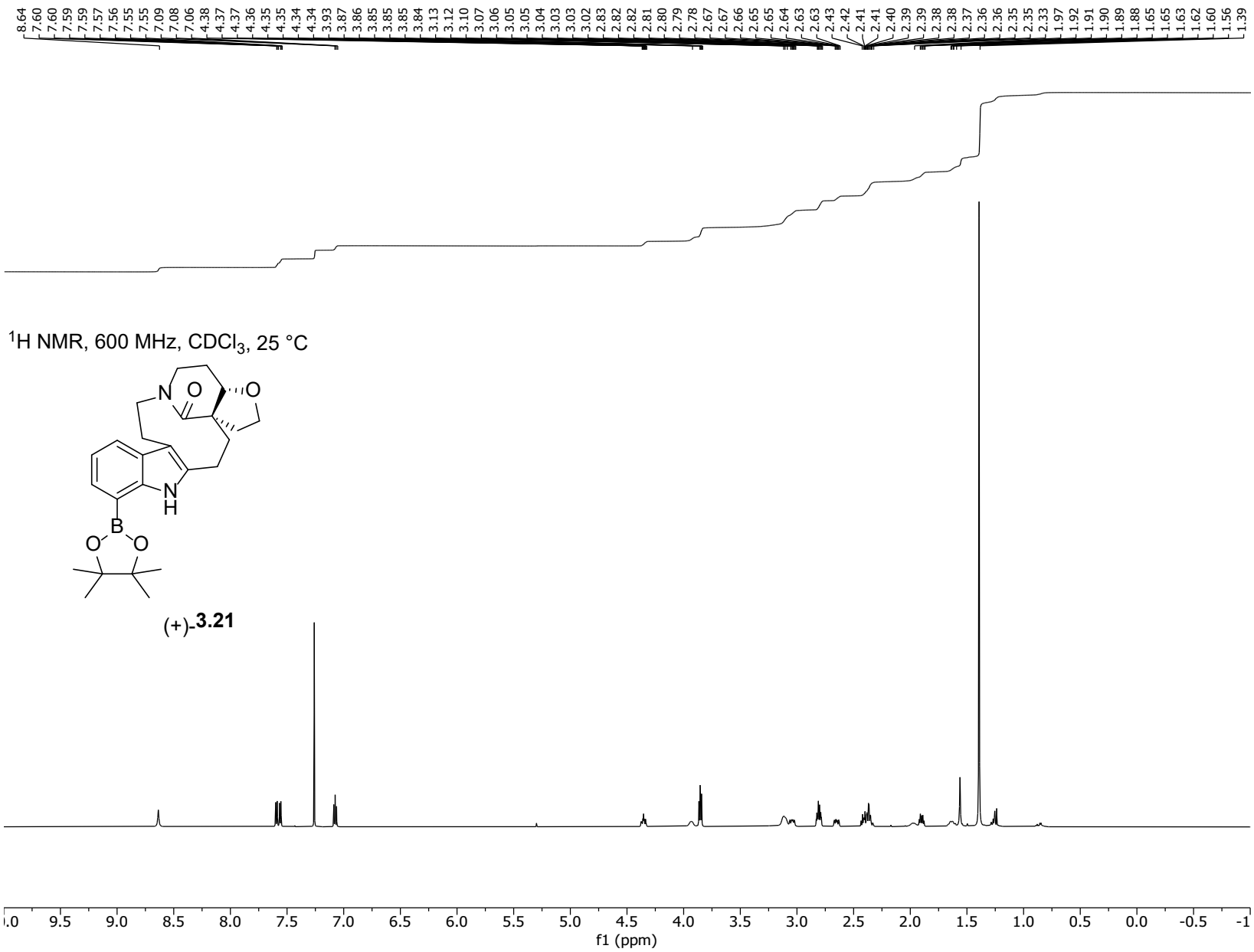
8.64 7.60 7.60 7.59 7.59 7.57 7.56 7.55 7.55 7.09 7.08 7.06 4.38 4.37 4.37 4.36 4.35 4.35 4.34 4.34 3.93 3.87 3.86 3.85 3.85 3.85 3.84 3.13 3.12 3.10 3.07 3.06 3.05 3.05 3.04 3.03 3.03 3.02 2.83 2.82 2.82 2.81 2.80 2.79 2.78 2.67 2.67 2.66 2.65 2.65 2.64 2.63 2.63 2.43 2.42 2.41 2.41 2.40 2.39 2.39 2.38 2.38 2.37 2.36 2.36 2.35 2.35 2.33 1.97 1.92 1.91 1.90 1.89 1.88 1.65 1.65 1.63 1.62 1.60 1.56 1.39
^{1}H NMR, 600 MHz, $CDCl_3$, 25 °C
N
O
O
N
H
B
O
O
(+)-**3.21**
.0 9.5 9.0 8.5 8.0 7.5 7.0 6.5 6.0 5.5 5.0 4.5 4.0 3.5 3.0 2.5 2.0 1.5 1.0 0.5 0.0 -0.5 -1
f1 (ppm)

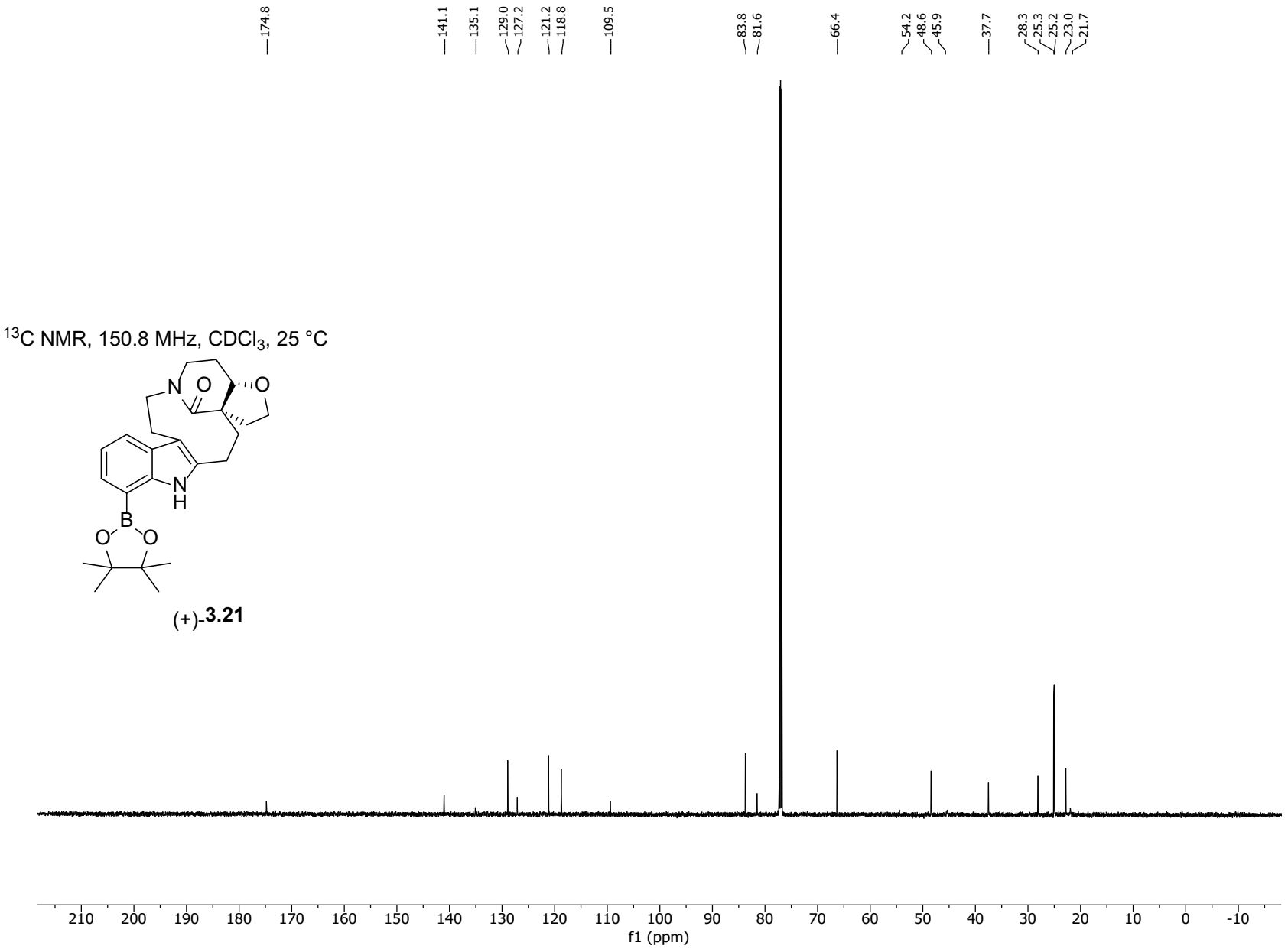
174.8
141.1
135.1
129.0
127.2
121.2
118.8
109.5
83.8
81.6
66.4
54.2
48.6
45.9
37.7
28.3
25.3
25.2
23.0
21.7
13C NMR, 150.8 MHz, CDCl3, 25 °C
N
O
O
N
H
B
O
O
(+)-3.21
210
200
190
180
170
160
150
140
130
120
110
100
90
80
70
60
50
40
30
20
10
0
-10
f1 (ppm)

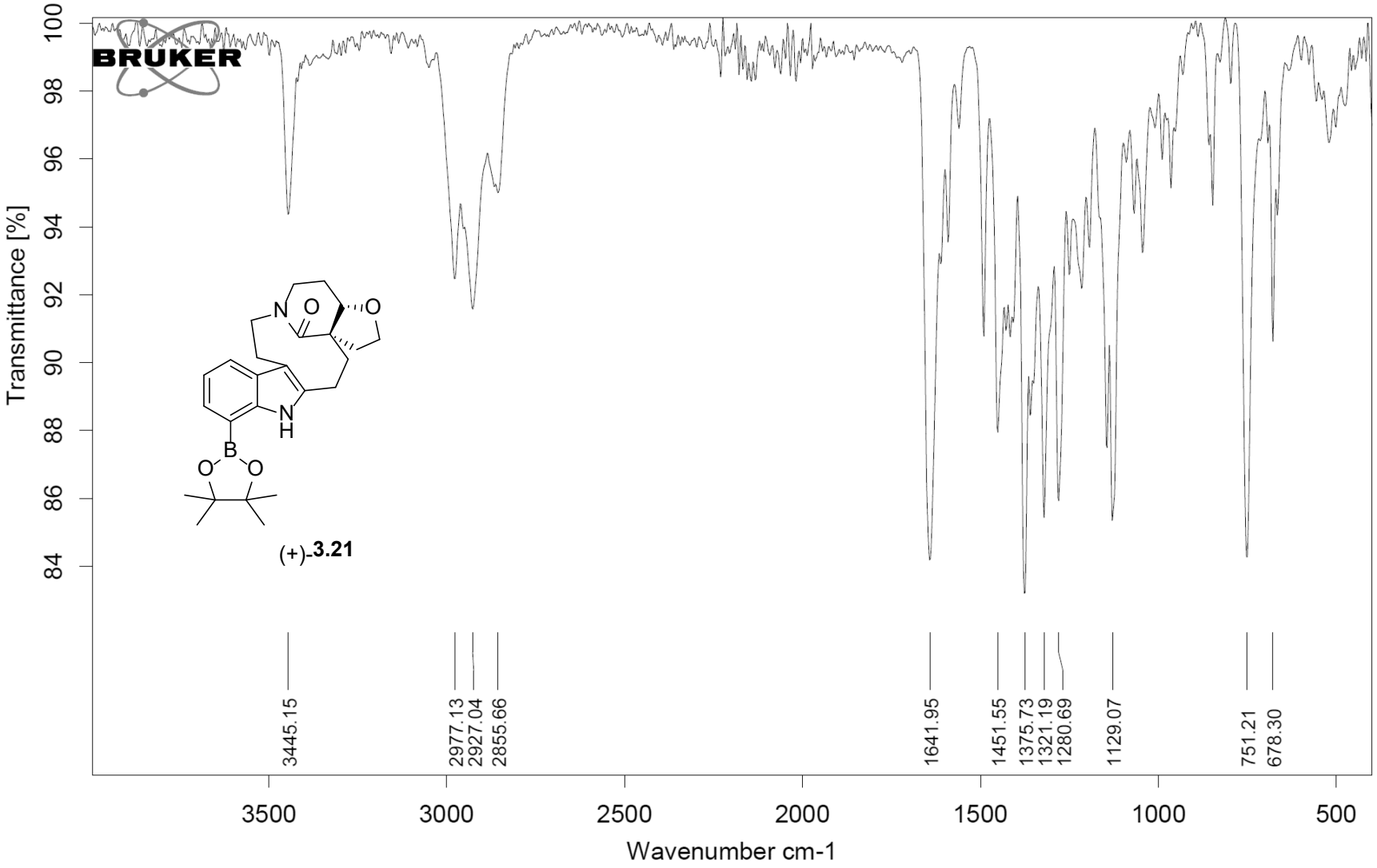
BRUKER
Transmittance [%]
100
98
96
94
92
90
88
86
84
3445.15
2977.13
2927.04
2855.66
1641.95
1451.55
1375.73
1321.19
1280.69
1129.07
751.21
678.30
3500
3000
2500
2000
1500
1000
500
Wavenumber cm-1
(+)-3.21

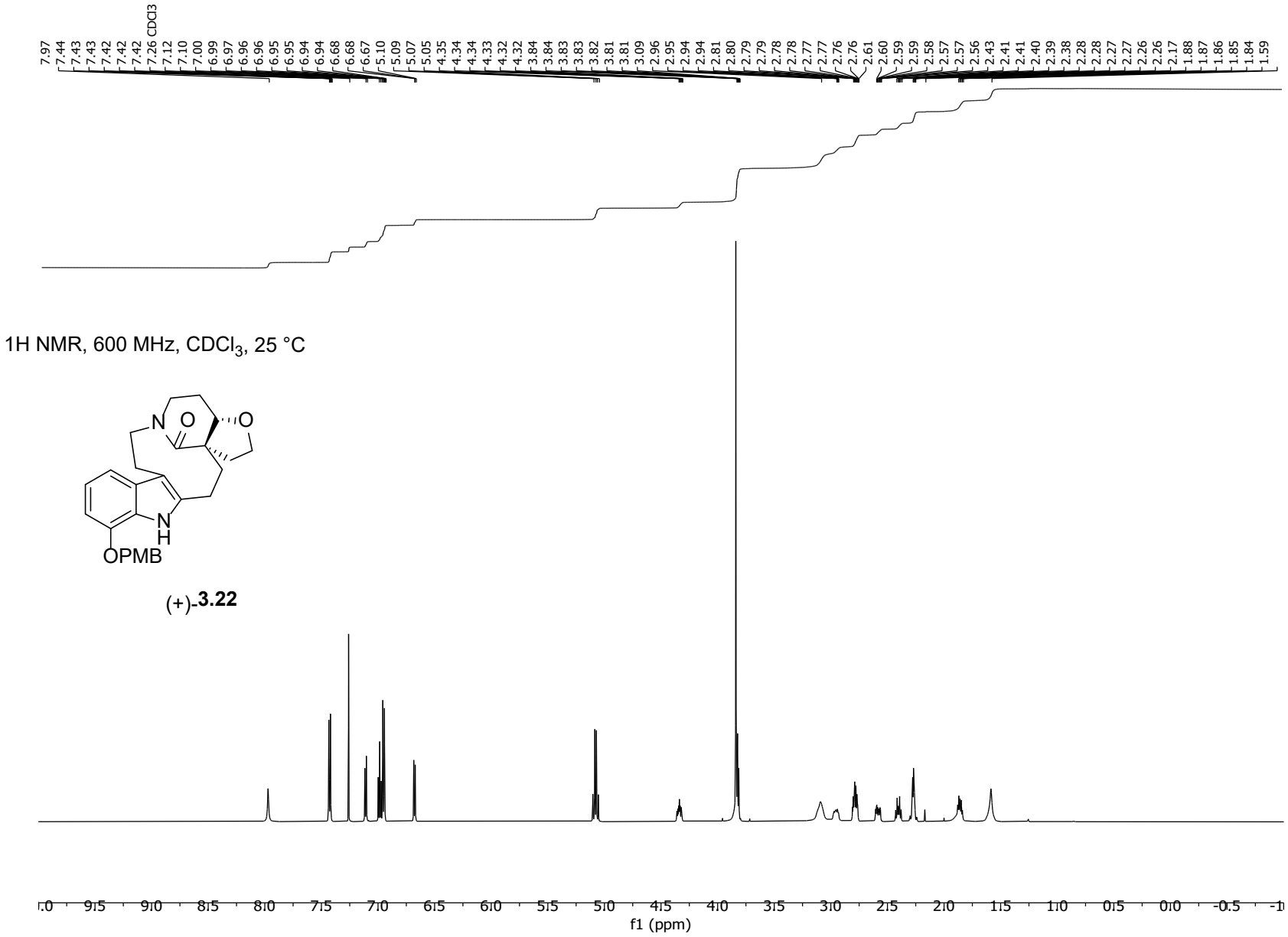
7.97 7.44 7.43 7.43 7.42 7.42 7.42 7.26 CDCl3 7.12 7.10 7.00 6.99 6.97 6.96 6.96 6.95 6.95 6.94 6.94 6.68 6.68 6.67 5.10 5.09 5.07 5.05 4.35 4.34 4.34 4.33 4.32 4.32 3.84 3.84 3.83 3.83 3.82 3.81 3.81 3.09 2.96 2.95 2.94 2.94 2.81 2.80 2.79 2.79 2.78 2.78 2.77 2.77 2.76 2.76 2.61 2.60 2.59 2.59 2.58 2.57 2.57 2.56 2.43 2.41 2.41 2.40 2.39 2.38 2.28 2.28 2.27 2.27 2.26 2.26 2.17 1.88 1.87 1.86 1.85 1.84 1.59
1H NMR, 600 MHz, CDCl3, 25 °C
N
O
O
N
H
OPMB
(+)-3.22
f1 (ppm)

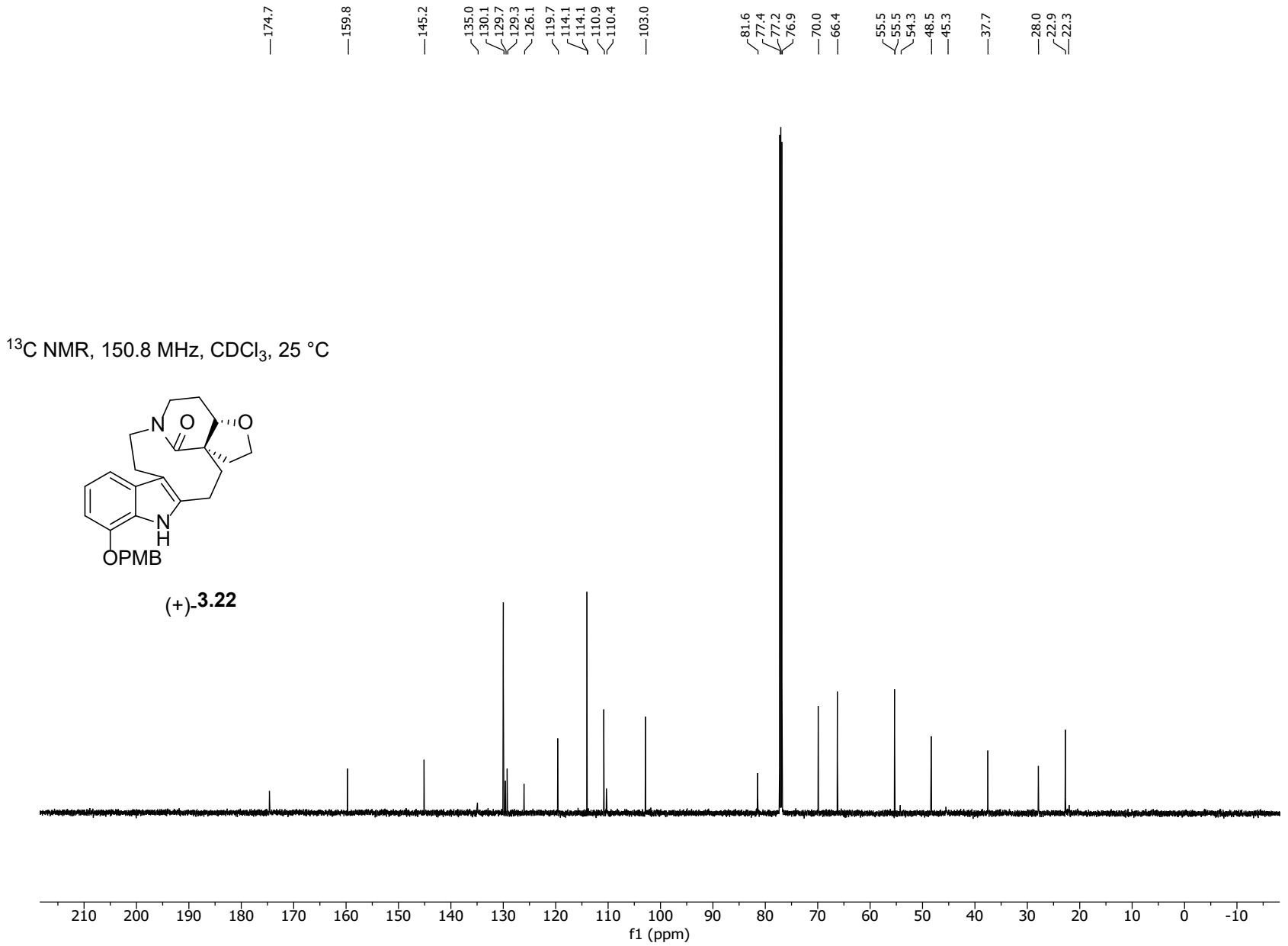
174.7
159.8
145.2
135.0
130.1
129.7
129.3
126.1
119.7
114.1
114.1
110.9
110.4
103.0
81.6
77.4
77.2
76.9
70.0
66.4
55.5
55.5
54.3
48.5
45.3
37.7
28.0
22.9
22.3
13C NMR, 150.8 MHz, CDCl3, 25 °C
N
O
O
N
H
OPMB
(+)-3.22
210
200
190
180
170
160
150
140
130
120
110
100
90
80
70
60
50
40
30
20
10
0
-10
f1 (ppm)

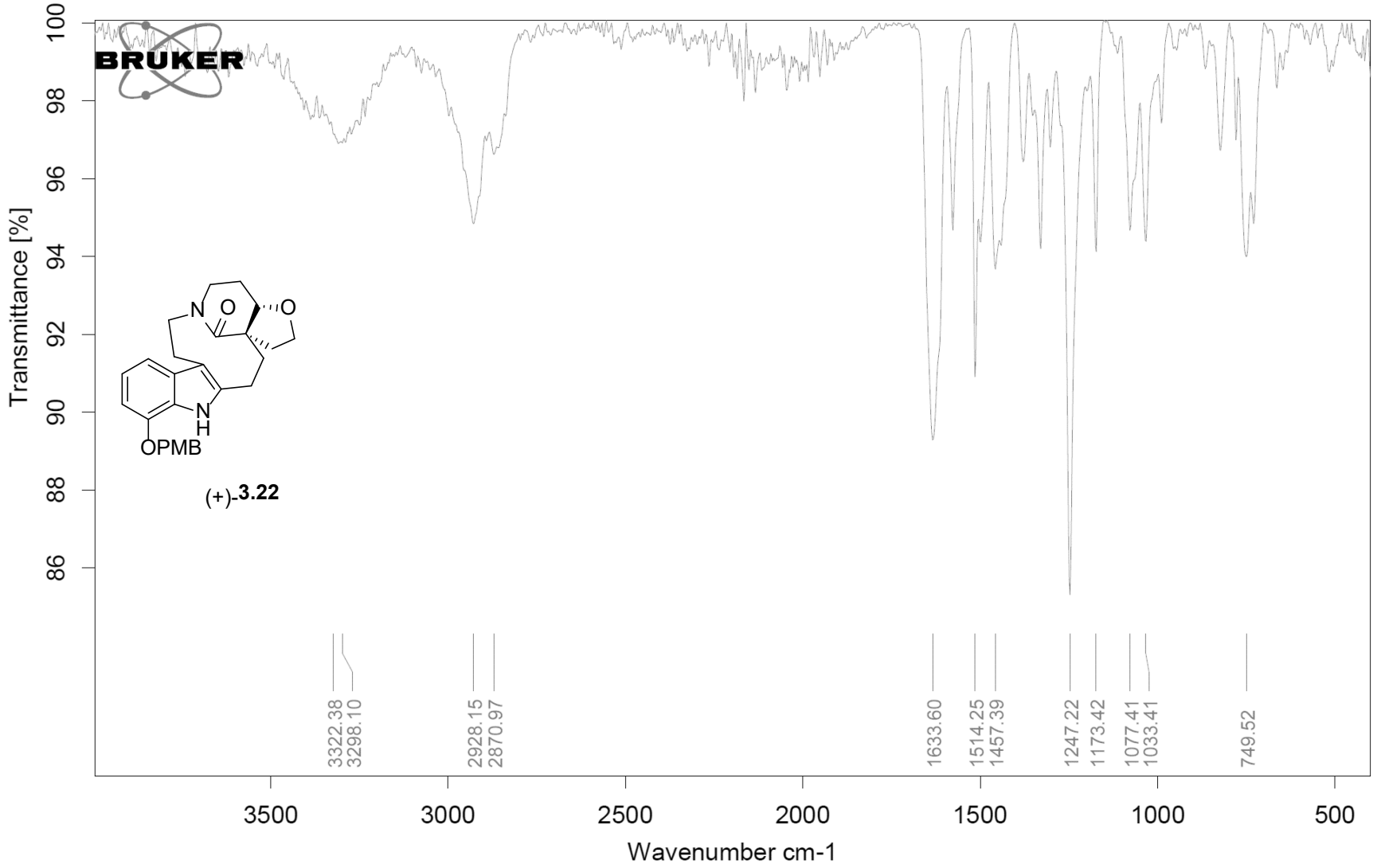
BRUKER
Transmittance [%]
100
98
96
94
92
90
88
86
N
O
O
N
H
OPMB
(+)-3.22
3322.38
3298.10
2928.15
2870.97
1633.60
1514.25
1457.39
1247.22
1173.42
1077.41
1033.41
749.52
3500
3000
2500
2000
1500
1000
500
Wavenumber cm-1

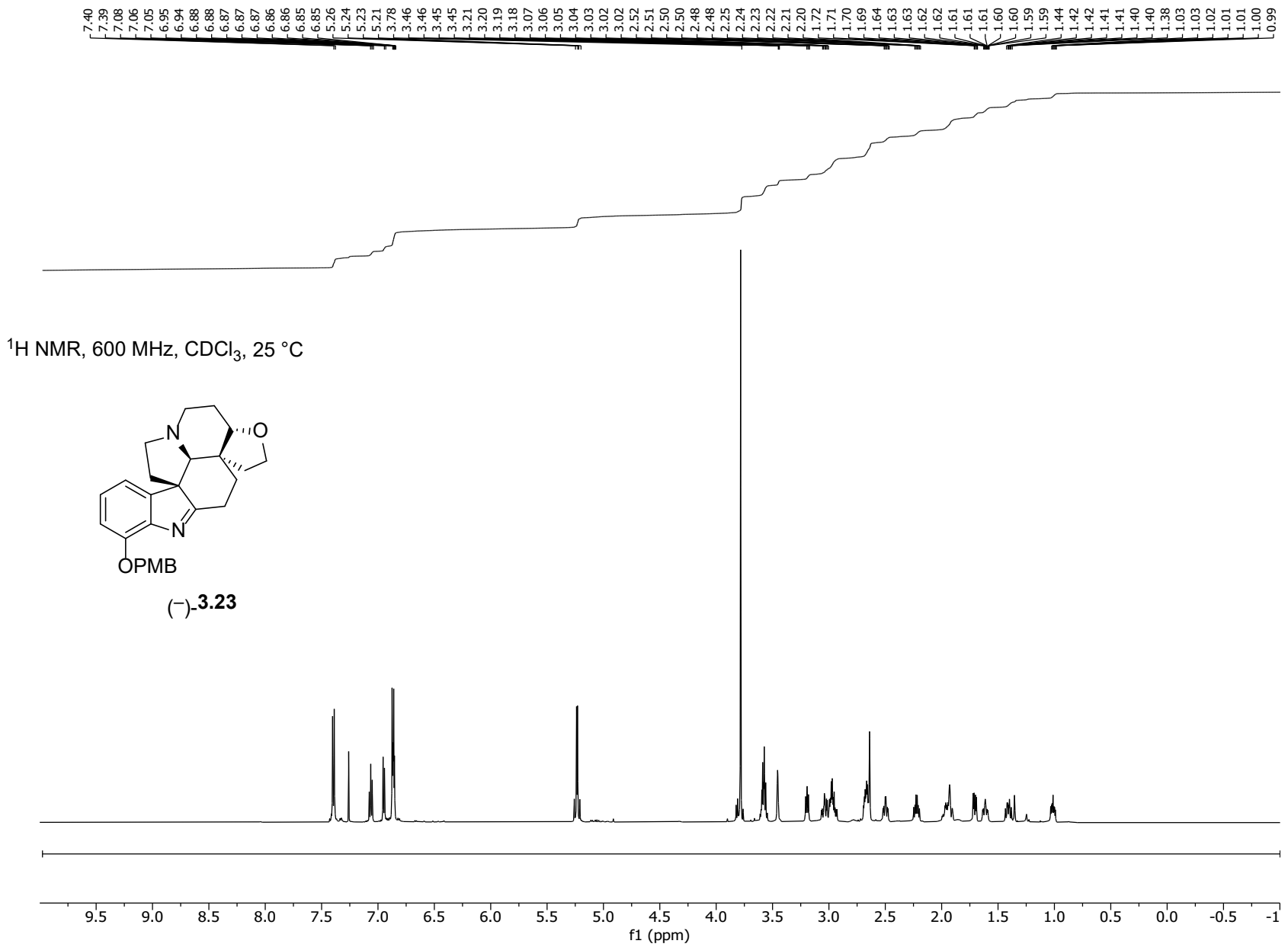
7.40 7.39 7.08 7.06 7.05 6.95 6.94 6.88 6.88 6.87 6.87 6.87 6.86 6.86 6.85 6.85 5.26 5.24 5.23 5.21 3.78 3.46 3.46 3.45 3.45 3.21 3.20 3.19 3.18 3.07 3.06 3.05 3.04 3.03 3.02 3.02 2.52 2.51 2.50 2.50 2.48 2.48 2.25 2.24 2.23 2.22 2.21 2.20 1.72 1.71 1.70 1.69 1.64 1.63 1.63 1.62 1.62 1.61 1.61 1.61 1.60 1.60 1.59 1.59 1.44 1.42 1.42 1.41 1.41 1.40 1.40 1.38 1.03 1.03 1.02 1.01 1.01 1.00 0.99
1H NMR, 600 MHz, CDCl3, 25 °C
N
O
N
OPMB
(−)-3.23
9.5 9.0 8.5 8.0 7.5 7.0 6.5 6.0 5.5 5.0 4.5 4.0 3.5 3.0 2.5 2.0 1.5 1.0 0.5 0.0 -0.5 -1
f1 (ppm)

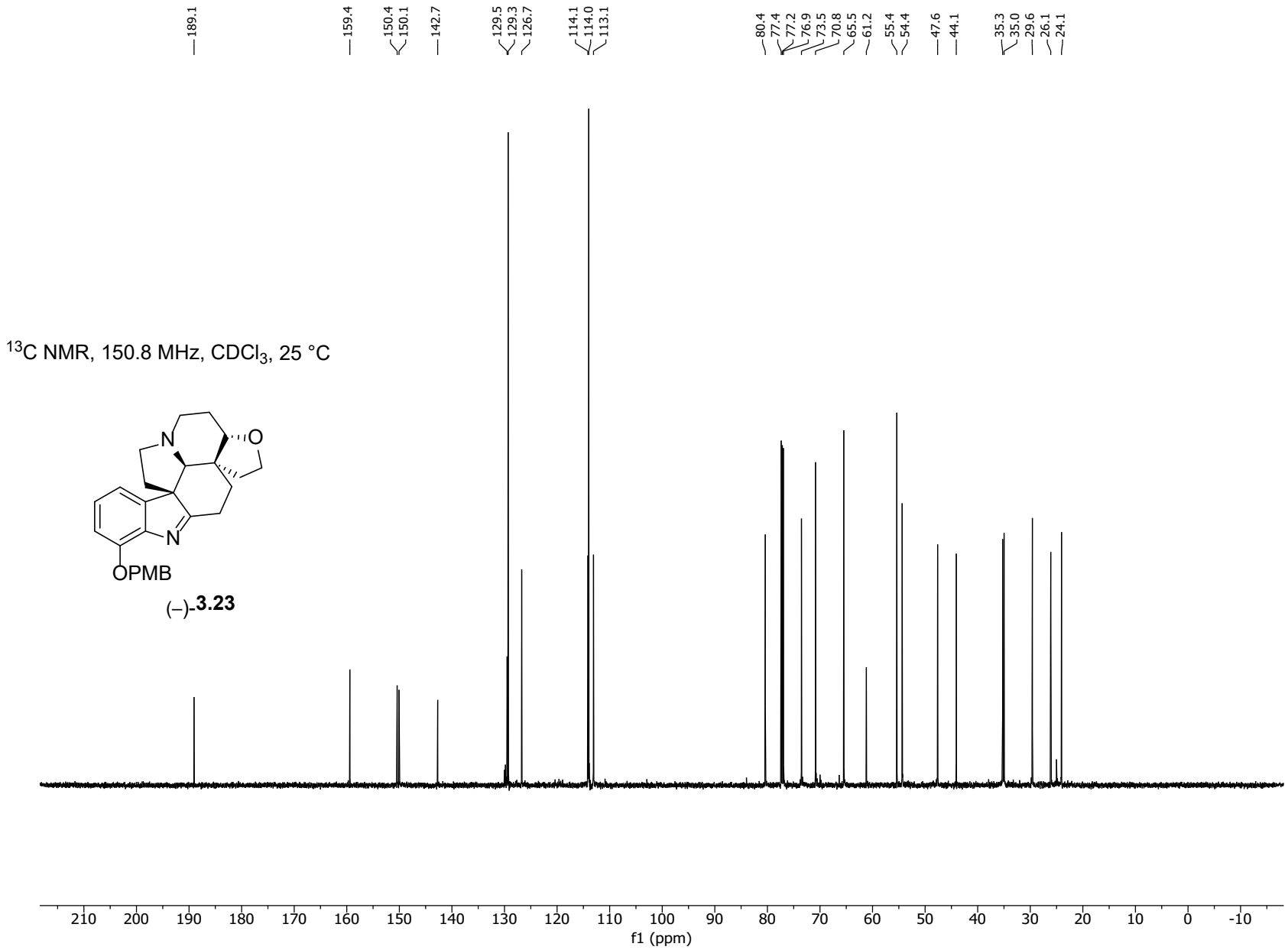
189.1
159.4
150.4
150.1
142.7
129.5
129.3
126.7
114.1
114.0
113.1
80.4
77.4
77.2
76.9
73.5
70.8
65.5
61.2
55.4
54.4
47.6
44.1
35.3
35.0
29.6
26.1
24.1
13C NMR, 150.8 MHz, CDCl3, 25 °C
N
O
N
OPMB
(–)-3.23
210 200 190 180 170 160 150 140 130 120 110 100 90 80 70 60 50 40 30 20 10 0 -10
f1 (ppm)

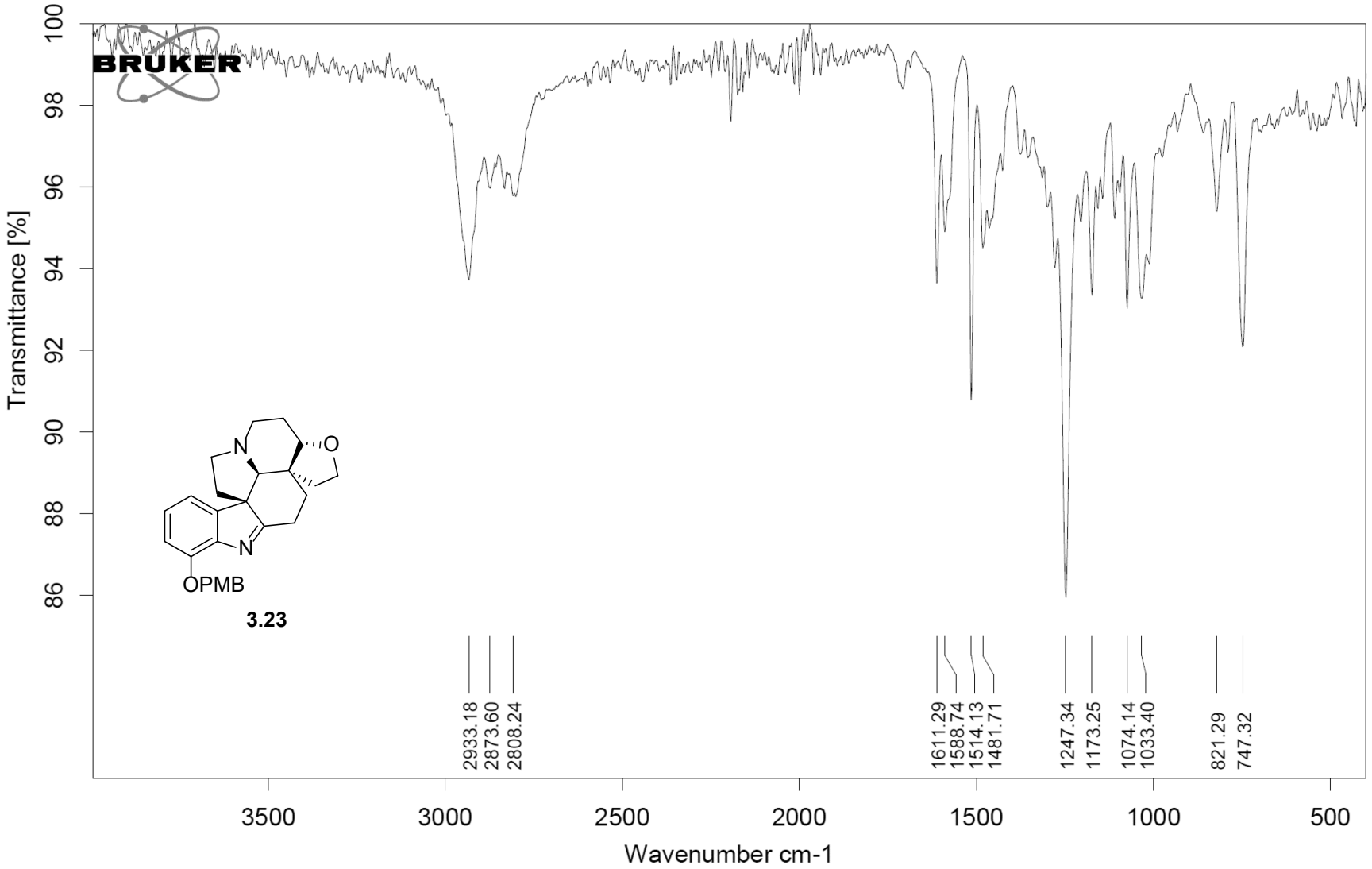
BRUKER
Transmittance [%]
100
98
96
94
92
90
88
86
N
O
N
OPMB
3.23
2933.18
2873.60
2808.24
1611.29
1588.74
1514.13
1481.71
1247.34
1173.25
1074.14
1033.40
821.29
747.32
3500
3000
2500
2000
1500
1000
500
Wavenumber cm-1

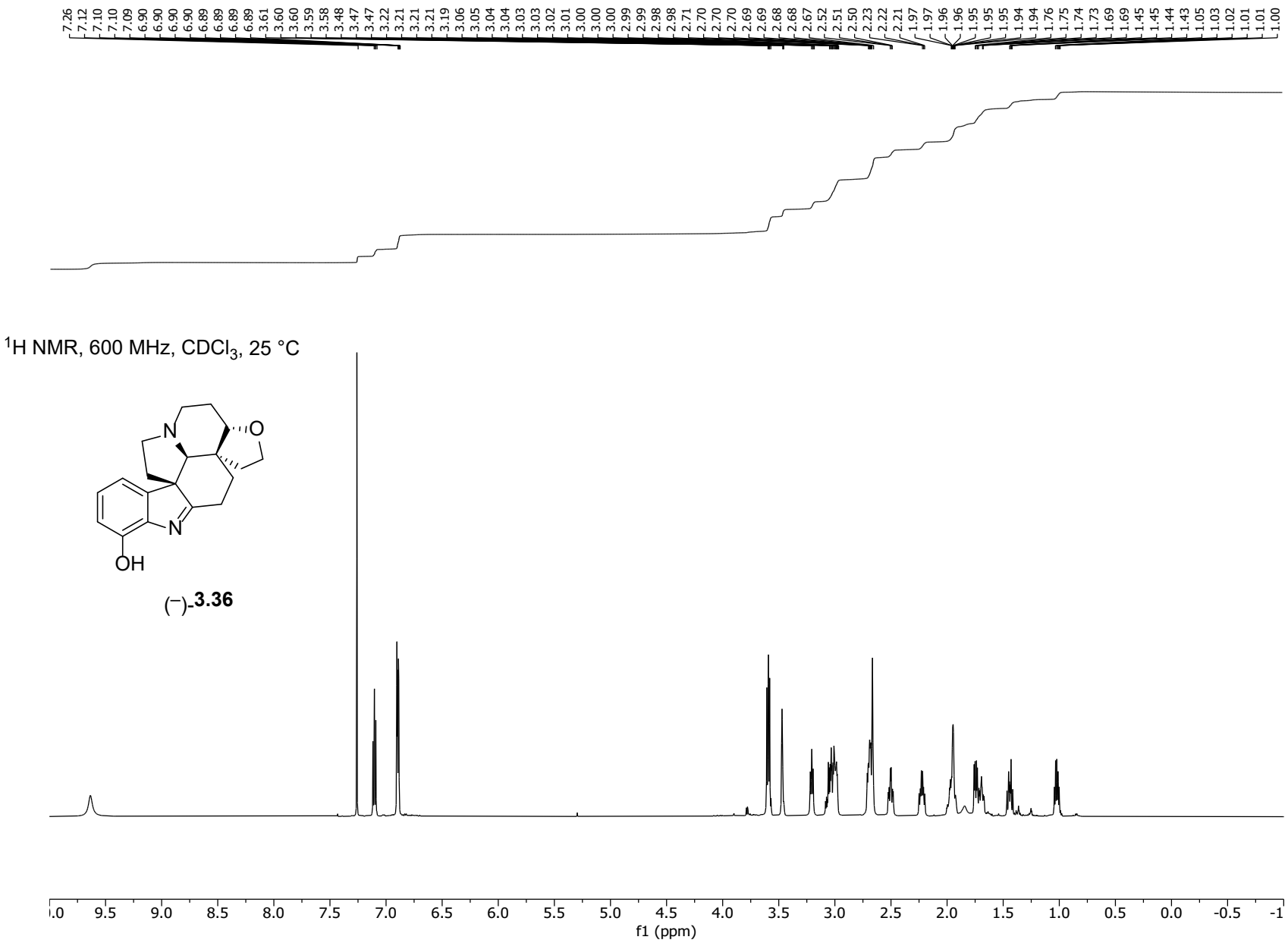
7.26 7.12 7.10 7.10 7.09 6.90 6.90 6.90 6.90 6.89 6.89 6.89 6.89 3.61 3.60 3.60 3.59 3.58 3.48 3.47 3.47 3.22 3.21 3.21 3.21 3.19 3.06 3.05 3.04 3.04 3.03 3.03 3.02 3.01 3.00 3.00 3.00 2.99 2.99 2.98 2.98 2.71 2.70 2.70 2.69 2.69 2.68 2.68 2.67 2.52 2.51 2.50 2.23 2.22 2.21 1.97 1.97 1.96 1.96 1.95 1.95 1.95 1.94 1.94 1.76 1.75 1.74 1.73 1.69 1.69 1.45 1.45 1.44 1.43 1.05 1.03 1.02 1.01 1.01 1.00
1H NMR, 600 MHz, CDCl3, 25 °C
N
O
N
OH
(−)-3.36
9.5 9.0 8.5 8.0 7.5 7.0 6.5 6.0 5.5 5.0 4.5 4.0 3.5 3.0 2.5 2.0 1.5 1.0 0.5 0.0 -0.5 -1
f1 (ppm)

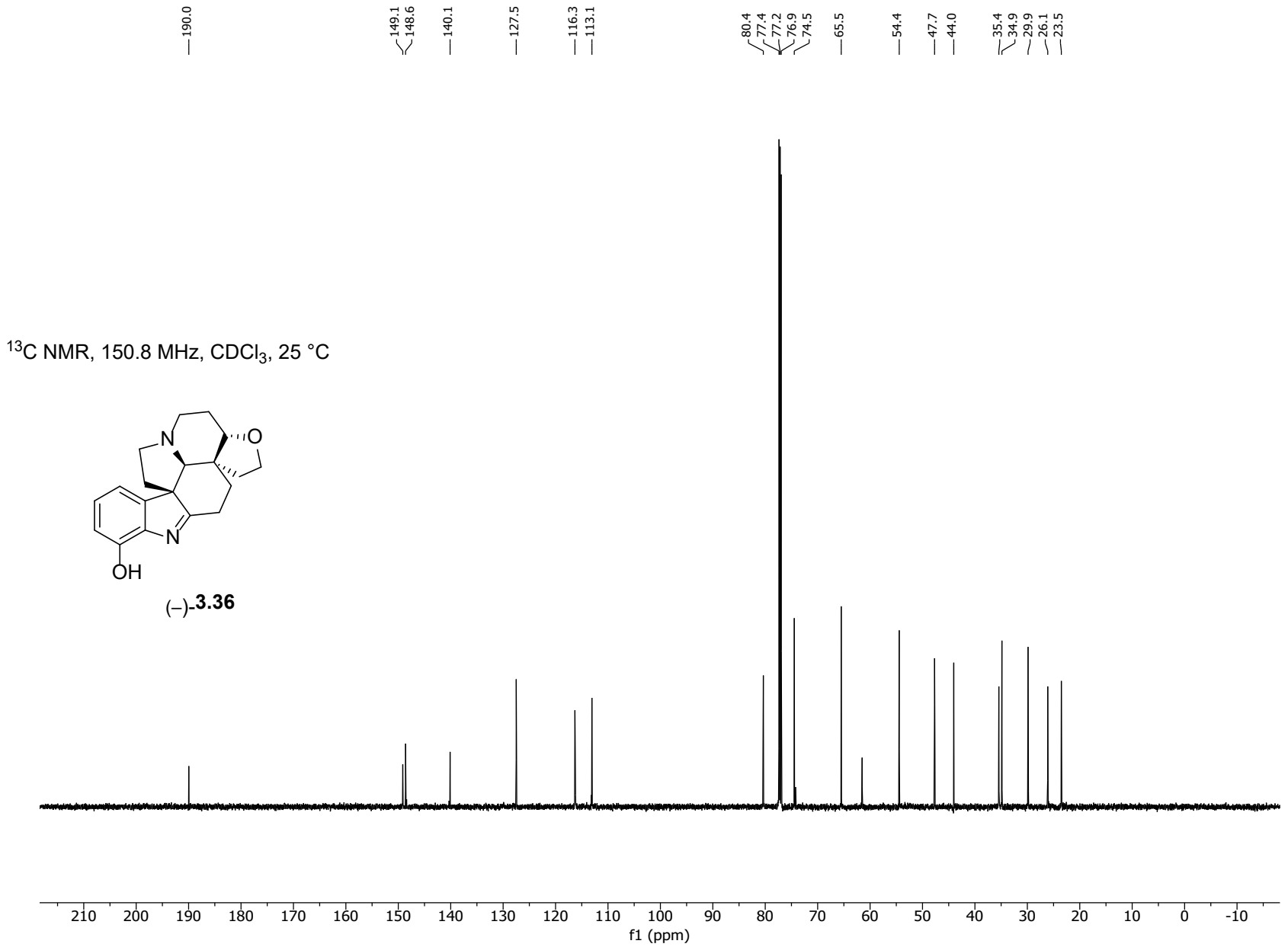
190.0
149.1
148.6
140.1
127.5
116.3
113.1
80.4
77.4
77.2
76.9
74.5
65.5
54.4
47.7
44.0
35.4
34.9
29.9
26.1
23.5
13C NMR, 150.8 MHz, CDCl3, 25 °C
N
O
N
OH
(–)-3.36
210 200 190 180 170 160 150 140 130 120 110 100 90 80 70 60 50 40 30 20 10 0 -10
f1 (ppm)

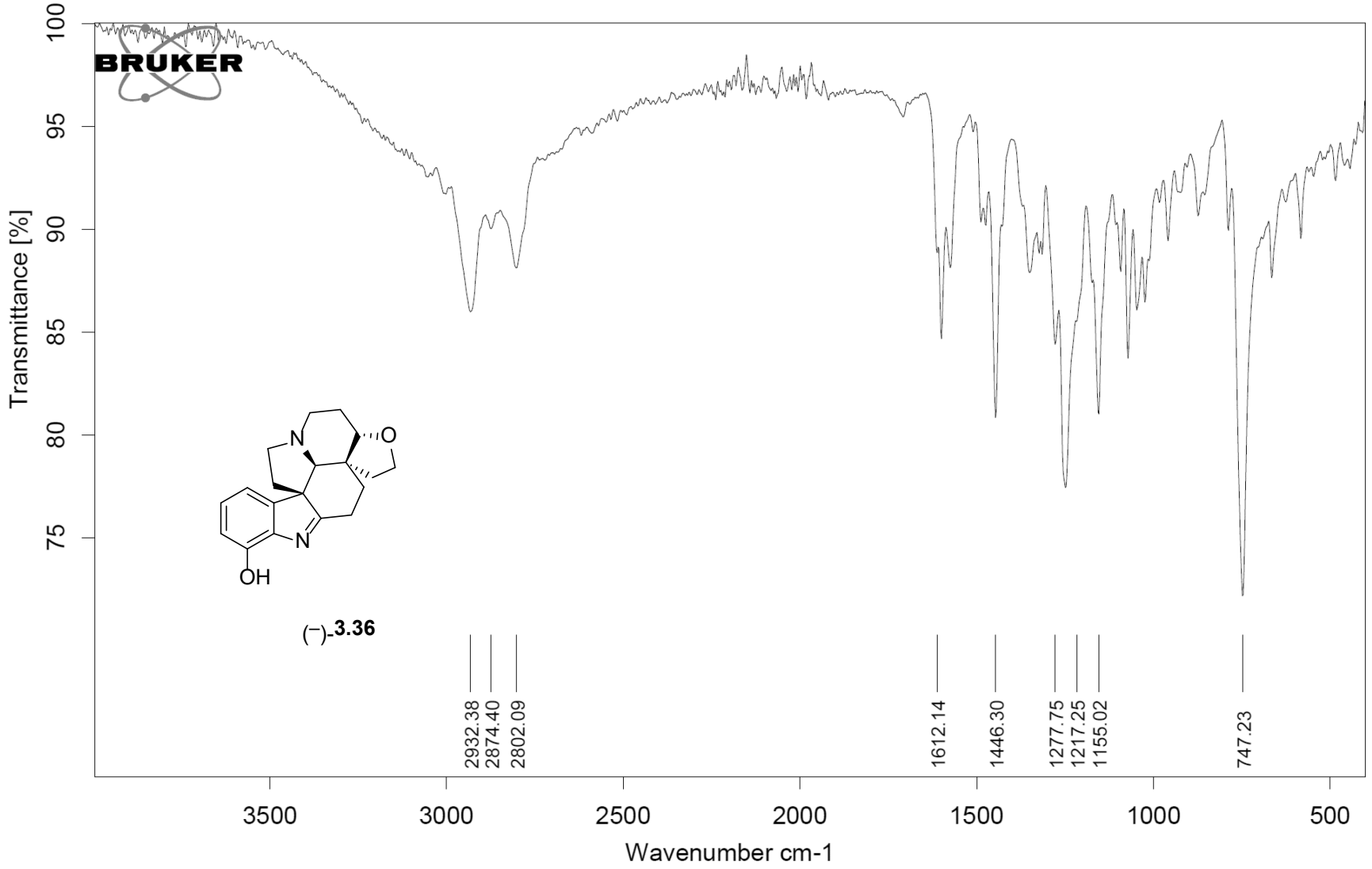
BRUKER
Transmittance [%]
100
95
90
85
80
75
3500
3000
2500
2000
1500
1000
500
Wavenumber cm-1
2932.38
2874.40
2802.09
1612.14
1446.30
1277.75
1217.25
1155.02
747.23
N
O
N
OH
(−)-3.36

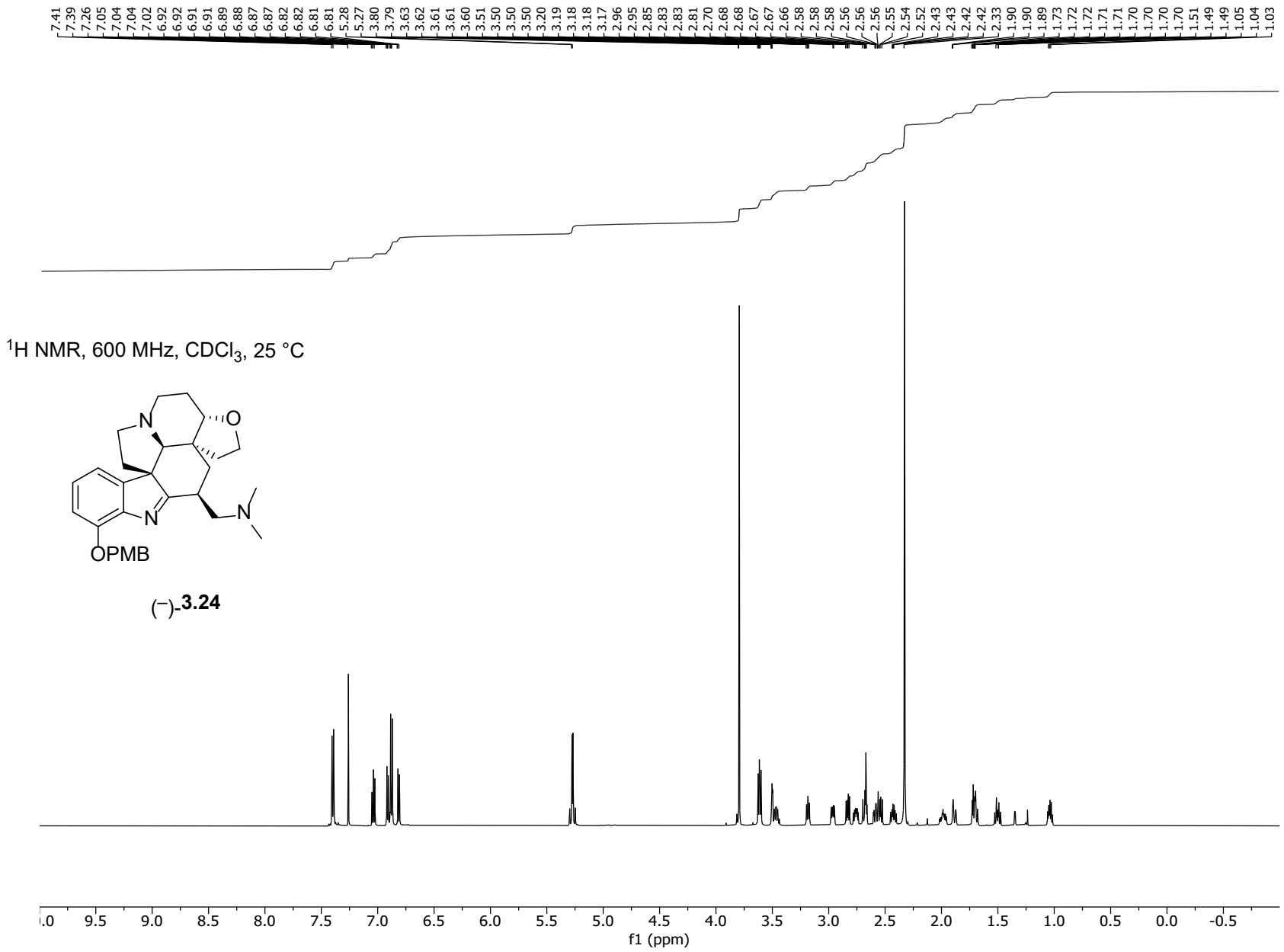
7.41 7.39 7.26 7.05 7.04 7.04 7.02 6.92 6.92 6.91 6.91 6.89 6.88 6.87 6.87 6.82 6.82 6.81 6.81 5.28 5.27 3.80 3.79 3.63 3.62 3.61 3.61 3.60 3.51 3.50 3.50 3.50 3.20 3.19 3.18 3.18 3.17 2.96 2.95 2.85 2.83 2.83 2.81 2.70 2.68 2.68 2.67 2.67 2.66 2.58 2.58 2.56 2.56 2.56 2.55 2.54 2.52 2.43 2.43 2.42 2.42 2.33 1.90 1.90 1.89 1.73 1.72 1.72 1.71 1.71 1.70 1.70 1.70 1.70 1.51 1.49 1.49 1.05 1.04 1.03
1H NMR, 600 MHz, CDCl3, 25 °C
N
O
N
N
OPMB
(−)-3.24
9.5 9.0 8.5 8.0 7.5 7.0 6.5 6.0 5.5 5.0 4.5 4.0 3.5 3.0 2.5 2.0 1.5 1.0 0.5 0.0 -0.5
f1 (ppm)

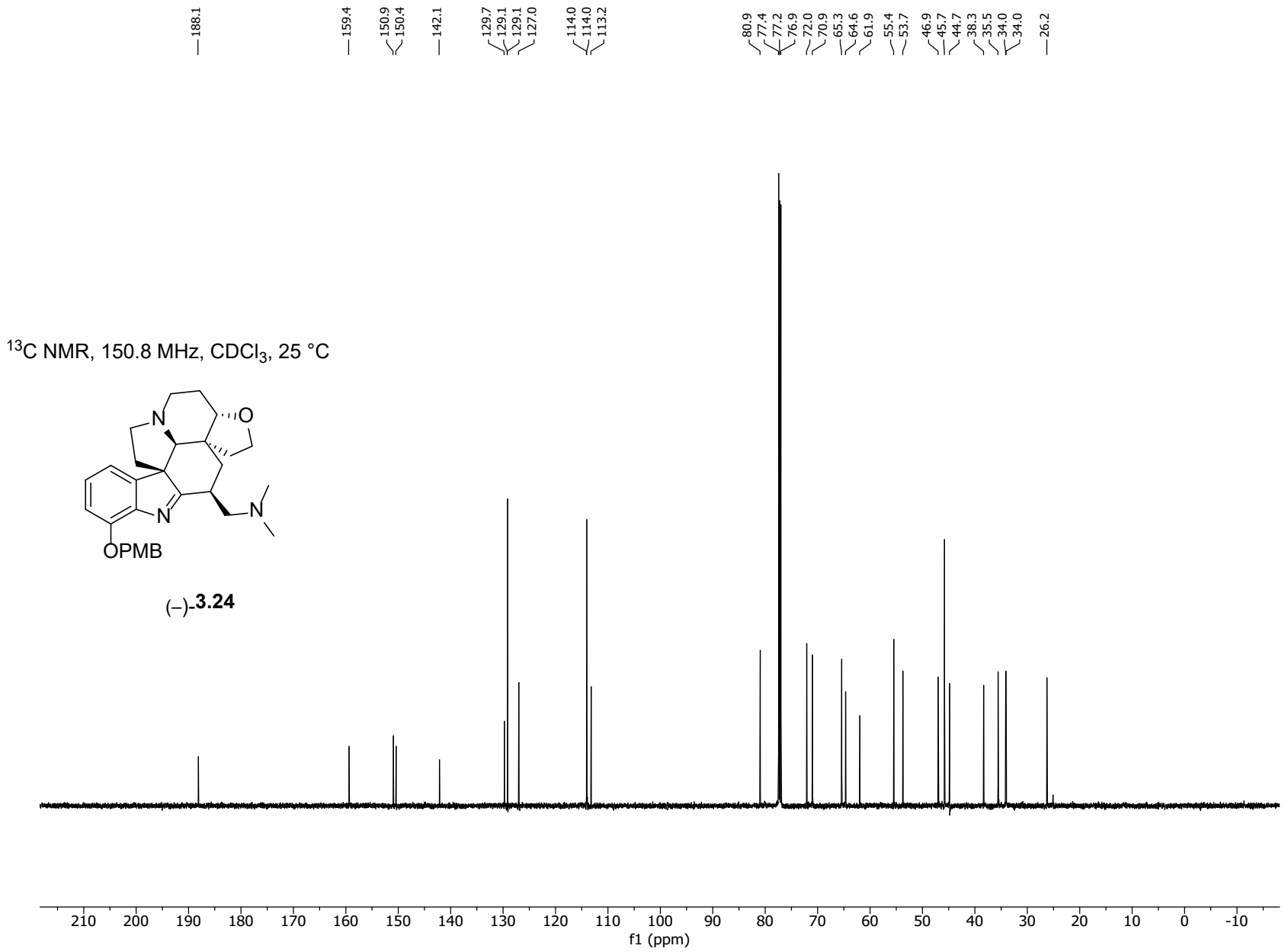
188.1
159.4
150.9
150.4
142.1
129.7
129.1
129.1
127.0
114.0
114.0
113.2
80.9
77.4
77.2
76.9
72.0
70.9
65.3
64.6
61.9
55.4
53.7
46.9
45.7
44.7
38.3
35.5
34.0
34.0
26.2
13C NMR, 150.8 MHz, CDCl3, 25 °C
N
O
N
N
OPMB
(–)-3.24
210 200 190 180 170 160 150 140 130 120 110 100 90 80 70 60 50 40 30 20 10 0 -10
f1 (ppm)

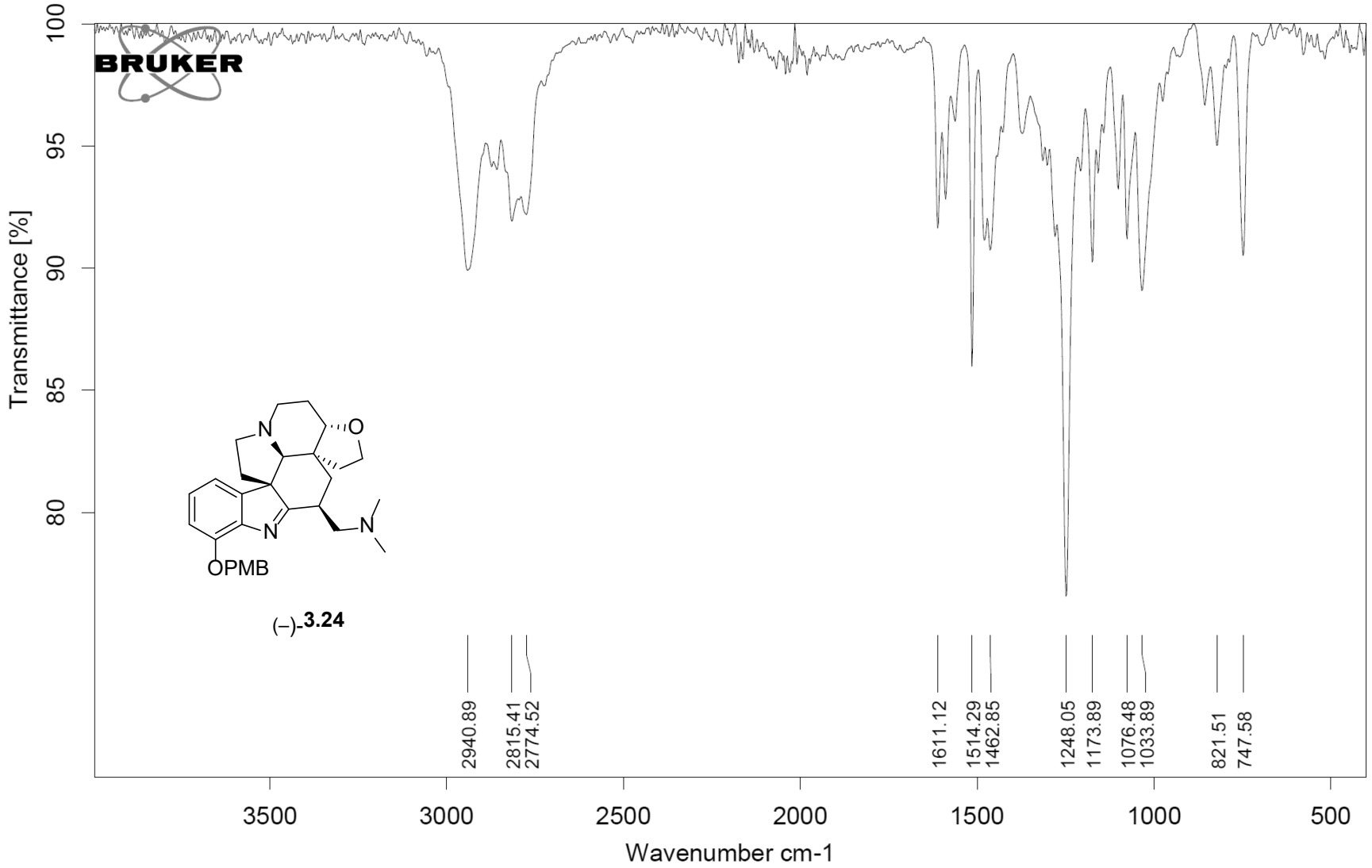
BRUKER
Transmittance [%]
100
95
90
85
80
N
O
N
N
OPMB
(–)-3.24
2940.89
2815.41
2774.52
1611.12
1514.29
1462.85
1248.05
1173.89
1076.48
1033.89
821.51
747.58
3500
3000
2500
2000
1500
1000
500
Wavenumber cm-1

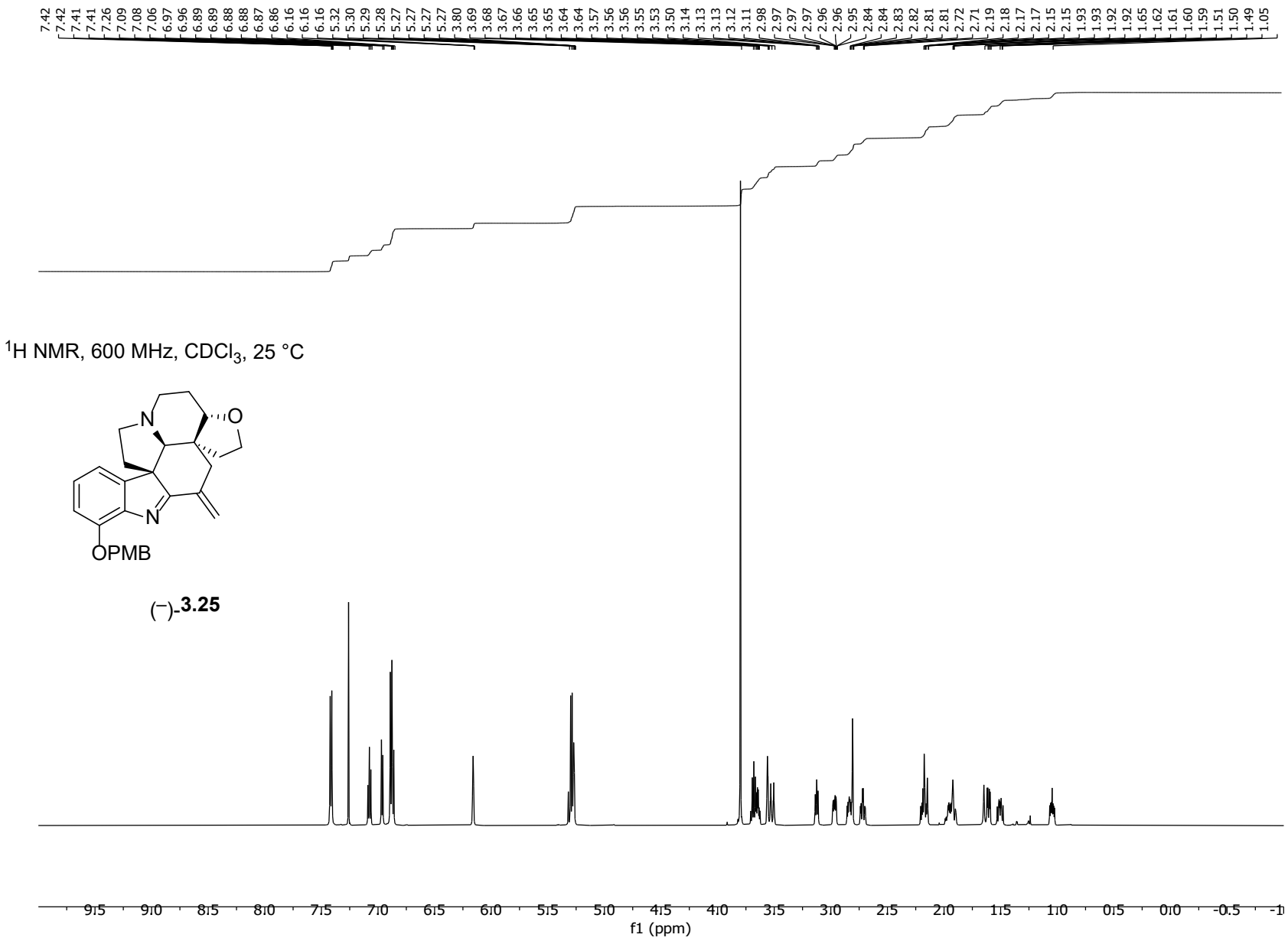
7.42 7.42 7.41 7.41 7.26 7.09 7.08 7.06 6.97 6.96 6.89 6.89 6.88 6.88 6.87 6.86 6.16 6.16 5.32 5.30 5.29 5.28 5.27 5.27 5.27 5.27 3.80 3.69 3.68 3.67 3.66 3.65 3.65 3.64 3.64 3.57 3.56 3.56 3.55 3.53 3.50 3.14 3.13 3.13 3.12 3.11 2.98 2.97 2.97 2.97 2.96 2.96 2.95 2.84 2.84 2.83 2.82 2.81 2.81 2.72 2.71 2.19 2.18 2.17 2.17 2.15 2.15 1.93 1.93 1.92 1.92 1.65 1.62 1.61 1.60 1.59 1.51 1.50 1.49 1.05
^{1}H NMR, 600 MHz, $CDCl_3$, 25 °C
N
O
N
OPMB
(−)-3.25
9.5 9.0 8.5 8.0 7.5 7.0 6.5 6.0 5.5 5.0 4.5 4.0 3.5 3.0 2.5 2.0 1.5 1.0 0.5 0.0 -0.5
f1 (ppm)

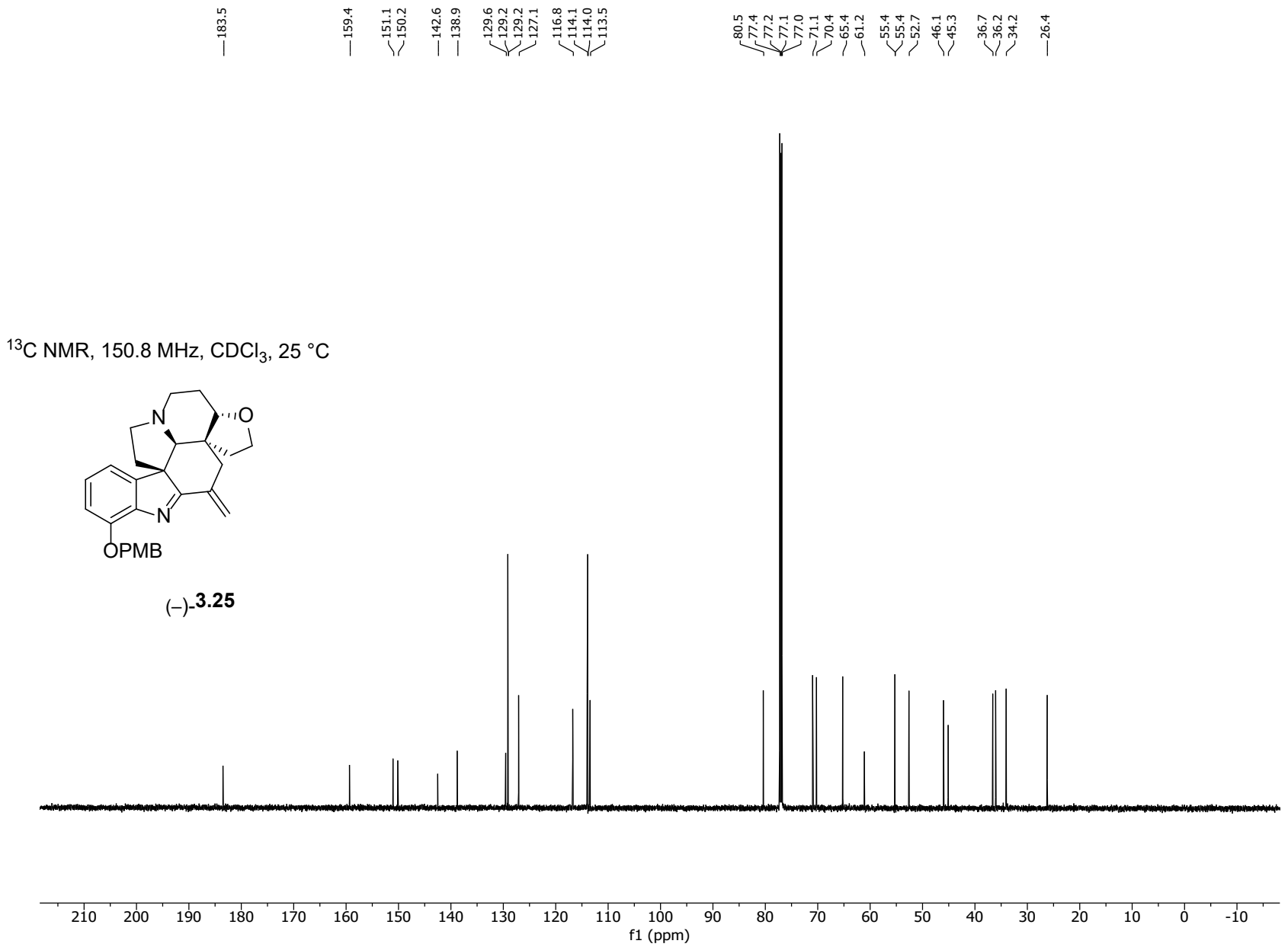
183.5
159.4
151.1
150.2
142.6
138.9
129.6
129.2
129.2
127.1
116.8
114.1
114.0
113.5
80.5
77.4
77.2
77.1
77.0
71.1
70.4
65.4
61.2
55.4
55.4
52.7
46.1
45.3
36.7
36.2
34.2
26.4
13C NMR, 150.8 MHz, CDCl3, 25 °C
N
O
N
OPMB
(–)-3.25
210
200
190
180
170
160
150
140
130
120
110
100
90
80
70
60
50
40
30
20
10
0
-10
f1 (ppm)

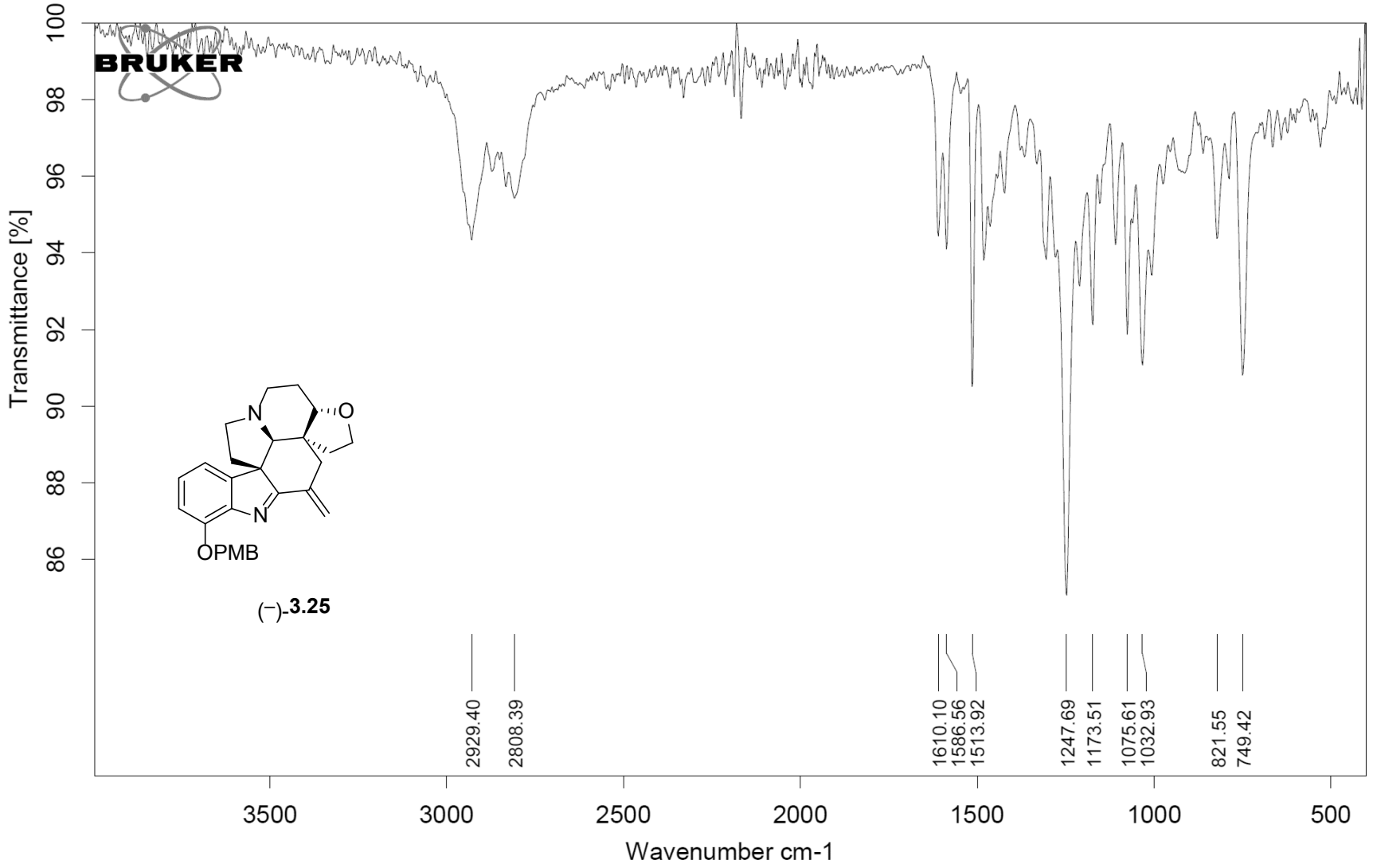
BRUKER
Transmittance [%]
100
98
96
94
92
90
88
86
N
O
N
OPMB
(−)-3.25
2929.40
2808.39
1610.10
1586.56
1513.92
1247.69
1173.51
1075.61
1032.93
821.55
749.42
3500
3000
2500
2000
1500
1000
500
Wavenumber cm-1

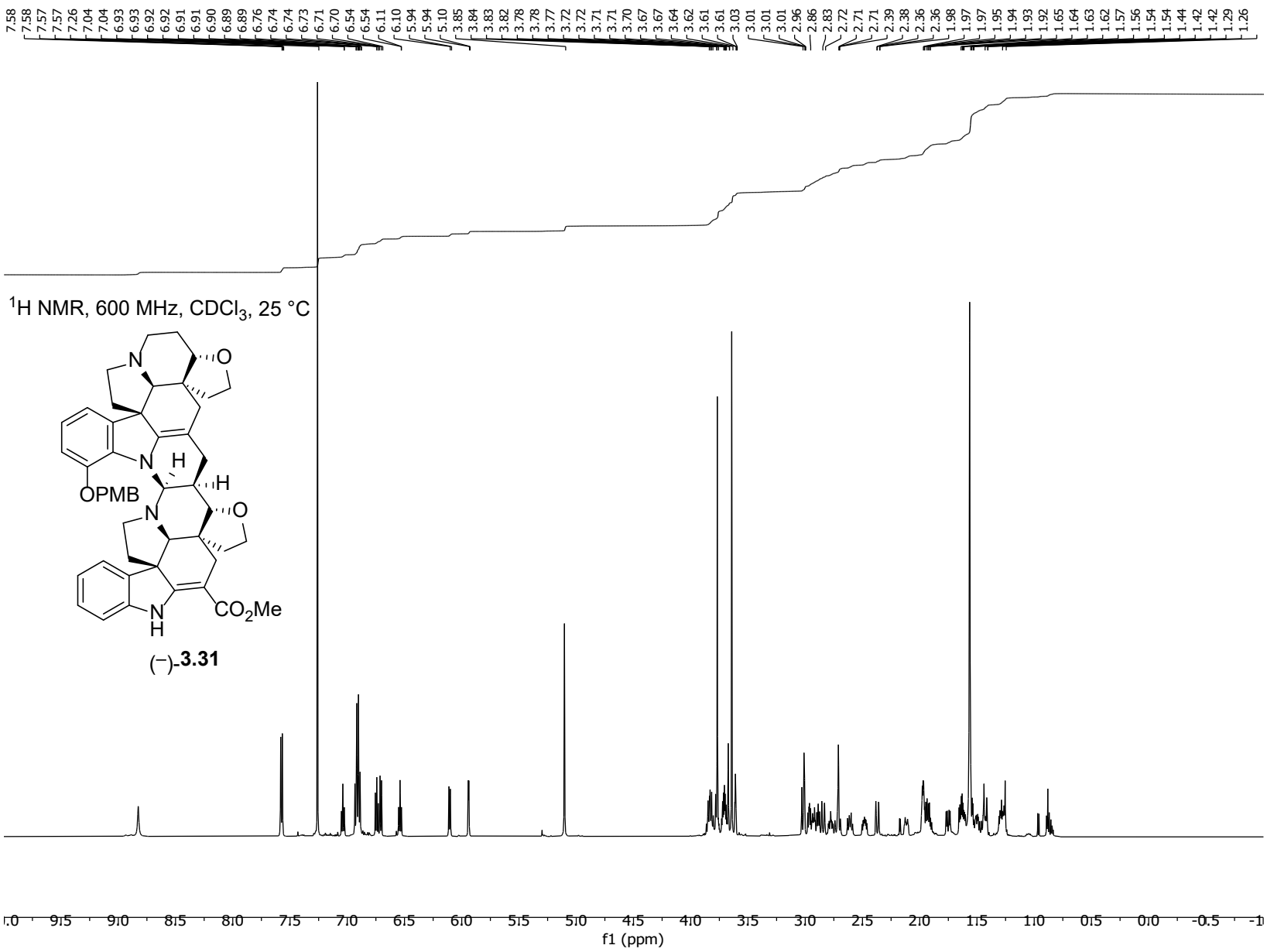
7.58 7.58 7.57 7.57 7.26 7.04 7.04 6.93 6.92 6.92 6.91 6.91 6.90 6.89 6.76 6.74 6.74 6.73 6.71 6.70 6.54 6.54 6.11 6.10 5.94 5.94 5.10 3.85 3.84 3.83 3.82 3.78 3.78 3.77 3.72 3.72 3.71 3.71 3.70 3.67 3.64 3.62 3.61 3.61 3.03 3.01 3.01 3.01 2.96 2.86 2.83 2.72 2.71 2.71 2.39 2.38 2.36 2.36 1.98 1.97 1.97 1.95 1.94 1.93 1.92 1.65 1.64 1.63 1.62 1.57 1.56 1.54 1.54 1.44 1.42 1.42 1.29 1.26
^{1}H NMR, 600 MHz, $CDCl_3$, 25 °C
OPMB
CO_2Me
(−)-**3.31**
f1 (ppm)

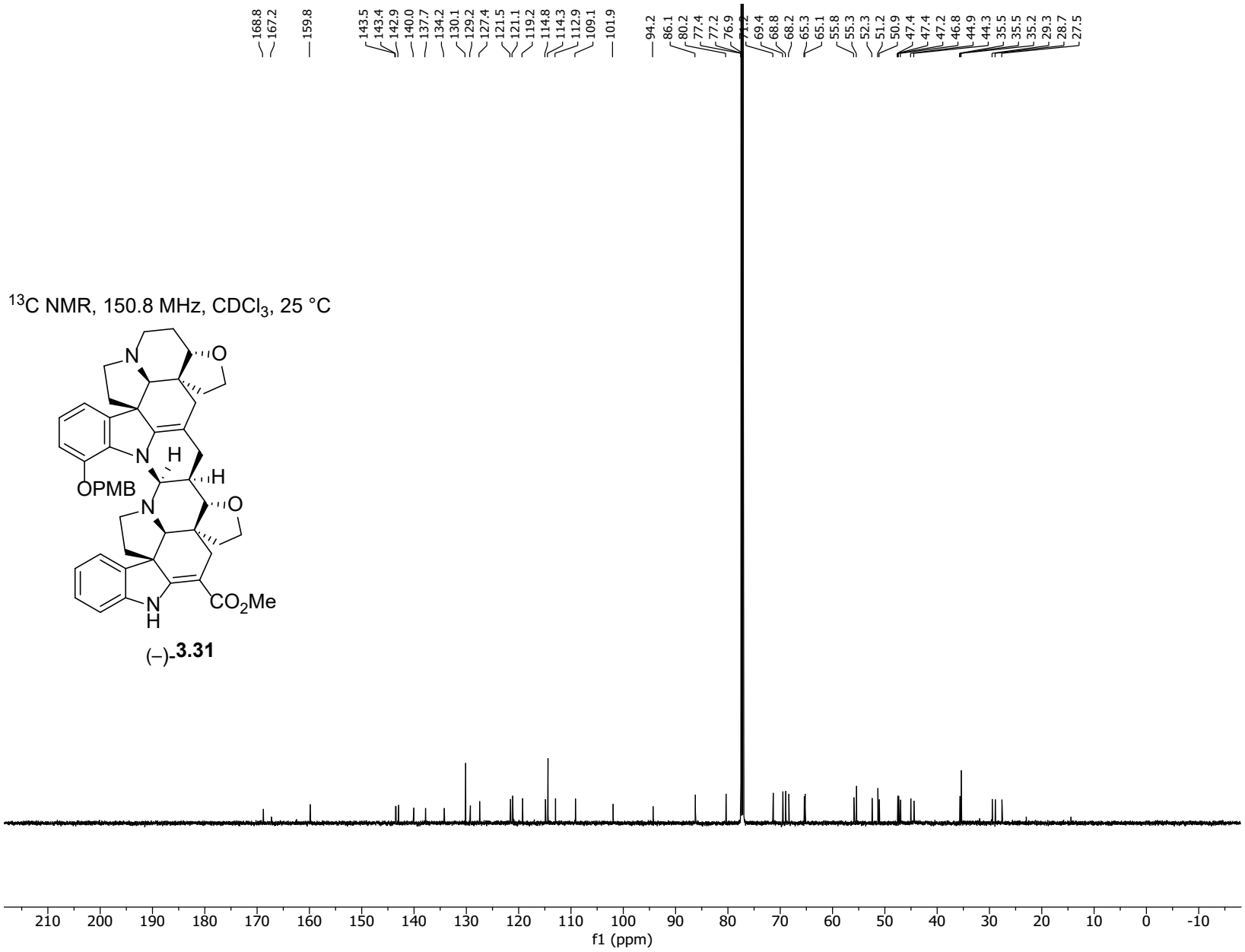

^{13}C NMR, 150.8 MHz, $CDCl_3$, 25 °C

(–)-**3.31**

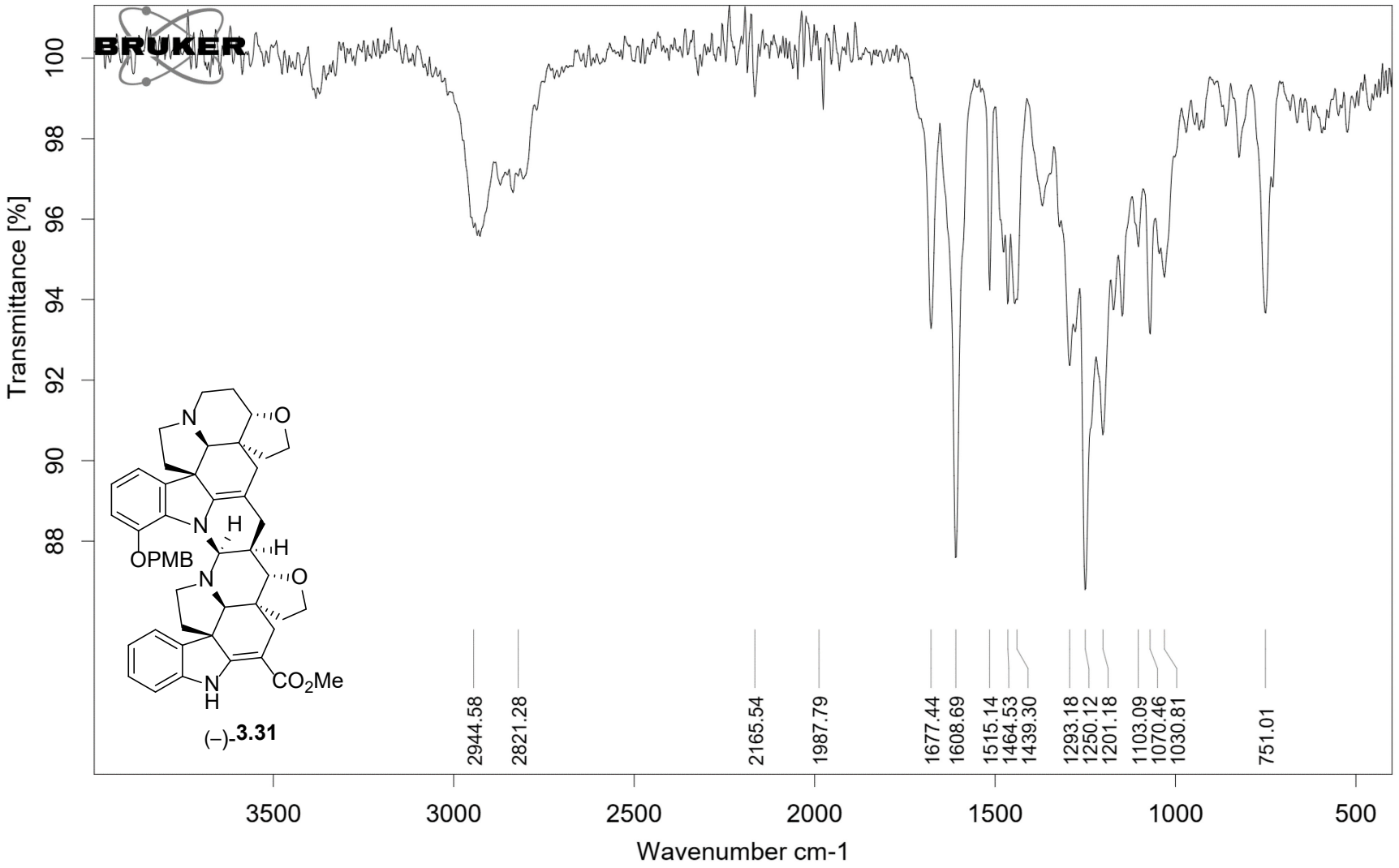
BRUKER
Transmittance [%]
100
98
96
94
92
90
88
3500
3000
2500
2000
1500
1000
500
Wavenumber cm-1
2944.58
2821.28
2165.54
1987.79
1677.44
1608.69
1515.14
1464.53
1439.30
1293.18
1250.12
1201.18
1103.09
1070.46
1030.81
751.01
OPMB
CO2Me
(–)-3.31

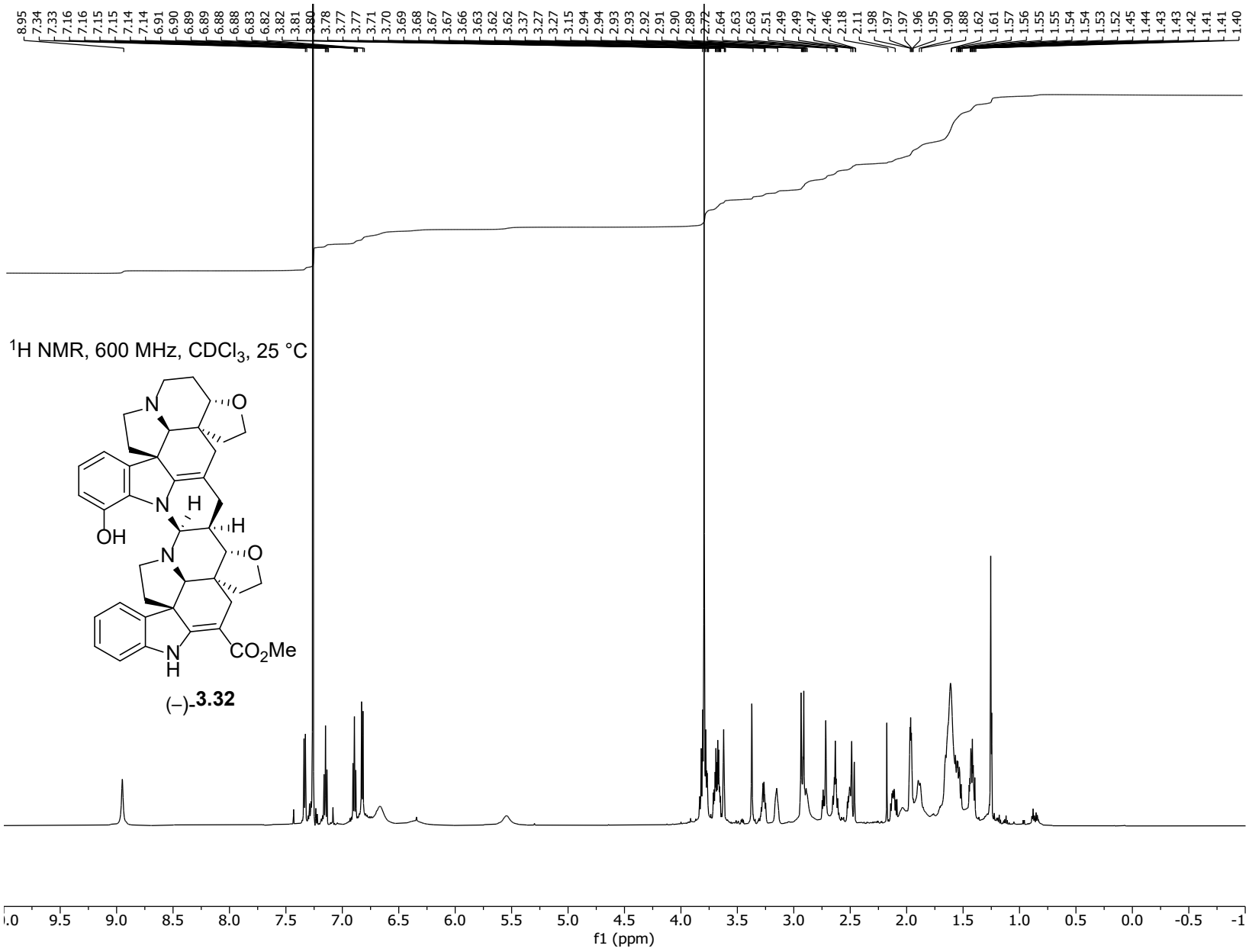
8.95 7.34 7.33 7.16 7.16 7.15 7.15 7.14 7.14 6.91 6.90 6.89 6.89 6.88 6.88 6.83 6.82 3.82 3.81 3.80 3.78 3.77 3.77 3.71 3.70 3.69 3.68 3.67 3.67 3.66 3.63 3.62 3.62 3.37 3.27 3.27 3.15 2.94 2.94 2.93 2.93 2.92 2.91 2.90 2.89 2.72 2.64 2.63 2.63 2.51 2.49 2.49 2.47 2.46 2.18 2.11 1.98 1.97 1.97 1.96 1.95 1.90 1.88 1.62 1.61 1.57 1.56 1.55 1.55 1.54 1.54 1.53 1.52 1.45 1.44 1.43 1.43 1.42 1.41 1.41 1.40
^{1}H NMR, 600 MHz, $CDCl_3$, 25 °C
N
O
N
H
H
OH
N
O
N
H
CO_2Me
(–)-**3.32**
9.5 9.0 8.5 8.0 7.5 7.0 6.5 6.0 5.5 5.0 4.5 4.0 3.5 3.0 2.5 2.0 1.5 1.0 0.5 0.0 -0.5 -1
f1 (ppm)

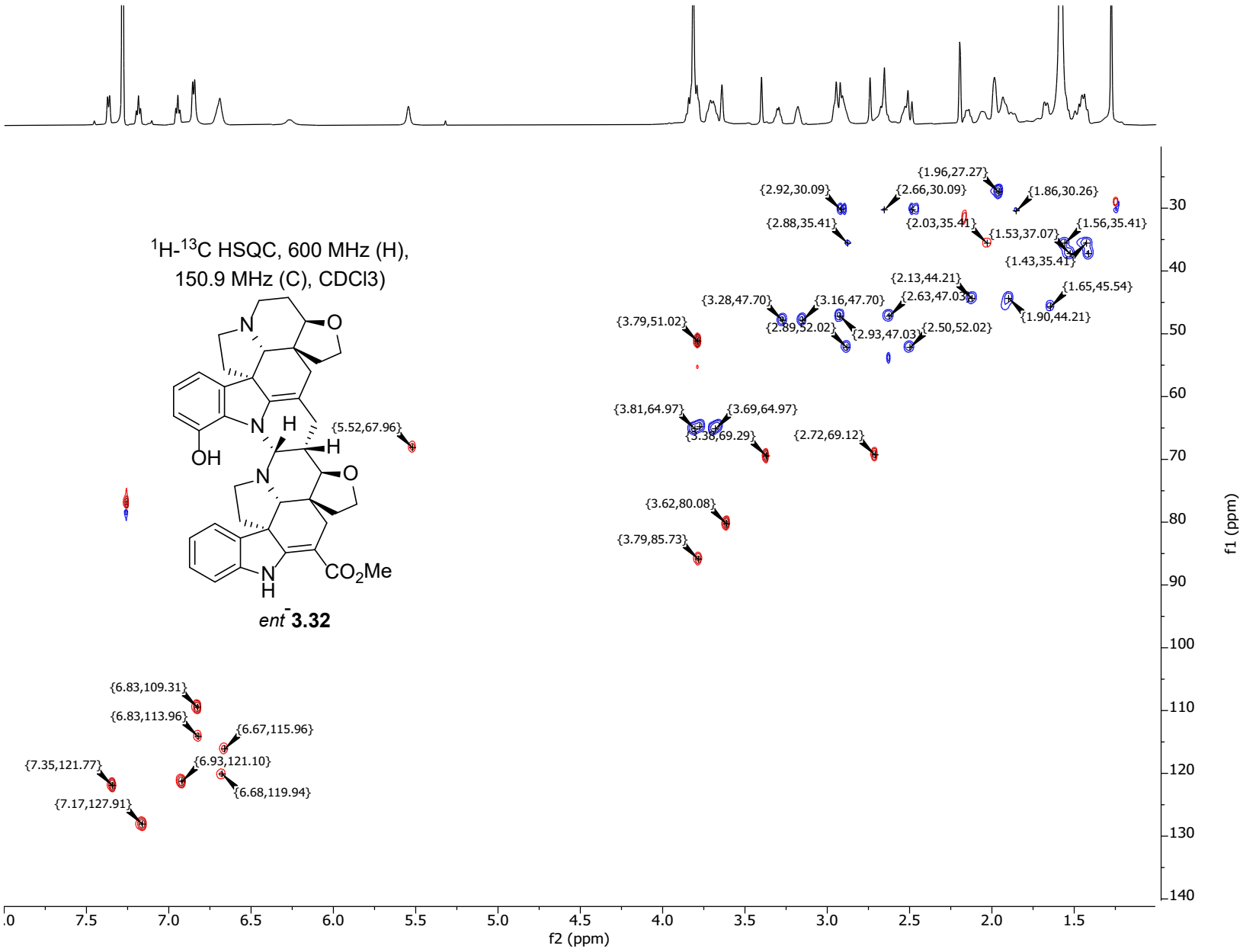
^{1}H-^{13}C HSQC, 600 MHz (H),
150.9 MHz (C), CDCl3)
ent-3.32
{1.96,27.27}
{2.92,30.09}
{2.66,30.09}
{1.86,30.26}
{2.88,35.41}
{2.03,35.41}
{1.53,37.07}
{1.56,35.41}
{1.43,35.41}
{2.13,44.21}
{1.65,45.54}
{3.28,47.70}
{3.16,47.70}
{2.63,47.03}
{1.90,44.21}
{3.79,51.02}
{2.89,52.02}
{2.93,47.03}
{2.50,52.02}
{5.52,67.96}
{3.81,64.97}
{3.69,64.97}
{3.38,69.29}
{2.72,69.12}
{3.62,80.08}
{3.79,85.73}
{6.83,109.31}
{6.83,113.96}
{6.67,115.96}
{6.93,121.10}
{7.35,121.77}
{6.68,119.94}
{7.17,127.91}
f1 (ppm)
f2 (ppm)

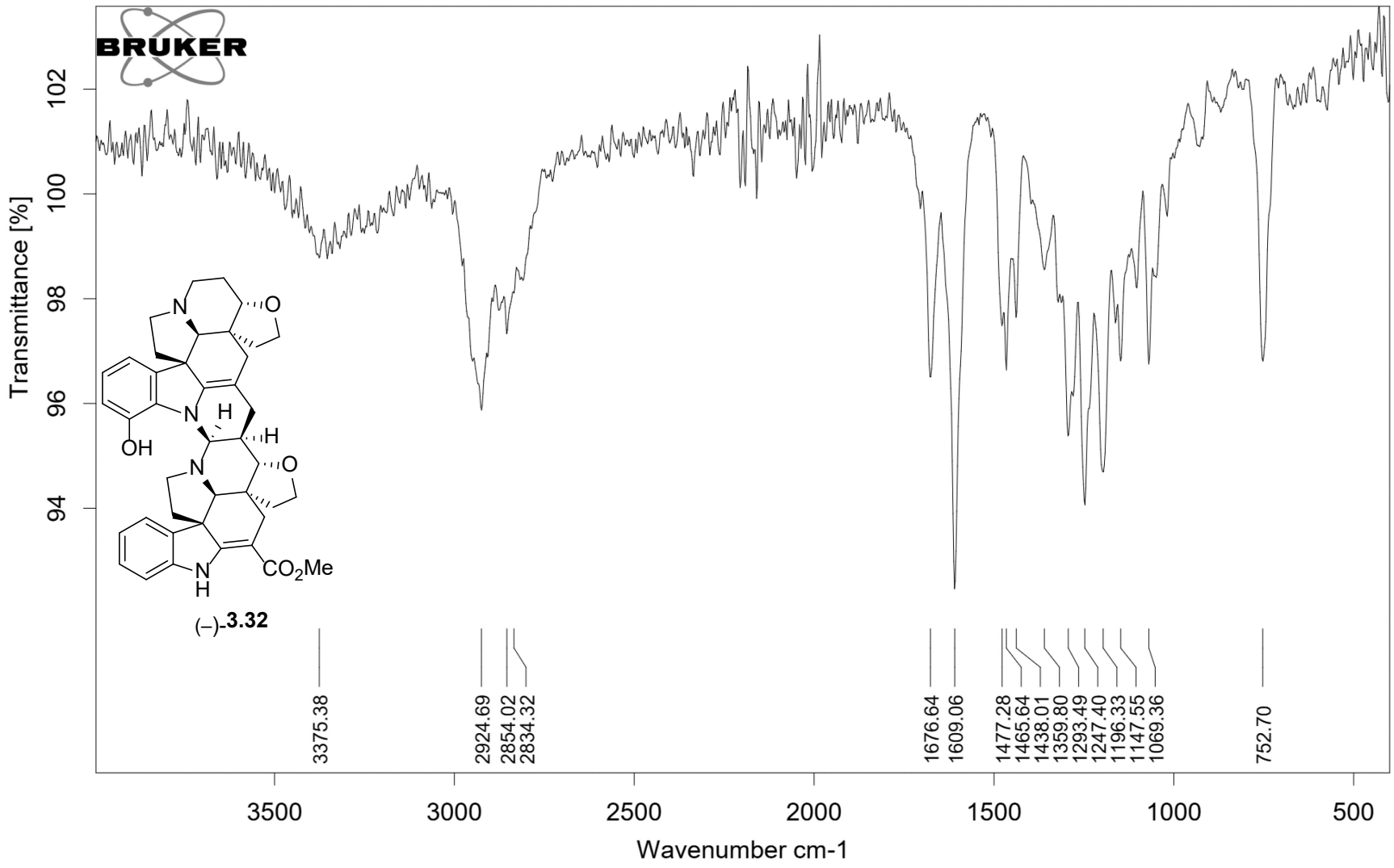
BRUKER
Transmittance [%]
102
100
98
96
94
3500
3000
2500
2000
1500
1000
500
Wavenumber cm-1
3375.38
2924.69
2854.02
2834.32
1676.64
1609.06
1477.28
1465.64
1438.01
1359.80
1293.49
1247.40
1196.33
1147.55
1069.36
752.70
N
O
N
H
H
OH
N
O
N
H
CO2Me

(–)-**3.32**

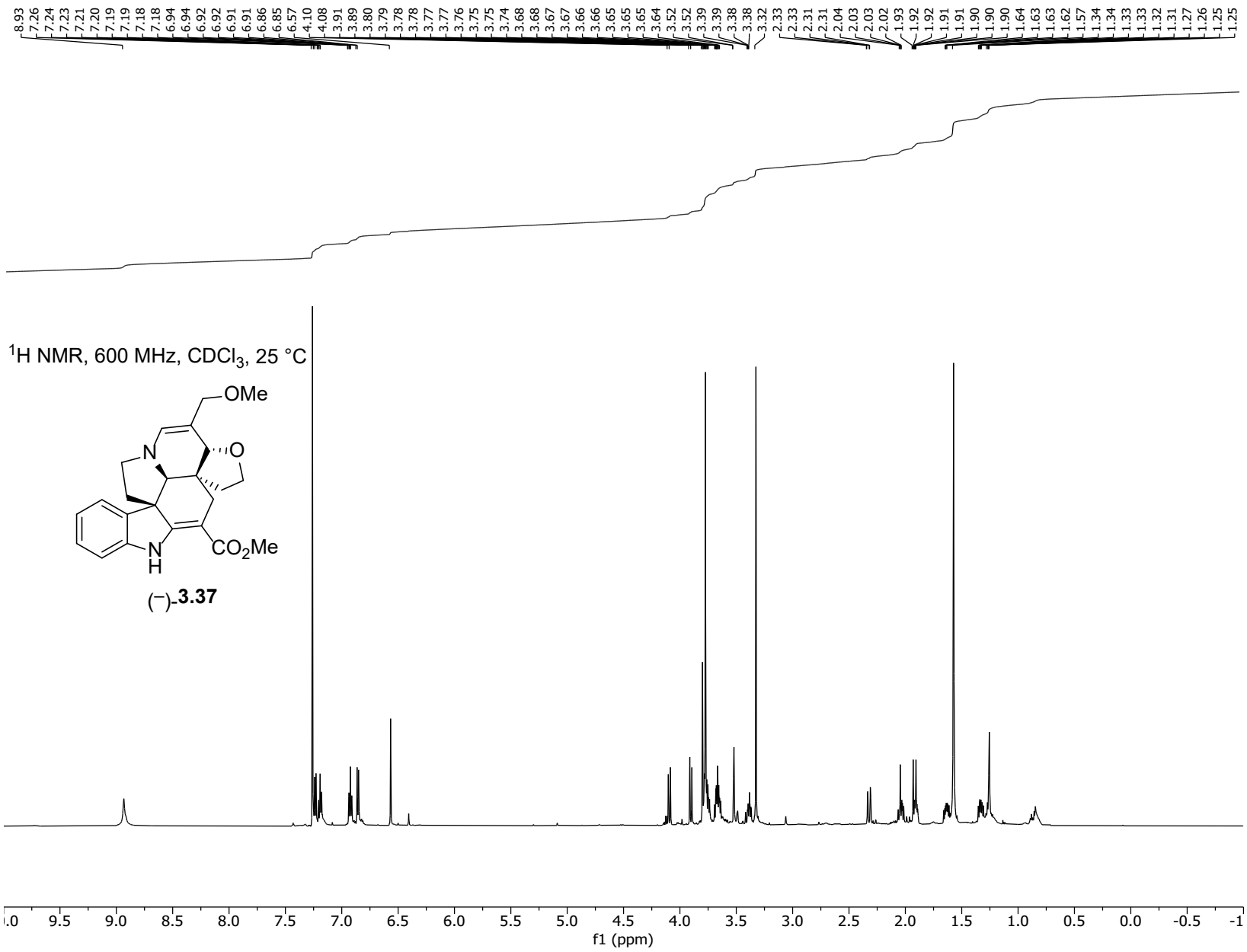
8.93 7.26 7.24 7.23 7.21 7.20 7.19 7.19 7.18 7.18 6.94 6.94 6.92 6.92 6.91 6.91 6.86 6.85 6.57 4.10 4.08 3.91 3.89 3.80 3.79 3.78 3.78 3.77 3.77 3.76 3.75 3.75 3.74 3.68 3.68 3.67 3.67 3.66 3.66 3.65 3.65 3.65 3.64 3.52 3.52 3.39 3.39 3.38 3.38 3.32 2.33 2.33 2.31 2.31 2.04 2.03 2.03 2.02 1.93 1.92 1.92 1.91 1.91 1.90 1.90 1.90 1.64 1.63 1.63 1.62 1.57 1.34 1.34 1.33 1.33 1.32 1.31 1.27 1.26 1.25 1.25
1H NMR, 600 MHz, CDCl3, 25 °C
OMe
N
O
N
H
CO2Me
(−)-3.37
f1 (ppm)

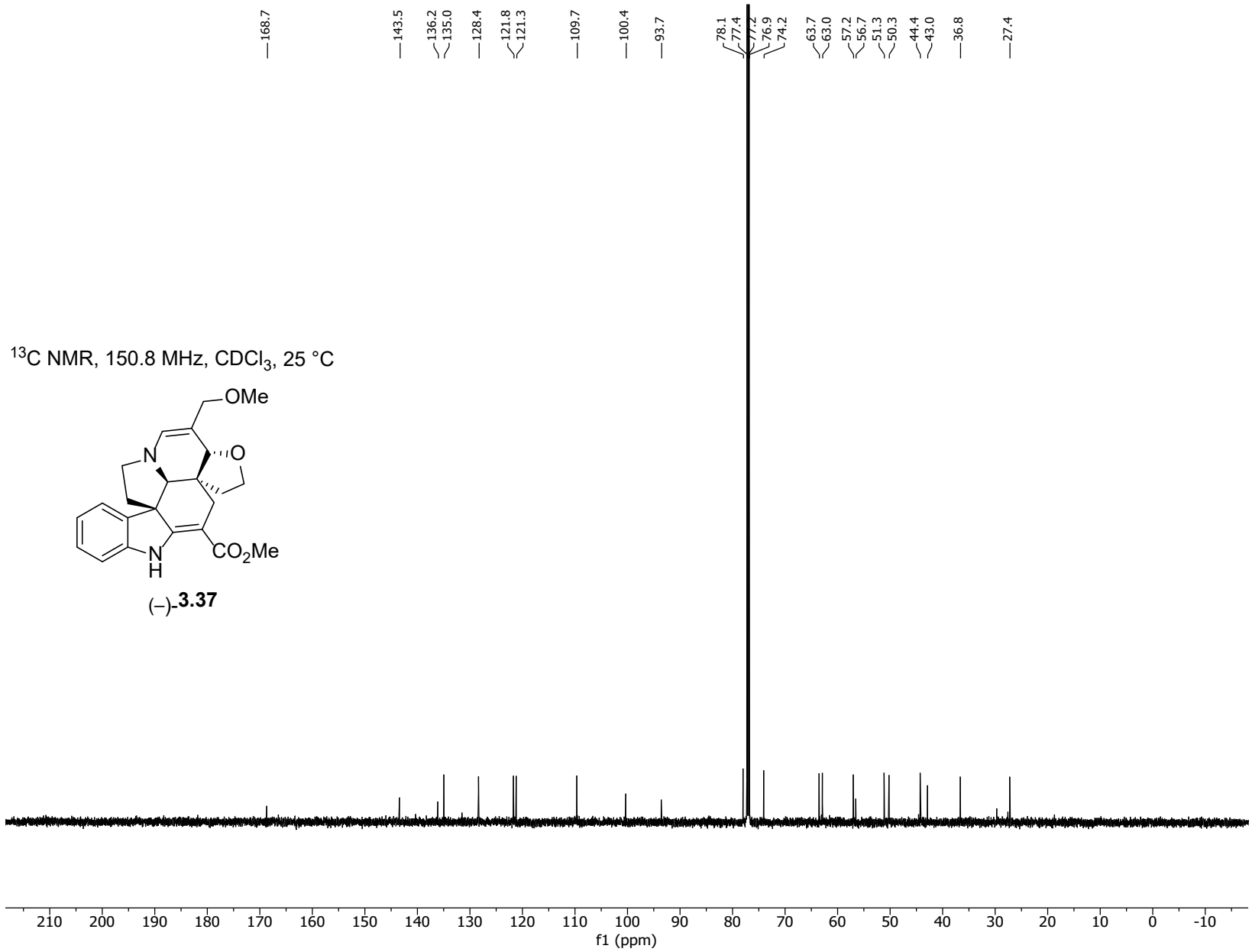

^{13}C NMR, 150.8 MHz, $CDCl_3$, 25 °C

(–)-**3.37**

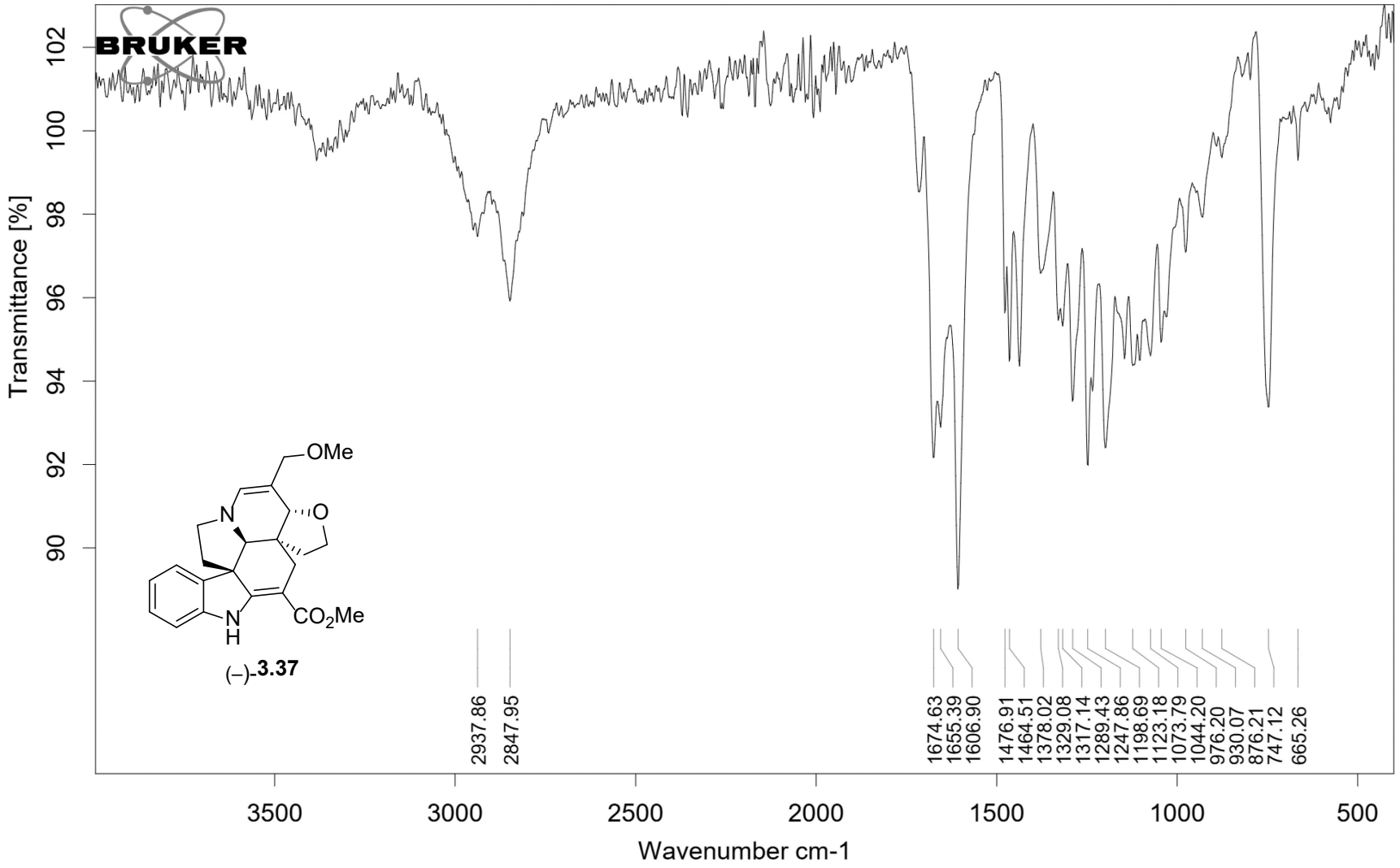
BRUKER
Transmittance [%]
102
100
98
96
94
92
90
OMe
N
O
N
H
CO2Me
(–)-3.37
2937.86
2847.95
1674.63
1655.39
1606.90
1476.91
1464.51
1378.02
1329.08
1317.14
1289.43
1247.86
1198.69
1123.18
1073.79
1044.20
976.20
930.07
876.21
747.12
665.26
3500
3000
2500
2000
1500
1000
500
Wavenumber cm-1

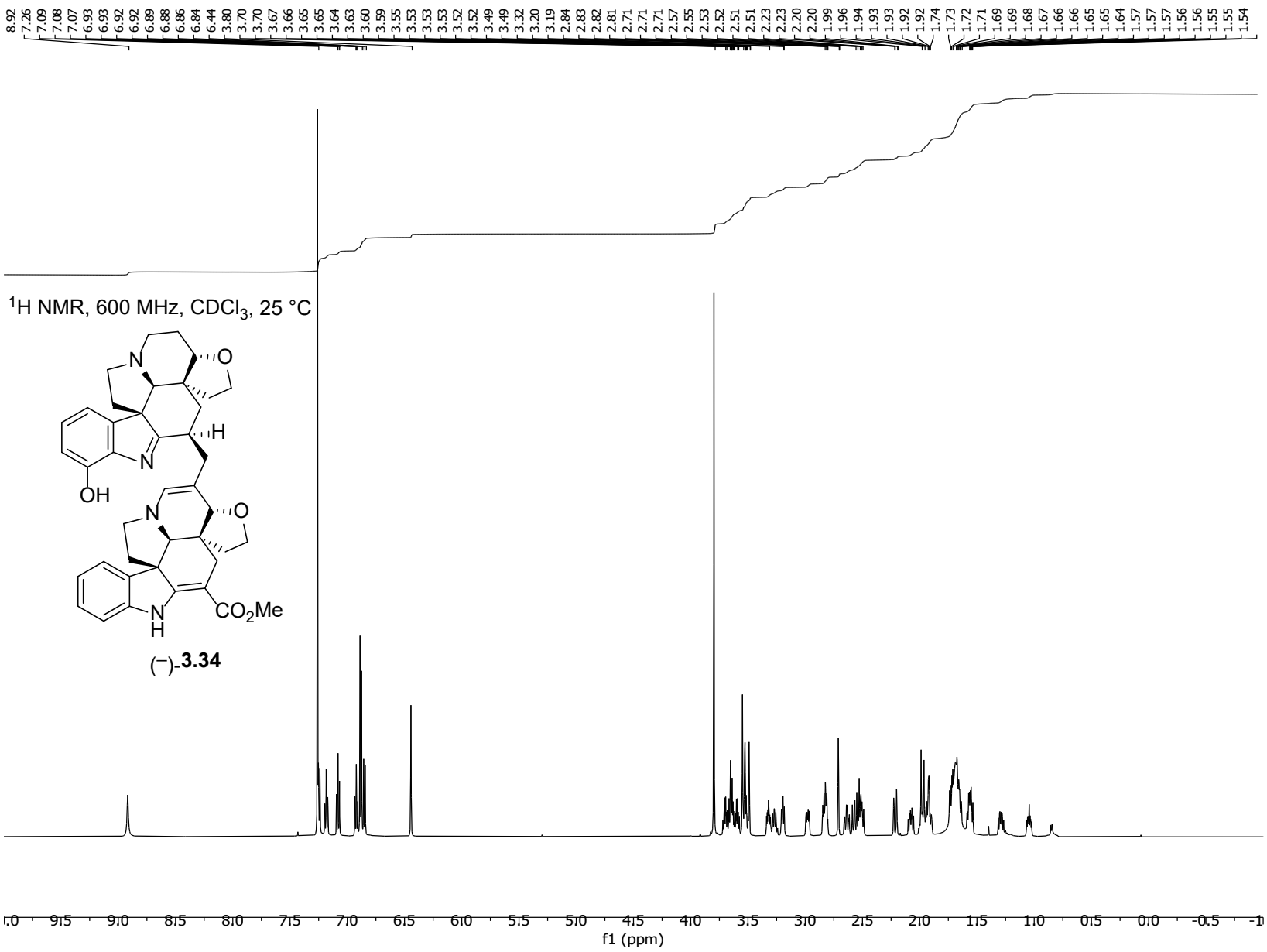
8.92 7.26 7.09 7.08 7.07 6.93 6.93 6.92 6.92 6.89 6.88 6.86 6.84 6.44 3.80 3.70 3.70 3.67 3.66 3.65 3.65 3.64 3.63 3.60 3.59 3.55 3.53 3.53 3.53 3.52 3.52 3.49 3.49 3.32 3.20 3.19 2.84 2.83 2.82 2.81 2.71 2.71 2.71 2.57 2.55 2.53 2.52 2.51 2.51 2.23 2.23 2.20 2.20 1.99 1.96 1.94 1.93 1.93 1.92 1.92 1.74 1.73 1.72 1.71 1.69 1.69 1.68 1.67 1.66 1.66 1.65 1.65 1.64 1.57 1.57 1.57 1.56 1.56 1.55 1.55 1.54
1H NMR, 600 MHz, CDCl3, 25 °C
N
O
H
N
OH
N
O
N
H
CO2Me
(−)-3.34
f1 (ppm)

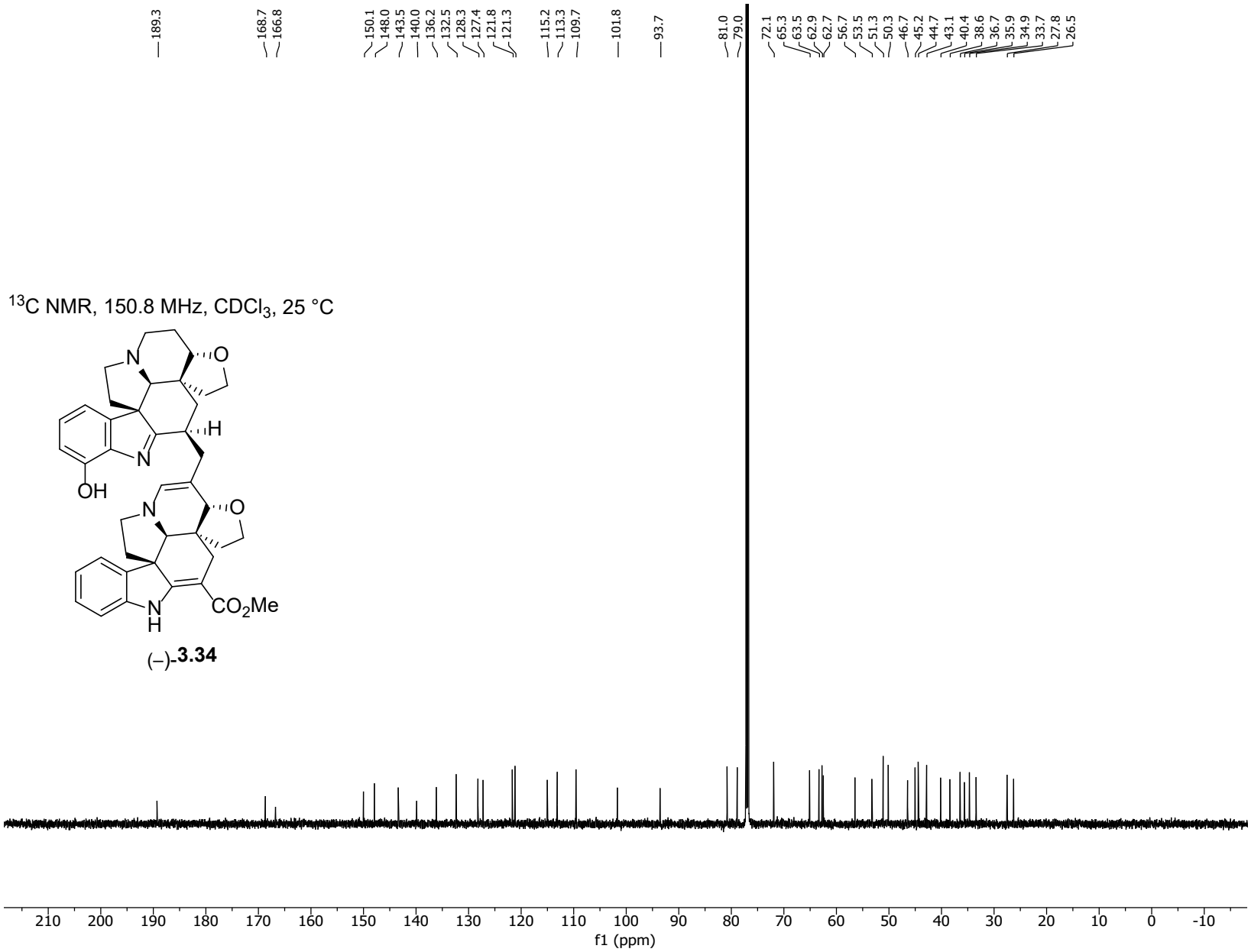

^{13}C NMR, 150.8 MHz, $CDCl_3$, 25 °C

(–)-**3.34**

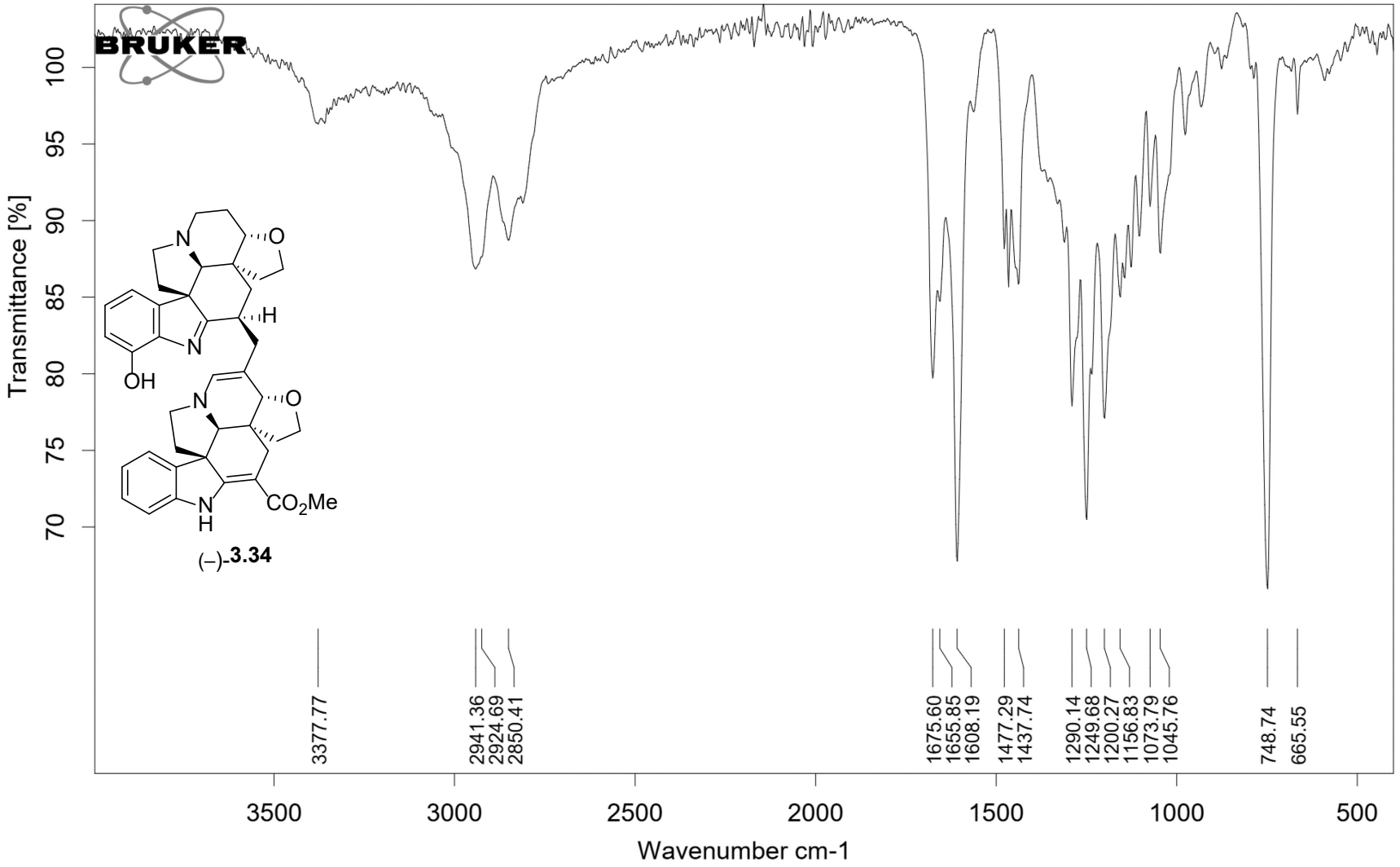
BRUKER
Transmittance [%]
100
95
90
85
80
75
70
3500
3000
2500
2000
1500
1000
500
Wavenumber cm-1
3377.77
2941.36
2924.69
2850.41
1675.60
1655.85
1608.19
1477.29
1437.74
1290.14
1249.68
1200.27
1156.83
1073.79
1045.76
748.74
665.55
N
O
H
N
OH
N
O
N
H
CO2Me
(–)-3.34

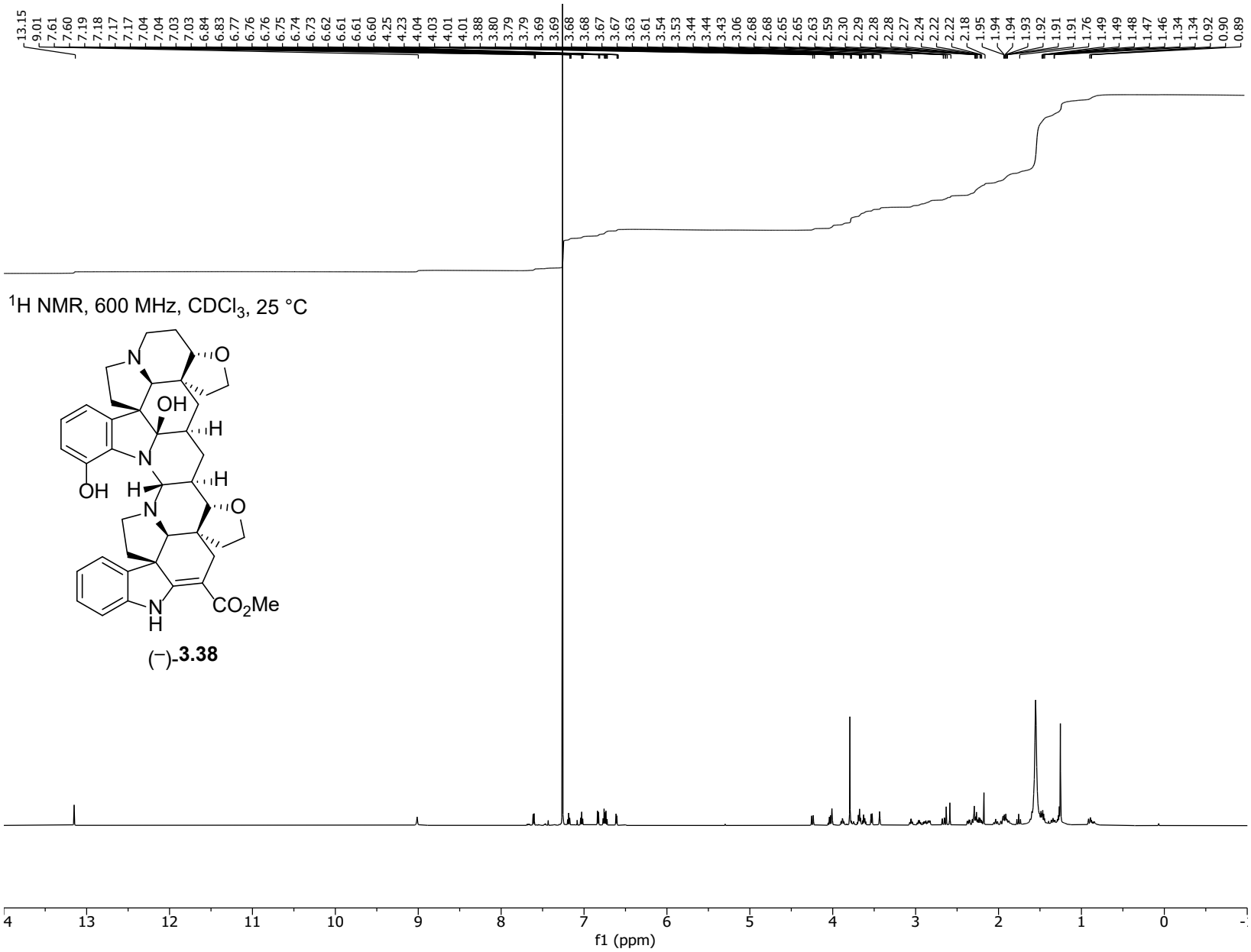
13.15
9.01
7.61
7.60
7.19
7.18
7.17
7.17
7.04
7.04
7.03
7.03
6.84
6.83
6.77
6.76
6.76
6.75
6.74
6.73
6.62
6.61
6.61
6.60
4.25
4.23
4.04
4.03
4.01
4.01
3.88
3.80
3.79
3.79
3.69
3.69
3.68
3.68
3.67
3.67
3.63
3.61
3.54
3.53
3.44
3.44
3.43
3.06
2.68
2.68
2.65
2.65
2.63
2.59
2.30
2.29
2.28
2.28
2.27
2.24
2.22
2.22
2.18
1.95
1.94
1.94
1.93
1.92
1.91
1.91
1.76
1.49
1.49
1.48
1.47
1.46
1.34
1.34
0.92
0.90
0.89
^{1}H NMR, 600 MHz, $CDCl_3$, 25 °C
OH
H
H
OH
H
O
O
CO_2Me
N
N
N
N
H
(−)-3.38
4
13
12
11
10
9
8
7
6
5
4
3
2
1
0
f1 (ppm)

^{13}C NMR, 150.8 MHz, $CDCl_3$, 25 °C

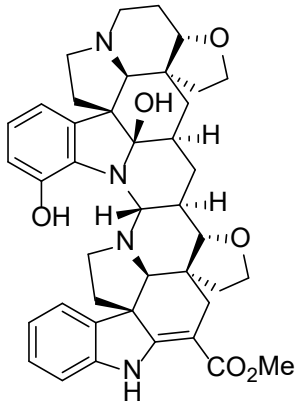

(–)-**3.38**

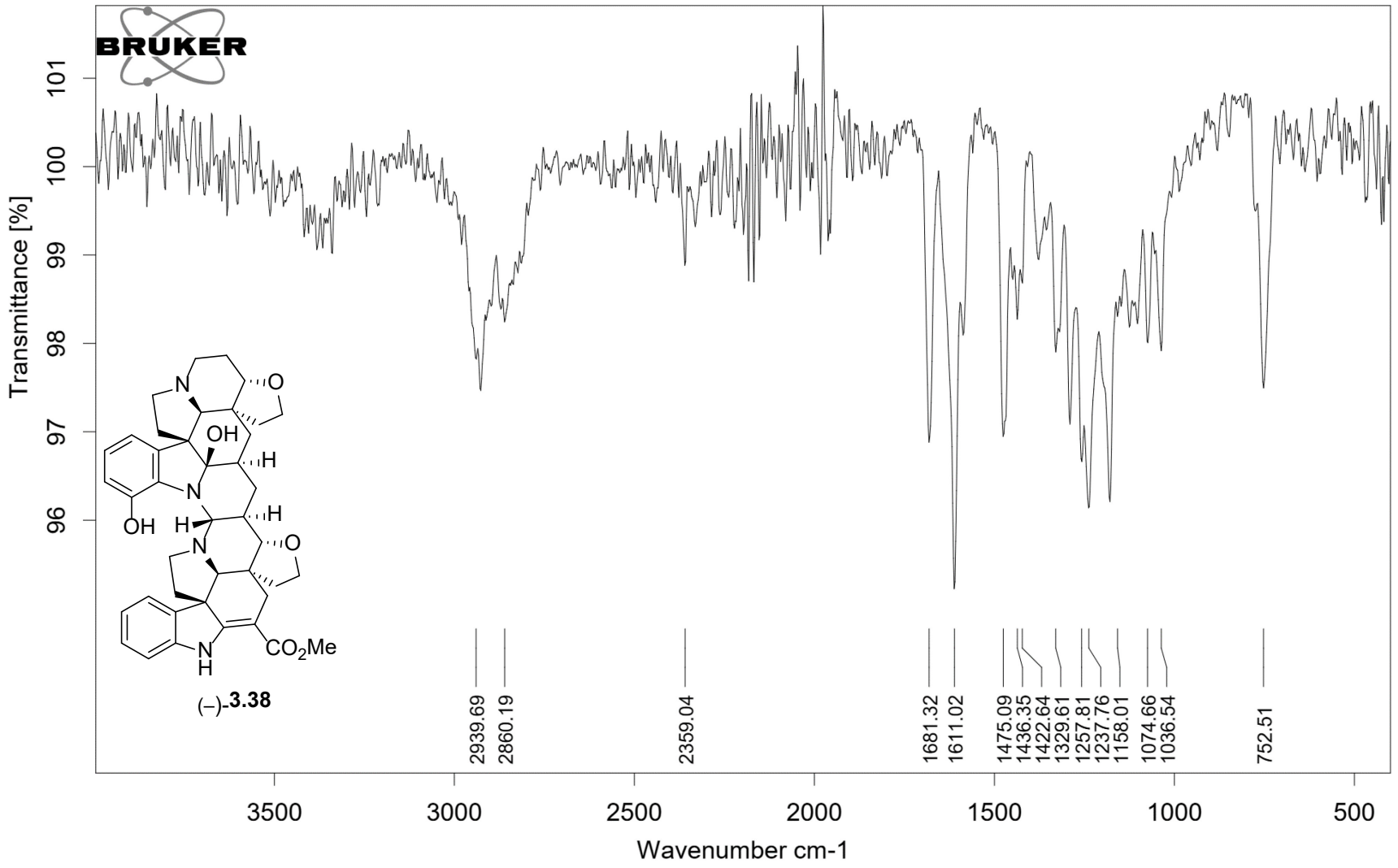
BRUKER
Transmittance [%]
101
100
99
98
97
96
3500
3000
2500
2000
1500
1000
500
Wavenumber cm-1
2939.69
2860.19
2359.04
1681.32
1611.02
1475.09
1436.35
1422.64
1329.61
1257.81
1237.76
1158.01
1074.66
1036.54
752.51
OH
OH
H
H
H
N
O
CO2Me
(–)-3.38

Curriculum vitae

Taylor Pinto

tpinto@mit.edu

Education

Graduate
Massachusetts Institute of Technology – Cambridge, MA August 2019 – Present
Ph.D. Candidate in Chemistry Degree expected Sept. 2024
Advisor: Professor Mohammed Movassaghi

Undergraduate
Tennessee Technological University – Cookeville, TN August 2014 – May 2019
Bachelor of Science in Chemistry, Summa Cum Laude, GPA 4.00
Bachelor of Science in Chemical Engineering, Summa Cum Laude, GPA 4.00

Research Experience

Graduate Research – Massachusetts Institute of Technology

- Research Advisor – Dr. Mohammed Movassaghi November 2019 – Present
  - Synthesis of Aspidosperma indole alkaloids
  - Contributed to synthesis of voacinol and voacandimine C

Undergraduate Research – Tennessee Technological University

- Research Advisor – Dr. William Carroll, Chemistry September 2018 – May 2019
  - Project: Amino acid synthesis using flow chemistry
  - Skills learned: Organic synthesis, NMR, experiment design
- Research Advisor – Dr. Daniel Swartling, Chemistry August 2014 – May 2018
  - Project: green synthesis of tetraphenylporphyrins using solar irradiation
  - Skills learned: Organic synthesis, NMR, Mass Spec, UV-Vis
- Research Advisor – Dr. Joseph Biernacki, Chemical Engineering Spring 2018
  - Project: Determining biodiesel heat of reaction
  - Skills learned: experiment design, isothermal calorimetry, data analysis

Work Experience

Eastman Chemical Company – Kingsport, TN
Intern

- Polymers Process Development May 2017 – August 2017
  - Worked on predicting product properties based on process conditions
  - Updated PI Process book displays for mixing systems
- Coatings Product Development May 2016 – August 2016
  - Worked on organic synthesis of new products for customer evaluation
  - Conducted stability test of the products
- Plasticizers Tech Service and App. Development May 2015 – August 2015
  - Worked on characterizing Eastman plasticizers

Publications

- Flynn, K. M.; Myeong, I.-S.; Pinto, T.; Movassaghi, M. "Total Synthesis of (-)-Voacinol and (-)-Voacandimine C." *J. Am. Chem. Soc*. **2022**, *144,* 9126-9131.
- Amin, S; et al. "Diels-Alder Reaction Using a Solar Irradiation Heat Source Designed for Undergraduate Organic Chemistry Laboratories" *J. Chem. Educ*. **2015**, *92*, 760-770.

Poster Presentations

- "Biogenesis-Inspired Synthesis of Complex Aspidosperma Alkaloids" Kristen M. Flynn, In-Soo Myeong, Taylor Pinto, Nadide Hazal Avci, and Mohammad Movassaghi
    - Merck-MIT Symposium 2022
    - MIT Chemistry Organic Retreat 2022
- "Investigating the use of Flow Chemistry for the Synthesis of 15N Labeled Amino Acids from Simple Starting Materials" Taylor Pinto and William Carroll
    - 257th ACS National Meeting, Orlando, FL, April 2019
- "Synthesis using solar irradiation and spectral analysis of meso-tetraphenylporphyrins" Taylor Pinto and Daniel Swartling
    - 255th ACS National Meeting, New Orleans, LA, March 2018
- "Continuing synthesis of meso-tetraphenylporphyrins using solar irradiation" Taylor Pinto and Daniel Swartling
    - 251st ACS National Meeting, San Diego, CA, March 2016
- "Preparation of tetraphenylporphyrins via solar irradiation" Taylor Pinto and Daniel Swartling
    - 249th ACS National Meeting, Denver, CO, March 2015

Recognitions

- Tau Beta Pi – Engineering Honor Society
- Omicron Delta Kappa – National Leadership Honor Society
- Alpha Lambda Delta – National Honor Society for First-Year Success
- TTU Chemistry Department Outstanding Freshman, Junior, and Senior
- TTU Chemistry Department awards in general chemistry, organic, physical chemistry, and analytical chemistry

Teaching Experience

Graduate Teaching Assistant – Massachusetts Institute of Technology

- 5.363 Organic Structure Determination lab September 2019 – December 2019
- 5.12 Organic Chemistry I February 2020 – May 2020

Laboratory Teaching Assistant – Tennessee Technological University August 2016 – May 2019

- Organic and General Chemistry Labs
- Responsible for monitoring lab safety and assisting with lab experiments

General Chemistry Tutor – Tennessee Technological University August 2015 – May 2016

Leadership

Undergraduate Research Mentor September 2021 – May 2023

- Mentoring an MIT undergraduate student in the Movassaghi group

MIT Chemistry Quality of Life Committee October 2020 – Present

- Chemistry Graduate Student Committee representative

Student Members of the American Chemical Society, TnTech chapter August 2014 – May 2019

- Treasurer, August 2016 – May 2017
- President, August 2018 – May 2019

American Institute of Chemical Engineers, TnTech chapter August 2014 – May 2016